INFORMATION TO USERS

This manuscript has been reproduced from the microfilm master. UMI films the text directly from the original or copy submitted. Thus, some thesis and dissertation copies are in typewriter face, while others may be from any type of computer printer.

The quality of this reproduction is dependent upon the quality of the copy submitted. Broken or indistinct print, colored or poor quality illustrations and photographs, print bleedthrough, substandard margins, and improper alignment can adversely affect reproduction.

In the unlikely event that the author did not send UMI a complete manuscript and there are missing pages, these will be noted. Also, if unauthorized copyright material had to be removed, a note will indicate the deletion.

Oversize materials (e.g., maps, drawings, charts) are reproduced by sectioning the original, beginning at the upper left-hand corner and continuing from left to right in equal sections with small overlaps.

Photographs included in the original manuscript have been reproduced xerographically in this copy. Higher quality 6" x 9" black and white photographic prints are available for any photographs or illustrations appearing in this copy for an additional charge. Contact UMI directly to order.

Bell & Howell Information and Learning
300 North Zeeb Road, Ann Arbor, MI 48106-1346 USA
800-521-0600

Epidermal Growth Factor Receptor and Insulin Receptor Traffic and Signal Transduction in Rat Liver.

Gianni M. Di Guglielmo
Department of Biochemistry
McGill University
Montreal, Canada

A Thesis submitted to the
Faculty of Graduate Studies and Research
in partial fulfillment of the requirements for the Degree of
Doctor of Philosophy

September 1998

Abstract

Previous studies have demonstrated that receptor tyrosine kinases (RTKs) use common intracellular signal transduction pathways. This is remarkable due to the divergent cellular responses elicited from different RTKs. The insulin receptor (IR) is involved in blood glucose homeostasis whereas the epidermal growth factor receptor (EGFR) has been linked to liver regeneration. We therefore used rat liver, an organ enriched in both EGF and insulin receptors, to study the specificity of signal transduction *in vivo*.

Upon EGF administration, the EGFR at the plasma membrane (PM) was tyrosine phosphorylated on the major *in vivo* activation site, Y^{1173}, and recruited the adaptor proteins SHC and GRB2. Following ligand-mediated endocytosis, the activated EGFR was associated on endosomal membranes with the signaling complex SHC/GRB2 and the guanine nucleotide exchange factor, SOS. EGF administration also led to tyrosine phosphorylation of the cytosolic proteins focal adhesion kinase (FAK) and SHC. These observations were associated with increased MAP kinase activity and the transcription of c-myc, c-fos and c-jun.

In response to insulin, IR kinase activity and autophosphorylation was observed at the PM but not after IR internalization into endosomes. This is postulated to be due to rapid degradation of insulin in the endosomal lumen allowing for the dephosphorylation of the IR by protein tyrosine phosphatase(s). To evaluate the role of endosomal degradation in IR signaling, an insulin analog, termed H2, was characterized for its clearance and processing in liver. Although liver uptake of H2 was similar to that of insulin, its clearance was slower. This correlated with reduced ligand dissociation from internalized IR as well as slower degradation kinetics.

In response to H2, IR traffic was delayed in the endosomal apparatus. This occurred with increased IR autophosphorylation and tyrosine kinase activity in this compartment. H2 but not insulin induced JNK activity and c-jun transcription. Insulin stimulated MAP kinase and glycogen synthase (GS) activities in rat liver. H2, however, was less efficient in inducing MAP kinase activity than insulin and GS activity was not observed. Impaired GS activity in response to H2 correlated with increased PKC activity. The above observations of insulin and H2 were not due to changes in SHC nor IRS-1 signaling.

These studies indicate that the modification of RTKs at the level of the endosome alters receptor traffic and specificity of signal transduction pathways and support the hypothesis that RTK endocytosis plays a role in the regulation of RTK signaling.

Résumé

De nombreuses études ont démontré que les récepteurs à activité tyrosine kinase utilisent des voies de transduction intracellulaires communes menant à des réponses cellulaires différentes. Le récepteur pour l'insuline est impliqué dans le contrôle du glucose sanguin tandis que le récepteur pour l'EGF participe à la régéneration du foie. Afin d'étudier la spécificité de signaiisation des récepteurs à activité tyrosine kinase *in vivo*, nous avons donc utilisé le foie de rat, organe riche en récepteurs pour l'EGF et l'insuline,

Après stimulation par l'EGF, le R-EGF est phosphorylé sur la tyrosine 1173 dans la membrane plasmique (MP). Il peut alors se fixer aux molécules adaptatrices SHC et GRB2. Après endocytose, le récepteur activé s'associe dans les endosomes avec le complexe SHC/GRB2 et le facteur d'échange SOS. Un traitment par l'EGF conduit aussi à la phosphorylation en tyrosine de FAK et SHC ainsi qu'à une augmentation de l'activité MAP kinase et à la transcription de c-fos, c-myc et c-jun.

Après un traitment par l'insuline, l'activité kinase et l'autophosphorylation du récepteur à l'insuline est retrouvée dans la membrane plasmique mais pas dans les endosomes. Ce phénomene pourrait être dû à une dégradation rapide de l'insuline dans la lumière endosomique, ceçi permettant une inactivation du récepteur par des tyrosines phosphatases. De manière à étudier le rôle de la dégradation endosomique de l'insuline dans la signalisation de son récepteur, une molécule analogue à l'insuline, H2, a été caractérisée. Bien que l'absorption hépatique de H2 soit similaire à celle de l'insuline, sa clairance est plus lente, du fait d'une dissociation réduite d'avec le récepteur et une dégradation minimisée.

Lors d'une stimilation par H2, le traffic du récepteur `a l'insuline est retardé dans l'appareil endosomique, avec une augmentation de l'autophosphorylation et de l'activité kinases. Contairement à l'insuline, H2 induit une activation de l'activité PKC ainsi que la transcription de c-jun. En revanche aucune activation de glycogène synthase n'est observée.

Nos resultats suggèrent que la modification des récepteur à activité tyrosine kinase dans le compartiment endosomique, affecte leur traffic intracellulaire ainsi que les voies de signalisation qu'ils déclenchent. Ces observations confirment que l'endocytose des récepteurs à activité tyrosine kinase joue un rôle dans la régulation de leur signalisation.

Contributions of Others

In this work, I present my original contribution to the study of EGF and insulin receptor internalization and signal transduction in a physiological system, rat liver. The work presented here is essentially my own with the following exceptions :

1) The Northern blotting analysis (Chapter 1, Figure 14 and Chapter 3, Figure 29A) was carried out by Dr. P.C. Baass with my assistance.

2) The insulin receptor kinase assay (Chapter 3, Figure 25) was carried out by Dr. P.G. Drake.

3) The Edman degradation data (Chapter 2, Table 3) was provided by Dr. F. Authier.

The data in Chapter 1 was published by G.M. Di Guglielmo, P.C. Baass, W.-J. Ou, B.I. Posner and J.J.M. Bergeron (1994) EMBO J. 13: 4269-4277. Dr. P.C. Baass assisted in the quantitative immunoblotting analysis. Dr. W.-J. Ou provided technical advice for the immunoprecipitation studies. Dr. B.I. Posner generously provided reagents and was involved on a conceptual basis.

The data in Chapter 2 represents my contribution to the manuscript published by F. Authier, G.M. Di Guglielmo, G.M. Danielsen and J.J.M. Bergeron (1998) Biochem. J. 332: 421-430. The published data solely generated by Dr. Authier (internalization studies, cross-linking studies, immunoblotting, etc.) was not included in Chapter 2 of this thesis. Dr. F. Authier assisted in the HPLC analysis. Dr. G.M. Danielsen generously provided the H2 insulin analog.

The data in Chapter 3 is in the manuscript entitled "Insulin and H2 mediated insulin receptor traffic and signal transduction in rat liver" by G.M. Di Guglielmo, P.C. Baass, P.G. Drake, L. Lavoie, G.M. Danielsen, B.I. Posner and J.J.M. Bergeron. Dr. P.C. Baass assisted in the quantitative immunoblotting analysis. Dr. P.G. Drake carried out the IR exogenous kinase assay (see above). Dr. L. Lavoie assisted in the glycogen synthase studies. Dr. G.M. Danielsen generously provided the H2 insulin analog. Dr. B.I. Posner generously provided reagents and was involved on a conceptual basis.

Dr. Bergeron supervised the work presented in this thesis and provided editorial assessment of the manuscripts.

Acknowledgments

I would like to thank my thesis supervisor, Dr. J.J.M. Bergeron for his guidance and enthusiasm.

I would like to thank Drs. P.C. Baass, F. Authier, L. Lavoie and P.G. Drake for their collaboration.

I would like to thank Drs. J. McGlade and T. Pawson for their SHC constructs, Dr. G. Danielsen for providing the insulin analog H2, Dr. M.F. White for the IRS-1 antibodies, Drs. R. St Arnaud, N. Sonenberg and P. Jolicoeur for the c-fos, c-myc and c-jun cDNA probes respectively, Dr. J. Woodgett for the GST-jun construct and Dr. M. Shanks for the IgG 151 hybridoma cells. I would also like to thank Dr. J. T. Parsons for the FAK 2A7 antibodies and Dr. D. Stern for the EGFR PY1173 phosphopeptide-specific antibodies.

I wish to thank Ms. P.H. Cameron, Mr. A. Fazel, Drs. F. Authier, W.-J. Ou, E. Chevet, M. Dominguez, P.C. Baass and R. Hemming, and the late Dr. W. Lai and Mr. J-J Doherty II for the training and time they generously provided in the course of my studies.

I wish to thank Dr. E. Chevet for translating the abstract.

I thank Drs. B.I. Posner, C.E. Smith, S. Miller, D.Y. Thomas, N. Lamarche, L. Larose, P. Branton and P.A. Walton for kindly allowing me access to their lab equipment and reagents.

I would like to thank Pam, David, Ali, Sophie, Michel, Eric, François, Hetty, Paul, Paulina, Joe and Victor for their friendship especially during the stressful times.

Thanks to Ms. M. Caron, P. Ramamurthy and K. Halse I never missed a deadline. Well, at least not the important ones. Special thanks to Ms. Ramamurthy for excellent clerical assistance.

Finally I'd like to thank Pat, Carmi and my parents for their patience, support and love.

Table of Contents

LIST OF FIGURES

LIST OF TABLES

ABBREVIATIONS

AP-1	activator protein 1
AP2	adaptor protein 2
ATP	adenosine triphosphate
BSA	bovine serum albumin
BW	body weight
cDNA	complementary DNA
CHO	chinese hamster ovary
cpm	counts per minute
CsCl	cesium chloride
DEPC	diethyl pyrocarbonate
DMEM	Dulbecco modified Eagle medium
DMSO	dimethyl sulfoxide
EAI	endosomal acidic insulinase
EDTA	ethylenediaminetetraacetic acid
EGF	epidermal growth factor
EGTA	ethylene glycol-bis (β-aminoethyl ether)-*N,N,N',N'*-tetraacetic acid
FGF	fibroblast growth factor
gab-1	GRB2 associated binding protein 1
GAP	GTPase activating protein
GAPDH	glyceraldehyde phosphate dehydrogenase
GE	Golgi endosome fraction
GRB2	growth factor receptor binding protein 2
GTP	guanosine triphosphate
HBS	HEPES buffered saline
HGF	hepatocyte growth factor
HPLC	high pressure liquid chromatograpy
HEPES	N-(2-Hydroxyethyl)-1-piperazine N'-2-ethane sulfonic acid
HRP	horse radish peroxidase
IGF-1(R)	insulin-like growth factor-1(receptor)
IP	immunoprecipitation
IPTG	isopropyl β-D-thiogalactopyranoside
IRS-1	insulin receptor substrate-1
kDa	kilo Dalton
KIU	kallikrein inhibitor units
LSPB	Laemmli sample preparation buffer
MAPK	mitogen-activated protein kinase
MBP	myelin basic protein
SOS	Son-of-sevenless
Na_3VO_4	sodium orthovanadate
NGF	nerve growth factor
OD	optical density
ODC	ornithine decarboxylase
OsO_4	osmium tetrachloride
PEPCK	phosphoenolpyruvate carboxy kinase
PBS	phosphate buffered saline
PH	pleckstrin homology domain
PI	phosphatidylinositol
PI 3'-kinase	phosphatidylinositol 3' kinase
PKC	protein kinase C
PM	plasma membrane
PMSF	phenylmethylsulfonyl fluoride

p-NPP	para-nitrophenylphosphate
PTB	phosphotyrosine binding domain
PY	phosphotyrosine
RTK(s)	receptor tyrosine kinase(s)
SD	standard deviation
SDS-PAGE	sodium dodecyl sulfate polyacrylamide gel electrophoresis
SH2 / 3	src homology 2 /3 domain
SHC	SH2 containing / homologous to collagen protein
SHPTP	SH2 containing phosphotyrosine phosphatase
SIE	serum inducible element
SRE/SRF	serum response element / serum response factor
TCF	ternary complex factor
TFA	trifluoroacetic acid
TGFα	transforming growth factor α
TP	total particulate fraction
Tris	2(hydroxymethyl) 2-amino-1,3 propanediol
Tween-20	polyoxyethylenesorbitan monolaurate
TX-100	Triton X-100
WGA	wheat germ agglutinin

Introduction

Cells in multi-cellular organisms communicate and cooperate with the extracellular environment and each other and in this way regulate cell metabolism, proliferation and differentiation. Methods of communication include the release of hydrophobic and hydrophilic signaling factors in an autocrine, paracrine, or endocrine fashion.

Hydrophobic molecules cross the cell membrane and carry out their effects by directly interacting with intracellular molecules. Hydrophilic factors, including growth factors and polypeptide hormones, cannot penetrate the cell membrane and must therefore interact with specific receptors on the cell surface that transmit extra-cellular signals to the interior of the cell. Among these receptors are cytokine receptors, serine/threonine kinase receptors and receptor tyrosine kinases (RTKs). Upon binding of the ligand with their respective receptors, the ligand-receptor complexes dimerize/oligomerize homotypically or heterotypically. For many receptors this aggregation stimulates cytoplasmic intrinsic enzymatic activity or the association with molecules that contain enzymatic activity. These form part of signaling cascades that feed the information from the receptor to the interior of the cell where changes in gene expression, protein translation and cytoskeletal structures are induced.

The demonstration of protein tyrosine phosphorylation came about in the late 1970's by a number of groups studying the properties of transforming proteins from polyoma virus, Rous sarcoma virus and Abelson murine leukemia virus (Hunter, 1996). The finding that the *v-src* gene product had an associated kinase activity allowed investigators to postulate that protein phosphorylation was involved in cellular transformation (Collett and Erikson, 1978). Soon after the demonstration of protein tyrosine phosphorylation (Eckhart *et al.*, 1979), a number of protein tyrosine kinases, both viral oncogenes and cellular proto-oncogenes, were described including the epidermal growth factor receptor (EGFR) (Ushiro and Cohen, 1980), the insulin receptor (IR) (Kasuga *et al.*, 1983; Rosen *et al.*, 1983) and the platelet derived growth factor receptor (PDGFR) (Ek *et al.*, 1982).

The mechanism of RTK activation was elucidated in the mid-1980s by studies on the EGFR (Hunter, 1996). By using cross-linking, solid matrix immobilization and native gel electrophoresis, it was shown that dimerization played an critical role in the activation of RTKs (Schlessinger, 1986). For autophosphorylation of the IR, the mechanism has been suggested to occur intra-molecularly or inter-molecularly based on its heterotetrameric ultrastructure (see below). The first protein tyrosine phosphatase (PTPase) was not identified molecularly until the late 1980's (Tonks *et al.*, 1988). In recent years the crystal structure of PTPases such as SHP-2 (reviewed by Barford and Neel, 1998) and RTKs

such as the FGFR and IR (reviewed by Hubbard *et al.*, 1998) have given insight on their mode of activation (see below).

Co-evolving with the identification and cloning of RTKs and PTPases was the mapping of signal transduction pathways by genetic analysis of *D. melanogaster* and *C. elegans*. Biochemically, these pathways were elucidated with the realization that many proteins have distinct domains (SH2 domains) that allow them to interact with phosphotyrosine residues (Margolis *et al.*, 1990). Following the identification of the SH2 domain, the description of other domains (e.g., PTB and SH3 domains) allowed investigators to map the interaction of RTKs with their substrates and/or adaptor proteins (reviewed by Pawson and Scott, 1997).

The complex mapping diagrams of RTK signal transduction have shown that although protein-protein interaction domains exhibit specificity, there is a high degree of crosstalk among members of RTKs and other signaling systems (e.g., serpentine receptors). Indeed, RTKs involved in metabolic actions in the cell (e.g., the IR) have been shown to use common pathways as RTKs involved in tissue regeneration (e.g., the EGFR) (see below). A further complication lies upon the fact that RTKs internalize immediately following challenge at the cell surface with their respective ligands (reviewed by Baass *et al.*, 1995; Bevan *et al.*, 1996). They may interact with specific subsets of substrates/adaptors as they are inactivated and/or degraded by intracellular processes.

I. Receptor Tyrosine Kinases

Many of the activities of vertebrate cells are controlled by extracellular signaling molecules. Transmembrane receptors transduce these signals across the cellular membrane to the interior of the cell. One type of receptor has intrinsic protein tyrosine kinase activity and belongs to the RTK family (Figure 1). RTKs are activated by hormones and polypeptide growth factors. Most known ligands for RTKs are secreted, soluble proteins, but membrane-bound proteins as well as extracellular matrix proteins also activate RTKs. They are closely related in their catalytic domains which has allowed for homology cloning of many RTKs that lack identified ligands, termed orphan receptors. Signaling by RTKs involves ligand-mediated receptor dimerization, which results in transphosphorylation and the receptor subunits and activation of the catalytic domains for the phosphorylation of cytosolic substrates (Hubbard *et al.*, 1998)

RTK basic structure

RTKs are type I transmembrane proteins with the N-termini outside the cell, a single membrane-spanning domain and a catalytic intracellular domain (Figure 1). The extracellular domain of RTKs is composed of several hundred amino acids that contain

characteristic patterns of structural motifs. Most RTKs extracellular domains are modified by N-linked glycosylation. The transmembrane domain consists of a stretch of hydrophobic residues and the cytoplasmic domain consists of a juxtamembrane region, the kinase domain and a C-terminal region. The kinase domain is approximately 250 residues in length and carries out the phosphotransfer reaction. It is closely related to that of cytoplasmic protein tyrosine kinases and protein-serine/threonine kinases (Hanks and Hunter, 1995) and the crystal structure indicates allosteric regulation of activity (see below). The C-terminal domain varies in length from a few up to 200 residues and the function varies among members of the RTKs.

RTK extracellular domain

RTK extracellular domains are composed of combinations of various sequence motifs. The IR and EGFR have Cys-rich regions that form disulfide bonds. The IR also has three fibronectin type III (FNIII) repeats. The IR is derived from a proteolytically cleaved polypeptide to yield a mature receptor in which the α and β subunits are covalently linked by disulfide bonds and function as a heterotetrameric molecule. The PDGF and the fibroblast growth factor receptor (FGFR) family members have immunoglobulin-like (Ig) domains. The NGF receptor contains two Ig-like domains and a Leu-rich motif, which is believed to function in cell adhesion. The hepatocyte growth factor receptor (HGFR) is a heterodimer that, like the IR, is formed by proteolytic cleavage of a precursor, which results in a receptor with two subunits held together by a disulfide bond.

Although the functions of the structural motifs found in ligand-binding domains are unclear, they have been postulated to specify interaction with the cognate ligand. Dimerization of two receptor molecules is critical for RTK signaling and some motifs in the extracellular domain may serve this function. Indeed, the crystallization of vascular endothelial growth factor supports the model that dimerized ligands induce the formation of a symmetric dimer of receptor extracellular domains (Hubbard *et al.*, 1998). Interactions with other cell surface proteins facilitating adhesion or direct communication between cells, or interactions with the extracellular matrix may be other functions for RTK extracellular domains.

RTK intracellular domain

Most protein kinases share a conserved catalytic domain. Sequences on either side of this domain and some large inserts within the domain itself are not required for activity and may have functions that are not involved in phosphotransfer. RTK catalytic domains are composed of ~250 amino acids and have sequence similarities (sequence identities range from 32 to 95%) (Hanks and Hunter, 1995). The catalytic domain structure is generally composed of two lobes. The N-terminal lobe is responsible for binding

Mg^{+2}/ATP. Protein substrates and Mg^{+2}/ATP are brought together in the cleft which allows phosphotransfer to be catalyzed. The motif responsible for this is the Gly-X-Gly-X-X-Gly-X-$_{(15-20)}$-Lys (where X is any amino acid). The second lobe forms the catalytic loop. This region is highly conserved in both protein kinase families, yet it discriminates between RTKs and protein serine/threonine kinases (Taylor *et al.*, 1995).

Dimerization model of RTK activation

Signal transduction from RTKs follows several well defined steps originating at the cell surface upon binding of ligand to the receptor. These steps are summarized and further developed in the following sections.

1) Following ligand binding, receptors dimerize via ligand-induced conformational changes in the external domain.

2) Receptor dimerization leads to intermolecular autophosphorylation. The ligand-induced dimerization of the extracellular domains result in the juxtaposition of the cytoplasmic domains. Autophosphorylation within the dimer occurs at a distinct set of sites, most of which lie outside the catalytic domain. The IR is unique in that it is already predimerized in a heterotetrameric complex. Thus, it undergoes different modes of activation/inactivation that are mediated by the tyrosine phosphorylation sites within its catalytic domain (see below).

3) Transphosphorylation results in the activation of the dimeric RTKs and the subsequent recruitment and phosphorylation of cytoplasmic substrates that have an increased affinity for the receptor due to its autophosphorylation.

RTK function

RTKs act as receptors for growth factors, differentiation factors, and for factors that stimulate metabolic responses (van der Geer *et al.*, 1994). Expression of almost all RTKs is restricted to specific cell types in the organism. The pattern of expression depends upon the nature of the regulatory elements in the RTK gene promoter and enhancer. In the cells types where a particular RTK is expressed, its function is dictated by activating ligands that bind to its extracellular domain. The response to ligand-dependent RTK activation in a given cell depends upon the intracellular proteins that are targets for phosphorylation and/or regulation by the activated RTK (van der Geer *et al.*, 1994).

EGF receptor

The EGFR is a 170 kDa glycoprotein that is expressed on the basolateral surface of polarized cells and spans the membrane once. In the absence of ligand it is found dispersed over the cell membrane and is inactive.

EGFR extracellular domain

The extracellular domain of the EGFR consists of 621 amino acid residues including 50 cysteines structured into 25 disulfide bonds that have recently been determined by mass spectroscopy (Abe *et al.*, 1998). This domain binds EGF and five related molecules including TGFα (van der Geer *et al.*, 1994). The ligand binding domain for EGF and TGFα maps to a region located between residues 321-367 of the receptor although the binding sites for these ligands do not perfectly overlap (Winkler *et al.*, 1989). This may be responsible for the apparent differences in biological endpoints in response to these ligands. The ligand binding domain is flanked by two Cys-rich domains whose function has been proposed to maintain receptor structural integrity rather than mediating ligand recognition (Abe *et al.*, 1998).

All known growth factor receptors appear to undergo receptor dimerization upon ligand binding (reviewed by Hubbard *et al.*, 1998). This phenomenon was first demonstrated for the EGFR where dimerization was shown to be a crucial for kinase activation. Dimerization is presumed to occur due to conformational changes in the extracellular domain, which stabilize the interactions between two occupied receptor molecules. Two properties of the EGFR essential to its function have been attributed to the dimeric form of the receptor, including the presence of high affinity EGF binding sites and the activation of the tyrosine kinase activity (Sorkin *et al.*, 1994). Dimerization was directly tested by multi-angle laser light scattering (SEC-MALLS) and it was demonstrated that two EGF molecules bind two monomeric EGFRs to induce dimerization (Odaka *et al.*, 1997).

EGFR intracellular domain

Ligand induced receptor dimerization results in the proximity of the two cytosolic tails and a subsequent conformational change. This conformational change is believed to result in the stimulation of the catalytic activity and the consequent transphosphorylation of the receptor molecules (Hubbard *et al.*, 1998). All five autophosphorylation sites in the EGFR are located in the C-terminus region, unlike the IR which contains three regulatory tyrosine residues in the kinase domain (Figure 1).

Regulation of EGFR signaling by autophosphorylation sites has been demonstrated by C-terminal deletions of EGFR that resulted in enhanced transforming ability of the receptor (Yarden and Ullrich, 1988). Further studies on receptors with deletions or point mutations in autophosphorylation sites demonstrated that while the mutant receptors exhibited normal V_{max}, they exhibited a lower K_m for the phosphorylation of exogenous substrate (Honegger *et al.*, 1988). It has been proposed that autophosphorylation sites serve to fine-tune kinase activity by acting as competitive inhibitors for exogenous substrate

phosphorylation (Honegger *et al.*, 1988, Decker *et al.*, 1993). The autophosphorylation sites are first to be phosphorylated upon kinase activation due to the proximity of these sites in adjacent dimerized receptors. By competing with exogenous substrates for binding to the substrate binding region of the kinase, the autophosphorylation sites prevent the phosphorylation of substrates with high K_m, and thus further modulate signal transduction.

The major sites of EGFR autophosphorylation *in vitro* were identified to be Y^{1068}, Y^{1148} and Y^{1173} (Downward *et al.*, 1984) with two additional minor sites at Y^{992} and Y^{1086} (Margolis *et al.*, 1989). However, the major *in vivo* site of phosphorylation is Y^{1173} with Y^{1148} and Y^{1068} phosphorylated to a lesser degree (Downward *et al.*, 1984). The extent of phosphorylation of these sites *in vivo* is not clear but differences may account for tissue-specific variations in the signal transduction pathways initiated by the EGFR.

EGFR function

The major function of the EGFR has been shown to be cell proliferation. EGF has been demonstrated to be a primary mitogen for hepatocytes and hepatoma cells and stimulates hepatocyte DNA synthesis (Fausto *et al.*, 1995). EGF has been implicated as a hepatotrophic factor during liver regeneration. Indeed, circulating levels of EGF, TGFα, and HGF increase dramatically after partial hepatectomy, a procedure which results in large scale hepatocyte proliferation (Diehl and Rai, 1996). These are strong inducers of DNA synthesis in cultured hepatocytes. The EGFR may be involved in liver regeneration and development through the interaction with TGFα. Overexpression of TGFα induces liver neoplasia, pancreatic metaplasia and abnormal mammary gland development in transgenic mice (reviewed by Fausto *et al.*, 1995). EGF and TGFα generally exert the same effects on cell proliferation and function in a variety of cell types. TGFα synthesis is stimulated in liver cells in culture as well as *in vivo* by the activation of the EGFR (Fausto *et al.*, 1995). TGFα is expressed at high levels in early postnatal life and is associated with hepatocyte proliferation during this time. In adult rats, TGFα levels attenuate when the liver reaches its liver-mass/body-mass ratio. This observation indicates that environmental factors provide a mechanism which inhibit signal transduction from the activated EGFR.

Insulin receptor

The IR is a type I transmembrane glycoprotein derived from a precursor that is proteolytically cleaved to yield an α (135 kDa) and β (94 kDa) subunit which are covalently linked by disulfide bonds to form the functional heterotetrameric ($\alpha_2\beta_2$) IR. The α subunit is entirely extracellular. The β subunit contains the transmembrane domain, as well as the cytosolic kinase domain, internalization motifs and autophosphorylation sites (Figure 1).

IR extracellular domain

The α subunit contains the insulin binding region of the receptor. Insulin binds to a domain near the N-terminus (amino acids 20-120) of the α subunit (De Metys *et al.*, 1990), although other regions in the α subunit, such as the Cys-rich domain, may be involved in determining the specificity of ligand binding (Taylor *et al.*, 1991). The IR can bind to insulin-like peptides including the insulin-like growth factors, IGF-1 and IGF-2, but the affinity for these ligands is ~100-fold less than that for insulin. There is an alternative splicing site surrounding exon 11 of the IR gene, which results in two possible receptor isoforms differing in 12 amino acids near the C-terminus of the α subunit (White and Kahn, 1994). All three target tissues, liver, muscle and adipose tissue, express the longer receptor isoform (White and Kahn, 1994). The presence of the 12 extra amino acids causes a 2-fold reduction in the affinity of the receptor for insulin binding. With respect to the liver, the presence of the lower affinity receptor isoform may be explained as an evolutionary adaptation to the 2 to 3 fold higher doses of insulin seen by this organ due to its anatomical relationship with the pancreas.

Scatchard analysis of insulin binding to its receptor results in a curvilinear plot. This was initially suggested to represent a heterogeneous population of IRs; one consisting of a low number of high affinity receptors and the other a high number of low affinity receptors (Kahn *et al.*, 1974). Later the plot was explained by assuming negative cooperative interactions between insulin binding sites. This is consistent with the observation that the IR dimer ($\alpha\beta$) demonstrates a linear Scatchard plot with an affinity corresponding to the low affinity state of the heterotetrameric receptor ($\alpha_2\beta_2$). The assembly of two dimers into the heterotetrameric form has been suggested to cause a conformational change thereby increasing the affinity of the receptor for insulin (Taylor *et al.*, 1991).

IR intracellular domain

Upon insulin binding to its receptor, a conformational change is transmitted to the intracellular domain and results in the activation of the tyrosine kinase activity of the receptor which is delineated by residues 1002-1257 (Taylor *et al.*, 1991). While kinase activity is not necessary for receptor expression and cell surface targeting of RTKs, including the IR, it is crucial for efficient internalization, signal transduction and the induction of both early and late cellular responses initiated by ligand binding.

In the absence of ligand binding, the extracellular domain of the IR has a strong inhibitory effect on kinase activity (Taylor *et al.*, 1992). Insulin binding removes this inhibitory influence and the kinase is activated, probably as the result of conformational changes which are transmitted to the intracellular domain. The active form, however, is the

$\alpha_2\beta_2$ form. Although insulin can bind to the $\alpha\beta$ form, binding does not activate tyrosine kinase activity. Thus, receptor kinase activation as well as tyrosine autophosphorylation appears to occur through a trans-mechanism in which insulin binding to one $\alpha\beta$ dimer results in the activation and phosphorylation of the adjacent, covalently bound β subunit.

The IR cytosolic tail is poorly homologous to other RTK C-termini. Upon ligand binding and RTK activation, the receptor undergoes autophosphorylation. There are three domains in the β subunit containing autophosphorylation sites; the juxtamembrane region (Y^{972}), the regulatory region within the kinase domain (Y^{1158}, Y^{1162} and Y^{1163}), and the C-terminus (Y^{1328} and Y^{1334}) (White and Kahn, 1994). These major sites of receptor autophosphorylation have been shown to be phosphorylated in response to insulin in rat hepatoma cells (Tornqvist *et al.*, 1988) and adipocytes (Wang *et al.*, 1996).

IR activation correlates temporally with phosphorylation of the residues in the kinase domain, rather than those in the C-terminus. Crystallization of the IR kinase domain has given insight on the mechanism of kinase activation (Hubbard *et al.*, 1994). In the catalytic domain, Y^{1162} folds over the ATP and substrate binding pockets and is believed to prevent access to these sites. Autophosphorylation of all three tyrosine residues in the regulatory region stimulates kinase activity (White and Kahn, 1994) by displacing Y^{1162} (Hubbard *et al.*, 1994). In many cell types, the regulatory region is only bisphosphorylated, possibly limiting the amplitude of the insulin response, however, in rat hepatocytes, trisphosphorylation predominates, indicating a tissue specific mechanism for up-regulation of the insulin response (Issad *et al.*, 1991). Once phosphorylated and activated, the IR has been shown to remain active even in the absence of ligand (Rosen *et al.*, 1983).

The two tyrosine residues (Y^{1328} and Y^{1334}) in the C-terminus undergo rapid ligand induced autophosphorylation. Deletion of the C-terminus which remove these two tyrosine phosphorylation sites has no effect on the insulin stimulated autophosphorylation in other regions, receptor kinase activity or endocytosis (Thies *et al.*, 1989). However, cells expressing these truncated receptors were inefficient in stimulating glucose transport and glycogen synthase and demonstrated increased mitogenic activity in response to ligand. This indicates that the phosphorylation of the C-terminal tyrosines may modulate between metabolic and mitogenic signaling. Indeed, mutation of these two tyrosine residues to phenylalanine, results in normal metabolic effects but leads to increased mitogenesis. Thus the C-terminus tyrosine residues normally exert an inhibitory effect on the mitogenic properties of the IR (Takata *et al.*, 1991). The juxtamembrane region of the IR β-subunit is essential for signal transmission. This region contains Y^{972}, which resides in an NPXY motif (X represents any amino acid). This mutation impaired the ability of the receptor to

phosphorylate an endogenous 185 kDa protein substrate (IRS-1; White and Kahn, 1994). This tyrosine motif is involved in IR substrate recognition (see below).

IR function

In post-natal animals the main function of insulin is to maintain blood glucose homeostasis (Mortimore *et al.*, 1967). Liver, adipose and muscle tissue are the major sites of glucose uptake from the bloodstream. In adipose tissue and muscle, glucose cannot readily cross the plasma membrane to be deposited into glycogen and therefore relies on insulin to induce glucose uptake into the cell. This is carried out by insulin dependent recruitment of glucose transporters (GLUT4) to the plasma membrane (Holman and Cushman, 1994). IR signal transduction also modifies the intracellular enzymes that effect glucose deposition (e.g., glycogen synthase, PP1, etc.) as well as amino acid transport into the cell (Messina, 1989; Srivastava and Pandey, 1998) and the regulation of the cell surface Na^+/K^+-ATPase (Sweeney and Klip, 1998).

Anatomically positioned to receive the first bolus of insulin released from the pancreas, the liver has > 1 x 10^5 IRs/hepatocyte (Kahn *et al.*, 1974). The liver removes > 45% of circulating insulin in one pass (Jaspan *et al.*, 1981). The functions of insulin on the regulation of glucose metabolism in the liver are well established. In response to insulin stimulation lipogenesis is increased and gluconeogenesis decreases. Insulin can affect the regulation of these pathways by modulating the expression of key enzymes (Messina, 1989). For example, the rate limiting step in gluconeogenesis is the conversion of oxaloacetate to phosphoenolpyruvate, which is catalyzed by the cytosolic enzyme phosphoenolpyruvate carboxy kinase (PEPCK). Insulin acts to inhibit the transcription of the PEPCK gene both in intact liver as well as in cultured hepatoma cells. In addition, insulin (in the presence of glucose) results in the increase of glucose kinase gene expression, which catalyses the first step (glucose to glucose-6-phosphate) of the glycolytic pathway in liver (Doiron *et al.*, 1994). These actions of insulin are involved in the regulation of blood glucose levels.

Although the metabolic effects represent the major physiological actions of insulin, its growth promoting actions may play an important role in fetal growth, organogenesis and tissue repair and regeneration. The mitogenic responses to insulin include the stimulation of DNA synthesis and promotion of cell growth. However, many of the studies observing the activation of a mitogenic pathway in response to insulin have used cells overexpressing the IR or with respect to liver, hepatoma cell lines. In addition, many cell types express the insulin-like growth factor 1 receptor (IGF-1R) . Insulin binds the IGF-1R at high hormone concentrations. The binding of insulin to the IGF-1R in 3T3 mouse fibroblasts results in 10 fold greater mitogenicity than mediated through the IR kinase (Taylor *et al.*, 1991). As

a consequence, some of the insulin mediated mitogenic responses observed in culture may in fact be carried out by insulin-activated IGF-1Rs. Interestingly, experiments carried out by Osterop and colleagues (1992) revealed that the higher the number of transfected IRs in Chinese hamster ovary (CHO) cells, the lower the level of [^{3}H]-thymidine incorporation was in response to insulin. Although these results indicate a possible role for insulin in mitogenic signaling, they may not reflect the signal transduction pathways of the IR in liver. Indeed, this organ receives insulin regularly and in large doses but does not appear to undergo a mitogenic response. Acting alone, insulin is not an initiator of hepatocyte proliferation. However, the infusion of anti-insulin serum into rats after partial hepatectomy, impaired the regenerative capacity of the liver, supporting the role of insulin as a co-mitogen during hepatic regeneration.

Many of the effects observed in response to insulin stimulation are cell and tissue specific and involve a discrete subset of proteins. Responses to insulin stimulation are also dependent on the dose and length of exposure. Evidence exists indicating that the IR exerts its metabolic and mitogenic effects through divergent signal transduction pathways. In both cases however, it appears that protein phosphorylation plays a central role (Saltiel, 1994).

II. RTK Signal Transduction

Substrates and/or adaptor molecules involved in the propagation of signal transduction pathways originating from RTKs have structural hallmarks that allow them to interact with both receptors and other constituents of signal transduction pathways (Pawson and Scott, 1997). Many of these structural domains have been crystallized and the amino acid sequences they interact with have been mapped. Some of the motifs found in many downstream signaling molecules originating from RTKs and in particular the IR and EGFR are PH, PTB, SH2 and SH3 domains.

Domains in signal transduction molecules

A number of domains are involved in the mediation and association of signaling molecules involved in signal transduction.

PH domain

Pleckstrin homology (PH) domains were originally recognized as a repeat in the protein pleckstrin and later found in various signaling and cytoskeletal proteins, including several phospholipase C (PLC) isoforms, growth factor receptor binding protein 7 (GRB7), Ras GTPase-activating protein (RasGAP), insulin receptor substrate 1 (IRS-1), and the guanine nucleotide exchange factor son-of-sevenless (SOS) (reviewed by Lemmon and Ferguson, 1998). Although the sequence (~120 amino acids) which comprises the PH

domain is poorly conserved, a common structure is formed composed of a seven stranded β-barrel and an α helix at the C-terminus. This domain is believed to be involved in protein-protein and lipid-protein interactions. Several PH domains have been shown to bind to the βγ-complexes of heterotrimeric G proteins (Touhara *et al.*, 1994). In addition, the PH domain has been shown to bind phosphatidylinositol-4,5-bisphosphate, primarily through ionic interactions (Hyvönen *et al.*, 1995), a mechanism which may mediate the membrane localization of these proteins.

SH2 domain

Src homology 2 domains (SH2) were first recognized as a region of homology between the c-fps and c-src gene products (Sadowski *et al.*, 1986). These noncatalytic regions, present in a wide variety of signaling proteins, are involved in mediating protein-protein interactions. SH2 domains consist of ~100 amino acid residues which bind to phosphorylated tyrosine residues (Pawson and Scott, 1997). Specificity in SH2 recognition of phosphotyrosines was realized from the observation that not all tyrosine phosphorylated receptors bound the same subset of SH2 containing molecules. It has been determined that the specificity of SH2 recognition is carried by the amino acids on the carboxyl side of the phosphotyrosine residue (Songyang and Cantley, 1995).

PTB domain

The phosphotyrosine binding domain (PTB) or phosphotyrosine interacting (PI) domain was first identified in the adaptor molecule SHC and later in other molecules such as IRS-1 (van der Geer and Pawson, 1995a). The PTB domains of SHC and IRS-1 recognize phosphotyrosine motifs in specific amino acid sequences that form a β turn. This sequence is usually NPXpY. Specificity is conferred by hydrophobic amino acids that are five to eight residues NH2-terminal to the phosphotyrosine (Trüb *et al.*, 1995). This recognition is different from that of SH2 domains that interact with residues C-terminal to the phosphotyrosine. PTB domains may serve a somewhat different purpose from SH2 domains since they are found primarily as components of docking proteins that recruit additional signaling proteins to the vicinity of an activated receptor (Pawson and Scott, 1997).

SH3 domain

SH3 domains are small protein domains (55-70 amino acids) that are found in a number of proteins that associate with and regulate the cytoskeleton as well as in signal-transduction proteins (Pawson and Scott, 1997). SH3 binding sites appear to be proline rich motifs of ~10 amino acids. Two classes of binding sites can be defined; class I sites, Arg-X-X-Pro-X-X-Pro, (X may be Pro or any hydrophobic residue) and class II sites, whose consensus sequence appears in the opposite orientation (Mayer and Eck, 1995).

These two classes may confer specificity to the SH3-proline region interaction. There is also evidence for a role for SH3 domains in directing the cellular localization of signaling molecules (Bar-Sagi *et al.*, 1993).

It is possible to divide proteins bearing SH2/SH3 and PTB motifs into two main classes. Type I defines proteins that, in addition to SH2 and/or SH3 domains, contain enzymatic activities. These include PLC-γ, $pp60^{c\text{-}src}$, RasGAP and SOS (Hunter, 1996). These proteins are believed to become activated upon phosphorylation and/or association with neighboring proteins. The second class of proteins includes those that have no apparent catalytic function. These include GRB2, SHC, IRS-1 and the p85 subunit of PI 3'-kinase. These proteins function as adaptors and/or docking proteins, mediating the association between cellular proteins, or as regulatory subunits of enzymes, effectively linking activated receptors to downstream signaling molecules (Mayer and Baltimore, 1993).

BPS domain

Localized to a region of ~50 amino acids in the GRB10 molecule, the BPS domain was termed to denote its location between the PH and SH2 domains (He *et al.*, 1998). The BPS domain does not bear any obvious resemblance to other known protein interaction domains but is highly conserved among the GRB10-related proteins (He *et al.*, 1998). The BPS domain interaction with the IR is dependent upon RTK activity and autophosphorylation and may play a role in stabilizing other intermolecular interactions such as SH2 binding. Since this domain has been recently described, the precise role it plays in signal transduction remains to be determined.

EGFR and insulin receptor signal transduction

Although the EGFR and the IR exhibit different physiological end points which are cell type dependent, a number of their signal transduction pathways have been mapped and several common molecules have been implicated to propagate signals from both receptors:

The Ras pathway

The Ras pathway, elucidated by the cooperation of genetic and biochemical studies, delineates signaling from the plasma membrane to the nucleus (Figure 2).

SHC

All three *shcA* gene products ($p46^{SHC}$, $p52^{SHC}$ and $p66^{SHC}$) were named based on molecular mass and peptide structural motifs; a C-terminal SH2 domain and an adjacent Gly/Pro rich region which has homology to the α1 chain of collagen (Pelicci *et al.*, 1992). The $p52^{SHC}$ isoform was originally identified as a 55 kDa polypeptide substrate of the

EGFR in rat liver (Wada *et al.*, 1992; Donaldson and Cohen, 1992) that was recruited and internalized with the receptor into endosomes (Wada *et al.*, 1992).

The N-terminal PTB domain of SHC has been identified to regulate specific protein-protein interactions (Trüb *et al.*, 1995; van der Geer *et al.*, 1995b). The SHC proteins are highly conserved, ubiquitously expressed and are tyrosine phosphorylated in response to the activation of a wide variety of receptor tyrosine kinases (Yokote *et al.*, 1994; Pronk *et al.*, 1994; Sasaoka *et al.*, 1994b). Some recent evidence has indicated that $p46^{SHC}$ and $p52^{SHC}$ are involved in mitogenesis and $p66^{SHC}$ plays a role in attenuating this signal (Migliaccio *et al.*, 1997).

SHC and the EGFR

SHC proteins act as adaptor proteins and do not possess enzymatic activity. They are able to interact with several proteins via their SH2 domains which appear to bind preferentially to pYMXM motifs (X represents any amino acid). In addition, the SHC PTB domain can interact with EGFR NPXpY motifs ($NPVpY^{1086}$ and $NPDpY^{1148}$)(van der Geer *et al.*, 1995b). There is evidence, *in vitro*, that the PTB domain of SHC binds to the EGFR more strongly than its SH2 domain. The binding of SHC to the EGFR seems to be mediated mainly by the interaction of the PTB domain with Y^{1148}, which may be further stabilized by the interaction of SHC SH2 domain with Y^{1173} (Batzer *et al.*, 1995).

The direct interaction between SHC and the phosphorylated EGFR is proposed to result in the phosphorylation of SHC. SHC has three tyrosine phosphorylation sites: Y^{239}, Y^{240}, and Y^{317} (van der Geer *et al.*, 1995b). SHC phosphorylation results in the association of SHC with growth factor receptor binding protein 2 (GRB2; see below) which implicates SHC in the Ras signaling pathway. Although Y^{317} is found within a pY(L/I/V)NV sequence which corresponds with the consensus GRB2 SH2 binding motif (Songyang *et al.*, 1993), it is Y^{239} and Y^{240} that preferentially interact with the SH2 domain of GRB2 (van der Geer *et al.*, 1996). Although the SHC-GRB2 interaction has been shown in a number of cell types, binding of SHC to the EGFR does not appear to be essential for SHC phosphorylation and its association with GRB2.

SHC and the IR

Insulin treatment of fibroblasts or CHO cells overexpressing the IR also results in the rapid tyrosine phosphorylation of SHC (Pronk *et al.*, 1994; Sasaoka *et al.*, 1994b). Although association between the activated IR and SHC was undetected, indirect evidence for the requirement of SHC in IR mitogenic signaling has come from microinjection studies (Sasaoka *et al.*, 1994b). In these studies anti-SHC antibodies microinjected into Rat-1 fibroblasts (overexpressing EGF, insulin and IGF-1 receptors) reduced the ability of the

three ligands to stimulate DNA synthesis. The high concentration of receptors in these cells may result in the reduced specificity and abnormal regulation of signaling from the IR.

Although the juxtamembrane domain of the IR contains an NPXpY^{972} motif (the consensus SHC PTB domain binding sequence) there is no evidence for the association of SHC with the IR in response to insulin *in vivo*. This may be due to the fact that the sequence surrounding this tyrosine does not contain a hydrophobic residue at the -5 position (Trüb *et al.*, 1995).

GRB2/SOS

Growth factor binding protein 2 (GRB2) is a 26 kDa adaptor protein that was cloned using the CORT method and which consists entirely of an SH2 domain flanked by two SH3 domains (Lowenstein *et al.*, 1992). The SH2 domain binds tyrosine phosphorylated residues in a number of proteins, including the EGFR and SHC (Rozakis-Adcock *et al.*, 1992). The SH3 domains bind to the proline rich region in the C-terminus of the guanine nucleotide exchange factor, son of sevenless (SOS) (reviewed by Vojtek and Der, 1998).

Mammalian cells contain two related but distinct SOS proteins (150-170 kDa), SOS1 and SOS2, which are widely expressed during development and in adult tissues (Vojtek and Der, 1998). A region of 117 amino acids in the C-terminus, which differs between SOS1 and SOS2, imparts an increase in apparent binding affinity of SOS2 towards GRB2, indicating that the two SOS isoforms may contribute differently to receptor-mediated Ras activation (Yang *et al.*, 1995). The GRB2/SOS complex is present in untreated as well as growth factor treated cells (Cussac *et al.*, 1994). In addition, Buday and Downward (1993) observed an EGF dependent increase in the number of GRB2/SOS complexes.

GRB2/SOS and the EGFR

GRB2 (associated with SOS) binds with high affinity to phosphorylated Y^{1068} and to a lesser extent to pY^{1086} of the activated EGFR. The GRB2/SOS complex may also bind to pY^{1148} and pY^{1173} of the receptor indirectly, via the adaptor SHC (Batzer *et al.*, 1995). Studies by Cussac and colleagues (1994) reveal that the GRB2 SH2 domain has the highest affinity for the SHC tyrosine phosphorylated site, followed by EGFR sites. The SHC/GRB2/SOS complex that forms upon EGF stimulation has nucleotide exchange activity toward Ras (Vojtek and Der, 1998). Some studies, however, suggest the guanine nucleotide exchange activity is not measurably affected by growth factor stimulation, and binding of GRB2/SOS to phosphotyrosine residues (Buday and Downward, 1993; Cussac *et al.*, 1994). GRB2/SOS translocation seems to be the important function, since the targeting of SOS to the PM is sufficient to cause the activation of Ras (Buday and

Downward, 1993). Indeed, SOS translocates to the particulate fraction upon EGF stimulation (Buday and Downward, 1993).

EGF treatment of cells results in a mobility shift of SOS as seen by SDS-PAGE, presumably due to the increase in serine/threonine phosphorylation (Burgering *et al.*, 1993). This phosphorylation occurs relatively late compared to the formation of the SHC/GRB2/SOS complex and Ras activation, which suggests that SOS phosphorylation is not involved in the initial activation of Ras and has been suggested to be a negative regulatory mechanism (Pronk *et al.*, 1994).

GRB2/SOS and the IR

The putative GRB2 binding sites on the IR have very low affinity for the GRB2 SH2 domain and consequently, GRB2 does not bind this receptor directly (Skolnik *et al.*, 1993b; Pronk *et al.*, 1994; Cussac *et al.*, 1994). However, GRB2 may be involved in IR signaling through its interaction with tyrosine phosphorylated IRS-1 (preferentially Y^{895}) and/or SHC (Y^{317}, Y^{239}, Y^{240}) (Skolnik *et al.*, 1993; van der Geer *et al.*, 1995b) although the presence of SOS in GRB2/IRS-1 complexes was not detected in fibroblasts overexpressing the IR (Pronk *et al.*, 1994). Most evidence indicates that it is the interaction of GRB2/SOS with phosphorylated SHC which results in the activation of Ras and the MAP kinase cascade in response to insulin (Skolnik *et al.*, 1993; Sasaoka *et al.*, 1994a). IRS-1 and SHC appear to compete for a limited pool of GRB2 and the extent of GRB2 associated with SHC correlates with downstream mitogenic signaling (Yamauchi *et al.*, 1994b). Thus, SHC appears to be involved in mitogenic signaling from the activated IR while IRS-1 may function in the metabolic pathway through PI3'-kinase activity.

Ras

The *ras* genes encode a family of related G proteins, 21 kDa guanosine triphosphatases (GTPase), localized to the inner face of the plasma membrane due to a series of C-terminal lipid modifications (Sprang, 1997; Vojtek and Der, 1998). A wide variety of stimuli can induce the activation of Ras including the activation of RTKs such as the EGFR and IR (Lowy and Willumsen, 1993). The biological activity of Ras is determined by the bound nucleotide; Ras-GDP being the inactive form and Ras-GTP, the active form (reviewed by Sprang, 1997). The majority of Ras in quiescent fibroblasts is found in the inactive GDP bound form. When Ras binds GTP, it undergoes a conformational change which is necessary to initiate downstream signals. The ratio of GTP-bound to GDP-bound Ras becomes elevated in growth factor stimulated cells (Satoh *et al.*, 1990). Growth factor stimulation may increase the ratio of GTP to GDP-bound Ras by either activating or recruiting guanine nucleotide exchange factors (GNEF) (see GRB2/SOS), or by inactivating Ras GTPase activating protein (RasGAP).

Activated (GTP-bound) Ras can interact with a number of effectors including AF6/canoe, RIN1 and PI 3'-kinase. It has also been shown to stimulate the MAP kinase cascade: Raf (c-Raf1, A-Raf and B-Raf), MEK (MAP kinase/ERK kinases 1 and 2) and MAP kinase/ERK1/2 (Vojtek and Der, 1998). While Ras activation is most commonly thought of as promoting mitogenic responses, in some cell types it is involved in the induction of differentiated phenotypes. The differentiation of 3T3-L1 fibroblasts to adipocytes is dependent on Ras activation, as is the differentiation of PC12 cells in response to NGF. The final outcome of the activation of Ras is most likely a consequence of the tissue-specific differences in Ras isoform expression (Lowy and Willumsen, 1993) and the type and state of differentiation of the cell.

The intrinsic GTPase activity of Ras limits the lifetime of the active GTP-bound form by the slow hydrolysis of GTP to GDP. *In vitro*, the half-life ($t_{1/2}$) of conversion of GTP to GDP is > 1 hour. However, the $t_{1/2}$ of Ras-GTP in quiescent cells is a few minutes. The GTPase activating protein, RasGAP was the first protein identified to be implicated in the control of Ras activity (Trahey and McCormick, 1987). RasGAP is as a cytoplasmic 120 kDa protein that appears to be ubiquitously expressed. The amino terminus of RasGAP contains two SH2 and one SH3 domain, while the active domain of RasGAP can be localized to the C-terminal portion of the protein (Lowy and Willumsen, 1993). RasGAP binds to the phosphorylated tail of the EGFR via its SH2 domain and becomes tyrosine phosphorylated in response to EGF stimulation (Liu and Pawson, 1991). RasGAP, which binds preferentially to Ras in the GTP bound form (Scheffzek *et al.*, 1997), functions catalytically to accelerate the intrinsic GTPase activity of Ras by up to five orders of magnitude (Gideon *et al.*, 1992). Thus, RasGAP functions as a potent negative regulator of normal Ras activity.

MAP kinase cascade

Ras controls the activation of the mitogen-activated protein kinase (MAP kinase) cascade in response to growth factor stimulation (Vojtek and Der, 1998). The MAP kinase signaling cascade modulates important cellular processes such as transcription and protein synthesis. Raf-1 functions directly downstream of Ras and is the first component of the MAP kinase cascade.

Raf-1

Raf-1 is a 72-74 kDa cytoplasmic protein that is ubiquitously expressed in all adult tissues and displays a considerable degree of evolutionary conservation (Storm *et al.*, 1990). It is comprised of an N-terminal regulatory region and a C-terminal domain that has serine/threonine kinase activity (Avruch *et al.*, 1994). The regulatory region (CR1) contains a zinc finger motif and multiple serine/threonine phosphorylation sites (CR2)

(Chow *et al.*, 1995). Deletion of the N-terminal domain activates the oncogenic potential of Raf-1 suggesting that this domain functions to suppress the catalytic activity of Raf-1 in unstimulated cells.

Raf-1 interacts directly with Ras-GTP both *in vitro* and *in vivo* and is mediated by sequences in the CR1 domain of Raf-1 and the effector region of Ras (Chuang *et al.*, 1994). Studies targeting Raf-1 to the plasma membrane stimulated MAP kinase activity 20-fold in the absence of Ras activation (Stokoe *et al.*, 1994). This indicates that the role of Ras activation may be to recruit Raf-1 to the cell surface. However, several lines of evidence reveal that Raf-1 requires more than recruitment to the plasma membrane to become fully activated. Indeed, Raf-1 constitutively localized to the PM can be further activated by treatment with EGF. Evidence further indicates that once Raf-1 is activated the interaction with Ras is no longer required (Stokoe *et al.*, 1994).

The precise mechanism of Raf-1 activation at the plasma membrane remains unclear but the protein 14-3-3 has been suggested to play a key role (reviewed by Burbelo and Hall, 1995). Following receptor or non-receptor tyrosine kinase activation, Raf-1 is phosphorylated on serine and tyrosine residues. The highly phosphorylated Raf-1 has increased protein serine/threonine kinase activity. The kinase(s) responsible for Raf-1 serine phosphorylation are unclear, although kinases downstream in the MAP kinase cascade have been shown to phosphorylate Raf-1 (Anderson *et al.*, 1991). While PKC is able to phosphorylate Raf-1 *in vitro*, it does not appear to be involved in Raf-1 phosphorylation in response to EGF. The activation of Raf-1 is dependent on the phosphorylation of specific sites.

MEK

Raf-1 induces the activation of MAP kinase $p44^{MAPK}$ and $p42^{MAPK}$ (see below) but not Jun N-terminal kinase (JNK) or p38. This is carried out via MEK which is a direct downstream Raf-1 substrate (Macdonald *et al.*, 1993). MEK is part of an evolutionary conserved family of protein serine/threonine kinases which are activated by serine/threonine phosphorylation by Raf-1 (Seger and Krebs, 1995). Although several other kinases can function as MEK activators, for example MEKK, the Raf family members play an important role in response to growth factor stimulation. Activated MEK is highly specific for downstream components of the MAPK cascade, $p44^{MAPK}$ and $p42^{MAPK}$ (Seger and Krebs, 1995). MEK is capable of phosphorylating the regulatory threonine and tyrosine residues of the MAP kinases. Therefore, it belongs to the family of dual specificity protein kinases (Seger and Krebs, 1995).

MAP kinase

Three forms of MAP kinase (also known as extracellular signal-regulated kinases or ERKs) have been identified, $p44^{MAPK}$ (ERK1) and $p42^{MAPK}$ (ERK2), and an alternative

spliced form $p40^{MAPK}$ (Seger and Krebs, 1995). The MAP kinases are proline-directed serine/threonine kinases, which are activated as a result of the phosphorylation of threonine and tyrosine residues in a TXY motif. This is carried out by MEK1 and MEK family members (Cobb *et al.*, 1991). Activated MAPK have been shown to phosphorylate substrates upstream in the kinase cascade for example, MEK, Raf-1 as well as the EGFR at position T^{669} in the juxtamembrane domain (Northwood *et al.*, 1991). This may be a mechanism of negative feedback regulation, designed to limit the activation time of the MAP kinase pathway. Following activation, MAP kinase phosphorylates cytoplasmic targets such as Rsk (Sturgill *et al.*, 1988) and Mnk (Wang *et al.*, 1998) and is able to translocate to the nucleus where it phosphorylates and activates key transcription factors such as Myc (Seth *et al.*, 1991) and $p62^{TCF}$/Elk-1 (Gille *et al.*, 1992).

Nuclear transcription

Quiescent cells respond to extracellular signals such as EGF and insulin by the transcriptional induction of early response genes including c-myc, c-fos and c-jun (Greenberg and Ziff, 1984; Quantin and Breathnack, 1988). Induction of expression of these genes is rapid (within 30 min) and independent of new protein synthesis, indicating a direct consequence of post-translational modifications of pre-existing transcription factors. Resting cells express low levels of transcription factors, such as Jun, Fos, Myc and $p62^{TCF}$/Elk-1, which are maintained in inactive states (Boyle *et al.*, 1991). When activated, these factors regulate the transcription of various cellular genes, thereby playing a role in cell growth, differentiation, and development.

Rapid and transient induction of c-fos and c-jun gene transcription is observed in rat hepatic cells in response to insulin (Gurney *et al.*, 1992), as well as in regenerating liver, 10-60 min after partial hepatectomy (Mohn *et al.*, 1990). The c-fos gene has several regulatory sequences in its promoter region, including the serum response element (SRE), the sis-inducible element (SIE) and the AP-1 binding site. The SRE is a component of the c-fos promoter that contributes to mitogen-induced c-fos gene expression (Treisman, 1995). The factors that bind this element to form a ternary complex include the serum response factor $p67^{SRF}$ and the ternary complex factor, $p62^{TCF}$/Elk-1. Mitogen stimulated transcription of c-fos can be accounted for, in part, by the phosphorylation and activation of $p62^{TCF}$/Elk-1 by MAP kinase (Gille *et al.*, 1992).

Regulation of transcription of the proto-oncogene c-myc plays a role in cellular proliferation (Marcu *et al.*, 1992). The increased transcription of the c-myc gene has been demonstrated in response to factors such as EGF and insulin, as well as after partial hepatectomy. However, the observation that transfection of c-myc into primary hepatocytes did not initiate DNA synthesis (Skouteris and Kaser, 1992) suggests that other

components are required. In addition, several c-myc transgenic mouse strains expressing high levels of Myc do not form malignant hepatic carcinomas (Sandgren *et al.*, 1989). Normal rat liver epithelial cells transfected with a c-myc gene were not transformed, but c-myc in combination with the Raf-1 gene was efficient in causing liver cell transformation (Garfield *et al.*, 1988). Thus Myc may function in association with other components acting downstream of the Ras pathway to cause hepatic cell proliferation.

The c-myc proto-oncogene product is a nuclear protein that functions as a transcription factor (Marcu *et al.*, 1992). It binds as a heterodimer with Max, to the DNA sequences CACGTG. The major phosphorylation site on Myc *in vivo* (S^{62}), a site of phosphorylation by MAP kinase *in vitro* is associated with enhanced transcription factor activity. The ODC gene is a transcriptional target of Myc and is capable of negatively regulating its transcription, adding another level to transcriptional control to the actions of Myc (Marcu *et al.*, 1992).

The activation of the Ras pathway results in changes in gene transcription which prepares hepatocytes for proliferation, i.e., a decrease in albumin gene expression and an increase in ODC levels (Nakamura *et al.*, 1983). In addition, EGF stimulation of primary hepatocytes and partial hepatectomy results in the induction of Ras mRNA transcription (Kost and Michalopoulos, 1990).

IRS signal pathway

Upon insulin administration, the most prominent tyrosine phosphorylated protein, in adipose tissue, muscle and liver, is the insulin receptor substrate, IRS-1. IRS-1 is a minor cytoplasmic protein which was purified and cloned from rat liver and found to be highly conserved and expressed in most cell types and tissues (Sun *et al.*, 1991). Four related proteins have recently expanded this family, including IRS-2, IRS-3, Gab-1 and $p62^{dok}$ (reviewed by White, 1998). Although these docking proteins are not related by extensive amino acid sequences identities, they are all IR substrates and contain common hallmark structures including an NH2-terminal PH domain and/or PTB domain that mediates protein-lipid or protein-protein interactions; multiple COOH-terminal tyrosine residues that act as SH2 domain binding sites; proline-rich regions that are SH3 domain binding sites and serine/threonine-rich regions which may regulate overall function through protein-protein interactions (White, 1998).

IRS-1 protein levels appear to be differentially regulated in target tissues such as muscle and liver (Saad *et al.*, 1992). Gene knock out experiments have concluded that there exists both IRS-1 dependent and IRS-1 independent signal transduction pathways originating from the IR. In the livers of $IRS\text{-}1^{-/-}$ animals, the presence of a tyrosine phosphorylated protein was observed in anti-PI 3'-kinase immunoprecipitates after insulin

stimulation. This protein was found to be related to IRS-1 and so termed IRS-2 (Araki *et al.*, 1994). Most tissues appear to express both IRS-1 and IRS-2, but the ratio of these two proteins differs depending on the cell type, which may be involved in the fine tuning of signaling from the IR.

The predicted open reading frame in the cDNA of IRS-1 encodes a 131 kDa protein, however IRS-1 migrates between 165-170 kDa in resting cells and 175-185 kDa in stimulated cells (White and Kahn, 1994), probably due to secondary structure and the increase in ligand-induced tyrosine phosphorylation, respectively. Although there is no transmembrane spanning region, based on primary sequence analysis, the N-terminus (residues 13-115) of IRS-1 contains a conserved PH domain. This domain is also called the IRS homology domain 1 (IH1) (White, 1998). The IRS-1 PH domain is 62% identical to the PH domain of IRS-2, a difference which may serve to target the IRS isoforms to different subcellular locations. Evidence indicates that the PH domain of IRS-1 is not required for the engagement of downstream signals but rather is one of the elements that mediates the efficient coupling with the IR. Indeed, insulin stimulated IRS-1 phosphorylation is greatly reduced if the PH domain is deleted (Myers *et al.*, 1995).

IRS-1 contains a region immediately downstream from the PH domain which has also been implicated in the interaction between the IR and IRS-1. This region, called IH2, resembles a PTB domain and binds the NPXpY^{972} motif found in the juxtamembrane region of the activated IR (White, 1998). The phosphorylation of IRS-1 requires the phosphorylation of this tyrosine residue as receptors which contain substitutions or deletions of the NPXY^{972} motif are unable to mediate the phosphorylation of IRS-1, the activation of PI 3'-kinase or glucose transporter translocation in transfected CHO cells. A small proportion of IRS-1 was observed associated with activated IR in CHO cells transfected with both IRs and IRS-1, and a direct interaction between the N-terminus of IRS-1 and phosphorylated Y^{972} has been demonstrated using the yeast two hybrid system (O'Neill *et al.*, 1994). In these cells, IRS-1 is expected to bind to the catalytic domain of the receptor, forming an enzyme/substrate complex, but this is expected to be transient and unstable and the dissociation of the phosphorylated IRS-1 may be favored. Tyrosine phosphorylation of NPXpY^{972} may be important for substrate selection since receptors which lack this motif do not phosphorylate IRS-1. Thus the high efficiency and specificity of interaction between the IR and IRS-1 requires both membrane localization of IRS-1 and IRS-1 recognition sites on the receptor.

IRS-1 does not possess catalytic activity but instead acts as an adaptor protein. IRS-1 contains at least 21 potential tyrosine phosphorylation sites, some of which are phosphorylated in response to insulin stimulation. Nine of these are located in YMXM

motifs, which interact with the SH2 domains of various signal transduction molecules such as PI3'-kinase, GRB2, and the tyrosine phosphatase, SHP-2 (Pawson and Scott, 1997). In this way, IRS-1 may act to bring proteins in proximity to the IR which can then phosphorylate and activate them or to cause, through induction of conformational changes, the activation of these proteins.

IRS-1 and mitogenic signaling

Although IRS-1 overexpression has been reported in hepatocellular carcinoma and its expression is important during liver regeneration (Ito *et al.*, 1996), most of the studies addressing the potential role of IRS-1 in mitogenic responses to insulin have been carried out in cell lines overexpressing the IR. Microinjection of anti-IRS-1 antibodies inhibited insulin and IGF-1 stimulated DNA synthesis and cell growth in HIRcB fibroblasts. This implicated IRS-1 in the mediation of mitogenic signaling from the IR (Myers *et al.*, 1994) and was postulated to occur as a result of the association of IRS-1 with GRB2 linking SOS and the Ras pathway to IRS-1. However, insulin stimulated association of SOS or SOS activity with IRS-1 could not be detected in fibroblasts expressing high numbers of IRs (Pronk *et al.*, 1994; Sasaoka *et al.*, 1994a), which indicated that the association of SOS with IRS-1 does not contribute significantly to the activation of the MAP kinase pathway in response to insulin. Alternatively, IRS-1 may associate with 14-3-3 directly and affect Raf-1 signaling independent of Ras activation (Craparo *et al.*, 1997)

The level of expression of IRS-1 was shown to activate or inhibit insulin signaling depending upon the cell context. In CHO cells expressing high levels of IRs, increased expression of IRS-1 resulted in the attenuation of insulin stimulated DNA synthesis and c-fos gene transcription (Yamauchi *et al.*, 1994b). Thus the role of IRS-1 in insulin induced mitogenic signaling remains unclear, although the specific concentrations of both the IR and IRS-1 as well as the cell type appear to be involved in determining downstream signaling (Yamauchi *et al.*, 1994a).

Serine/threonine IRS-1 phosphorylation

IRS-1 becomes phosphorylated on additional serine and threonine residues after insulin stimulation (Tanti *et al.*, 1994). There are over thirty potential serine/threonine phosphorylation sites on IRS-1. Several kinases, including MAP kinase, casein kinase II (CKII) (Tanasijevic *et al.*, 1993) and PI3'-kinase (Lam *et al.*, 1994), have been proposed to phosphorylate serine and/or threonine residues in IRS-1 in an insulin dependent manner. The phosphorylation of these residues may be involved in the regulation of signal transduction. Indeed, it has been shown that the serine/threonine phosphorylation of IRS-1 by okadaic acid caused a decrease in the ability of the IR to phosphorylate IRS-1 and a reduction in the ability of proteins such as PI 3'-kinase to dock to IRS-1 (Tanti *et al.*,

1994). This may also be the result when MAP kinase phosphorylates IRS-1 on residues located near those which are known to recruit the SH2 domains of PI 3'-kinase. Thus, the regulation of signal transduction by serine/threonine phosphorylation of IRS-1 may be twofold; as interference for the binding of downstream effectors to IRS-1 and/or as a negative feedback mechanism which ensures a limited duration of signal transduction. The precise nature of the regulation would be dependent on the subset of kinases which are activated by insulin treatment in a given cell type.

PI 3'-kinase

PI3'-kinase is a heterodimeric enzyme composed of a p85 regulatory subunit, containing one SH3 and two SH2 domains, and a p110 subunit which is a dual specificity kinase with both lipid and serine kinase activity (Lam *et al.*, 1994; Stevens, 1995). Insulin injection in mice results in the ~6-fold increase in IRS-1 associated PI 3'-kinase activity in the liver (Araki *et al.*, 1994). The p85 subunit does not appear to be phosphorylated in response to insulin stimulation in many cultured cells (Backer *et al.*, 1992). The two SH2 domains of the p85 subunit bind strongly to phosphorylated Y^{939} and Y^{608} (both in YMXM motifs) of IRS-1, in response to insulin stimulation (Myers *et al.*, 1994). Upon binding to phosphotyrosine containing peptides, the p85 subunit of PI 3'-kinase undergoes a conformational change and activates the p110 subunit (White, 1998). The association with IRS-1, which accounts for as much as 70% of total cellular PI 3'-kinase in stimulated cells (Backer *et al.*, 1992) may serve to recruit PI 3'-kinase to the plasma membrane and may be important for the interaction with lipid substrates. The role of 3'-phosphorylated phosphoinositols generated by PI 3'-kinase activation remains to be shown although several lines of evidence indicate a role for PI 3'-kinase in the regulation of intracellular traffic of proteins (Stephens, 1995; Shepherd *et al.*, 1996).

In CHO-IR cells, PI 3'-kinase has been proposed to function upstream of Ras and Raf-1 in mediating the insulin signal transduction pathway leading to the transcriptional activation of the c-fos SRE (Yamauchi *et al.*, 1993). It is not clear how this interaction results in the activation of Ras, but indicates an alternative to GRB2/SOS interactions with Ras as a mechanism for Ras activation. Rodriguez-Viciana and colleagues (1994) propose that Ras can regulate PI3'-kinase activity. The p110 subunit of PI3'-kinase was shown to co-immunoprecipitate with Ras. This interaction appears to involve the effector region of Ras and is highest when Ras is GTP-bound.

While the exact role of PI 3'-kinase in insulin signaling remains unclear, the importance of PI 3'-kinase in insulin action has been demonstrated. Wortmannin, a specific inhibitor of PI 3'-kinase (both lipid and serine kinase activities) blocks the antilipolytic action of insulin on adipocytes (Okada *et al.*, 1994), the insulin induced

glucose uptake (via GLUT4 transport; Kotani *et al.*, 1995) and glycogen synthesis, insulin induced inhibition of glycogen synthase kinase-3 (GSK-3) activity (Shepherd *et al.*, 1995), as well as insulin-induced inhibition of PEPCK gene expression (Sutherland *et al.*, 1995).

Glycogen synthase

Glycogen synthase (GS) activation is a key step in glycogen deposition in liver, skeletal muscle, and adipose tissue. GS activity is regulated by the phosphorylation state of specific serine residues. Activation occurs by dephosphorylation by type-1 protein phosphatase (PP1) (Cohen, 1989) and inactivation is carried out by phosphorylation on multiple serine residues by several protein kinases (Roach, 1986). Although insulin activates GS and stimulates glycogen synthesis in all three target tissues, the underlying molecular mechanism is unclear.

The MAP kinase pathway is unlikely to be involved in the activation of GS by insulin since the MEK inhibitor, PD98059 (Dudley *et al.*, 1995), does not prevent GS activation by insulin and EGF activates ERK but not GS (Peak *et al.*, 1998). Another member of the MAP kinase family, the JNK, has been implicated in the activation of PP1 and GS by insulin in skeletal muscle (Moxham *et al.*, 1996). Studies in many cell types have indicated that PI 3'-kinase is involved in the GS activation by insulin because this process was shown to be abrogated by wortmannin (Hurel *et al.*, 1996). However, PI 3'-kinase seems not to be sufficient for the activation of GS at least in 3T3 L1 adipocytes where it was shown that PI 3'-kinase overexpression increases PI3'-kinase activity above that induced by insulin stimulation but did not enhance basal and insulin stimulated GS activity (Frevert and Kahn, 1997). Finally studies on the involvement of $p70^{S6}$ kinase in GS activation by insulin on the basis of the sensitivity of this process to the inhibitor rapamycin have given different results depending on the tissue or the experimental conditions used (Azpiazu *et al.*, 1996).

In the L6 skeletal muscle cell line, the wortmannin-sensitive pathway resulting in the activation of GS has recently been more clearly delineated. Protein kinase B (PKB, Akt or RAC) phosphorylates and inactivates GSK-3 (Cross *et al.*, 1995), and both inactivation of PKB (Alessi *et al.*, 1996) and inactivation of GSK-3 (Klippel *et al.*, 1997) are wortmanin-sensitive and stimulated by insulin. Activation of PKB is stimulated by the lipid products of PI 3'-kinase (Klippel *et al.*, 1997, Franke *et al.*, 1997). In liver, phosphorylation and inactivation of GS by GSK-3 has been demonstrated (Randhawa *et al.*, 1990), but whether this kinase is involved in the control of GS by insulin is not known. Recently, activation of PKB and inactivation of GSK-3 by insulin have been demonstrated in primary cultures of rat hepatocytes (Peak *et al.*, 1998). However, in this study, the low magnitude (30%) of GSK-3 inactivation cannot account for the marked (2-4

times) stimulation of GS by insulin (Peak *et al.*, 1998). In addition, inactivation of GSK-3 was also induced by EGF which did not activate GS (Peak *et al.*, 1998). Hence the relative contribution of GSK-3 inactivation in the activation of GS by insulin remains unclear in liver cells.

Activation of PP1 by insulin has been demonstrated in skeletal muscle (Dent *et al.*, 1990), rat adipocytes (Begum, 1995), and in differentiated 3T3-L1 adipocytes (Brady *et al.*, 1997). In skeletal muscle, this activation is achieved by $p90^{rsk2}$ kinase which phosphorylates the glycogen targeting subunit of PP1 (Gm or Rgl) at a specific serine residue (Dent *et al.*, 1990). In liver, targeting of PP1 to glycogen particles by the Gl subunit confers to the enzyme specific properties: a high ratio of synthase phosphatase over phosphorylase phosphatase activities (Bollen *et al.*, 1988). Activation of hepatic GS by insulin can be mediated by the activation of the glycogen synthase phosphatase following the inactivation of phosphorylase by the hormone (Stalmans *et al.*, 1987). Hepatic glycogen synthase phosphatase and phosphorylase phosphatase activities were shown to increase by 35% by in vivo insulin treatment (Toth *et al.*, 1988). Glucagon induced depressed synthase phosphatase activity was restored by insulin in perfused rat liver (Miller *et al.*, 1981) but no change in synthase phosphatase activity was observed in acutely insulin stimulated cultured hepatocytes despite enhanced glycogen synthase activity (Miller *et al.*, 1986).

PKC

The protein kinase C (PKC) family represents a family of structurally and functionally related serine/threonine kinases derived from multiple genes as well as from alternative splicing of single mRNA transcripts (reviewed by Mellor and Parker, 1998). The individual isoforms differ in their regulatory domains and in their dependence on Ca^{+2}, as well as in their tissue distribution and intracellular localization (Newton, 1997, Goodnight *et al.*, 1995).

PKCs appear to play a dual role in the insulin signaling network. First, PKCs control insulin-dependent receptor kinase activation and may regulate IRS-1 signaling as well (Coghlan *et al.*, 1994). Second, at least in certain cells and tissues, insulin activation of PKCs is required to evoke insulin effects on glucose transport and its intracellular metabolism (Schubert *et al.*, 1996). Although involvement of PKC in insulin action remains unclear (Frevert and Kahn, 1996), overexpression of PKC α and β has been reported to impair insulin stimulated glycogen synthase activity and therefore may be involved in the regulation of this pathway (Bandyopadhyay *et al.*, 1997). Furthermore, recent studies have implicated the interaction of specific PKC isoforms with the IR and altered receptor intracellular routing (Formisano *et al.*, 1998).

III. Endocytosis and RTK traffic

The model of ligand mediated receptor endocytosis is based on observations of Anderson, Brown and Goldstein and colleagues on low-density lipoprotein (LDL) internalization (reviewed by Bergeron *et al.*, 1985). It was followed by the discovery of the near exclusive location of LDL receptors (LDLRs) in coated pits and entry of LDL into the secondary lysosome via membrane-bound structures. The general application of the LDL pathway to the endocytosis of insulin, EGF and other peptide hormones has elucidated differences in the handling of ligands by target cells. These differences are found on the cell surface as well as in the intracellular compartments accumulating and concentrating ligands and receptors prior to intracellular processing and sorting (Baass *et al.*, 1995; Bevan *et al.*, 1996).

Cell surface events

Ligands bind their corresponding receptors on the cell membrane and the subsequent internalization of receptor-ligand complexes involves specialized membrane indentations. These indentations fall into a number of cellular structures including clathrin-coated pits and caveolae, although clathrin-mediated endocytosis is believed to be the most common route of ligand entry in rat liver (see below).

Coated pits/vesicles and endocytosis

Clathrin-coated pits are cell surface microdomains where randomly moving membrane proteins are segregated from resident plasma membrane proteins, and are internalized into the cell. Ligands and membrane proteins are selectively taken up while other proteins of the plasma membrane are prevented from being internalized. Coated pits are relatively uniform in size (~100-150 nm in diameter) and were first observed by Roth and Porter (1964) as bristle coated invaginations of the plasma membrane. Soon thereafter the major protein component of the coat was identified as clathrin (Pearse, 1976). The purification of coated vesicles has allowed the major structural units of the coat, clathrin triskelion and adaptors, to be identified. The characteristic ultrastructural hexagon and pentagon lattice of coats is made up of clathrin while the inner shell of the coat consists of adaptor proteins that interact with the cytoplasmic domains of the receptors in the membrane of the pit/vesicle (Schmid, 1997).

Clathrin triskelions pack together to form polyhedral lattices (Schmid, 1997). Each triskelion is a three-legged structure consisting of three heavy chains and three tightly associated light chains. The latter have been suggested not to be required for cage assembly in *in vitro* studies where intact, proteolytically-truncated, or light-chain depleted triskelions were found to spontaneously self-assemble into structures similar to the coat on

a coated vesicle (Luzio and Stanley, 1983). Light chains have been suggested to participate in regulating clathrin assembly and disassembly *in vivo* (Brodsky *et al.*, 1991).

The adaptor proteins (AP) are the three major type of coat proteins. Two structurally related classes of APs are present in most cell types: AP2 is the plasma membrane coated pit adaptor and AP1 is the Golgi-associated coated pit adaptor (reviewed by Schmid, 1997). Sequence data has shown that particular subunits of these heterotetrameric molecules are closely related to each other (Pearse and Robinson, 1990). A third adaptor protein, AP3, is Golgi and endosome-associated and is implicated in the formation of synaptic vesicles from endosomes (Faundez *et al.*, 1998).

A working model for their role in coated pit assembly, budding and receptor sorting has emerged from the large amount of information about their biochemical and functional properties *in vitro* (Schmid, 1997). APs are thought to initiate coated pit assembly on the membrane, to regulate coated pit growth and to mediate receptor-sorting into coated pits by binding directly or indirectly to the cytoplasmic tails of receptor molecules (Pearse, 1990). The EGFR has been shown to interact with adaptors, by co-immunoprecipitation of PM adaptors and EGFR in EGF treated cells (Sorkin and Carpenter, 1993; Nesterov *et al.*, 1995a; Boll *et al.*, 1995).

The process of coated pit formation involves the recruitment and assembly of clathrin and associated proteins and other factors at the plasma membrane to form a pit, which subsequently invaginates, buds and produces a coated vesicle (Schmid, 1997). The number of coated pits and vesicles at the PM as well as the dynamics of their formation have been estimated by several investigators. Biochemical analyses of receptor internalization kinetics demonstrate that following ligand stimulation, receptors (EGFR and IR) known to use the coated pit pathway, are rapidly lost from the PM ($t_{1/2}$ ~1 min) (Di Guglielmo *et al.*, 1994; Burgess *et al.*, 1992).

Although clathrin self-assembly and rebinding to members is spontaneous *in vitro*, coated vesicle budding and endocytosis is severely inhibited in ATP-depleted cells (Schmid and Carter, 1990). This process is also inhibited in *D. melanogaster* bearing the *shibire* mutation (Kosaka and Ikeda, 1983), or in cells overexpressing mutant dynamin (van der Bliek *et al.*, 1993). This indicates that energy and dynamin, a microtubule-associated GTPase, are necessary to drive efficient endocytosis (van der Bliek *et al.*, 1993). Indeed, studies preventing GRB2 and dynamin association with the EGFR inhibited internalization (Wang and Moran, 1996). The interference with clathrin structure formation by using mutant dynamin was shown to have the same effect on the internalization of the EGFR (Vieira *et al.*, 1996). Finally dynamin mutants prevented the internalization of the IR (Ceresa *et al.*, 1998). Furthermore the small Ras-like GTPase, Rab5 has been reported to

be involved in endocytosis at the PM level. It is associated with the PM, clathrin-coated vesicles and early endosomes (Chavrier *et al.*, 1990).

Recently, AP2 has been shown to be constitutively associated with Eps15 (Benmerah *et al.*, 1998), a highly conserved protein organized in three distinct structural domains. Its NH2-terminal domain is composed of three imperfect repeats of 70 amino acids homologous to each other and to domains found in proteins in mammals, yeast, and nematodes. These domains, called EH for Eps15 Homology (Wong *et al.*, 1995), were recently shown to mediate interaction with other proteins (Salcini *et al.*, 1997). Moreover, two yeast proteins containing EH domains, End3p and Pan1p, have been implicated in endocytosis (Wendland *et al.*, 1996). The COOH-terminal domain is characterized by the presence of repeats of a DPF sequence and contains the AP2-binding site (Iannolo *et al.*, 1997). The observation that Eps15 is associated with AP2 and is homologous to yeast proteins involved in endocytosis strongly implicates Eps15 in coated pit-mediated endocytosis.

Endocytic signals

At least two types of internalization signals have been described: the tyrosine based motif and the dileucine based motif. The most thoroughly examined of these is the former motif, which consists of a sequence of 4-6 amino acids, specifically containing a tyrosine that is crucial for proper endocytic targeting (reviewed by Trowbridge *et al.*, 1993). Alteration of specific tyrosine residues within the cytoplasmic domains of many constitutively internalizing receptors and other membrane glycoproteins was also found to severely impair their endocytosis. These tyrosines, which usually resides in a YXXØ or NPXY motif (where X is any amino acid and Ø is a hydrophobic residue), has been shown capable of forming a tight turn in secondary structure (Trowbridge *et al.*, 1993).

Receptors that lack tyrosine signals but participate in receptor-mediated endocytosis have revealed other possible endocytic signals. CD4, human FcII B2 receptor (Trowbridge *et al.*, 1993), the GLUT4 glucose transporter (Corvera *et al.*, 1994) and the IR (Haft *et al.*, 1998) contain dileucine sequence motifs in their cytoplasmic domains that are believed to influence internalization.

Ligand-dependent internalization of receptors such as EGFR, PDGFR and IR has been postulated to occur by induction of a structural change in the cytoplasmic domain of receptors. This is followed by ligand binding and autophosphorylation of tyrosine residues that would allow receptors to expose a recognition determinant for coated pits similar to the internalization signals of constitutively internalizing receptors. Mutational analyses of the EGFR (Chang *et al.*, 1993) have revealed putative internalization domains within the carboxyl terminus of these receptors that share no sequence similarity (β-turn) and

juxtamembrane localization with internalization domains of other receptors. Moreover, the EGFR and IR cytoplasmic domains both contain multiple copies of the LDLR related NPXY sequence patterns as well as dileucine motifs. However the three NPXY sequences in the EGFR do not appear necessary for ligand internalization since the deletion of the C-terminal region of the EGFR cytoplasmic tail containing them does not inhibit the process (Prywes *et al.*, 1986). However, deletion of the membrane-proximal region of the IR cytoplasmic domain containing NPXY impairs internalization (Thies *et al.*, 1989).

Caveolae and non-clathrin-mediated endocytosis

Endocytosis of membrane and fluid also occurs through a pathway that is independent of clathrin. Internalization still continues after endocytosis from clathrin-coated pits is inhibited under conditions of incubation in hypertonic medium (Daukas and Zigmond, 1985), potassium depletion (Larkin *et al.*, 1983), or acidification of the cytosol (Sandvig *et al.*, 1987). Clathrin-independent endocytosis has been demonstrated in unperturbed cells and may contribute up to half of the total membrane and fluid-phase uptake of the cell. The coated pit and clathrin-independent pathway of EGFR endocytosis can be distinguished by their kinetic characteristics with rapid internalization occurring via the coated pit pathway (especially at low cell surface receptor occupancy) and constitutive internalization occurring via a clathrin-independent pathway in macropinocytosis. Clathrin-independent internalization may be responsible for the uptake of molecules that do not use coated pits, such as GPI-anchored proteins, or this process may play a role in turnover of membrane proteins.

Although caveolae were described 30 years ago as flask-shaped pits containing a small diameter of 50-80 nm (Palade and Bruns, 1968), clathrin-independent endocytosis mediated by caveolae in rat liver remains unclear. The integral membrane protein of caveolae, caveolin, was found to be most prominently expressed in adipose, lung and muscle tissues and was virtually undetectable in liver and other tissues (Scherer *et al.*, 1994). However, in cultured hepatocytes caveolin is expressed and has been co-localized with dynamin, a major component of the membrane budding mechanism to caveolae (Henley *et al.*, 1998). These differences may be a reflection of the stress cells undergo in cell culturing and may cause them to adopt a non-polarized morphology and express gene products not present in quiescent cells in the organism.

Intracellular events

The endosomal apparatus is positioned both temporally and physically between the plasma membrane (PM) and the lysosome (Figure 3). Based on the time required for an internalized receptor to accumulate in the endocytic apparatus two main compartments have been defined and termed early and late endosomes. Receptor-ligand complexes are

delivered into early endosomes (within 2-5 min) which are located at the cell periphery and consist of weakly acidic tubular elements (pH 6-6.5) (reviewed by Authier *et al.*, 1994b). For many ligand-receptor complexes as in the case of insulin and its receptor, endosomal acidification results in the dissociation of the ligand from its receptor. Ligand degradation may then occur in this compartment (Authier *et al.*, 1994b; Authier *et al.*, 1998). It is early in the endosomal pathway that a mechanism exists which sorts the receptors to be recycled to the PM from those targeted to the lysosome for degradation (Lai *et al.*, 1989a). This mechanism is dependent, at least to some extent, on receptor occupancy levels. Late endosomes which are moderately acidic (pH 5-6), fill more slowly (10-20 min) and consist of tubulovesicular structures of varying sizes located in the Golgi-lysosome area of the cell. Some receptor recycling may occur at this point as well. The precise fate of ligand-receptor complexes within the endosomal apparatus varies with each particular ligand and receptor (Baass *et al.*, 1995).

EGFR endocytosis

Endocytosis of RTKs has been shown to be a readily saturable process. Indeed, overexpression of transmembrane receptor with tyrosine-containing sorting sequences can saturate the endocytic transport machinery (Warren *et al.*, 1997). However, saturation of RTK endocytosis does not affect endocytosis of other receptors within the same cell. These findings indicate that a distinct and saturable RTK-specific component of the endocytic machinery is required for RTK internalization. Further evidence for this idea comes from the finding that recombinant IRs are efficiently internalized when expressed in Rat-1 cells but not when expressed in B82L mouse cells (which are capable to efficiently internalize recombinant EGFR). Moreover, fusion of IR-expressing B82L cells with non-transfected Rat-1 cells restores efficient IR internalization, indicating that Rat-1 cell cytosol can supply a factor that is absent in mouse B82L cell cytosol (reviewed by Schmid, 1997).

Ligand-dependent redistribution of EGFRs into coated pits has been reconstituted *in vitro* using perforated cells (Lamaze *et al.*, 1993). EGFR endocytosis in this assay shows similar biochemical requirements to those of transferrin receptor (TfnR) endocytosis, and both receptors are found together in coated pits and coated vesicles after *in vitro* incubations in the presence of cytosol, ATP and GTP (Lamaze *et al.*, 1993). Furthermore, the requirements for endocytosis of EGFR *in vitro* parallel those for endocytosis *in vivo*. Specifically, ligand-dependent RTK sequestration into coated pits is not observed when mutant EGFR, lacking either an active kinase domain or the C-terminal regulatory domain which contains the internalization motifs, are used (Schmid, 1997).

Although AP2 can form stable complexes with the activated EGFR *in vivo* (Sorkin and Carpenter, 1993), deletion or mutagenesis of the AP2 binding site has little effect on

the rate of EGFR endocytosis *in vivo* (Nesterov *et al.*, 1995b). This finding is consistent with *in vitro* results showing that soluble AP2 complexes are not rate limiting for EGFR endocytosis, whereas they are for endocytosis of the TfnR (Lamaze *et al.*, 1993). Taken together, these data indicate that a cytosolic component other than AP2 is required for the recruitment of activated EGFR into coated pits.

Two candidates for an EGFR recruitment factor have been proposed. The recent finding that Eps15, an EGFR tyrosine kinase substrate, interacts constitutively with AP2 complexes *in vivo* makes a possible candidate for such a recruitment molecule (see below). A second report showing that microinjection of a fushion protein corresponding to the SH2 domain of the GRB2 inhibited endocytosis of the EGFR (Wang and Moran, 1996). This finding, coupled to with the fact that dynamin binds to the SH3 domain of GRB2 supports a role for GRB2 in EGFR internalization.

In liver the EGFR is dispersed on the sinusoidal and lateral surfaces of the plasma membrane (Lai *et al.*, 1989a). Upon ligand binding, the receptor is redistributed to coated pits and rapidly internalized. Chen and colleagues (1989) have suggested that a region (residues 1022-1186) in the C-terminus of the unoccupied EGFR masks the internalization sequences. Upon receptor activation and autophosphorylation of the tyrosine residues in this inhibitory domain, a conformational change results which releases this inhibition, and permits endocytosis. Tyrosine kinase activity is required for ligand induced EGFR internalization (Glenney *et al.*, 1988), and results in an internalization rate 5-fold higher than that of the kinase negative receptor (Chen *et al.*, 1989).

The internalization sequences required for ligand induced endocytosis and down-regulation of the EGFR have been mapped to residues 973-1022. This region, conferring both calcium regulation and receptor endocytosis, was called the CaIn domain (Chen *et al.*, 1989). Further analysis revealed that these two EGF dependent functions were in fact mediated by distinct regions in the CaIn domain. The endocytic motifs of the EGFR (^{996}QQGFF and ^{973}FYRAL) were predicted to form a tight turn, a structure present in IR internalization codes as well (Chang *et al.*, 1993). The three NPXY sequences in the EGFR tail, unlike those in the IR, do not appear to be essential for internalization, since their deletion does not impair this process (Chang *et al.*, 1993).

Although activated EGFR follows the established endocytic pathway, RTK-specific regulators affecting sorting at both early (Sorkin and Carpenter, 1993; Wang and Moran, 1996; Lamaze *et al.*, 1993) and late (Kurten *et al.*, 1996) trafficking steps have been identified. Many of these regulators, for example, Snx-1 (sorting nexin 1) (Kurten *et al.*, 1996) and PI 3'-kinase (Joly *et al.*, 1994) appear to affect sorting of only a subset of RTKs. The specificity found in sequences required for internalization suggests that the

mechanisms of internalization (as well as intracellular trafficking) are controlled by receptor specific endocytosis molecules. The AP2 complex has been implicated in this role for the EGFR.

AP2

EGFR recruitment into coated pits is postulated to occur via an AP2 complex, already localized at the PM, that recognizes and associates with sorting signals on activated EGFRs (Boll *et al.*, 1995). This interaction is postulated to cause an increase in the affinity of AP2 for clathrin and result in the rapid assembly of the clathrin coated pits (Pearse and Robinson, 1990).

The EGFR was found to be capable of recruiting AP2, in an EGF dependent manner, without receptor activation or autophosphorylation. However, this interaction was 6 to 8-fold less than in the wild-type receptor (Sorkin and Carpenter, 1993; Boll *et al.*, 1995). This correlates with the reported ability of inactive EGFR to internalize and/or down regulate in a ligand dependent manner, but at decreased rates compared with wild-type receptors. Although AP2 lacks the SH2 domain needed to interact directly with phosphorylated tyrosine residues, receptor autophosphorylation appears to be required for high levels of AP2 binding (Nesterov *et al.*, 1995a). Phosphorylation may be involved in causing a conformational change in the receptor tail leading to the exposure of AP2 binding motifs. These motifs have been mapped to residues 970-991 in the regulatory C-terminus of the EGFR (Boll *et al.* 1995; Nesterov *et al.*, 1995a), located within a larger region known to be involved in endocytosis of the receptor (see above). The identified AP2 binding domain is not conserved in the IR or TfnR. Deletion of the AP2 binding determinant abolishes complex formation. However, internalization of this mutant receptor is indistinguishable from the wild type receptor (Nesterov *et al.*, 1995b). This indicates that processes other than AP2 binding regulate receptor endocytosis.

There is evidence for a role for AP2 later in the endocytic process. The presence of a significant population of endocytic membranes and vesicles coated with adaptors but devoid of clathrin, has been demonstrated by double immunofluorescence microscopy and biochemical analyses (Chakrabarti *et al.*, 1993). A specific role for AP2 in the fusion of early endosomes has been proposed (Beck *et al.* 1992). In addition, microinjection of anti-AP2 antibodies limits the accumulation of internalized ligand to late perinuclear compartments (Chin *et al.*, 1989). Since perinuclear localization is the result of a sequential transport of internalized receptors through multiple compartments (early to late endosomes) this observation implies a possible role for AP2 at a number of steps in the endocytic pathway.

Dynamin

Dynamin is a 100 kDa GTPase that plays an essential role in coated vesicle formation and localizes to the plasma membrane around the neck of emerging coated pits (reviewed by Damke, 1996). Wang and colleagues (1996) have demonstrated that GRB2 associates with dynamin and the EGFR and is therefore implicated in the internalization of this RTK. In these studies internalization of the TfnR was not affected by the microinjection of inhibitory GRB2 peptides. This implies that internalization via GRB2 and dynamin may be specific for RTKs that recruit GRB2 upon ligand activation. Ligand-induced EGFR endocytosis is potently inhibited in cells overexpressing a dynamin mutant (K44A mutant) as compared to cells overexpressing the wild type dynamin (Vieira *et al.*, 1996). In these studies EGFR signal transduction was also largely modified. Recently, Ringerike and colleagues (1998) have reported that the overexpression of the K44A dynamin mutant disrupts high-affinity binding of EGF with its receptor. Further work involving dynamin and RTK internalization is therefore necessity to clarify this discrepancy.

Eps15

Eps15 is an EGFR substrate (Fazioli *et al.*, 1993) that is characterized by the presence of a protein-protein interaction domain, the EH domain, and the ability to bind to AP2 (see above). Microinjection of antibodies against Eps15 inhibits internalization of EGF and Tfn indicating the involvement of these proteins in receptor endocytosis (Carbone *et al.*, 1997). Studies by Benmerah and colleagues (1998) have shown that the interaction of Eps15 and AP2 is essential for ligand mediated receptor endocytosis. In perforated A431 cells, GST-COOH terminus of Eps15-(the AP2 binding domain)-fusion proteins inhibited EGFR internalization. This family of proteins, targeted to endosomes, may be key to understanding the role of the EGFR substrate Eps15 (Fazioli *et al.* , 1993). This protein accompanies the adaptor protein complex AP2 to the endosome after receptor activation. The functional significance of Eps15 is linked to the clathrin internalization machinery. Recently, a protein related to FYVE protein Hrs (also an EGFR substrate) and the yeast vacuolar targeting protein Vps27p has been identified and termed EAST (EGFR Associated protein with SH3 and TAM domains) (Lohi *et al.*, 1998). EAST has been identified as an EGFR substrate for tyrosine phosphorylation *in vivo* and is proposed to serve as a scaffold that links the EGFR, Eps15 and Eps15-associated proteins with the internalization machinery (Lohi *et al.*, 1998).

FYVE proteins

These proteins originally observed by Stenmark *et al.* (1996) possess common motifs, some of which are putative zinc fingers. These motifs target proteins to

endosomes. The FYVE proteins are named for their first four proteins shown to contain the motif (Fab1, YOTB/zk632.12, Vac1 and EEAI) (Patki *et al.*, 1997). The family has now expanded to several other proteins including the HGFR and EGFR substrate Hrs which has been clearly localized to endosomes (Komada *et al.*, 1997) as is the PI 3'-kinase effector EEAI also found via the same motifs to be targeted to endosomes.

Snx-1

The internalization codes mentioned above are thought to be involved in the early steps of EGFR internalization. The targeting and sorting of the EGFR to the lysosome relies on the vesicular trafficking machinery, such as the protein Snx-1, but does not require RTK activity (Kurten *et al.*, 1996).

Internalized EGF/EGFR

Internalized receptors are sorted in the endosomal apparatus where they either recycle to the plasma membrane or are targeted to the lysosome for degradation. These processes have implications on the magnitude and duration of signaling. EGF does not dissociate from its receptor in the endosomal compartment, but it does undergo partial proteolysis as it traffics from early endosomes to the lysosome (Renfrew and Hubbard, 1991a,b). It is generally believed that the vast majority of EGFR undergoes degradation in the lysosomal compartment (Renfrew and Hubbard, 1991b). However, Lai and colleagues (1989a) demonstrated that EGFR down regulation (degradation) in rat liver fractions, occurred only when > 50% of the receptors were occupied. At lower receptor occupancy levels, the receptor was internalized and was subsequently recycled to the PM. These observations imply that intracellular traffic is a function of intracellular ligand association with their receptors. This hypothesis is supported by the studies on TGFα induced EGFR internalization (Ebner and Derynck, 1991).

Although both EGF and TGFα follow similar kinetics of internalization, TGFα dissociates from the EGFR at a higher pH (half-maximal dissociation at pH 6.9) (Ebner and Derynk, 1991). This indicates that during endocytosis and the acidification of the endosome, TGFα dissociates from the EGFR in an early endosome, while EGF dissociates only in the lysosome or a prelysosomal compartment.. At physiological concentrations, more TGFα than EGF recycles back to the PM, and fewer EGFRs are degraded, resulting in a shorter lag before restimulation can take place (Ebner and Derynk, 1991; Waterman *et al.*, 1998).

Evidence indicates that endosomal sorting is controlled by tyrosine kinase activity (Honegger *et al.*, 1987; Felder *et al.*, 1990). French and colleagues (1994) have concluded that kinase activity was not crucial for lysosomal targeting although it enhanced downregulation, possibly by stabilizing interactions with the endocytic apparatus (see AP2;

Herbst *et al.*, 1994). A model was proposed for postendocytic sorting, where lysosomal targeting of the EGFR is mediated by specific and saturable components that interact with the cytoplasmic tail of the occupied receptor (French *et al.*, 1994). Indeed residues 1022-1123 in the C-terminus of the EGFR have been shown to play a role in receptor targeting to the lysosome (Kornilova *et al.*, 1996).

IR endocytosis

In the rat liver hepatocyte, IRs in their unbound state are preferentially associated with surface microvilli, and excluded from coated pits (Bergeron *et al.*, 1979). Studies by Carpentier and McClain (1995) reveal that the C-terminus of the IR functions to anchor the unoccupied receptors to the microvillar membrane. Insulin binding to the receptor results in the activation of the RTK which initiates internalization by releasing this constraint. How this occurs is unclear but may to be controlled by the dileucine motif (Haft *et al.*, 1998). In H35 hepatocytes, occupied receptors appeared to be excluded from coated pits (Knutson, 1991). Likewise, in HepG2 hepatoma cells, where coated pit formation was inhibited by the depletion of potassium under hypotonic conditions, insulin-IR complexes endocytosed normally even in the absence of clathrin coats. While, these observations were carried out in conditions of high receptor occupancy, under more physiological conditions of low insulin concentrations and low receptor occupancy, internalization was inhibited by potassium depletion consistent with a coated pit mechanism. These results, and those derived from CHO cells, indicate that the insulin-IR complex may be internalized by both smooth and coated pits in a manner that may be related to receptor occupancy (Backer *et al.*, 1991; McClain and Olefsky, 1988).

Insulin mediated endocytosis requires specific amino acid residues found in the juxtamembrane domain (encoded by exon 16) of the receptor. This region, capable of inducing endocytosis of an IR lacking the portion encoded by exons 17-22 (Carpentier and McClain, 1995), contains two endocytic sequences; a strong code, $GPLY^{965}$ and a weak code, $NPEY^{972}$ (Rajagopalan *et al.*, 1991). Mutation of these codes to APLA and APEA, reduced internalization to 32% and 87% respectively, as compared to wild type IR internalization. Both codes form a tight β turn structure exposing a tyrosine residue, an essential recognition motif which is present in the internalization codes of many receptors. In addition to these endocytic codes, efficient internalization of the IR requires the activation of its catalytic kinase activity and tyrosine phosphorylation (Backer *et al.*, 1991). An active IR kinase may be required to induce a conformational change which would result in the exposure of internalization codes, as has been suggested for the EGFR (Cadena *et al.*, 1994). Alternatively, an active tyrosine kinase receptor may be needed to phosphorylate substrates involved in mediating receptor internalization.

pp120/HA4

An IR substrate, pp120/HA4, that is predominantly expressed in the liver was assessed for receptor internalization (Formisano *et al.*, 1995). The transfection of antisense pp120/HA4 cDNA into H35 hepatoma cells inhibited insulin-induced receptor internalization 2 to 3-fold, implicating this protein in the regulation of endocytosis. The effect of this protein in increasing internalization appeared to be specific for the IR. Based on the observation that pp120/HA4 shared some homology with sequences thought to be important recognition elements for AP2 adaptor proteins (implicated in EGFR internalization, see above), it was proposed to be part of a complex contributing to the interaction of the activated insulin receptor with clathrin coated pits. However, immunolocalization of pp120/HA4 in rat liver revealed that this protein was associated exclusively to the bile canulicular membrane (Margolis *et al.*, 1988), and consequently unlikely to be directly involved in IR internalization. Furthermore, pp120/HA4 may be involved in internalization of the shorter form of the IR (IR A; lacking the 12 amino acids encoded by exon 16) that is absent from the liver (which contains the B form). Co-expression of pp120/HA4 and the shorter form of the IR (IR A) in NIH 3T3 cells induced IR internalization 2-3 fold greater than the overexpression of IR A alone. When the B form of the receptor was co-expressed with pp120/HA4, no difference in receptor internalization was observed (Li Calzi *et al.*, 1997).

Enigma

Using the yeast two hybrid system, a protein which specifically interacts with the internalization region of the IR was uncovered (Wu and Gill, 1994). This protein, termed enigma, contains three LIM domains in its C-terminus. LIM domains were first identified as regions of homology in the homeodomain proteins lin-11, isl-1 and mec-3, involved in *D. melanogaster* development. These domains have been proposed to function in protein-protein interactions and have been identified cytoplasmic proteins that interact with the cytoskeleton and focal adhesions (Schmeichel and Beckerle, 1994). Mutation of the strong IR endocytic code (GPLY^{965} to APLA) almost completely abolished this interaction, whereas the mutation of NPEY^{972} to APEA decreased this interaction by 40%. These results were in accordance with the decreased internalization rates observed for these mutant receptors and demonstrate that LIM domains are capable of interacting with the tyrosine tight turn motif of these endocytic codes. Enigma failed to interact with the endocytic codes of the constitutively internalizing LDLR, TfnR or the EGFR (^{996}QQGFF), revealing the specificity in the recognition of enigma for internalization motifs (Wu and Gill, 1994). This was confirmed by peptide library screening with a GST-Enigma LIM3

domain probe. The peptide that preferentially bound the probe was Gly-Pro-Hyd-Gly-Pro-Hyd-Tyr-Ala, a peptide similar to the IR GPLY domain (Wu *et al.*, 1996).

Dynamin

Dynamin has been reported to physically interact with the IR via SHC and GRB2 (Baron *et al.*, 1998) and has been suggested to play a role in IR internalization (Ceresa *et al.*, 1998). The latter study demonstrates that a dominant negative mutant of dynamin (the K44A mutant) inhibits IR internalization and alters signal transduction. In these studies IR autophosphorylation and IRS-1 phosphorylation were unaltered by inhibition of IR internalization, however, SHC and MAP kinase activation were partially inhibited. It remains unclear if overexpression of the K44A dynamin mutant interferes with the interaction of insulin with its receptor as is the case of EGF and the EGFR (Ringerike *et al.*, 1998).

Internalized insulin/IR

Internalization of the insulin-IR complex constitutes the major mechanism of insulin degradation and down-regulation of cell surface receptors. The acidic pH of the endocytic compartment causes the dissociation of insulin from its receptor. Several studies have demonstrated that the endosome is a major site of degradation of insulin (Doherty *et al.*, 1990; Backer *et al.*, 1990; Authier *et al.*, 1994a). Insulin degradation is initiated in rat liver endosomes as rapidly as 1 min after insulin administration to hepatic circulation. The degradation of insulin appears to be carried out by an endosomal acidic insulinase (EAI), found in the lumen of hepatic endosomes (Authier *et al.*, 1994a,b). The insulin protease characterized in cell-free endosomes demonstrates optimal activity between pH 5.0 and 5.5. Doherty and colleagues (1990) demonstrated that the inhibition of insulin release from the receptor reduces degradation of insulin.

While insulin is degraded in the endosome, the IR may recycle back to the plasma membrane or translocate into lysosomes for degradation. Prolonged insulin stimulation, or receptor saturating doses of insulin, causes the degradation of the internalized receptor in rat liver (Burgess *et al.*, 1992).

Endocytosis and mitogenesis

Remarkably, proteins linked to internalization have been linked to cancer. These include AF-1p (the orthologue of the EGFR substrate, Eps15) which causes transformation of NIH 3T3 cells (Fazioli *et al.*, 1993). In addition, endophilin is also an apparent cause of a myeloid leukemia due to chromosomal translocation. Endophilin is a constituent of the internalization machinery via association with dynamin (Floyd and De Camilli, 1998). Finally, the internalization protein AP-180 is implicated in cancer due to a chromosomal translocation related to histiocytic lymphoma (Dreyling *et al.*, 1996).

Other links between the endocytic machinery and cancer causation have been reviewed by Floyd and De Camilli (1998) for the early endocytic GTPase Rab5 partner tuberin (Xiao *et al.*, 1997, McLauchlan *et al.*, 1998) a gene homologous to the beta subunit of clathrin adapters AP1 and AP2 (Peyrard *et al.*, 1994) and the amphiphysin II variant (BIN1). BIN1 was identified as a tumor suppressor underexpressed in human cancer (Sakamuro *et al.*, 1996) and another amphyphysin II splice form was demonstrated to bind and enhance the transformation induced by c-abl (Kadlec and Penderast, 1997). Amphyphysin is a dynamin and synaptojanin binding protein again found associated with the internalization machinery (Floyd and De Camilli, 1998). Finally, the TSG101 homologue of VPS23 (an endosomal protein in yeast) is responsible for forming tumors in mice (Li and Cohen, 1996). Taken together with work of Gill and colleagues (Masui *et al.*, 1991) and French and Lauffenburger (1997) it is clear that traffic of protooncogene products and RTKs such as the EGFR are transforming. Furthermore, downstream substrates of the EGFR including all three separate isoforms of SHC are differentially recruited to the activated EGFR in plasma membrane or endosomes (Di Guglielmo *et al.*, 1994). Such differential recruitment may be related to different downstream outcomes mediated by the activation or attenuation of signal transduction (Migliaccio *et al.*, 1997).

IV. Downregulation of RTK signaling

Signaling cascades are activated in response to ligand binding and receptor activation. Control of complex physiological processes such as differentiation and proliferation require mechanisms to control these signals. The ligand and activated receptor complex may undergo modifications which result in the attenuation of signaling. These modifications may take on the form of dephosphorylation of internalized receptors by PTPases or receptor desensitization via phosphorylation of serine/threonine residues. Endocytosis of the receptor-ligand complexes and ligand and/or receptor degradation in endosomes/lysosomes may also play an important role in the regulation of signaling from RTKs. Both spatial and covalent forms of negative regulation exists (Sorkin and Waters, 1993; Baass *et al.*, 1995).

Serine/threonine phosphorylation

Negative covalent regulation of the EGFR is achieved primarily by phosphorylation of the receptor on serine/threonine residues (Lund and Wiley, 1993). For example, phosphorylation of the EGFR at T^{654} by PKC not only reduces affinity for ligands but also inhibits receptor activation (Lund *et al.*, 1990). MAP kinase has also been implicated in the serine/threonine phosphorylation of T^{669} in the juxtamembrane domain of the EGFR and inactivate it in a negative feedback mechanism (Northwood *et al.*, 1991).

In the case of the IR, activation of different PKC isoforms by high glucose levels causes a rapid inhibition of IR activity. This effect is most likely mediated through serine phosphorylation of the β subunit. (Haring *et al.*, 1996). Specifically, PKC α, δ and ζ have been demonstrated to bind the IR in response to ligand stimulation and modulate receptor traffic and degradation (Formisano *et al.*, 1998).

Protein tyrosine phosphatases

To date, approximately 80 PTPases have been described that can be classified into three main groups: (1) receptor-like PTPases - composed of a variable extracellular domain, a single hydrophobic transmembrane domain and one or two intracellular catalytic domains; (2) intracellular PTPases - which contain a single catalytic domain and possess carboxyl and amino-terminal extensions thought to be responsible for subcellular localization and/or enzymatic regulation (reviewed by Mauro and Dixon, 1994) and; (3) dual-specificity PTPases - a class of PTPases able to dephosphorylate both phosphotyrosine and phospho-serine/threonine residues (reviewed by Tonks and Neel, 1996). Although the dual-specific PTPases have been shown to regulate the activity of the MAP kinase enzyme family (Tonks and Neel, 1996), the physiological substrates and *in vivo* functions for most PTPases remain elusive.

Attenuation of RTK activity is thought to involve two main processes: (1) dissociation and degradation of ligand and; (2) dephosphorylation of specific tyrosine residues required to deactivate the RTK. Although proteolytic activity towards insulin in endosomes has been well established (Authier *et al.*, 1994b) the degradation of EGF is less clear. Although limited proteolysis of EGF has been documented in the endosomal apparatus, the ligand retains biological activity (Renfrew and Hubbard, 1991b). Unlike insulin, EGF associated with its receptor are both targeted to the lysosome for efficient degradation (Lai *et al.*, 1989a).

Dissociation and degradation of ligand is necessary to prevent continuous stimulation of RTK autophosphorylation. The IR retains its phosphorylation state and tyrosine kinase activity after insulin is removed from the β-subunit (Rosen, 1983) therefore dephosphorylation of specific β-subunit tyrosine residues is necessary to deactivate the RTK activity and down-regulate insulin-signaling (reviewed by Sale, 1992). Studies of rat hepatoma cells demonstrated that internalized IRs were dephosphorylated and inactivated prior to recycling back to the plasma membrane (Backer *et al.*, 1989). Other work in rat liver (Khan *et al.*, 1989; Di Guglielmo *et al.*, 1994), permeabilized adipocytes (Mooney *et al.*, 1992), and CHO cells (Bernier *et al.*, 1994) demonstrated that the activated IR is rapidly dephosphorylated *in vivo*. Thus tyrosine phosphorylation of the IR is a dynamic, rapidly reversible process.

The EGFR has been shown to bind a number of phosphatases including PTP-PEST, SH-PTP2 and SHP-1 (Charest *et al.*, 1997; Tomic *et al.*, 1995; Wong and Johnson, 1996). However when these EGFR/PTPase complexes were immunoprecipitated and incubated, they were not found to affect EGFR phosphorylation implying that they are not the physiological PTPases that dephosphorylate the EGFR *in vivo*. The use of purified enzymes and recombinant catalytic domains have revealed several PTPases that are active against the autophosphorylated IR *in vitro* including the receptor-like PTPases, CD45, leukocyte antigen-related PTP (LAR) and leukocyte common antigen-related PTP (LRP or R-PTP), and the cytosolic PTPases, PTP1B and TC-PTP (Goldstein, 1993). Using phosphopeptides modeled on the kinase regulatory domain of the IR, differences have been observed in the *in vitro* specificity and rates by which particular PTPases dephosphorylate the three phosphotyrosines in the IRK kinase domain (Goldstein, 1993). Although promising, the PTPase responsible for the dephosphorylation of the IR in insulin target tissues remains elusive.

A different approach involving cellular location was used to identify the compartments in the cell that harbor insulin and EGF receptor specific PTPases in order to then attempt their identification. Faure and colleagues (1992) identified PTPase activity towards the IR and EGFR in rat liver endosomes. In these studies, ^{32}P-labeling of IRs and EGFRs in intact endosomal membranes (*in situ* labeling) allowed for an assessment of PTPase activity in a more physiological environment where the potential spatial relationship between the IR and membrane-associated PTPase(s) was not disrupted. Whether this PTPase(s) represents a transmembrane protein and/or an intracellular enzyme tightly associated with the endosomal membrane remains unclear. However, it appears that IR-associated PTPase(s), either present or recruited to the endosomal compartment with internalized IRs, are responsible for IR dephosphorylation *in vivo*.

In contrast to rat liver, studies of IR internalization in isolated adipocytes reveal that the intracellular IR tyrosine kinase activity and phosphorylation is elevated compared to IRs at the cell surface and a direct correlation exists between endosomal IR tyrosine phosphorylation and signal transduction in adipocytes (Klein *et al.*, 1987, Kublaoui *et al.*, 1995). In rat liver the majority of IR phosphorylation occurs at the plasma membrane and is attenuated as the receptor internalizes into endosomal apparatus (Burgess *et al.*, 1992). Whether these differences reflect tissue-specific regulatory mechanisms related to the different physiological roles of adipose and liver remain to be established.

V. Hypothesis and thesis objectives

Cell culture studies were instrumental in the identification of RTK substrates and pathways involved in signal transduction. However, removing these cells from their normal physiological environment may result in the loss of structural cues and hormonal regulation. We have therefore used young adult male rat liver to assess the regulation of signal transduction pathways from the IR and EGFR *in vivo*.

The major organ responsible for whole body homeostasis is the liver, which is composed primarily of quiescent and highly differentiated parenchymal cells. Hepatocytes carry out the specialized functions of the liver, including production of the majority of plasma proteins, and regulation of carbohydrate, urea, fatty acid and cholesterol metabolism. In addition, the liver displays the remarkable and unique capacity to undergo hyperplasia and to repopulate lost tissue and cells resulting from physical, infectious and toxic injury (reviewed in Steer, 1995; Diehl and Rai, 1995). Young adult male rat liver expresses equivalent numbers of EGF and insulin receptors and therefore provides a physiological model for the study of the metabolic and mitogenic signal transduction pathways from these two RTKs. The relative absence of IGF-1Rs in adult rat liver (Santos *et al.*, 1994) also allows for the direct evaluation of IR signal transduction uncomplicated by secondary effects via other receptor systems.

Hypothesis

Using rat liver as an experimental system, the hypothesis that the endosomal apparatus plays a role in regulating RTK traffic and signal transduction was evaluated.

Thesis objectives:

1) To assess if the EGFR and IR access signaling molecules of the Ras pathway in rat liver and to correlate this with RTK activation at the plasma membrane and/or the endosomal apparatus.

2) To study the clearance of the insulin analog, H2, by rat liver. Endosomal degradation of H2 as well as its association with the endosomal IR will be compared to studies using native insulin.

3) To assess the effect of the insulin analog H2 on IR traffic and signal transduction in rat liver.

Figure 1. Receptor tyrosine kinase structure.

The structure of 6 RTK families are shown in panel A. They include the EGF receptor (EGFR), insulin receptor (IR), platelet derived growth factor receptor (PDGFR), fibroblast growth factor receptor (FGFR), nerve growth factor receptor (NGFR or Trk), and hepatocyte growth factor receptor (HGFR). The EGFR is a transmembrane glycoprotein that is monomeric at the plasma membrane (B). Upon binding of ligand, it dimerizes (not shown), and via its intrinsic tyrosine kinase activity, it autophosphorylates the five cytosolic tyrosine residues indicated (Y^{992}-Y^{1173}). The ligand binding region (residues 321-367), the transmembrane domain (redidues 622-644), the ATP binding site (K721) and the catalytic domain (residues 694-940) are indicated. The IR is a heterotetrameric molecule composed of 2 α and 2 β subunits (B). Upon ligand binding it oligomerizes and becomes autophosphorylated on the six tyrosine residues indicated (Y^{972}-Y^{1334}). The ligand binding domain (residues 1-121), the transmembrane domains (residues 930-952 of the β subunit), the ATP binding site (K1030) and the catalytic domain (residues 1002-1257) are indicated. The numbering system used to identify specific residues of the IR include the 12 amino acids encoded by exon 16. This is the IR form expressed in liver parenchyma.

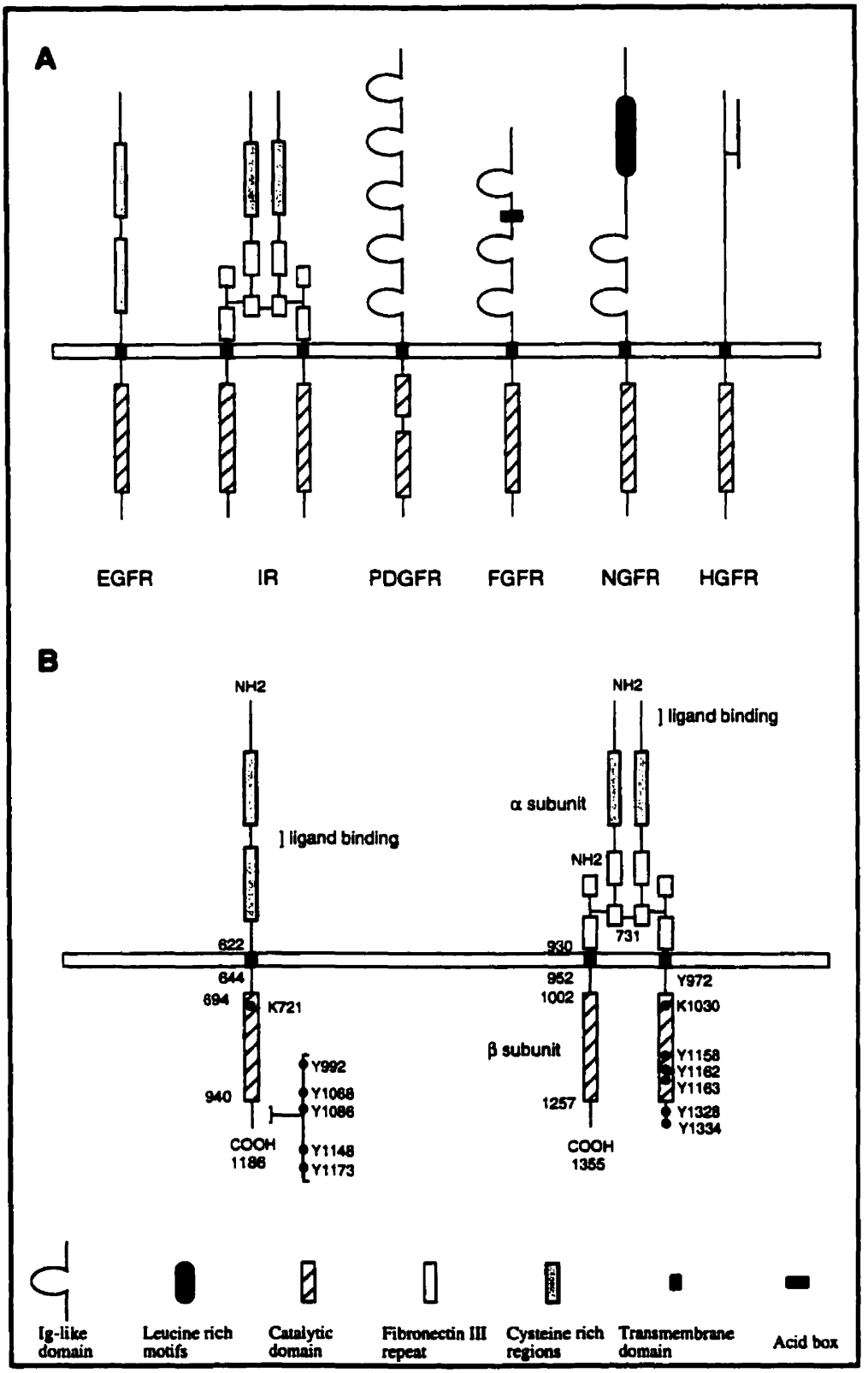
A
EGFR
IR
PDGFR
FGFR
NGFR
HGFR
B
NH2
] ligand binding
622
644
694
K721
940
Y992
Y1068
Y1086
COOH
1186
Y1148
Y1173
α subunit
NH2
] ligand binding
731
930
952
1002
β subunit
1257
COOH
1355
Y972
K1030
Y1158
Y1162
Y1163
Y1328
Y1334
Ig-like domain
Leucine rich motifs
Catalytic domain
Fibronectin III repeat
Cysteine rich regions
Transmembrane domain
Acid box

Figure 2. Insulin and EGF receptor signaling pathways.

Binding of ligand at the cell surface induces receptor dimerization and activation of intrinsic tyrosine kinase activity. Following autophosphorylation of cytosolically exposed tyrosine residues, substrates and docking/adaptor proteins are recruited via SH2 or PTB domains and form complexes (see text). These complexes elicit a number of downstream signaling cascades including the MAP kinase cascade via activation of Ras. Downstream effects include mitogenesis, differentiation and metabolism.

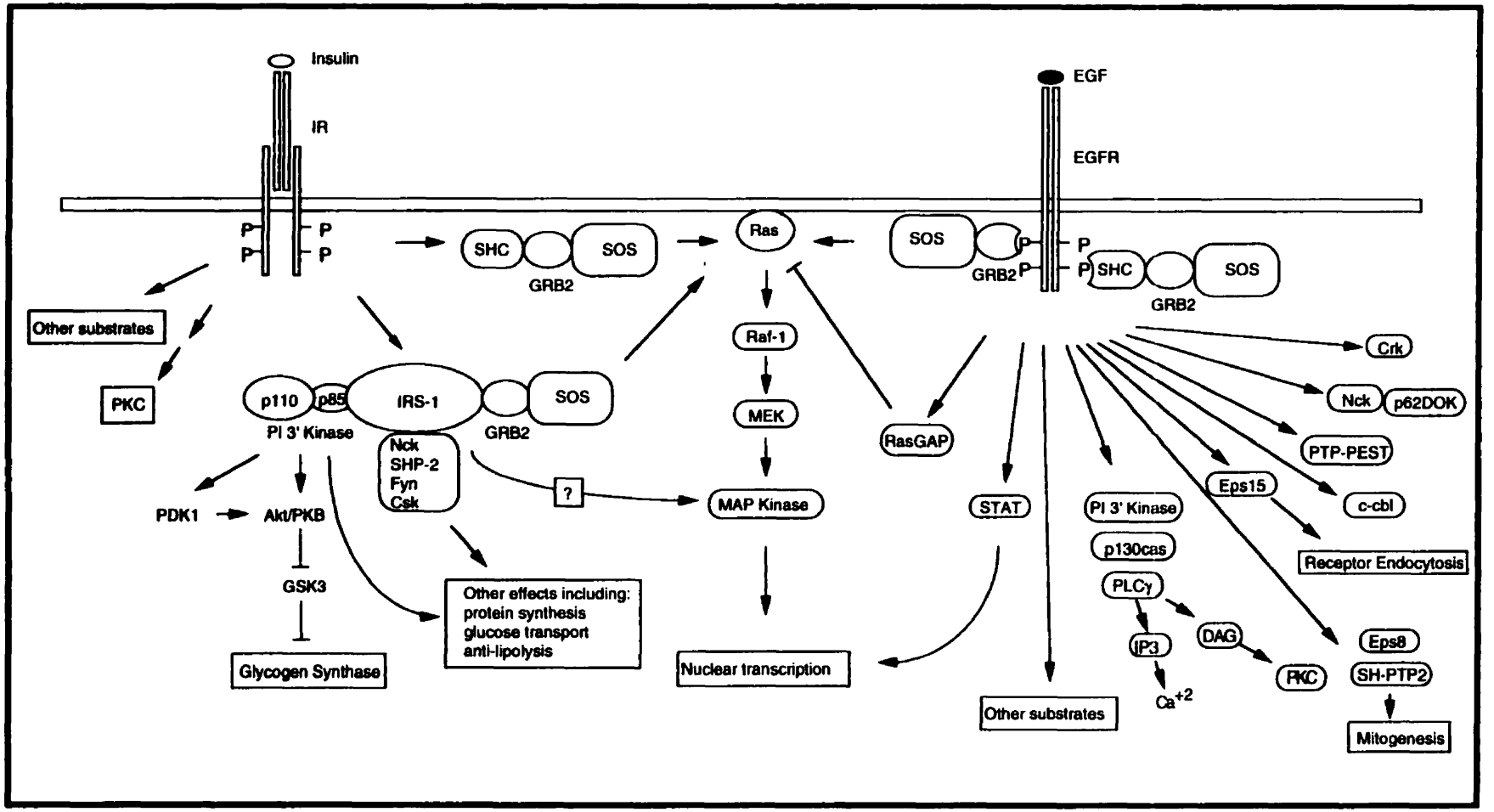
Insulin
IR
EGF
EGFR
P
P
P
P
SHC
SOS
GRB2
Ras
SOS
GRB2
P
P
P
P
SHC
SOS
GRB2
Other substrates
PKC
p110
p85
PI 3' Kinase
IRS-1
SOS
GRB2
Nck
SHP-2
Fyn
Csk
?
Raf-1
MEK
MAP Kinase
RasGAP
STAT
PDK1
Akt/PKB
GSK3
Glycogen Synthase
Other effects including:
protein synthesis
glucose transport
anti-lipolysis
Nuclear transcription
Other substrates
PI 3' Kinase
p130cas
PLCγ
IP3
Ca+2
DAG
PKC
Crk
Nck
p62DOK
PTP-PEST
Eps15
c-cbl
Receptor Endocytosis
Eps8
SH-PTP2
Mitogenesis

Figure 3. Ligand mediated insulin and EGF receptor endocytosis.

Upon insulin or EGF binding to their respective cell surface receptors, receptors oligomerize and redistribute to clathrin coated pits and internalize into the endosomal apparatus. This is aided by a number of molecules that associate with the receptor cytosolic domains (see text). Once inside the cell, the acidic pH of the endosomal lumen mediates ligand dissociation of insulin from its receptor and insulin is degraded. The IR then recycles back to the plasma membrane. EGF does not dissociate from its receptor at ligand concentrations > 50% receptor occupancy (Lai *et al.*, 1989a), and accompanies the receptor to the lysosome for degradation. At EGF concentrations < 50% receptor occupancy, or if TGFα is used as ligand, the EGFR dissociates from the ligand in the endosomal apparatus and recycles back to the plasma membrane.

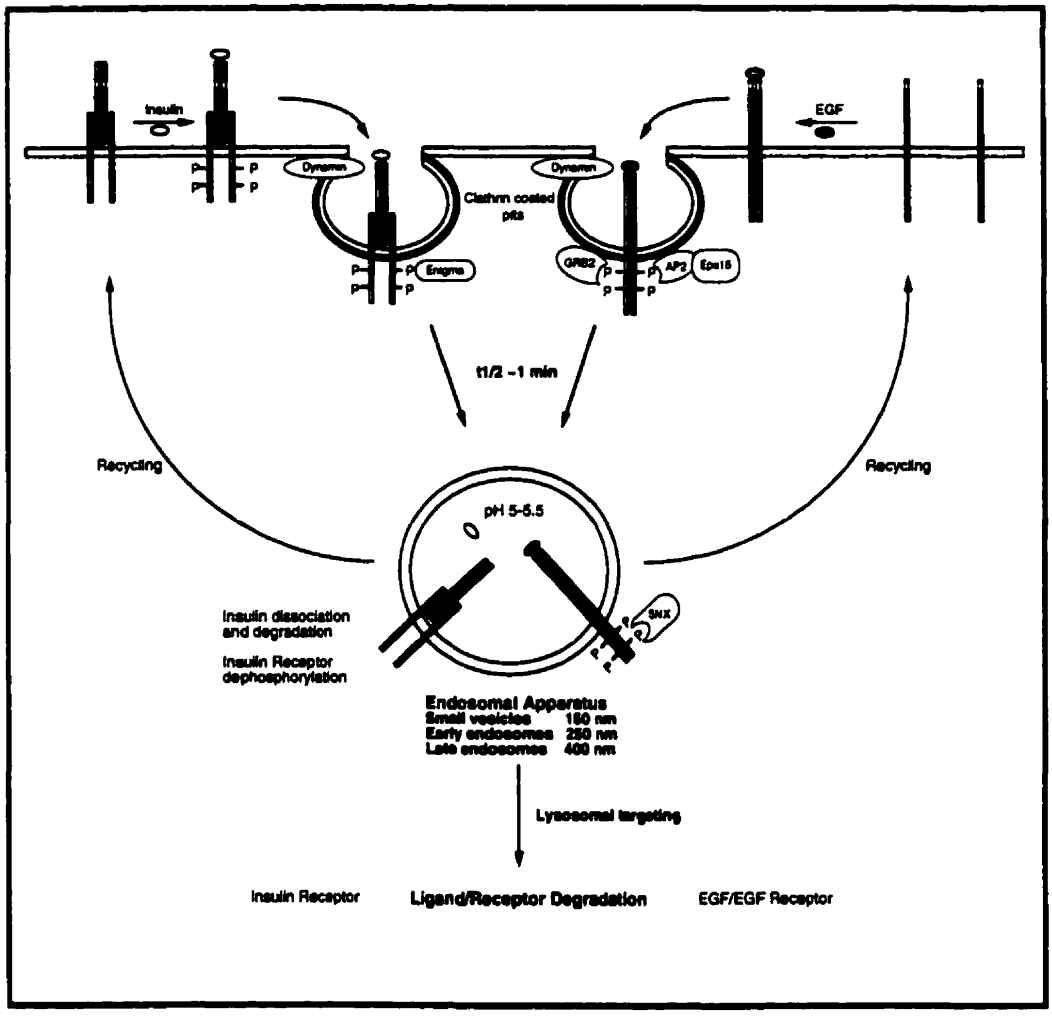
Insulin
EGF
Dynamin
Dynamin
Clathrin coated pits
Endophilin
GRB2
AP2
Eps15
t1/2 ~1 min
Recycling
Recycling
pH 5-5.5
SNX
Insulin dissociation and degradation
Insulin Receptor dephosphorylation
Endosomal Apparatus
Small vesicles 150 nm
Early endosomes 250 nm
Late endosomes 400 nm
Lysosomal targeting
Insulin Receptor
Ligand/Receptor Degradation
EGF/EGF Receptor

Materials and Methods

Materials

Receptor-grade EGF was purchased from Collaborative Research Inc. (Lexington, MA), insulin was obtained from Eli Lilly (Indianapolis, IN) or Sigma Chemical Company (St. Louis, MO) and the insulin analog H2 was obtained from Dr. G.M. Danielsen (Novo Nordisk, Denmark). Antibodies used for immunoprecipitation and immunoblotting are described in Table 1. Protein A and Protein G Sepharose were obtained from Pharmacia Biotech Inc. (Baie d'Urfé, PQ). Reagents for protein determination and SDS-PAGE were from BioRad Laboratories (Mississauga, Ont.). Nitrocellulose membrane (BA85) was obtained from Xymotech (Mt. Royal, PQ). [^{125}I]-goat anti-rabbit IgG (8.70 μCi/μg), [^{125}I]-goat anti-mouse IgG (19.9 μCi/μg) were obtained from NEN-Mandel (St. Laurent, PQ) and ICN Biomedicals (Mississauga, Ont.) respectively. HRP-conjugated goat anti-rabbit IgG, and Protein A-HRP were purchased from BioRad Laboratories (Mississauga, Ont.) while the HRP-conjugated goat anti-mouse IgG was purchased from Jackson ImmunoResearch Laboratories, Inc. (West Grove, PA). The ECL Detection kit was obtained from Amersham (Oakville, Ont.). Restriction enzymes were obtained from Pharmacia Biotech Inc. (Baie d'Urfé, PQ). The GeneClean II Kit for insert purification was purchased from Bio101 Inc. (La Jolla, CA). [α-^{32}P] dCTP (3000 Ci/mmol) was purchased from NEN-Mandel (St. Laurent, PQ). The Random Primer DNA Labeling System was purchased by Gibco BRL (Burlington, PQ). Hybond-N membrane was obtained from Amersham (Oakville, Ont.). Kodak XAR-5 OMAT X-ray film was purchased from Picker International (Montreal, PQ).

All other reagents and chemicals were obtained from Anachemia (Lachine, PQ), Boehringer Mannheim (Laval, PQ), Gibco BRL (Burlington, PQ), Fisher Scientific (Montreal, PQ), Pharmacia Biotech Inc. (Baie d'Urfé, PQ), Sigma Chemical Company (St. Louis, MO). Reagents for molecular biology were of nucleic acid grade (DNase and RNase free).

Animals

Male Sprague-Dawley rats (100-125 g BW) were used in subcellular fractionation or RNA isolation protocols. Lab Chow and water were available *ad libitum* and animals were fasted 14-16 hours before the administration of polypeptide growth factors or hormones. Female New Zealand White rabbits (2-2.5 kg) were used to raise anti-SHC antibodies. Male BALB C/BYT mice (25-30 g) were used for the production of monoclonal anti-EGFR antibodies (clone IgG 151). All animals were obtained from Charles River Laboratory (St. Constant, PQ).

Methods

Subcellular fractionation

Fasted rats were anesthetized with an injection of sodium pentobarbital (65 μg/g BW) (Somnotol, MTC Pharmaceuticals, Cambridge, Ont.). EGF (10 μg/100 g BW), insulin (15 μg/100 g BW) or the insulin analog, H2 (15 μg/100 g BW) was administered to rats via injection into the hepatic portal vein. At various times post-injection, the animals were sacrificed and their livers were rapidly removed and minced in ice cold homogenization buffer [0.25 M sucrose, 20 mM Tris base (pH 7.4), 1 mM $MgCl_2$] containing 5 mM iodoacetamide, 165 KIU/ml aprotinin, 0.5 mM PMSF, 4 mM NaF, 100 mM Na_3VO_4, 5 mM $NaMoO_4$, 10 mM β-glycerophosphate, 2 mM benzamidine, 5 mM p-NPP. Aprotinin, PMSF, and iodoacetamide were added to buffers immediately before use. Subsequent steps were carried out at 4°C and all buffers and gradients contained the above inhibitors unless otherwise indicated.

The isolation of plasma membranes (PM) was carried out as described by Di Guglielmo *et al.* (1994). Livers were homogenized using a Dounce homogenizer ("B" or loose pestle) in 5 ml homogenization buffer/g liver. Homogenates were centrifuged at 280 x g_{av} for 5 min (Sorvall SS-34 rotor). The resulting supernatant (S1) was collected and the pellet (P1) was resuspended in half the original volume using the Dounce homogenizer and centrifuged at 280 x g_{av} for 5 min to obtain P2 and S2. S2 and S1 were combined and centrifuged at 1,500 x g_{av} for 10 min to obtain P3 and S3. Pellets P2 and P3 were combined, resuspended and the molarity was adjusted to 1.42 M sucrose. This homogenate was overlaid with 0.25 M sucrose and centrifuged at 82,000 x g_{av} for 1 h (Beckman SW-28 rotor). The pellicule at the 0.25 M and 1.42 M interface was collected, and the molarity was adjusted to 0.39 M sucrose. Following centrifugation at 1,500 x g_{av} for 10 min (Sorvall SS-28), the resulting pellet (PM) was resuspended in homogenization buffer.

To obtain the total particulate fraction (TP), one ml of the homogenate (5 ml/g liver) was centrifuged at 300,000 x g_{av} (Beckman rotor TLA 100.2) for 30 min. The pellet was resuspended in 2 ml of homogenization buffer.

The GE fraction was prepared as described by Di Guglielmo *et al.* (1994). In homogenization buffer, livers were homogenized using a Potter-Elvehjem homogenizer (power setting 3) to generate homogenates (5 ml/g liver) which were then centrifuged for 10 min at 1,500 x g_{av} (Sorvall SS-34) and the supernatant collected and centrifuged at

200,000 x g_{av} for 30 min (Beckmann 60 Ti rotor). The supernatant was used as the cytosolic (Cyt) fraction. The microsomal pellet was resuspended to a molarity of 1.15 M sucrose and overlaid with 1.00 M and 0.25 M sucrose cushions and centrifuged at 200,000 x g_{av} for 1.5 h (Beckman SW28 rotor). The GE fraction was collected at the 0.25 M and 1.00 M sucrose interface. Fractions were aliquoted and stored at -70°C.

Yields and recoveries

The protein concentration of these subcellular fractions was measured using the Bradford method (1976) and BSA as a standard. The yield (mg protein/g liver) of each fraction was calculated and is indicated in Table 2. The yields obtained for the PM and GE fractions (Table 2) were consistent with the yields described by Kay *et al.* (1986) and by Wada *et al.* (1992), respectively.

The EGFR content in the TP, PM and GE fractions was determined by quantitative immunoblotting using phosphoimager analysis (Fuji BAS2000 Phosphoimager). In the TP fraction, the EGFR content was determined to be 2.54 ± 0.26 arbitrary U/mg cell fraction protein and was unchanged from 0 to 60 min after EGF injection. The EGFR content of the PM fraction at 0 and 15 min after EGF injection was found to be 12.2 ± 3.4 and 2.40 ± 0.02 U/mg cell fraction protein, respectively. For the GE fraction at 0 and 15 min after EGF injection, the values were 12.8 ± 2.5 and 57.8 ± 4.1 U/mg cell fraction protein, respectively. Using the yields for each fraction (see Table 2), recoveries were calculated to be 24.3% for the PM and 18.1 % for the GE.

Generation of polyclonal anti-SHC antibodies

GST-SHC expression and purification

E. Coli transformed with the pGEX vector containing the SHC SH2 domain insert were obtained from Drs. Jane McGlade and Tony Pawson (Samuel Lunenfeld Research Institute, University of Toronto). A single colony was used to inoculate 200 ml of LB broth (Sambrook *et al.*, 1989) containing 40 µg/ml of ampicillin. The culture was grown overnight at 37°C in a shaking incubator and then diluted into 1 liter of fresh LB/ampicillin and grown for an additional hour. One hundred mM IPTG was added (0.1 mM final concentration) for 4 h to induce fusion protein expression. Cells were pelleted by centrifugation at 5,000 x g_{av} for 10 min and then resuspended in 30 ml ice-cold PBS/0.5 mM PMSF. Cells were lysed, 1 ml at a time, using a 5 mm diameter probe sonicator (setting 100; 50 watts) twice for 15 seconds. Ten percent TX-100 (v/v) was added to make a 1% final concentration, and incubated for 30 min on ice. The cells were centrifuged at

10,000 x g_{av} (Beckman JA20 9500) for 10 min at 4°C to remove insoluble material. The supernatant was collected and 2 ml 50% glutathione-agarose bead slurry (in PBS) were added and the mixture rotated for 1 h at 4°C. The beads are then washed 3 times with 50 ml of ice-cold PBS with intervening 2 min centrifugations at 500 x g_{av}. The fusion protein was eluted by the addition of 1 ml 50 mM Tris (pH 8)/10 mM reduced glutathione for 15 min at 4°C. The eluant was collected after 30 sec centrifugation at 4°C at 10,000 x g_{av}.

Immunization and blood collection

Prior to antigen injection, 10 ml preimmune blood were taken from the central ear artery of female New-Zealand White rabbits. The rabbits were then injected intramuscularly with 2 mg (500 µl) of the purified GST-SHC SH2 fusion protein in PBS and an equal volume of Freund's complete adjuvant. Boosters of 1 mg fusion protein/ Freund's incomplete adjuvant were given 30 and 60 days after the initial immunization. Ten ml of blood was taken each week, incubated for 30 min at 37°C, and then overnight at 4°C. Serum was obtained by centrifugation at 2200 rpm (Beckman, JS-4.2) for 30 min at 4°C.

GST-SHC bead preparation

Five hundred µg CB-Sepharose was prepared overnight in 200 ml of 0.1 M HCl and then centrifuged at 1,000 g_{av} for 10 min at 4°C. Fifty ml of 0.1 M $NaHCO_3$ (pH 8.0) were added to the beads and re-centrifuged under the same conditions. This yielded 1.5 ml wet bead volume to which was added 4.37 mg of GST-SHC in 1.5 ml PBS. Following rotation for 4 h at 4°C, 50 ml of 0.05 M Tris (pH 8.0) were added and incubated overnight at 4°C. The beads were washed one time each with 6 ml 0.1 M Tris (pH 11), 6 ml 0.1 M Tris (pH 8), and 6 ml 0.1 M glycine (pH 2.5).

Antibody affinity purification

Ten ml of serum (see Immunization and Bleeds) were added to the GST-SHC beads, rotated overnight at 4°C and then poured into a 0.5 cm x 10 cm column. The column was washed with 20 ml of 0.1 M Tris (pH 8.0). The anti-SHC antibodies were eluted off the column with 5 ml of 0.1 M Tris (pH 11) followed by 5 ml of 0.1 M Tris (pH 8) and finally 5 ml of 0.1 M glycine (pH 2.5). Ammonium sulfate (50% final concentration) was added to the combined eluants, stirred for 1 h at 4°C and centrifuged at 8,000 g_{av} for 20 min. The pellet was resuspended in 0.5 ml PBS and dialyzed overnight in PBS. The affinity purified anti-SHC antibodies were diluted with PBS to 2 ml.

Generation of monoclonal anti-EGFR antibodies

IgG 151 hybridoma cell culture

IgG 151 hybridoma cells were obtained from Dr. M. Shanks (Johns Hopkins University, Baltimore, MD). Cells were cultured in DMEM, 10% NCTC, 20% fetal

bovine serum, 10% v/v hybridoma cloning factor, 50 µg/ml Streptomycin base and 50 U/ml Penicillin G (pH 7.2). Culture medium was replaced every 2 days until cells were reached confluency. Confluent cells were trypsinized (0.05% trypsin for 2 min at 37°C) and replated at a 10 % cell density in culture medium.

Ascites fluid production and collection

Male BALB C / BYT mice were primed with an intraperitoneal injection of 0.5 ml of Freund's incomplete adjuvant. One week later, 1 ml of IgG 151 hybridoma cell suspension (9.8 x 10^6 cells / ml DMEM) was injected intraperitoneally. Ten days later, the ascites fluid was tapped, centrifuged at 1,600 g_{av} for 10 min and the supernatant collected and stored at -20°C.

Immunoprecipitation

Cytosolic fractions were diluted to 1 mg/ml with immunoprecipitation buffer [1% TX-100 / HBS (50 mM HEPES (pH 7.5), 150 mM NaCl, 10% glycerol]. Solubilization of PM and GE fractions was carried out for 30 min at 4°C with immunoprecipitation buffer containing 0.5% deoxycholate. Solubilized samples were centrifuged at 10,000 x g_{av} for 5 min at 4°C. Anti-EGFR (IgG 151), anti-SHC, anti-IRS-1 (JD66), anti-FAK (2A7) or anti-phosphotyrosine (PY) antibodies were added to the supernatants which were incubated for 2 h at 4°C. The immune complex was precipitated using 80 µl of a 20% protein A-Sepharose slurry or 75 µl of 20% protein G-Sepharose slurry (α-FAK and α-PY) for 1 h at 4°C with rotation. The beads were centrifuged (10,000 x g_{av} for 30 sec at 4°C) and resuspended in immunoprecipitation buffer three times and once with HBS alone. Immunoprecipitated proteins were removed from the beads by the addition of Laemmli sample preparation buffer (Laemmli, 1970).

Immunoblotting

Samples, in sample preparation buffer, were boiled for 5 min, electrophoresed in 8% SDS-polyacrylamide gels (10% resolving gel for proteins less than 30 kDa) as described by Laemmli (1970) and transferred to nitrocellulose for one hour in 192 mM Glycine, 25 mM Tris base buffer (12V, 400 mA). The blots were then incubated in 5% skimmed milk (SM) in TNT buffer [0.15 M NaCl, 0.05% Tween-20, 10 mM Tris (pH 7.5)] for 1.5 h with three changes of solution. Immunoblots probed with α-PY antibodies were incubated in 2% BSA/TNT. Blots were then incubated in various antibodies (see Table 1), overnight at room temperature and then gently shaken in 0.5% SM/TNT or 0.5% BSA/TNT for 15 min (changing the buffer every 5 min). The blots were then incubated with [^{125}I]-conjugated (200 000 cpm/ml) or HRP-conjugated secondary antibodies (1:5000

for HRP-protein A or 1:10000 for HRP-goat anti-mouse), in 0.5% SM/TNT or 0.5% BSA/TNT, for 45 min and then shaken for 25 min with 5 changes of buffer. The chemiluminescence reaction, with the HRP-conjugated secondary antibodies, was carried out as described by the manufacturer. For visualization, the blots were exposed to Kodak X-OMAT X-ray film. Quantitation of [^{125}I] signals was carried out using a BAS 2000 Fuji Bio-Imaging Analyzer (Fuji BioMedical Systems, Inc., Bethesda, MD), with the gradation, resolution and sensitivity settings as described by the manufacturer for immunoblots.

RNA isolation

Total RNA was isolated from liver using Acid Guanidinium Thiocyanate/ Phenol/ Chloroform extraction described by Chomczynski and Sacchi (1987). Male Sprague-Dawley rats were injected with EGF (10 μg/100 g BW), insulin or H2 (15 μg/100 g BW). Animals were sacrificed at various times after injection and the livers were rapidly removed. Livers were either stored in liquid nitrogen or immediately homogenized in 1 ml/100 mg liver of ice-cold denaturing solution (4 M guanidinium thiocyanate, 25 mM sodium citrate, 0.5% sarcosyl, 0.1 M β-mercaptoethanol) with 100 μl of Antifoam A emulsion, using a Brinkmann Polytron (Brinkmann Instruments, Westbury, NY). After homogenization, 0.1 ml/100 mg liver of 2 M sodium acetate (pH 4), 1 ml/100 mg liver of water-saturated phenol, and 0.2 ml/100 mg liver of chloroform-isoamyl alcohol (49:1) were added with thorough mixing by inversion after addition of each reagent. The suspension was incubated 15 min at 4°C and then centrifuged at 10,000 x g_{av} (Sorvall SS-34 rotor) for 20 min at 4°C. The aqueous phase was transferred to a fresh tube and the RNA was precipitated with 1 vol of 100% isopropanol overnight at -20°C. Samples were centrifuged at 10,000 x g_{av} for 20 min at 4°C. The pellets were dissolved in 0.3 ml denaturing solution and the RNA was precipitated with 1 ml 100% isopropanol for 2 h at -20°C. Samples were then centrifuged for 10 min at 4°C in a microfuge and the pellets were resuspended in 100 μl 75% ethanol to remove trace amounts of guanidinium contaminants. Samples were centrifuged for 5 min at 4°C in a microfuge and the pellet was dried under vacuum. RNA was dissolved in DEPC-treated water and were stored at -70°C until use.

The concentration of RNA in the samples was determined by spectrophotometric measurement of the absorbance at λ of 260 nm. The yield of total RNA isolated from rat liver was calculated to be 7.09 ± 1.14 μg/mg liver (n=58). The purity of the isolated RNA was determined by calculating the ratio of OD 260/280 and was determined to be 1.80 ± 0.11. The integrity of the isolated RNA was tested by electrophoresis in denaturing

agarose/formaldehyde gels to detect the relative amounts of the 28S and 18S ribosomal RNA bands.

Northern Blotting

Probe preparation

cDNA probes for c-myc, c-jun and c-fos, obtained from Drs. N. Sonenberg, P. Jolicoeur, and R. St. Arnaud, respectively, were labeled with [α-^{32}P] dCTP by oligolabeling with Klenow DNA polymerase and hexanucleotides as primers using the Random Primer Labeling System as described by the manufacturer. The specific activity was 6.53 x 10^8 cpm/mg cDNA fragment.

Prehybridization and hybridization

Twenty micrograms of total RNA were loaded per lane on a 1.2% (w/v) agarose gel containing 0.66 M formaldehyde/1 x HEPES-EDTA (pH 7.8) and electrophoresis was carried out at 25 V for 15 h. The gel was gently shaken 2 x 30 min with 10 x SSC buffer [1.5 M NaCl, 0.15 M sodium citrate (pH 7)]. The RNA was transferred to Hybond-N nylon membranes using the LKB.VacuGene XL (Pharmacia Canada Ltd. Baie D'Urfe, PQ) vacuum apparatus at 50 cm H_2O for 1.5 h. The blots were prehybridized in hybridization buffer [50% deionized formamide, 5 x SSC, 20 mM Tris-HCl (pH 7.5), 1 x Denhardt's solution, 10% Dextran Sulfate, 0.1% SDS, 200 mg/ml denatured ssDNA] without probe overnight at 45°C. [α-^{32}P] dCTP-labeled cDNA probe was hybridized (10^6 cpm/ml) to the filters at 45°C for 2-3 h in fresh hybridization buffer. The blots were then shaken 2 x 15 min (1 x SSC, 0.1% SDS) at room temperature, and 3 x 20 min (0.2 x SSC, 0.1% SDS) at 68°C. Quantitation of [α-^{32}P] signals was carried out using a BAS 2000 Fuji Bio-Imaging Analyzer (Fuji BioMedical Systems Inc., Bethesda, MD), with the gradation, resolution and sensitivity settings as described by the manufacturer.

In vitro kinase assays

All subcellular fractions generated for use in *in vitro* kinase assays were isolated as described above (see Subcellular Fractionation) with the exception that iodoacetamide was omitted from all buffers.

Exogenous IR tyrosine kinase activity

Exogenous IR tyrosine kinase activity was determined as described by Burgess *et al.* (1992). Membrane fractions (PM and GE), which were generated as described above (see Subcellular Fractionation), were solubilized in 1% TX-100 in Buffer A [50 mM HEPES (pH 7.6), 1 mM PMSF, 1 mM benzamidine, 20 µM leupeptin, 20 µM pepstatin A, 1 U/ml aprotinin, 100 µM vanadate] for 1 h at 4°C with agitation. The suspensions were

centrifuged at 100,000 x g_{av} for 1 h (Beckman SW 60 Ti) and the resulting supernatants were recycled 6 times through 2 ml WGA-Sepharose 6MB columns. The columns were washed with 80 ml of 0.1% TX-100, 50 mM HEPES (pH 6.0), 150mM NaCl, 10 mM $MgSO_4$, 1 mM PMSF, 1 mM benzamidine, and 100 µM vanadate. This was followed by a wash with 20 ml of 0.1% TX-100, 50 mM HEPES (pH 7.6), 150 mM NaCl, 1 mM PMSF, 1 mM benzamidine and 100 µM vanadate. Elution of bound glycoproteins was effected with 2.5 ml/column of 0.3 M N-acetyl-D-glucosamine and 0.1% TX-100 in Buffer A.

Aliquotes (20 µl) of partially purified IR that bound 10 fmol [^{125}I]-insulin were added to a reaction mixture containing 87.5 mM HEPES (pH 7.4), 40 mM MgCl2, 25 µM [γ-^{32}P]-ATP (5 µCi/sample), and 5.0 mg/ml poly Glu/Tyr (4:1) in a reaction volume of 100 µl. After 10 min at 25°C, the reaction was terminated by spotting 50 µl aliquots on Whatman 3MM paper disks with immersion in ice-cold 10 % TCA, 10 mM sodium pyrophosphate. The disks were washed, immersed in Opti-Fluor scintillation fluid (Packard, Merriden, CT) and associated radioactivity was quantitated in a Beckman LS6000SC β-counter.

PI 3'-kinase activity

The PI 3'-kinase assay was performed as described by Fukui and Hanafusa (1989). Rat liver cytosolic fractions were isolated at various times after the injection of insulin or the insulin analog H2 (15 µg/100 g BW) or EGF (10 µg/100 g BW) as described above (see Subcellular Fractionation). The PI 3'-kinase assay were carried out as described by Fukui and Hanafusa (1989). Cytosol was incubated with anti-IRS-1 antibodies (see Immunoprecipitation). The protein A-Sepharose beads containing the IRS-1 immunoprecipitates were washed (centrifugation in an Eppendorf microfuge followed by resuspension in buffer) 3 times with 20 mM HEPES buffer (pH 7.5) containing 10% glycerol, 0.1% TX-100, 150 mM NaCl, 10 µg/ml Aprotinin, 10 µg/ml Leupeptin, and 1 mM PMSF. The beads were then washed once with PBS, once with 0.5 M LiCl / 0.1 M Tris HCl (pH 7.5), once with distilled water, and once with 0.1 M NaCl / 1 mM EDTA / 20 mM Tris HCl (pH 7.5). All preceding steps were carried out at 4° C. Protein A-Sepharose immunoprecipitates were then suspended in 50 µl kinase buffer [20 mM Tris HCl (pH 7.5), 100 mM NaCl, 0.5 mM EGTA]. One µl of a 10 mg/ml stock of PI dissolved in DMSO was added and the mixture was incubated for 10 min at 25°C. [γ^{32}P]-ATP (10 µCi per assay) and $MgCl_2$ (20 mM final concentration) were added to start the reaction and incubated for 3 min at 25°C. The reaction was stopped by the addition of 150 µl of chloroform / methanol / 11.6 N HCl (100:200:2) and 100 µl of chloroform were added to separate the phases. The organic phase was washed with one volume of

methanol/HCl (1:1). The lipid samples were concentrated under vacuum, spotted onto Silica Gel 60 Plates (Merck & Co. Inc., Rahway, N.J.) and allowed to migrate in chlororform/methanol/28% ammonium hydroxide/water (43:38:5:7). Visualization was carried out by exposing air dried plates to Kodak O-MAT X-ray film at room temperature.

MAP kinase activity

MAP kinase assays were performed as described by Canossa *et al.* (1994). Rat liver cytosolic fractions were isolated at various times after the injection of insulin or the insulin analog H2 (15 μg/100 g BW) or EGF (10 μg/100 g BW) as described above (see Subcellular Fractionation). For the co-injection studies (Chapter 3), H2 (15 μg/100 g BW), or glucagon (20 μg/100 g BW) were coinjected with EGF (0.1 μg/100 g BW or 1 μg/100 g BW) and the animals were sacrificed 5 min post injection. MAP kinase was immunoprecipitated from 500 μg of cytosolic fraction using 5 μl of anti-ERK 1 antibody as described above. The immunocomplexes were washed twice with kinase buffer [10 mM Tris HCl (pH 7.4), 150 mM NaCl, 10 mM $MgCl_2$, 0.5 mM dithiothreitol] and then incubated for 5 min at 37° in 40 μl of kinase buffer containing 1 mM ATP, 2.5 μCi [γ^{32}P]-ATP and 10 mg/ml MBP. Reactions were stopped by boiling in Laemmli sample preparation buffer. Samples were processed for SDS-PAGE and exposed to X-ray film. Quantitation of the dried [^{32}P] gels was carried out by using a BAS 2000 Fuji Bio-Imaging Analyzer (Fuji BioMedical Systems, Inc., Bethesda, MD), with the gradation, resolution and sensitivity settings as described by the manufacturer.

PKC activity

PKC assays were performed as described by Yasuda *et al.* (1990). Aliquots of 1 cytosolic fractions (1 mg) were added to 250 μl of a 50% slurry DEAE-Sepharose in buffer A: 20 mM Tris, pH 7.5, 0.5Mm EDTA, 0.5 mM EGTA, 0.01 mM β-mercaptoethanol. Following rotation for 15 min at 4°C, beads were washed (see above) with buffer A. Bound proteins were eluted from the beads with 2 ml of buffer A containing 200 mM NaCl. Protein kinase C activity was then measured using a commercially available PKC assay kit (Gibco-BRL; Burlington, Ont.). This PKC assay kit is based on measurement of the phosphorylation of Ac-MBP(4-14). Briefly, aliquots of DEAE-Sepharose purified fractions (5 μg protein) were incubated in 35 μl of buffer containing 20 mM Tris (pH 7.5), 20 mM $MgCl_2$, 1 mM $CaCl_2$, 20 μM ATP (1 μCi/sample), and 50 μM Ac-MBP(4-14) for 5 min at 30°C. Twenty-five μl aliquots were then spotted on phosphocellulose disks and immersed in 500 ml of 1% (v/v) H_3PO_4 for 5 min. The acid wash was repeated followed by two more washes with distilled water. The phosphocellulose disks were then quantitated for associated radioactivity as described for the IRK activity assay. PKC

specificity was confirmed by using the PKC pseudosubstrate inhibitor peptide PKC (aa 19-36) (Yasuda *et al.*, 1990).

Glycogen synthase activity

Glycogen synthase activities were measured by monitoring the incorporation of [^{14}C]-glucose into glycogen as described by Thomas *et al.*, (1968). Rat livers from overnight fasted animals were removed at various times after the hepatic portal vein injection of 15 µg/100 g BW of insulin or the insulin analog H2 or 10 µg/100 g BW of EGF. Livers (100 mg) were homogenized in 1 ml of homogenization buffer: 50 mM Glycylglycine, 0.5 % Glycogen (w/v), 100 mM NaF, and 20 mM EDTA (pH 7.0). The homogenates were then assayed for glucose-6-phosphate independent glycogen synthase (GSa) and total glycogen synthase (GSa+GSb) activities as described by Thomas *et al.* (1968). Briefly, 20 µl aliquots of homogenates were incubated in 100 µl GSa buffer: 25 mM glycylglycine (pH 7.4), 0.275 mM [U-^{14}C]UDP-glucose (0.12 µci.ml, 0.44 Ci/mol), 1 % glycogen, 1 mM EDTA, 10 mM sodium sulfate for 30 at 30°C. Aliquots (90µl) were spotted on 2 cm^2 ET-31 Whatman papers and washed in 66% (v/v) ethanol at 4°C for 30 min. Two additional washes (30 min each) were then performed at room temperature. Papers were immersed in acetone, dried, and counted for incorporated radioactivity as described for IR kinase ativity. Total glycogen synthase (GSa+b) activity was assayed similarly to GSa with the exception that the reaction mixture contained 5 mM glucose-6-phosphate and lacked sodium sulfate. Activity ratios represent GSa activity divided by total glycogen synthase activity (GSa+b).

JNK activity

Cytosolic fractions (500 µg protein) isolated from rat liver after the injection of 15 µg insulin or H2/ 100 g BW were immunoprecipitated as descibed above with 5 µl of anti-JNK antibodies. The immunocomplexes were washed twice with kinase buffer [10 mM Tris HCl (pH 7.4), 150 mM NaCl, 10 mM $MgCl_2$, 0.5 mM ditiothreitol] and then incubated for 5 min at 37° in 40 µl of kinase buffer containing 1 mM ATP, 2.5 µCi [γ^{32}P]-ATP and 5 µg GST-c-jun. Reactions were stopped by boiling in Laemmli sample preparation buffer and the samples were processed for SDS-PAGE. Following staining with Coommassie brilliant blue, the band corresponding to GST-c-jun was excised from each lane and immersed in Opti-Fluor scintillation fluid and the radioactivity determined using a Beckman LS6000SC β-counter

Ligand radioiodination

Insulin or H2 was radioiodinated to specific activities of 350-380 µCi/µg as described by Frank *et al.* (1983) with some modifications. A 10 µg sample of insulin or H2 [in 10 µl of 0.4 M $NaPO_4$ (pH 7.4)] was added to 100 µl of 2 M urea, 1 mCi Na[^{125}I]

(in 20 µl of 0.1 N NaOH) and 2 µg lactoperoxidase [in 10 µl of 0.4 M sodium phosphate buffer (pH 7.4)]. The reaction was initiated with 10 µl of 0.12 mM hydrogen peroxide and was carried out for 15 min at room temperature. The reaction was stopped by the addition 10 µl 0.25 mM sodium metabisulfite and stabilized with 100 µl BSA (10 mg/ml stock).

HPLC separation of radiolabeled ligands

HPLC analysis was performed as described by Authier *et al.* (1995). Immediately following radioiodination of insulin or H2, the reaction mixture was loaded on a reverse phase HPLC column (Waters µBondapak C18, 0.39 cm x 0.39 cm, 10 µm particle size) and chromatographed with a mixture of 0.1 % (v/v) TFA in HPLC grade water (solvent A) and 0.1 % (v/v) TFA in acetonitrile (solvent B) as eluant, at a flow rate of 2 ml/min. Elution was performed by isocratic elution of 30% solvent B. Eluates were monitored on-line for absorbance at 280 nm with an LC spectrophotometer and for radioactivity with a radioisotope detector (Beckman, model 170). The major components in the eluates (peaks II and IV; see Chapter 2) were collected and freeze-dried.

Automated Edman degradation

To ensure identity of the radiolabeled tyrosine residue in the H2 analog molecule, a mixture of peak IV (2 x 10^6 cpm) and ~300 pmol of the native H2 analog (see above) were subjected to N-terminal sequencing with an Applied Biosystems model 476A analyser as previously described (Authier *et al.*, 1991).

Intra-endosomal processing of [^{125}I]-labeled insulin or H2

Ligand dissociation assay

Dissociation of [^{125}I]-labeled ligands from the endosomal IR was assessed by precipitation with polyethylene glycol (PEG) in the absence or presence of the detergent Brij-35, as previously described by Pease *et al.* (1987). In intact endosomes, both receptor-bound and free intraluminal ligands are PEG-precipitable. In Brij-35-permeabilized endosomes, only receptor-bound ligands remain PEG-precipitable. After incubation of endosomal fractions containing [^{125}I]-labeled insulin or H2 for 5 min in buffered 0.15 M KCl at 37°C, Brij-35 (0.1 % final) or KCl (0.15M) was added. After 10 min at 4 °C with constant shaking, a PEG solution (12.5% w/v) in 50 mM Tris/HCl buffer containing bovine γ-globulin (1 mg per sample) was added, and the resulting precipitate was pelleted and counted for radioactivity in a 1282 LKB γ-counter.

Ligand degradation assay

Endosomal fractions (50 µg) isolated in the absence of protease inhibitors 4 min after the injection of [^{125}I]-labeled ligands was suspended at a concentration of 1 mg/ml in 0.15 M KCl containing 5 mM $MgCl_2$, 50 mM citrate phosphate buffer (pH 3-8.5), and,

where indicated, 1mM ATP. Sample were incubated at 37°C for 0-60 min, after which the integrity of the ligands was assessed by precipitation with TCA as described by Authier *et al.* (1995). This was performed by the addition of two ml of ice-cold TCA to each sample followed by incubation for 15 min at 4°C. The samples were then centrifuged at 10,000 x g_{av} for 20 min at 4°C, and the resulting supernatants and pellets were assessed for radioactivity using a 1282 LKB γ-counter.

HPLC analysis of insulin and H2 degradation by the solubilized GE (SGE) fraction

GE fractions were isolated as described above (Subcellular Fractionation) in the absence of protease or phosphatase inhibitors. The soluble GE extract (SGE) from the endosomes was isolated by freeze/ thawing in 5 mM sodium phosphate (pH 7.4) followed by disruption with a small Dounce homogenizer (15 strokes with a tight type A pestle). Following centrifugation at 300,000 x g_{av} for 30 min, soluble proteins (~0.01 μg) were incubated with 10^{-6} M insulin or the insulin analog, H2, in 0.25 ml of 62.5 mM citrate-phosphate buffer (pH 5.0) for 2 hr. The samples were then acidified with acetic acid (20% final) and immediately loaded onto a reverse-phase HPLC column (Waters, μBondapak C18). Elution was performed by using two sequential linear gradients with the same solvents as described for the purification of native radiolabeled isomers: first, a gradient of 0-20% (v/v) solvent B was achieved within 15min followed by a gradient of 20-45% (v/v) solvent B achieved by 70 min post-loading. HPLC analysis was carried out with detection at 214 nm using a Beckman spectrophotometer (model 166). The control incubations were carried as described above, in the absence of endosomal fraction proteins.

Table 1. Antibodies for Immunoprecipitation and Western Blotting (part 1 of 2)

Antibody	Raised to:	Type	Specificity	Dilution	Source
anti-EGFR(IgG 151)	Extracellular domain of the EGFR	monoclonal	170 kDa EGFR	1:200 - 1:500*	Lai *et al.*, 1989
anti-EGFR	Synthetic peptide corresponding to residues 1164-1176 of the EGFR	polyclonal	170 kDa EGFR	1:1000	Wada *et al.*, 1992
anti-ERK 1 (C-16)	Amino acids 352-367 at c-terminus of rat MAPK p44	polyclonal	p44 ERK 1		Santa Cruz
anti-FAK	Residues 354-533 of chicken FAK	monoclonal	125 kDa FAK		Transduction Laboratories
anti-FAK 2A7	Purified PY protein from chicken embryo cells	monoclonal	125 kDa FAK	2ml/250mg fraction protein	Dr. J.T. Parsons
anti-GAP	TRP E fusion protein (residues 171-448) of human GAP	polyclonal	120 kDa GAP		UBI
anti-GRB2	Full length murine GRB2	polyclonal	23 kDa GRB2		UBI
anti-Insulin Receptor β subunit (α 960)	Synthetic peptide to residues 942-969 of the β-subunit of the insulin receptor	polyclonal	94 kDa β-subunit of the insulin receptor	1:500 1:200*	Burgess *et al.*, 1992
anti-IRS-1 (JD66)	Synthetic peptide to residues1221-1235 of C-term of IRS-1	polyclonal	185 kDa IRS-1	1:500 1:100*	Dr. M.F. White
anti-JNK (FL)	Full length human JNK1	polyclonal	p46 JNK1, p54 JNK2, JNK3		Santa Cruz
anti-MAPK	Synthetic peptide corresponding to residues 333-367 of rat Erk 1	polyclonal	44, 43 and 42 kDa isoforms of MAPK		UBI

Dilutions indicated are used for immunoblotting while the asterisk (*) indicates the dilution used in immunoprecipitation protocols. Where no dilution is indicated the concentration of antibody used was as recommended by the supplier.

Table 1. Antibodies for Immunoprecipitation and Western Blotting (part 2 of 2)

Antibody	Raised to:	Type	Specificity	Dilution	Source
anti-Phosphotyrosine	Phosphotyrosine-BSA	monoclonal	Phosphotyrosine containing proteins		Sigma
anti- PKC Isozymes	Peptides corresponding to specific regions of α, β, γ, δ, ε, ζ isozymes of PKC	polyclonal	α, β, γ, δ, ε, ζ isozymes of PKC		Gibco BRL
anti-Raf-1	Peptide to 12 C-terminal residues of Raf-1	polyclonal	74 kDa Raf-1		Santa Cruz
anti-SHC	SH2 domain of SHC (residues 366-473)	polyclonal	46, 55, and 66 kDa isoforms of SHC	1:1000 1:250 - 1:500*	Dr. T. Pawson
anti-SOS 1	C-terminal region of murine SOS1	polyclonal	175 kDa mSOS1		UBI
anti- p190	Recombinant human p190	monoclonal	p190 Rho GAP		Transduction Laboratories
anti-PY 1173	Residues 1247-1260 of the activated neu receptor	polyclonal	EGFR phosphorylated on Y-1173	1:750	Dr. D. Stern

Dilutions indicated are used for Western blotting while the asterisk (*) indicates the dilution used in immunoprecipitation protocols. Where no dilution is indicated the concentration of antibody used was as described by the supplier.

Table 2 Subcellular fractionation - Protein yields

Fraction	Yield (mg/g liver)	n
Cytosol	44.8 ± 7.5	55
Total Particulate	66.1 ± 8.4	29
Plasma membrane	2.7 ± 1.0	41
GE	0.4 ± 0.1	52

Rat liver homogenates were fractionated into cytosol and total particulate fractions, purified plasma membranes or GE fractions. The yield of protein (mean ± SD) is indicated as well as the number of fractionations performed (n).

Chapter 1
EGF and insulin receptor traffic and signal transduction in rat liver

Introduction

Liver parenchyma is a major target organ enriched in insulin and EGF receptors (Kahn *et al.*, 1974; Bergeron *et al.*, 1980; Cohen *et al.*, 1980). Morphological, subcellular fractionation and biochemical studies with this system have been used as a physiological model to assess receptor traffic (Geuze *et al.*, 1984), receptor activation (Kay *et al.*, 1986; Khan *et al.*, 1986) and the relationship between receptor compartmentalization as a consequence of ligand-mediated receptor endocytosis and signal transduction (reviewed by Bergeron *et al.*, 1995; Di Guglielmo *et al.*, 1998). As a consequence of these studies, a major physiological substrate for the EGFR tyrosine kinase was uncovered and termed pyp55 (Wada *et al.*, 1992; or pp55 by Donaldson and Cohen, 1992) and has been shown to be the PTB/SH2-containing adaptor protein SHC (Ruff-Jamison *et al.*, 1993; Di Guglielmo *et al.*, 1994).

In mammalian cells, SHC and GRB2 have been demonstrated to act as adaptors in the signaling pathway from the EGFR to Ras. The IR has also been shown to activate Ras in cell culture via IRS-1, SHC and GRB2/SOS (see Literature Review). The utilization of similar signaling pathways for the EGFR and IR is remarkable since their physiological responses are different. The acute action of insulin is related to metabolic effects, such as the regulation of glycogen formation and the maintenance of blood glucose homeostasis (Mortimore *et al.*, 1967). Although less well defined, activation of the EGFR in adult liver has been linked to organ repair through increased mitogenesis (Fausto, 1995). The aim of this chapter was to study IR and EGFR signal transduction in order to assess if both RTKs are able to access the Ras pathway in a physiological target tissue.

In the absence of ligand the majority of insulin and EGF receptors are found at the cell surface; however, upon ligand binding, the cognate receptors rapidly internalize into endosomes. Ligand mediated receptor endocytosis may be expected to attenuate Ras activation since Ras is located at the plasma membrane (Willingham *et al.*, 1980). Therefore the second aim of this chapter was to assess the relationship between RTK internalization and signaling.

A preparative subcellular fractionation approach was used to assess the hypothesis that receptor internalization into endosomes regulates the specificity of IR and EGFR signal transduction and the selection of signaling constituents of the Ras pathway.

Results

The injection of EGF or insulin into the hepatic portal circulation of young adult rats leads to the rapid autophosphorylation of their respective RTKs. Coincident with this is the immediate internalization of the RTKs into endosomes. To study the relationship between receptor trafficking and signaling, we isolated hepatic subcellular fractions and evaluated them for the presence of tyrosine phosphorylated and/or receptor associated signaling molecules as a consequence of ligand administration. Established protocols were followed to prepare plasma membrane (PM) and endosomal (GE) fractions which have been shown to be virtually free of cross contamination (Dunn and Hubbard, 1984; Khan *et al.*, 1986; Kay *et al.*, 1986; Lai *et al.*, 1989a,b; Doherty *et al.*, 1990; Wada *et al.*, 1992).

Receptor redistribution in subcellular fractions in response to ligand

Rat liver PM and GE fractions were isolated following the intraportal injection of a single receptor saturating dose of EGF [10 μg/ 100 g body weight (BW)] or insulin (15 μg/100 g BW). The relative amount of receptors in these fractions was assessed by immunoblotting with anti-EGFR or anti-IR β subunit antibodies (Figure 4A and B) and quantitated by phosphoimaging (Figure 4C and D). The initial $t_{1/2}$ of both EGFR or IR internalization was ~1 min in response to their respective ligands. The reduction of the EGFR signal in the PM fraction was 66% and occurred within 15 min of ligand administration (Figure 4C). In response to insulin the amount of IR loss from the PM compartment was 39% and was achieved within 5 min of ligand administration (Figure 4D). The reduced amounts of EGFR and IR in the PM were observed up to 60 min after ligand administration as previously described for receptor saturating doses of ligand (Lai *et al.*, 1989a; Burgess *et al.*, 1992).

Challenge with cognate ligands induced EGFR and IR accumulation in the GE fraction (Figure 4A and B, lanes 7-12). In response to EGF, the EGFR content in endosomes increased and peaked at 15 min post injection (Figure 4C). After 60 min of ligand administration the EGFR content in the GE remained 3-fold over the control. In response to insulin, the IR content in endosomes peaked 5 min post injection and decreased to near basal levels within 60 min (Figure 4D).

EGF and insulin receptor phosphorylation in response to ligand

The administration of a receptor saturating dose of EGF to the hepatic circulation of rats stimulated the tyrosine phosphorylation of two polypeptides of 170 kDa and 55 kDa in the PM and GE fractions (Figure 5A), previously demonstrated to be the phosphorylated EGFR and its major associated substrate in liver, pyp55 (Wada *et al.*, 1992; Donaldson and

Cohen, 1992). Both the EGFR and pyp55 were maximally phosphorylated within 30 sec in the PM fraction (Figure 5A, lane 2), while peak phosphotyrosine modification of these two proteins occurred 15 min after ligand administration in GE fraction (Figure 5A, lane 10). Other less prominent phosphotyrosine modified proteins were evident in the GE fraction in response to EGF. In response to insulin one major phosphotyrosine band of 94 kDa was observed in the PM fraction (Figure 5B, lane 2). This 94 kDa phosphoprotein was previously shown to be the β subunit of the IR (Burgess *et al.*, 1992).

The amounts of tyrosine phosphorylated EGFR and IR in PM and GE fractions were quantitated by phosphoimaging and plotted as arbitrary units per gram of liver, taking into account the yield and recoveries of the PM and GE fractions (Figure 5C and D). The EGFR was found to be the most highly phosphorylated in the GE fraction 15 min post ligand injection (Figure 5C). In contrast, the IR was mainly phosphorylated in the PM fraction and to a much lesser degree in GE fractions (Figure 5D). Therefore, despite an equal number of EGF and insulin receptors in liver parenchyma, a clear cut distinction was found between the intensity of signaling as evaluated by anti-phosphotyrosine immunoblotting (with EGFR > IR) and the compartments harboring the highest concentration of ligand dependent autophosphorylated receptor (the PM fraction for the IR and the GE fraction for the EGFR).

The major site of EGFR activation *in vivo* is phosphotyrosine (PY) 1173 (Downward *et al.*, 1984). Immunoblotting of PM and GE fractions with the phosphopeptide specific antibody (Pep(P) of Bangalore *et al.*, 1992) verified that the liver parenchymal EGFR was tyrosine phosphorylated at this site in response to EGF stimulation (Figure 5E). Moreover both the PM and GE fractions contained activated EGFR in response to ligand.

Since the EGFR was activated as early as 30 sec at the PM and extended to the GE fraction, we assessed SHC recruitment in PM and GE fractions as a function of EGF administration *in vivo* (Figure 6A). Two polypeptides of 46 and 55 kDa were found to associate with the PM in an EGF dependent manner. These corresponded to the two isoforms of SHC described by Pelicci *et al.* (1992). Additionally, in endosomes, the third polypeptide recognized by the antiserum, the 66 kDa isoform of SHC, was also recruited in an EGF dependent fashion.

The association of the adaptor protein GRB2 with the EGFR, phosphorylated at tyrosine residue 1068, as well as with phosphorylated SHC has been demonstrated to activate Ras through a physical link with SOS (see Literature Review). We therefore evaluated GRB2 recruitment to the activated EGFR in PM and GE fractions. Little detectable signal was observed in the PM (Figure 6C, lanes 1-6). In contrast, the

recruitment of GRB2 to endosomes was observed at the peak time of 15 min post EGF injection (Figure 6C). In response to insulin neither SHC nor GRB2 were recruited to PM or GE fractions (Figure 6B and D).

To evaluate if SHC and GRB2 are associated with the EGFR in the GE fractions, co-immunoprecipitation studies were carried out (Figure 7). Immunoprecipitation of the EGFR from control endosomes and endosomes isolated 15 min after EGF injection (Figure 7A-D, lanes 3 and 4) was carried out with the monoclonal anti-EGFR antibody IgG 151 (Lai *et al.*, 1989a). This was followed by immunoblotting with antibodies raised to phosphotyrosine (Figure 7A), the phosphopeptide encompassing the PY-1173 of the EGFR (Figure 7B), SHC (Figure 7C), GRB2 (Figure 7D) and SOS (Figure 7E). Immunoprecipitation and immunoblotting was also performed on GE fractions isolated 15 min after insulin injection (Figure 7A-D, lane 5) with no detectable signal observed above the control. These observations, when compared to the non-immunoprecipitated endosomal fractions isolated at 0 or 15 min after EGF injection (Figure 7A-D, lanes 1 and 2), demonstrate identical mobilities for the EGF specific immunoreactive polypeptides.

The EGFR was shown to be associated with pyp55, SHC and GRB2 in endosomes in a ligand dependent manner (Figure 7). To evaluate if these constituents were part of the same complex or if complexes of EGFR/SHC were distinct from those of the EGFR associated with pyp55 or GRB2, immunoprecipitation of solubilized endosomes with anti-SHC antibodies was followed by immunoblotting with anti-SHC (Figure 8A) or anti-GRB2 antibodies (Figure 8B). All three isoforms of SHC as well as GRB2 were found in the SHC immunoprecipitates in an EGF dependent manner. We therefore confirm that phosphotyrosine modified SHC (PY-SHC), GRB2 and the activated EGFR were in oligomeric association in the same complex on the endosomal membrane.

To quantitate the amount of tyrosine phosphorylated SHC and GRB2 recruited to PM and GE fractions in response to EGF, PM and GE fractions were immunoblotted as described in Figure 6 followed by phosphoimaging analysis (Figure 9). In response to EGF, a 3-fold recruitment of SHC was observed at the PM within 30 sec of ligand administration (Figure 9A). The amount of SHC that was present in the GE fraction was lower than that recruited to the PM fraction. The phosphorylation of SHC was also quantitated and plotted (Figure 9B). The largest pool of phosphorylated SHC was associated with the endosome and the maximum phosphorylation was 15 min after EGF administration. The ratio of phosphotyrosine modified SHC per molecule of SHC revealed a significantly higher level ($P < 0.001$) of phosphorylation in endosomes as compared to PM (Figure 9C). This is consistent with recruitment of SHC to the PM leading to partial tyrosine phosphorylation of SHC at this locus but with more extensive tyrosine

phosphorylation occurring during internalization into endosomes. The phosphotyrosine content of SHC was more pronounced in endosomes consistent with phosphorylation occurring at this locus. Remarkably, GRB2 was more prominently associated with endosomes than with the PM (Figure 9D).

Although the EGFR is exclusively membrane bound, several of its associated substrates i.e., GRB2 and SHC, are largely cytosolic. We therefore evaluated rat liver cytosol for its content of tyrosine phosphorylated proteins following EGF administration (Figure 10). Of the three major cytosolic proteins which were tyrosine phosphorylated, two were EGF dependent (120 kDa and 55 kDa) and one was constitutively present (190 kDa) and was virtually unchanged after insulin injection. The 55 kDa phosphoprotein was quantitated and was seen to be maximally phosphorylated 5 min after EGF administration (Figure 10B).

The identity of the cytosolic 120 kDa phosphotyrosine modified polypeptide was addressed. Immunoprecipitation with anti-RasGAP followed by immunoblotting with anti-RasGAP or anti-PY indicated that RasGAP was not the 120 kDa phosphoprotein (Figure 11A). However, the constitutively tyrosine phosphorylated 190 kDa polypeptide, was co-immunoprecipitated with RasGAP (Figure 11A) indicating that this polypeptide is RhoGAP, which has been observed to be associated with RasGAP when phosphorylated (Settleman *et al.*, 1992a,b). Cytosolic fractions were immunoprecipitated with anti-PY antibodies and immunoblotted with the pp120$^{c\text{-}src}$ substrate, unrelated to RasGAP, shown to be rapidly phosphorylated after growth factor stimulation (Downing and Reynolds, 1991). However, when cytosolic fractions were immunoprecipitated with anti-phosphotyrosine antibodies and immunoblotted with pp120 this polypeptide was not immunoreactive. The immunoprecipitates were also immunoblotted with anti-FAK antibodies and were found to give a positive signal (Figure 11B). Indeed, immunoprecipitating FAK from cytosol after the administration of EGF demonstrated that FAK was phosphorylated up to 60 min post ligand administration (Figure 11C). However, the amount of PY-modified FAK was small and there may be other phosphoproteins that may make up the pyp120 signal.

Ras-Map kinase cascade and nuclear transcription

The identity of the cytosolic 55 kDa phosphoprotein was attempted by immunoprecipitation and immunoblotting studies. Rat liver cytosolic fractions isolated after the injection of EGF were immunoprecipitated with anti-SHC antibodies and immunoblotted with anti-phosphotyrosine antibodies (Figure 12A). The cytosolic 55 kDa phosphoprotein corresponded to phosphotyrosine-modified SHC. Since SHC was

phosphorylated in the cytosol, we assessed if it was in a complex with GRB2 and SOS. Both GRB2 and SOS coprecipitated with the same kinetics of association as found for the tyrosine phosphorylation of SHC (Figure 12B and C).

Tyrosine phosphorylation of SHC and the association of GRB2 with the EGFR has been a hallmark of the upstream events leading to Ras activation (see Literature Review). Direct quantitation of GDP and GTP content of Ras was difficult to attempt due to the limitations of using rat liver. We therefore undertook an indirect method by measuring the relative mobilities of the downstream effectors, Raf-1 and MAP kinase, in SDS-PAGE. In response to a number of growth factors, both Raf-1 and MAP kinase are phosphorylated on serine residues and exhibit lagging mobilities in SDS-PAGE gels (Wartmann *et al.*, 1997). In the case of MAP kinase, this mobility shift is characteristic of activity. For Raf-1, mobility shifts are more unclear, although it has been suggested that serine phosphorylation of this molecule is part of a feed-back mechanism that inactivates this molecule (Wartmann *et al.*, 1997). In response to EGF but not insulin both Raf-1 and MAP kinase were shifted in SDS-PAGE (Figure 13). Approximately 40% of Raf-1 was hyperphosphorylated in response to EGF and was observed within 5 min and extended to 60 min after EGF injection (Figure 13B).

Once stimulated, MAP kinase phosphorylates a number of cytosolic proteins and/or translocates into the nucleus where it influences gene transcription by phosphorylating transcription factors (reviewed by Vojtek and Der, 1998). To assess nuclear transcription in response to EGF or insulin, total RNA from control rat livers or rat livers isolated after ligand administration was electrophoresed and Northern blotted with cDNA probes to the early response genes c-myc (Figure 14A), c-fos (Figure 14B) or c-jun (Figure 14C). The 2.4 kb c-myc, 2.2 kb c-fos and 2.5 kb c-jun transcripts were quantitated by phosphoimaging and demonstrate that EGF induced increases in all three transcripts within 30 min of ligand administration but insulin had little effect (Figure 14D-F).

From these results a pattern of signal transduction from the activated EGFR in rat liver has been shown to differ from the activated IR. These differences are based on signaling potential at the PM, endosome, and cytosol as well as substrate specificity.

Discussion

The assessment of compartmentalization during receptor signaling has revealed specific regulation *in vivo* during the early phases (0-15 min) of ligand-mediated EGFR internalization. First, a complex of activated EGFR and phosphotyrosine (PY)-modified SHC/GRB2/SOS was observed in endosomes. Second, a long lived signaling intermediate, consisting of a complex of PY-SHC/GRB2/SOS was uncovered in the cytosolic compartment. Remarkably, although tyrosine phosphorylation of SHC and association with GRB2/SOS was demonstrated to be a consequence of the activated EGFR, no comparable activation of these constituents were observed by the IR in liver parenchyma. Third, the specificity of signaling was clearly demonstrated by the prolonged hyperphosphorylation of Raf-1 and MAP kinase, and in nuclear transcription of c-myc, c-fos and c-jun after EGF but not insulin administration.

Electron microscopy, marker enzyme analysis (Khan *et al.*, 1986), the direct visualization of internalized [^{125}I]EGF by quantitative electron microscopy radioautography (Lai *et al.*, 1989b), latency studies for receptor kinase stimulation (Kay *et al.*, 1986) and proteinase sensitivity assays (Wada *et al.*, 1992) have all established that the endosome preparation is virtually free by plasma membrane fragments. Endosomes were the major particulate compartment which recruited GRB2 in response to EGF. The complex of PY1173 modified EGFR/PY-SHC/GRB2 and SOS represent the first evidence for such a complex *in vivo*. The physiological relevance for such a complex is probably related to Ras activation. GRB2 has been demonstrated to activate Ras via a direct physical linkage with activated receptor and SOS (see Literature Review).

Although endosomes are a major site of GRB2 recruitment and SHC phosphorylation, significant levels of both proteins were found associated with the PM up to 30 min post-EGF injection. We propose that the prolonged hyperphosphorylation of Raf-1 and Map kinase mobility shifts in response to EGF may be due to the pool of cytosolic signaling constituents most probably emanating from endosomes at times > 5 min. Such a scenario provides a rationale for the adaptor protein SHC, since this constituent is not a membrane protein and is able to form a signaling complex in the cytosol following its tyrosine phosphorylation. This model has also been used to describe cytosolic signaling in response to Tpr-Met signal transduction (Fixman *et al.*, 1996).

The kinetics of appearance of phosphotyrosine-modified SHC in the cytosol is consistent with its derivation from endosomes, since (1) the phosphotyrosine content of SHC was higher in endosomes than that seen at the peak time of activation in the PM (30 sec) and (2) the overall SHC content of endosomes was less than that found at the cell surface at 30 sec following EGF administration. The association of PY-SHC with GRB2

was previously shown by Rozakis-Adcock and colleagues (1992) to lead to Ras activation. Hence a cytosolic pool of activated PY-SHC/GRB2/SOS would be able to activate Ras regardless of its membrane location. The generation of these cytosolic activated signaling complexes, at times when the EGFR has internalized may increase the temporal window of signaling by activated EGFRs.

The comparatively low level of GRB2 recruited to the activated PM EGFR may be related to receptor traffic. For high efficiency internalization via coated pits, two regions in the cytosolic tail of the EGFR, corresponding to residues 993-1022 and 1024-1186, have been shown to independently restore ligand-mediated high efficiently internalization to receptors truncated at residue 968 (Chang *et al.*, 1993). The latter region, comprising residues 1024-1186, contains major sites of phosphorylation and recruitment of SHC and GRB2. Since the activated EGFR also associates at the cell surface with the clathrin adaptor AP2 (Sorkin and Carpenter, 1993, Nesterov *et al.*, 1995a, Boll *et al.*, 1995), this may lead to competition with the recruitment and/or tyrosine phosphorylation of PTB/SH2 signaling adaptors to the EGFR. We suggest that this may be responsible for the low level of GRB2 recruitment to the activated EGFR at the cell surface although this would not be predicted by studies suggesting that GRB2 assists EGFR internalization.

Tyrosine kinase activity of the EGFR has also been demonstrated to regulate sorting of internalized EGFR. Felder and colleagues (1990) have demonstrated that a kinase-defective point mutation of the EGFR was able to access the boundary of the endosomal membrane following receptor internalization, but was prevented from gaining access to the intraluminal microvesicle population of multivesicular endosomes. They postulated that the EGFR tyrosine phosphorylation of endosomal substrates may regulate this sorting event. The complex of activated EGFR, PY-SHC and GRB2 represents a candidate for the above, as well as having a role, albeit poorly defined in signal transduction at this locus.

In studies employing IRs transfected into CHO cells (CHO-IR cells), COS-1 cells of fibroblasts, tyrosine phosphorylation of SHC and association with GRB2 have been demonstrated (Pronk *et al.*, 1993; Skolnik *et al.*, 1993b). However, despite the similar number or insulin and EGF receptors in livers of young adult male rats (Burgess *et al.*, 1992; Wada *et al.*, 1992), SHC phosphorylation and association with GRB2 was undetected, nor was any Raf-1 mobility shift or nuclear transcription observed. We postulate that liver parenchyma has evolved endosomally directed mechanisms to regulate the specificity of IR and EGFR signal transduction (assessed in the following chapters).

Endosomes contain potent protein phosphatase (PTPase) activity that is capable of dephosphorylating EGF and insulin receptors (Faure *et al.*, 1992). Rat liver endosomes also contain insulin degrading activity (Doherty *et al.*, 1990; Authier *et al.*, 1994; 1998) but

little EGF degrading activity (Doherty *et al.*, 1990; Renfrew and Hubbard, 1991a,b). Indeed, most EGF is receptor-bound in endosomes (Lai *et al.*, 1989a) and may therefore account for the highly phosphorylated state of the EGFR at this locus. In contrast, insulin degradation in endosomes is efficient and would allow for the dephosphorylation of the IR. The studies of Backer *et al.* (1990) support this hypothesis. They find that an endosomal insulinase is absent in CHO cells and this may account for the enhanced tyrosine phosphorylation of the IR in CHO-IR cells and the subsequent phosphorylation of SHC as well as its association with GRB2.

Based on the hypothesis that the degradation of ligand plays a role in the signaling potential of a RTK in the endosome, we will attempt to characterize a recombinantly expressed modified insulin analog, termed H2 (Chapter 2).

Figure 4. Ligand-mediated EGF and insulin receptor internalization in rat liver.

Rat liver plasma membrane (PM) and endosomal (GE) fractions were isolated at the indicated times after EGF (10 μg/100 g body weight; A and C) or insulin (15 μg/100 g body weight; B and D) administration and immunoblotted with antibodies raised to the EGFR (A) or the β subunit of the insulin receptor (B). Each lane in A and B contains the equivalent of 100 μg of PM protein or 50 μg of GE fraction protein. The mobilities of the EGFR and the β subunit of the insulin receptor (IR-β) are indicated on the right. Quantitation of the relative amount of the EGFR (C), and the IR-β (D) in PM and GE fractions was carried out by phosphoimaging. Each point is the mean of 3 separate experiments ± SD expressed as arbitrary phosphoimager units per gram liver corrected for yields and recoveries as described in Materials and Methods.

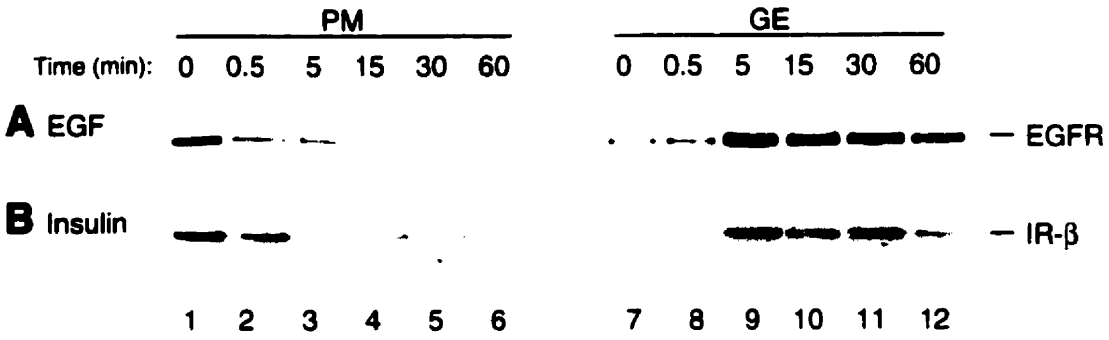
PM
GE
Time (min): 0 0.5 5 15 30 60
0 0.5 5 15 30 60
A EGF
B Insulin
EGFR
IR-β
1 2 3 4 5 6
7 8 9 10 11 12

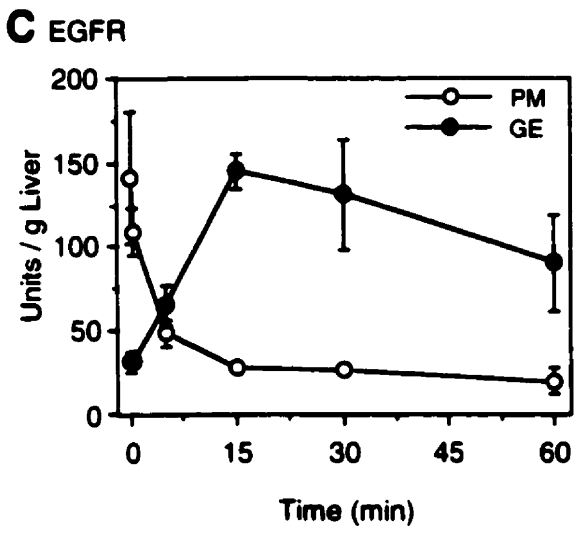
C EGFR
Units / g Liver
200
150
100
50
0
PM
GE
0 15 30 45 60
Time (min)

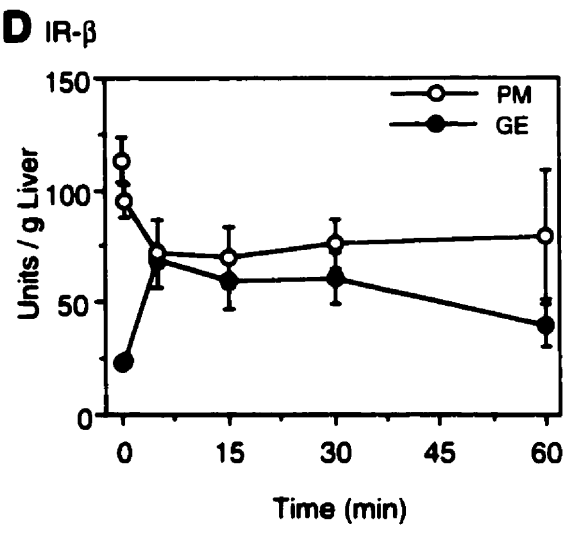
D IR-β
Units / g Liver
150
100
50
0
PM
GE
0 15 30 45 60
Time (min)

Figure 5. Ligand-mediated insulin and EGF receptor tyrosine phosphorylation in rat liver.

Rat liver plasma membrane (PM) and endosomal (GE) fractions were isolated at the indicated times after EGF (10 μg/100 g body weight; A, C and E) or insulin (15 μg/100 g body weight; B and D) administration and immunoblotted with anti-phosphotyrosine (αPY) antibodies (A-D) or antibodies recognizing a phosphopeptide encompassing Y^{1173} of the EGFR (αPY-1173; E). Each lane contains the equivalent of 100 μg of PM or 50 μg of GE fraction protein. The mobilities of the major tyrosine phosphorylated polypeptides are indicated on the right by their apparent molecular weight calculated from the standard molecular weight markers on the left. The relative amount of tyrosine phosphorylated EGFR (170 kDa polypeptide in panel A) and the tyrosine phosphorylated IR-β (94 kDa polypeptide in panel B) were quantitated by phosphoimaging and plotted vs. time in panels C and D. Each point is the mean of 3 separate experiments ± SD expressed as arbitrary phosphoimager units per gram liver corrected for yields and recoveries as described in Materials and Methods.

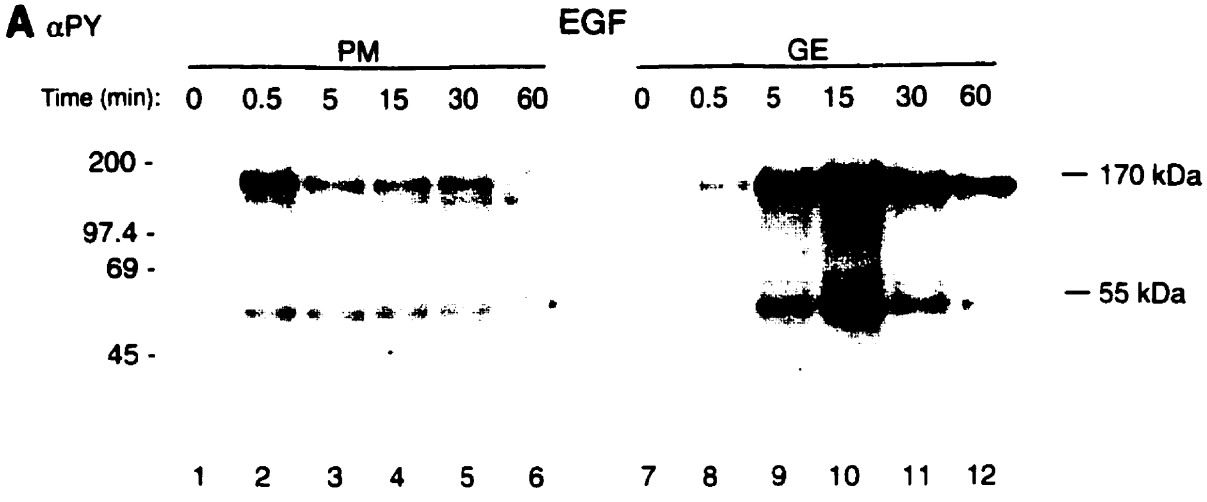
A αPY
EGF
PM
GE
Time (min): 0 0.5 5 15 30 60 0 0.5 5 15 30 60
200 -
97.4 -
69 -
45 -
— 170 kDa
— 55 kDa
1 2 3 4 5 6 7 8 9 10 11 12

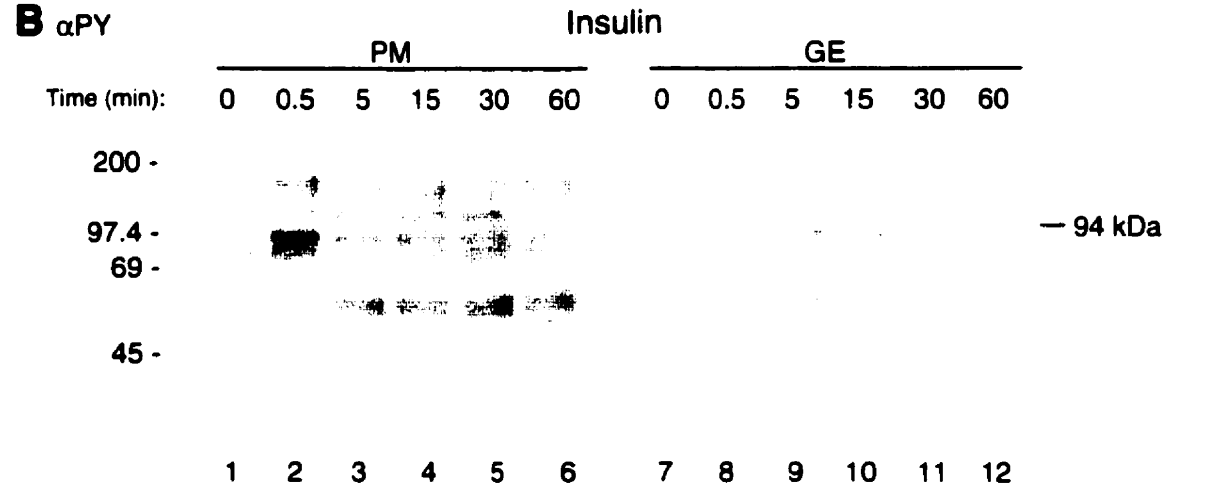
B αPY
Insulin
PM
GE
Time (min): 0 0.5 5 15 30 60 0 0.5 5 15 30 60
200 -
97.4 -
69 -
45 -
— 94 kDa
1 2 3 4 5 6 7 8 9 10 11 12

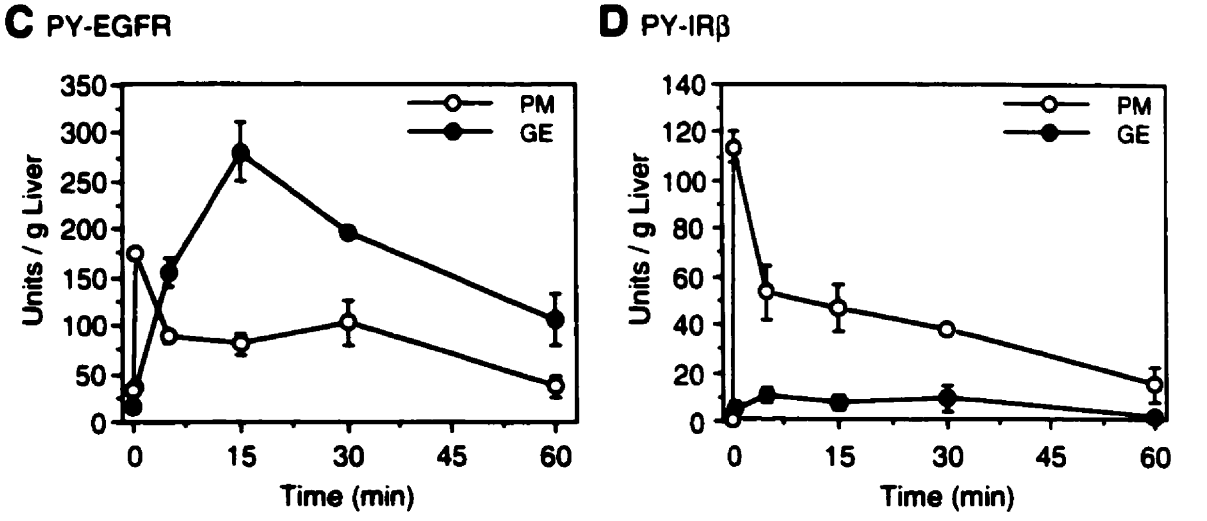
C PY-EGFR
D PY-IRβ
PM
GE
Units / g Liver
Time (min)
0 15 30 45 60
0 50 100 150 200 250 300 350
0 20 40 60 80 100 120 140

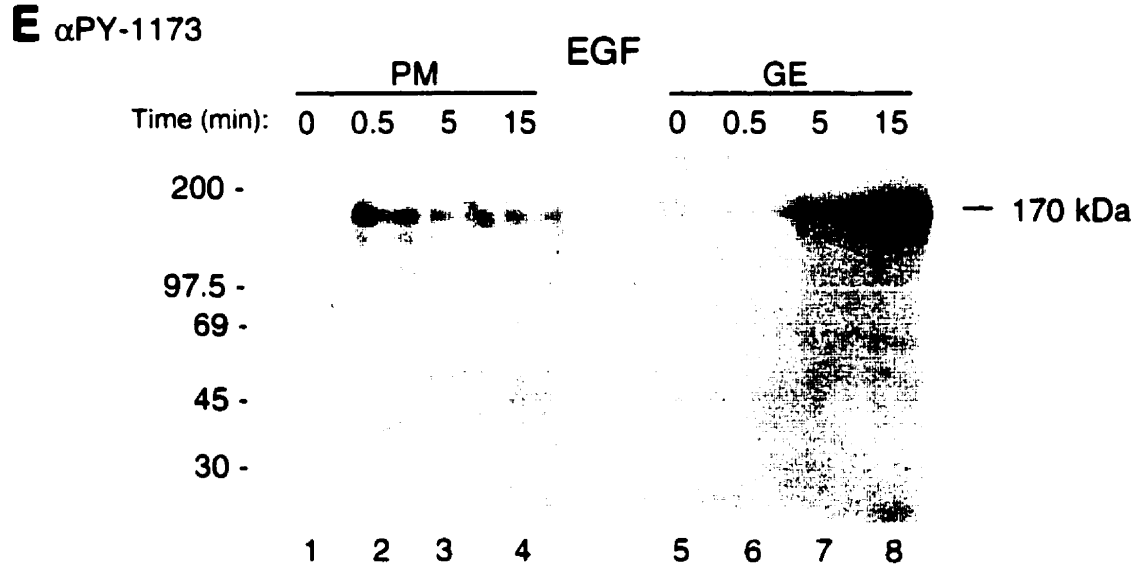
E αPY-1173
EGF
PM
GE
Time (min): 0 0.5 5 15 0 0.5 5 15
200 -
97.5 -
69 -
45 -
30 -
— 170 kDa
1 2 3 4 5 6 7 8

Figure 6. SHC and GRB2 recruitment to plasma membrane and endosomes in response to EGF or insulin administration.

Plasma membrane (PM) or endosomal (GE) fractions were isolated at the indicated times after EGF or insulin administration as described in Figure 1. Samples were immunoblotted with anti-SHC (A and B) or anti-GRB2 (C and D) antibodies. One hundred micrograms of PM or 50 μg GE fraction protein were applied to each lane. The mobilities of the three isoforms of SHC (46, 55, and 66 kDa) and the mobility of GRB2 (26 kDa) are indicated on the right.

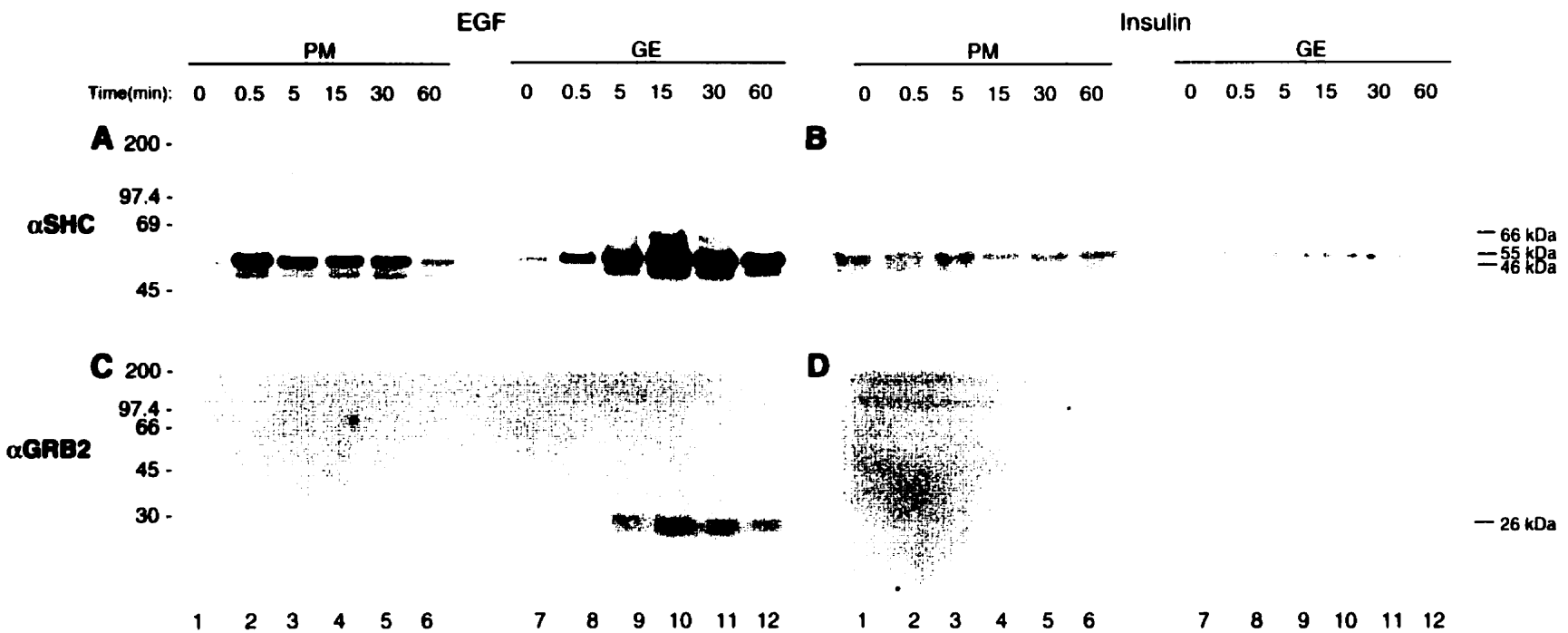
EGF
Insulin
PM
GE
PM
GE
Time(min): 0 0.5 5 15 30 60 0 0.5 5 15 30 60 0 0.5 5 15 30 60 0 0.5 5 15 30 60
A
B
200 -
97.4 -
69 -
45 -
αSHC
66 kDa
55 kDa
46 kDa
C
D
200 -
97.4 -
66 -
45 -
30 -
αGRB2
26 kDa
1 2 3 4 5 6 7 8 9 10 11 12 1 2 3 4 5 6 7 8 9 10 11 12

Figure 7. Internalized EGFR is associated with PY-SHC and GRB2/SOS.

Control endosomal (GE) or GE fractions isolated 15 min after the injection of EGF or insulin were immunoprecipitated with EGFR monoclonal antibody IgG 151 (indicated by IP: αEGFR). The immunoprecipitates were immunoblotted with antibodies raised to phosphotyrosine (αPY; A), the phosphorylated peptide encompassing PY^{1173} of the EGFR (α PY-1173; B), SHC (C), GRB2 (D), or mSOS (E). For panels A-D the non-immunoprecipitated GE fractions from control livers or those isolated 15 min after EGF injection are shown (lanes 1 and 2). The mobilities of the EGFR, SHC (pyp55 or 55 kDa), GRB2 (26 kDa), and mSOS (150 kDa) are indicated on the right. The cross-reactivity between immunoblotting secondary antibodies with the IgG heavy chain present in the immunprecipitates is indicated (IgG H).

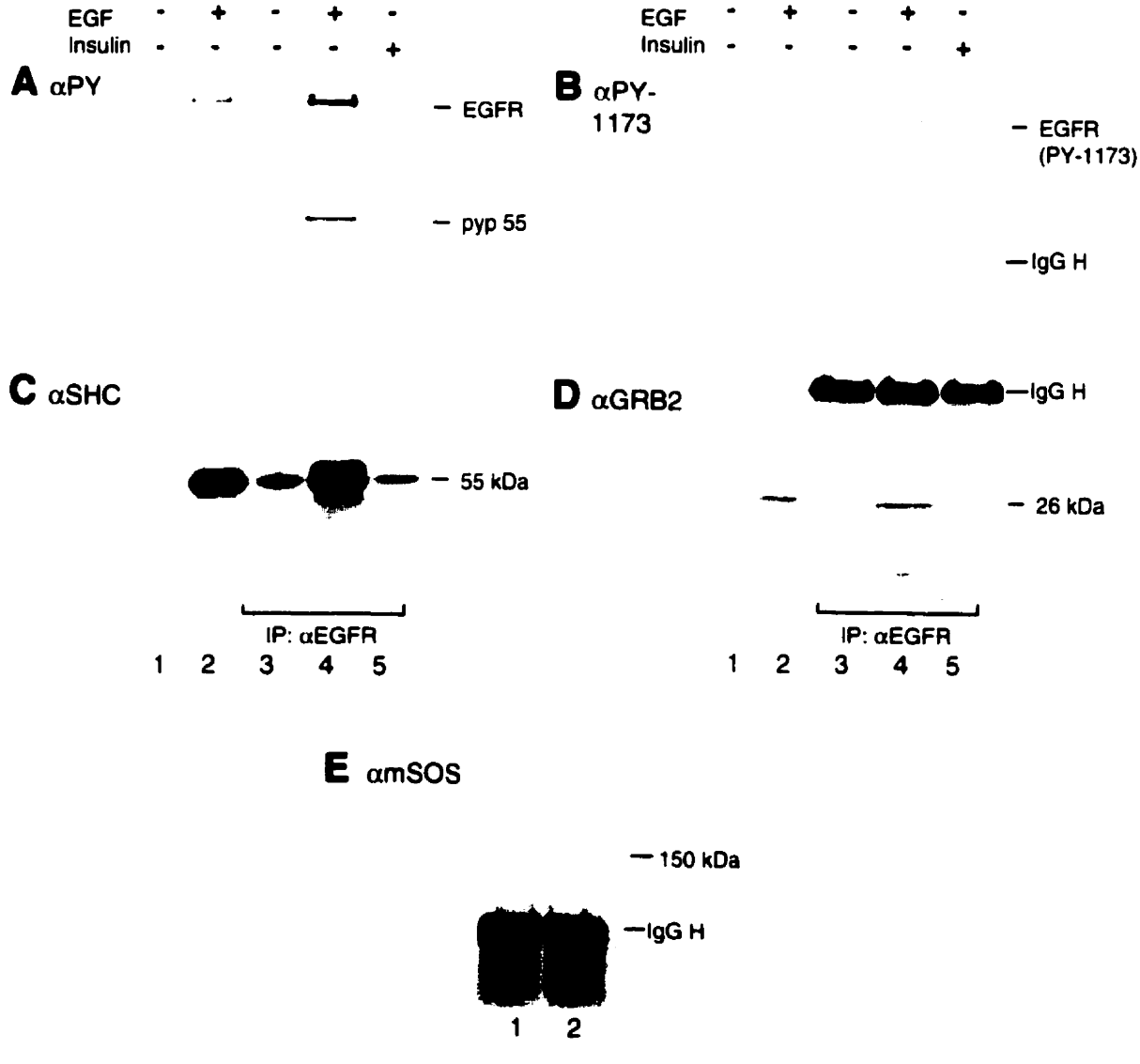
EGF - + - + -
Insulin - - - - +
A αPY
– EGFR
– pyp 55
B αPY-1173
– EGFR (PY-1173)
– IgG H
C αSHC
– 55 kDa
IP: αEGFR
1 2 3 4 5
D αGRB2
– IgG H
– 26 kDa
IP: αEGFR
1 2 3 4 5
E αmSOS
– 150 kDa
– IgG H
1 2

Figure 8. EGF mediated SHC and GRB2 association on endosomal membranes.

Control endosomal (GE) or GE fractions isolated 15 min after the injection of EGF were immunoprecipitated with anti-SHC antibodies (indicated by IP:αSHC). Immunoprecipitates were immunoblotted with antibodies to SHC (A) or GRB2 (B). The non-immunoprecipitated GE fractions from control livers or GE isolated 15 min after EGF injection are shown (A and B, lanes 1 and 2). The relative mobilities of the 3 isoforms of SHC (46, 55, and 66 kDa) and GRB2 (26 kDa) are indicated on the right. The cross-reactivity between immunoblotting IgG and immunoprecipitation IgG light chain is indicated (L).

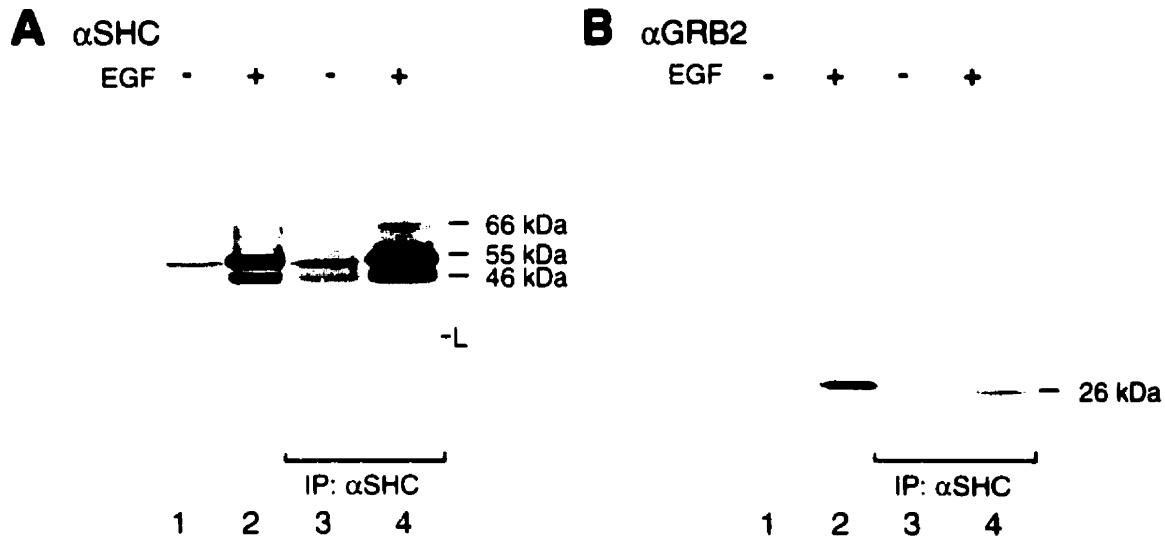
A αSHC
EGF - + - +
66 kDa
55 kDa
46 kDa
-L
IP: αSHC
1 2 3 4
B αGRB2
EGF - + - +
26 kDa
IP: αSHC
1 2 3 4

Figure 9. Quantitation of SHC and GRB2 recruitment, and SHC phosphorylation in plasma membranes or endosomes in response to EGF.

Immunoblotting of plasma membrane (PM) or endosomal (GE) fractions was performed as described in Figure 3. Quantitation was carried out by phosphoimaging of the amount of the 55 kDa isoform of SHC (A), the phosphotyrosine modified 55 kDa SHC (B), or the content of the adaptor protein GRB2 (D) in PM and GE fractions at the indicated times after EGF administration. Each point is the mean of 3 separate experiments ± SD expressed as phosphoimager units per gram liver corrected for yields and recoveries as described in Materials and Methods. The ratio of PY-SHC/SHC was quantitated for the timepoints 0.5 and 15 min in PM and GE fractions (C).

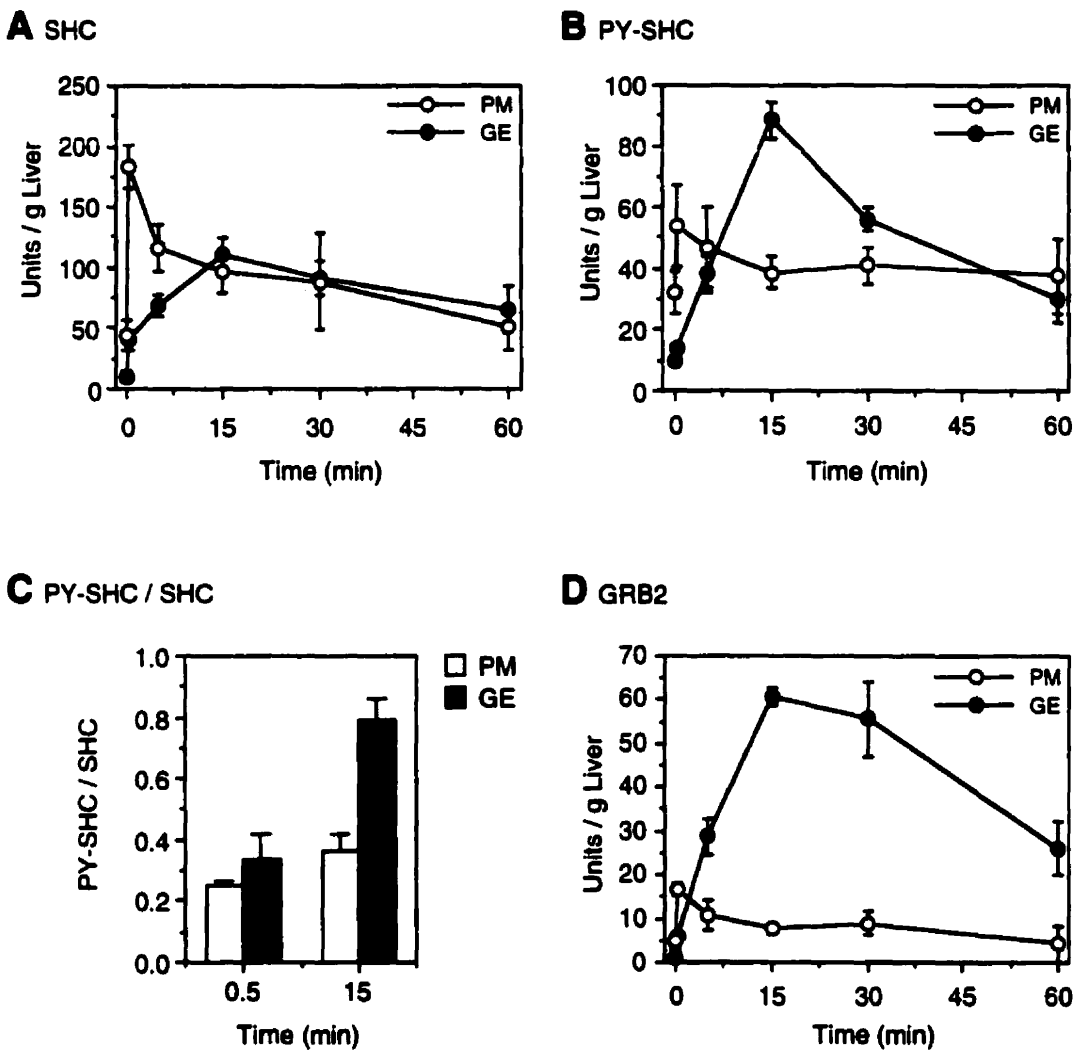
A SHC
B PY-SHC
C PY-SHC / SHC
D GRB2
PM
GE
Units / g Liver
PY-SHC / SHC
Time (min)
0
15
30
45
60
0.5
0.0
0.2
0.4
0.6
0.8
1.0
10
20
40
50
70
80
100
150
200
250

Figure 10. Phosphotyrosine protein profile in rat liver cytosolic fractions in response to EGF or insulin administration.

Control rat liver cytosol or cytosol isolated 0.5-60 min after the administration of receptor saturating doses of EGF (10 μg/100 g body weight) or insulin (15 μg/100 g body weight) were immunoblotted with anti-phosphotyrosine (αPY) antibodies (A). Each lane contains the equivalent of 300 μg of fraction protein. The mobilities of the three major phosphotyrosine proteins (55, 120 and 190 kDa) are indicated. The cytosolic 55 kDa phosphoprotein was quantitated by phosphoimaging and expressed as arbitrary units per gram liver of three experiments ± SD (B).

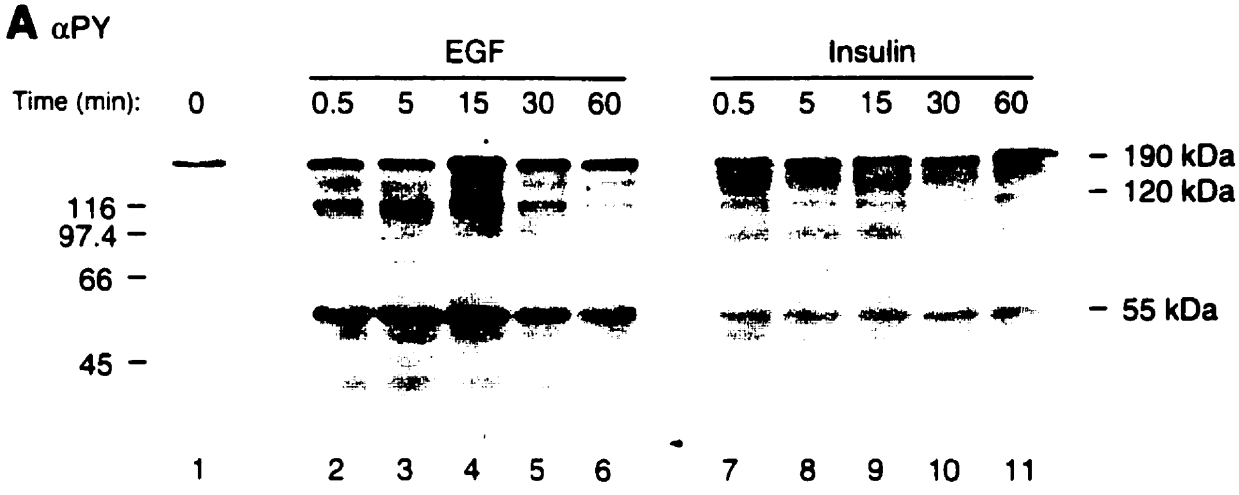
A αPY
EGF
Insulin
Time (min):
0
0.5
5
15
30
60
0.5
5
15
30
60
116
97.4
66
45
190 kDa
120 kDa
55 kDa
1
2
3
4
5
6
7
8
9
10
11

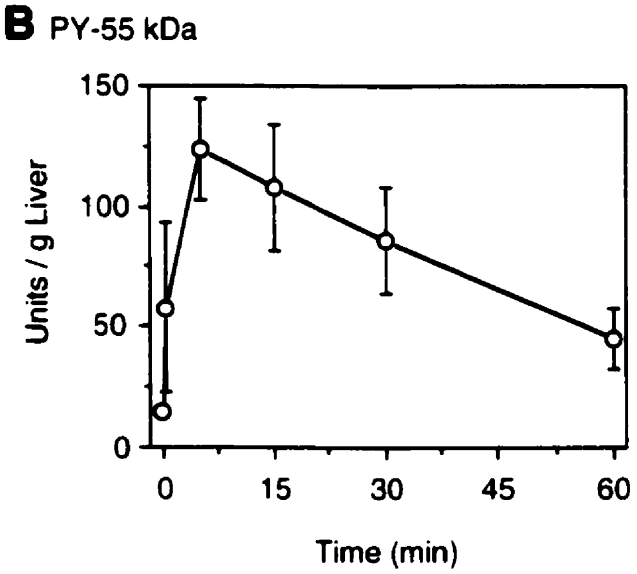
B PY-55 kDa
Units / g Liver
150
100
50
0
0
15
30
45
60
Time (min)

Figure 11. EGF-mediated tyrosine phosphorylation of FAK in rat liver cytosol.

Cytosolic fractions isolated after EGF administration were immunoprecipitated with anti-GAP (A), anti-phosphotyrosine (αPY) (B), or anti-FAK (C) antibodies and immunoblotted with anti-GAP, αPY and anti-RhoGAP antibodies (A); αPY, anti-pp120$^{c\text{-}src}$ and anti-FAK antibodies (B); or anti-FAK and αPY antibodies (C). The crossreactivity of immunoprecipitating IgG heavy chain and immunoblotting secondary antibody is indicated (IgG H).

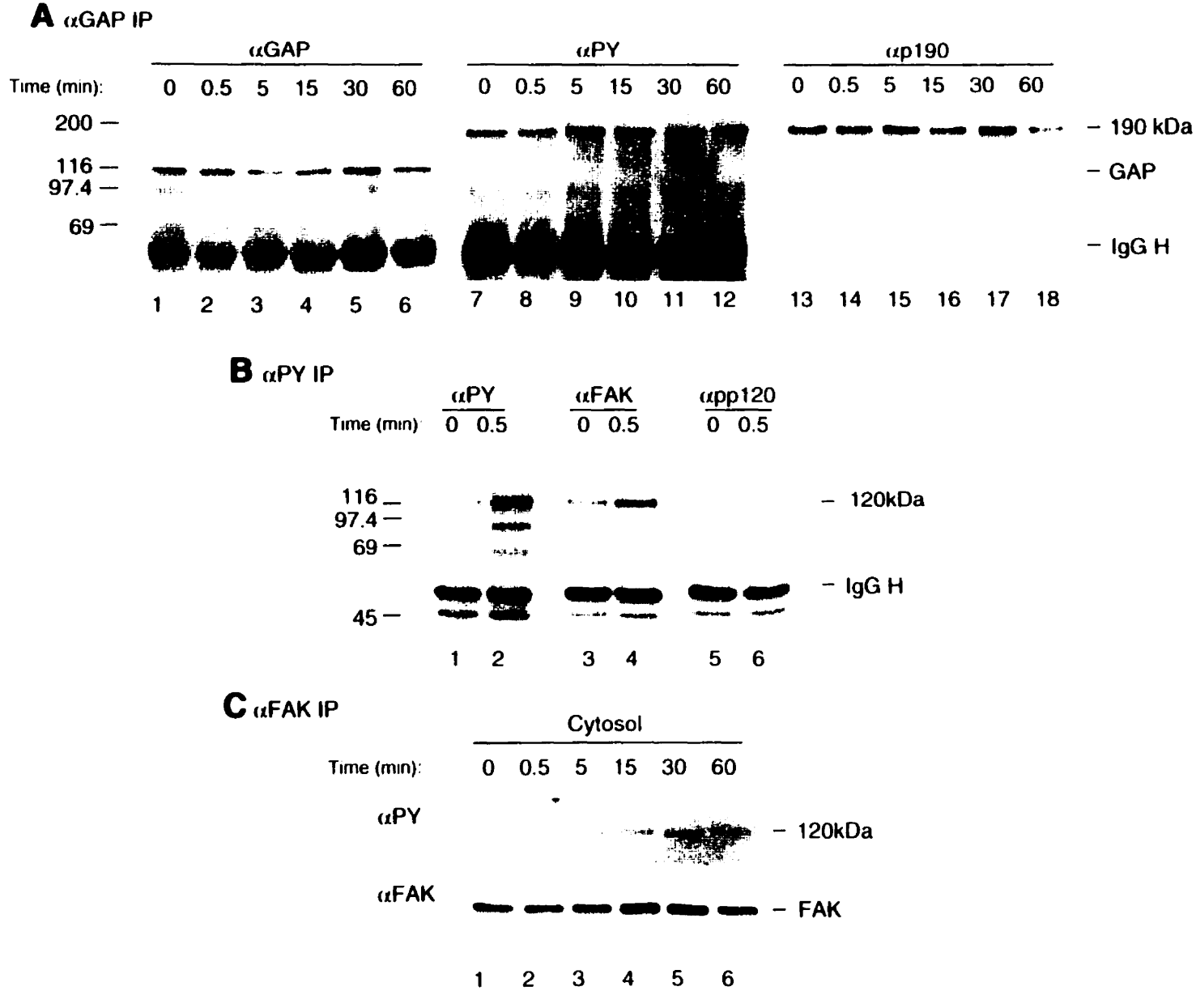
A αGAP IP
αGAP
αPY
αp190
Time (min):
0 0.5 5 15 30 60
200 —
116 —
97.4 —
69 —
– 190 kDa
– GAP
– IgG H
1 2 3 4 5 6 7 8 9 10 11 12 13 14 15 16 17 18
B αPY IP
αPY
αFAK
αpp120
Time (min)
0 0.5
116 —
97.4 —
69 —
45 —
– 120kDa
– IgG H
1 2 3 4 5 6
C αFAK IP
Cytosol
Time (min):
0 0.5 5 15 30 60
αPY
αFAK
– 120kDa
– FAK
1 2 3 4 5 6

Figure 12. EGF dependent association of PY-SHC with GRB2/SOS in rat liver cytosol

Rat liver cytosolic fractions were isolated after EGF administration (10 μg/100 g body weight) and immunoprecipitated with affinity purified antibodies raised to SHC. The immunoprecipitates were immunoblotted with antibodies raised to phosphotyrosine (αPY; A), GRB2 (B) or SOS (C) and their mobilities are indicated on the right (55, 26 and 170 kDa, respectively).

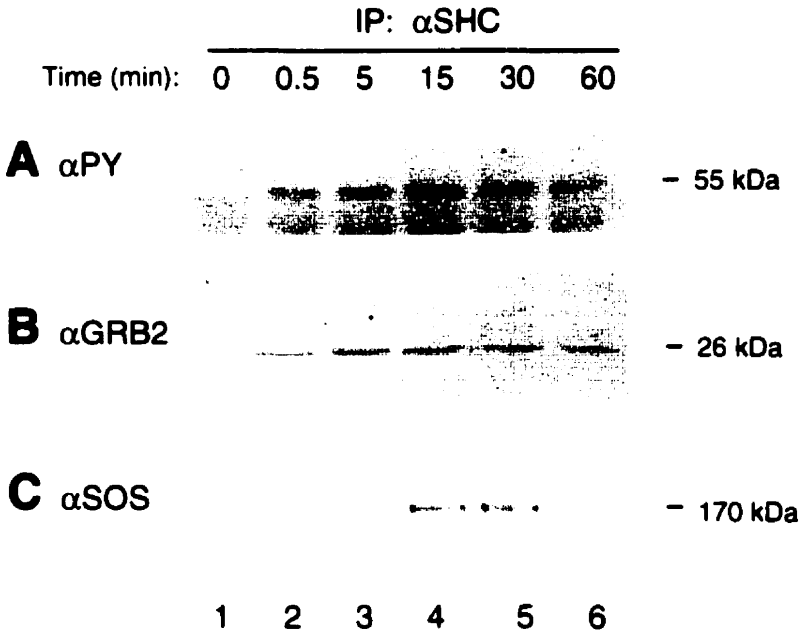
IP: αSHC
Time (min): 0 0.5 5 15 30 60
A αPY
– 55 kDa
B αGRB2
– 26 kDa
C αSOS
– 170 kDa
1 2 3 4 5 6

Figure 13. MAP kinase and Raf-1 mobility shifts in SDS-PAGE in response to EGF but not insulin administration

Rat liver cytosolic fractions were isolated at the indicated times after receptor saturating doses of EGF (10 μg/100 g body weight) or insulin (15 μg/100 g body weight) administration and immunoblotted with antibodies raised to Raf-1 (A) or MAP kinase which recognizes the 42, 43 and 44 kDa MAP kinase isoforms (C). The relative mobilities of Raf-1, the delayed mobilities corresponding to phosphorylated Raf-1 (P-Raf-1) or p44 MAP kinase (P-MAPK) are indicated. The amounts of Raf-1 and P-Raf-1 in cytosolic fractions in response to EGF were quantitated by phosphoimaging and expressed as Units/ g Liver (B). Each datapoint represents 3 experiments ± SD.

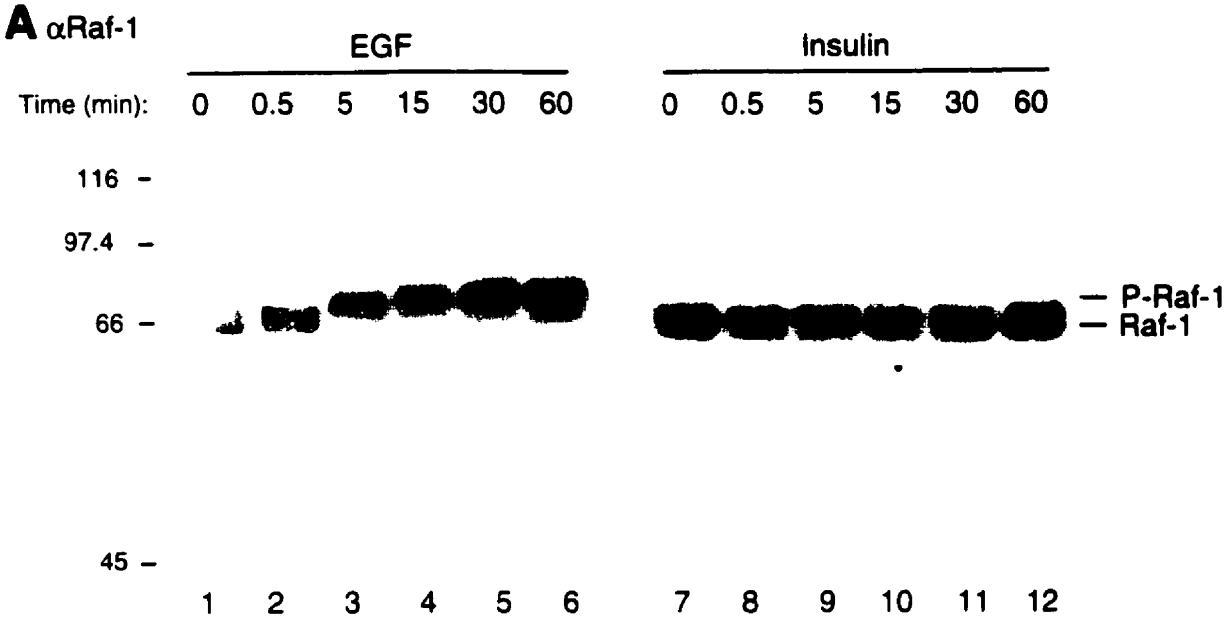
A αRaf-1
EGF
Insulin
Time (min): 0 0.5 5 15 30 60 0 0.5 5 15 30 60
116 –
97.4 –
66 –
45 –
— P-Raf-1
— Raf-1
1 2 3 4 5 6 7 8 9 10 11 12

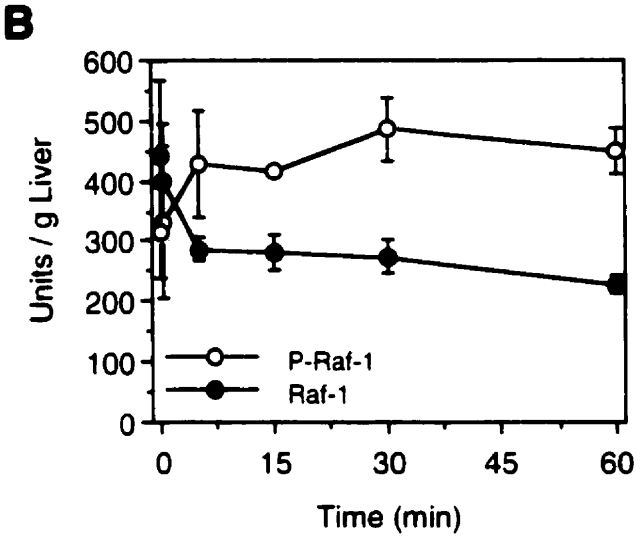
B
Units / g Liver
600
500
400
300
200
100
0
P-Raf-1
Raf-1
0 15 30 45 60
Time (min)

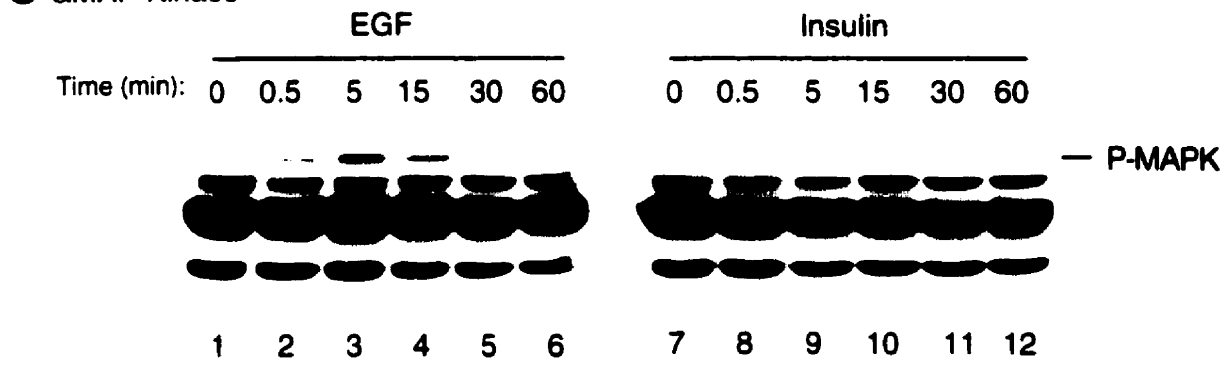
C αMAP Kinase
EGF
Insulin
Time (min): 0 0.5 5 15 30 60 0 0.5 5 15 30 60
— P-MAPK
1 2 3 4 5 6 7 8 9 10 11 12

Figure 14. Transcription of early response genes in response to EGF or insulin.

Total RNA was isolated from rat livers at the indicated times after the injection of EGF (10 μg/ 100 g body weight) or insulin (15 μg/ 100 g body weight). Twenty μg samples of RNA were resolved on a denaturing 1.2 % agarose/formaldehyde gels. The RNA was transferred onto Nylon membrane and hybridized with a [^{32}P]-dCTP labeled cDNA probe for c-myc (A), c-fos (B) or c-jun (C). The bands representing the c-myc (2.4 kb), c-fos (2.2 kb) and the two c-jun (2.5 and 3.2 kb) transcripts are indicated on the right. The [^{32}P] bands corresponding to the transcripts were quantified by phosphoimaging and expressed as arbitrary phosphoimager units (D-F). In the case of the c-jun transcript, the 2.5 kb transcript was quantitated. The results represent the mean ± SD of three separate experiments.

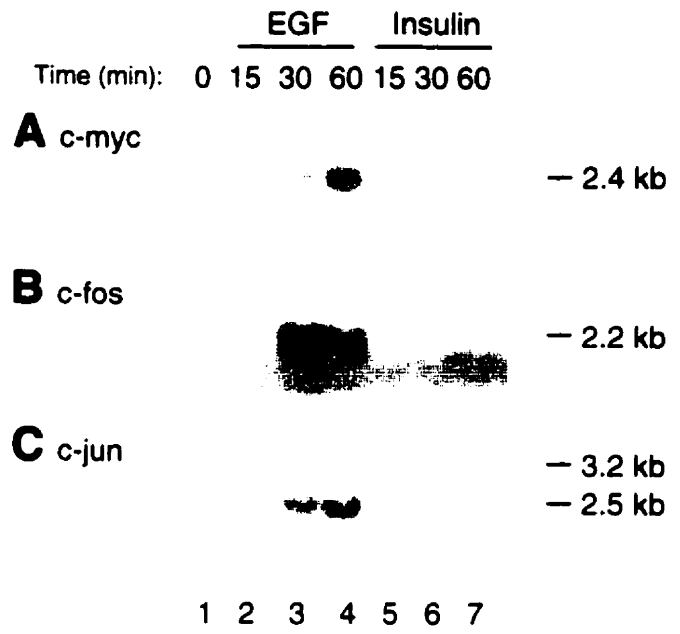
EGF
Insulin
Time (min): 0 15 30 60 15 30 60
A c-myc
— 2.4 kb
B c-fos
— 2.2 kb
C c-jun
— 3.2 kb
— 2.5 kb
1 2 3 4 5 6 7

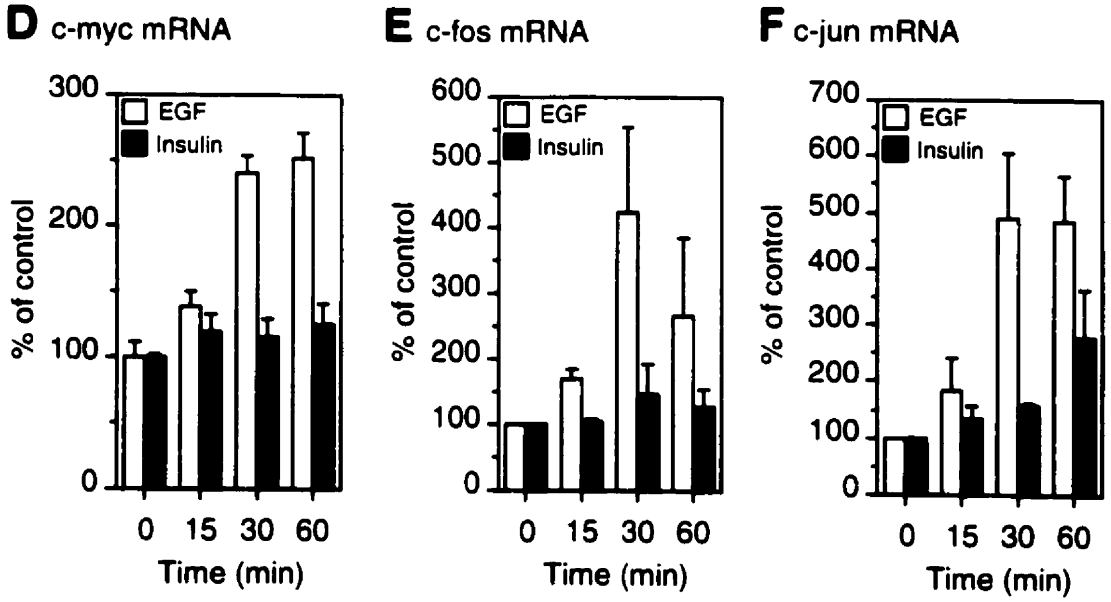
D c-myc mRNA
E c-fos mRNA
F c-jun mRNA
EGF
Insulin
% of control
Time (min)
0 15 30 60
300
200
100
0
600
500
400
700
600

Chapter 2
Endosomal processing of insulin and the insulin analog, H2, in rat liver

Introduction

Insulin degradation in liver parenchymal cells has been shown to be a consequence of receptor mediated endocytosis (Authier *et al.*, 1994b). Coincident with receptor activation at the cell surface, the insulin-IR complex internalizes into endosomes and the termination of signal transduction is achieved by endosomal insulin degradation and receptor dephosphorylation (see Literature Review). Endosomal proteolysis of the ligand is required to prevent any further ligand-driven receptor re-phosphorylation and the receptor is dephosphorylated by extraluminal endosomally associated phosphotyrosine phosphatases (Faure *et al.*, 1992).

Evidence for the role of endosomes in the degradation of internalized insulin has been documented in a number of studies (reviewed by Authier *et al.*, 1994b). Cell fractionation studies demonstrate internalized insulin in purified endosomes with little hormone observed in lysosomes of rat liver parenchyma (Pease *et al.*, 1985; Surmacz *et al.*, 1988). Purified endosomal fractions were shown to contain intact as well as degraded insulin (Backer *et al.*, 1990; Seabright and Smith, 1996) and inhibitors of lysosomal proteases did not modify endosomal insulin degradation in cell-free endosomes (Desbuquois *et al.*, 1990). Further proof comes via a thiol-dependent rat liver endosomal acidic insulinase (EAI) with a metal ion requirement that has been partially characterized (Doherty *et al.*, 1990; Authier *et al.*, 1994a).

EAI activity has been identified in insulin target tissues (Backer *et al.*, 1990; Doherty *et al.*, 1990) and is unrelated to insulin degrading enzyme (IDE) previously reported to be a candidate for hydrolysis of internalized insulin (Authier *et al.*, 1994b). The endosomal degradation of insulin results in a partially cleaved insulin molecule that can no longer bind to its receptor within endocytic structures (Seabright and Smith, 1996). Although some cleavage sites of insulin produced by rat hepatic endosomal insulinase activity have been identified (Seabright and Smith, 1996), little is known about the regions of the insulin molecule that are responsible for selective binding to EAI.

The metabolic and mitogenic potencies of insulin analogs such as [Asp^{B10}] insulin and the insulin analog, H2 have been extensively studied (Hansen *et al.*, 1996 and references therein). However, few studies have been directed towards the cell-mediated metabolism of these molecules. The roles of receptor mediated endocytosis and subsequent endosomal degradation in defining their degradation pathway remain undefined.

In this chapter we investigated the internalization and subsequent processing of the H2 analog [which displays a slower dissociation rate from the IR than insulin (Hansen *et al.*,

1996)] and to compare these two processes with wild-type insulin by using a quantitative subcellular fractionation of rat liver.

Results

Insulin dissociation from its receptor and ligand degradation within the endosomal lumen are believed to be mutually dependent mechanisms necessary in the initial steps of IR signal attenuation (Doherty *et al.*, 1990; Authier *et al.*, 1994a; Authier *et al.*, 1998). The aim of the work in this chapter is to biochemically characterize the degradation of insulin and H2 within the endosome and assess the dissociation of insulin or H2 from the IR in rat liver. By using established protocols (Authier *et al.*, 1995 and references therein), this was attempted by generating radioiodinated species of insulin or H2 and their association with subcellular fractions throughout the internalization pathway and be assessed by: (1) their degree of degradation by TCA precipitation and HPLC analysis; (2) their degree of association with the IR by PEG-precipitation and (3) the effect of pH on their dissociation and degradation states within endosomes using a cell free system.

Preparation of ^{125}I-labeled insulin or H2 on Tyrosine A14.

The primary amino acid sequences of human insulin and the recombinantly expressed insulin analog H2 are shown in Figure 15. The four amino acid substitutions introduced (His^{A8}, His^{B4}, Glu^{B10}, His^{B27}) decrease the rate of dissociation of H2 from the IR presumably due in part to the mutation at position B10 that is involved in the putative binding site with the IR (Hansen *et al.*, 1996). Since the structural differences of labeled hormones may affect their interactions with the IR and/or degradation, we attempted to generate equivalently radiolabeled isomers. Figure 16A shows a typical HPLC elution plot of [^{125}I]-labeled insulin. Previous studies have shown that the reverse-phase HPLC purification of radioiodinated insulin products results in a mixture of two products in which the A-chain tyrosines have been independently iodinated; A14 and A19 (Drejer *et al.*, 1991). The minor radioactive material (Figure 16A, peak I) co-eluting with unlabeled insulin was identified as insulin monoiodinated on Tyr^{19}, and the major radioactive product eluting last (Figure 16A, peak II) was shown to represent the insulin labeled on Tyr^{14} (Drejer *et al.*, 1991). The HPLC plot obtained after [^{125}I]-labeled H2 elution is shown in Figure 16B and matches that of [^{125}I]-labeled insulin (Figure 16A). To further characterize the radioiodinated H2-analog product IV, radiosequence analysis was carried out by automated Edman degradation (Table 3). The results indicate that the majority of radiolabel was released during the 14th cycle which was enriched in tyrosine, confirming that product IV of [^{125}I]-labeled H2 was radiolabeled on Tyr^{A14}.

Clearance of radiolabeled ligands from rat liver homogenates

The liver is anatomically positioned to receive the first bolus of insulin from the pancreas. To assess ligand uptake and clearance, [^{125}I]-labeled insulin or H2 was administered to rats and liver homogenates were assessed for content of radiolabel (Figure 17). Both insulin and H2 were observed in liver homogenates with a maximum peak of radiolabel quantitated 4-8 min post injection (Figure 17A). Clearance of radiolabeled insulin or H2 from the liver occurred at approximately the same rate ($t_{1/2}$ of ~9 min). The accumulation of H2 was observed to be greater than insulin (~ 23% and 19% of the dose per g of liver for H2 and insulin, respectively) and was significantly retained over insulin up to 30 min after ligand administration. To test if the greater amount of H2 vs. insulin accumulation in liver was due to slower ligand processing, TCA-precipitation of [^{125}I]-labeled insulin or H2 was assessed in rat liver homogenates isolated 4 min after the injection of radiolabeled insulin or H2 (Figure 17B). The results demonstrate a time-dependent increase in degradation of radiolabeled ligand with the rate of insulin proteolysis exceeding that of H2 by 15-20%. The $t_{1/2}$ of degradation for insulin and H2 was 23 min and 39 min, respectively (Figure 17 B).

Cell-free degradation of radiolabeled ligands within isolated endosomes

Having observed that the rate of insulin degradation by the liver was faster than H2, the role of an endosomal specific insulinase, EAI, was assessed. Endosomal (GE) fractions isolated after the administration of [^{125}I]-labeled insulin or H2 were isolated and assayed for their ability to degrade ligand *in vitro* (Figure 18). Following a time course of incubation in buffers of pH4 to pH7, the amount of degraded ligand was assessed by TCA precipitation. We observed that degradation of insulin and H2 within endosomes was dependent on the medium pH and occurred mainly at pH 6 (Figure 18A and B). Throughout the range of buffer pH tested, the GE fractions were found to contain ~ 1.5-2 times more insulin degradation products than H2 products.

Acidification of endosomes has been shown to be dependent on an ATP-driven proton pump (reviewed by Authier *et al.*, 1994b). It is within the acidic endosomal lumen that ligands have been suggested to dissociate from their cognate receptors and be degraded in the case of insulin. To directly assess lumen acidification on ligand proteolysis, GE fractions isolated after the injection of radiolabeled insulin or H2 were incubated in buffers of varying pH in the presence or absence of ATP (Figure 19). The addition of ATP to the incubation buffers shifted the buffer pH for maximal ligand degradation to pH 7 (Figure 19). Due to the previous observation that the endosomal pH pump is the most efficient in

neutral pH buffers (Debuquois *et al.*, 1990), this demonstrates that acidification of the endosome is necessary for both insulin or H2 degradation. However, the difference in the rate of degradation of insulin and H2 was still maintained with insulin processing ~1.5-2 times faster than H2.

Degradation of insulin and H2 by endosomal acidic insulinase

The degrading activity of an endosomal protease, termed endosomal acidic insulinase (EAI), has been demonstrated to be a soluble component of the endosomal lumen (Authier *et al.*, 1994a). To study the ability of EAI to recognize and degrade insulin and H2, endosomes isolated from control rats were disrupted by hypotonic shock and following sedimentation of membrane components via centrifugation, the resultant supernatant of the GE extract (SGE) was assayed for its ability to degrade insulin or H2 at pH 5 and 37°C. The incubation mixture was then analyzed by HPLC and the resultant HPLC profiles of the degraded ligands are shown in Figure 20. Intact insulin or H2 (no incubation) eluted in one peak and had a retention time of 52 and 53 min, respectively (Figure 20A and B). Incubation of the SGE with intact insulin resulted in a rapid generation of insulin peptide products with ~80% proteolysis within 2 hours (Figure 20C). With respect to H2, ~20% degradation was detected following the same incubation conditions (Figure 20D).

Dissociation state of intracellular radiolabeled ligands

To examine the possibility that the reduced intraendosomal degradation of H2 was due to altered dissociation from the IR in the acidic environment of the endosomal lumen, the dissociation of internalized radiolabeled ligands from the intracellular IR was studied using a PEG-precipitation protocol (Figure 21). GE fractions were isolated 2-60 min after the injection of radiolabeled insulin or H2 and precipitated with polyethylene glycol (PEG) in the presence or absence of the detergent Brij-35. We observed that internalized insulin was 62-76% PEG-precipitable in the presence of Brij-35 between 2 and 60 (Figure 21A). However internalized H2 was > 95% PEG-precipitable in the presence of the detergent up to 8 min post-injection (Figure 21A). In rat liver endosomes isolated from 15 and 60 min after H2 injection, the dissociation of ligand from the receptor increased to ~12%. This indicates that insulin dissociation from the IR was greater than that of H2 in the acidic lumen of endosomes.

To further test if the acidity of the endosomal lumen plays a role in ligand dissociation, dissociation of previously bound insulin and H2 from endosomes incubated

in varying pH buffers was examined (Figure 21B). No specific binding was detected below pH 5.5. At neutral pH, specific binding of insulin was 9.7%, whereas H2 binding was 37.7%. Therefore the release of PEG-soluble radioactivity for insulin was greater than H2 in buffers greater than pH 6.

From these results we observed that liver endosomes processes insulin faster than the insulin analog H2. This is based on both the rate of dissociation of ligand form the IR in an acidic environment as well as substrate specificity for the insulinase activity present in endosomes.

Discussion

The data presented in this chapter provide evidence for the hypothesis that altered ligand dissociation from its cognate receptor results in kinetic differences in hormonal processing. Hepatic endosomes are the major physiological locus of insulin degradation *in vivo* (Authier *et al.*, 1994b). In this chapter the observation that endosomal fractions accumulated ^{125}I-labeled insulin or H2 indicates that the H2 analog accessed the endosomal degradative compartment (Figures 18 and 21). The altered *in vivo* clearance of H2 can be ascribed to two mechanisms: (1) Reduced dissociation of H2-IR complexes within the acidic lumen of endosomes. (2) Reduced ability of the free H2 to be degraded by EAI. Both mechanisms have been postulated to cooperate for the efficient processing of insulin *in vivo* (Doherty *et al.*, 1990).

EAI hydrolyses insulin at a limited number of sites (Seabright and Smith; 1996). Although some positions of these cleavages are known (e.g.. Leu^{A13}-Tyr^{A14}, Ala^{B14}-Leu^{B15} and Phe^{B24}-Phe^{B25}), the residues of insulin required for binding to EAI have not been defined. However, we postulate that residues involved in the binding of insulin to the protease may be located at or near the sites at which insulin is hydrolyzed by the enzyme. The amino acid substitutions in H2 did not correspond to primary sites of cleavage of insulin within endosomes. Recent studies indicate that intermediates for endosomal insulin degradation resulted from an ordered sequential pathway involving an initial cleavage in the B-chain at Phe^{24}-Phe^{25}. (Seabright and Smith; 1996). However, replacement of amino acids near but not within the sites of cleavage of insulin may also significantly modify the ability of such analogs to act as effective substrates for the endosomal protease. Hence replacement of Thr^{B27} with the more hydrophilic His residue in the H2 analog may reduce the Phe^{B24}-Phe^{B25} cleavage. Since the substituted amino acids in the H2 analog have been implicated in the binding of insulin to the IR (Hansen *et al.*, 1996), our data indicate that the structural determinants required for binding to the IR vs. EAI may differ.

The endosomal processing of H2 by EAI is significantly slower than that of native insulin and the H2 analog also has an extended duration of receptor occupancy. Interestingly, EGF also undergoes limited proteolysis within endosomes of rat liver (Renfrew and Hubbard, 1991a). Furthermore, the vast majority of EGF remains bound to its receptor in endosomes (Renfrew and Hubbard, 1991b). Indeed, some proteolytic EGF products generated within endosomes, e.g. EGF-(residues 1-52), bind identically to the EGFR as intact EGF-(residues 1-53) (Renfrew and Hubbard, 1991b). Taken together, these studies combined with ours indicate that, within endosomes, the ligand integrity and

receptor bound ligand state may influence intracellular transmembrane signaling by enhancing association with internalized receptor kinase.

In light of these results we attempted to assess how the extended association of ligand (H2) with the IR at the endosomal locus would influence IR signal transduction.

Figure 15. Primary sequence of insulin and the insulin analog H2.

Primary structure of the human insulin polypeptide and the recombinantly expressed insulin analog H2 (Hansen *et al.*, 1996). The H2 analog contains 1 amino acid substitution in the A chain (Thr^{8} to His) and three substitutions in the B chain (Gln^{4} to His; His^{10} to Glu and Thr^{27} to His) (indicated in black). These substitutions confer to the H2 molecule a lower IR-dissociation rate constant than insulin. The k_d was calculated to be $5.52 \times 10^{-2}\ s^{-1}$ for insulin and $8.28 \times 10^{-4}\ s^{-1}$ for H2 (Hansen *et al.*, 1996).

INSULIN

A-chain

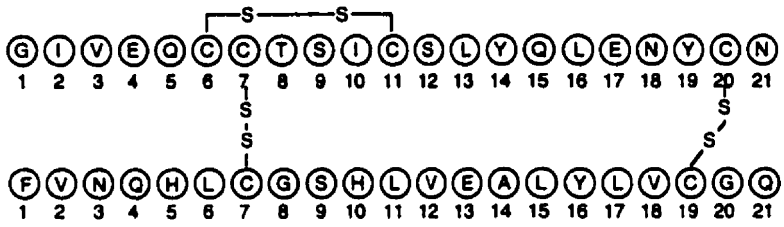

B-chain

H2

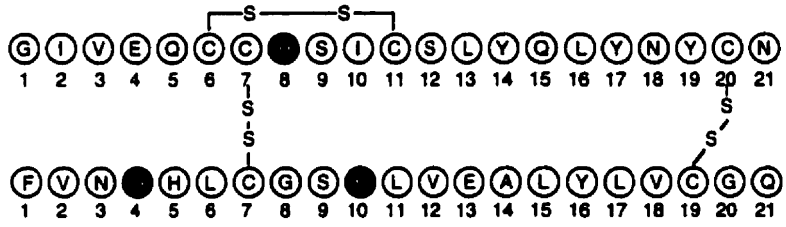

Figure 16. Reverse-phase HPLC purification of [^{125}I]-labeled insulin or H2

Insulin or the insulin analog, H2, were iodinated by the lactoperoxidase method, applied to a μBondapak C18 column and eluted using an acetonitrile gradient as described in Materials and Methods. The HPLC profiles of [^{125}I]-labeled insulin or [^{125}I]-labeled H2 are shown in Panels A and B, respectively, and plot radioactivity vs. elution time. Products I and III co-eluted ~17 min post injection into the column. The HPLC profiles in the right panels represent absorbance at 280 nm of unlabeled insulin and H2. The retention time of unlabeled insulin and H2 was measured to be ~13 min. Peaks II and IV were collected and lyophilyzed.

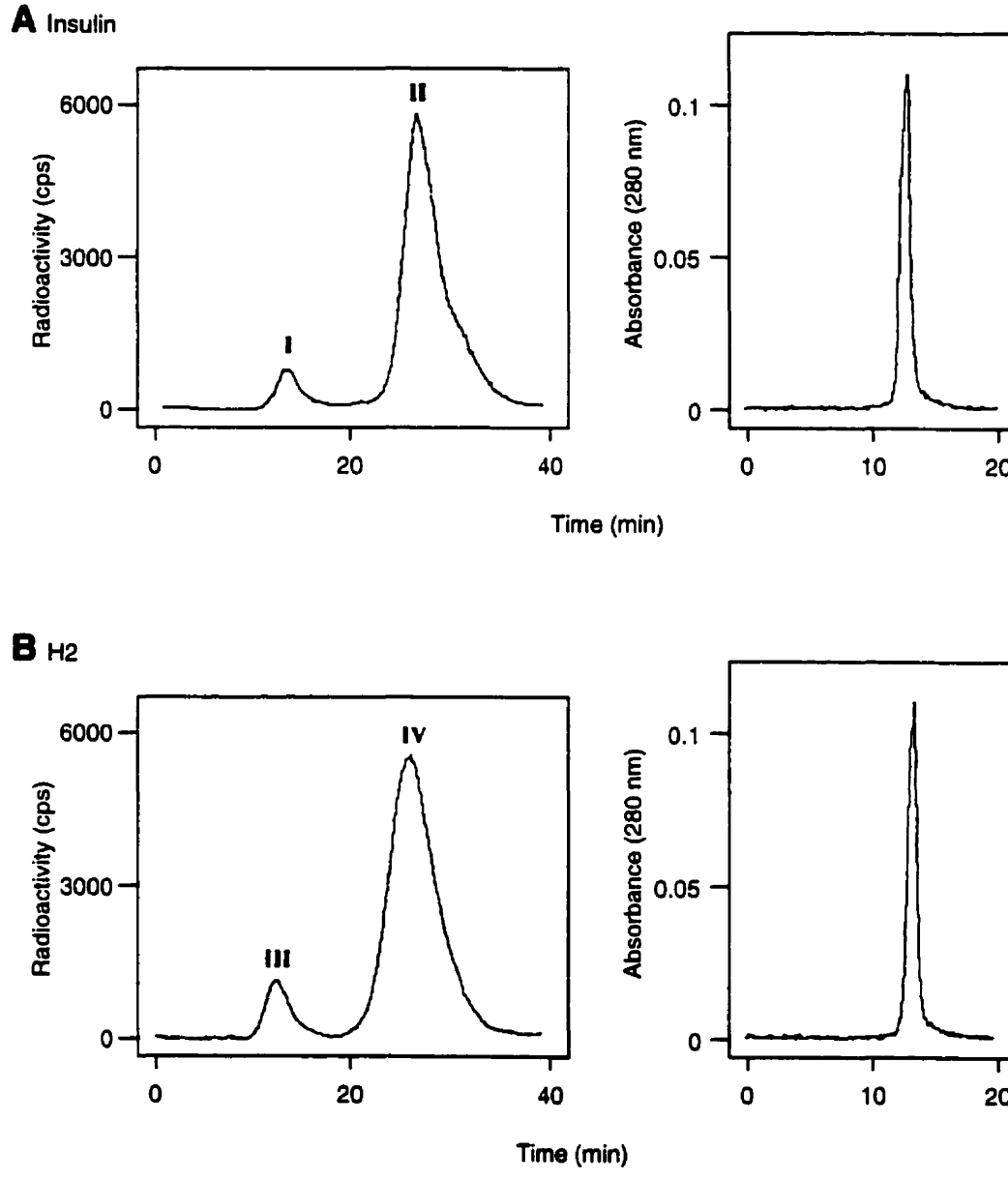
A Insulin
Radioactivity (cps)
6000
3000
0
I
II
0
20
40
Absorbance (280 nm)
0.1
0.05
0
0
10
20
Time (min)
B H2
Radioactivity (cps)
6000
3000
0
III
IV
0
20
40
Absorbance (280 nm)
0.1
0.05
0
0
10
20
Time (min)

Table 3. Automated Edman degradation of ^{125}I-labeled product IV and unlabeled H2.

N-terminal sequence analysis was employed to identify the iodinated tyrosyl residue within the radiolabeled product IV (see Figure 16B) and to monitor in parallel the phenylthiohydantoin-derivatized amino acid residues liberated from native H2 during each cycle. The released residues are shown by the single-letter amino acid code.

Cycle	Radioactivity (c.p.m.)	Residues (pmol)
1	120	G (89) + F (99)
2	86	I (97) + V (95)
3	187	V (100) + N (42)
4	248	E (65) + H (25)
5	312	Q (63) + H (27)
6	498	L (40)
7	394	-
8	552	H (41) + G (27)
9	525	S (17)
10	526	I (42) +(20)
11	618	L (20)
12	678	S (10) V (27)
13	653	L (35) + E (20)
14	23098	Y (27) + A (22)
15	9013	Q (20) + L (30
16	4125	L (29) + Y (28)
17	1871	E (17) + L (29)
18	1056	N (13) + (V (16)

Figure 17. Clearance and degradation of radiolabeled insulin or H2 in rat liver.

Rat liver homogenates were isolated at the indicated times after the administration of [^{125}I]-labeled insulin (—○—) or [^{125}I]-labeled H2 (—●—). The amount of radioactivity in the homogenates was quantitated by γ counter (A) and the degradation of [^{125}I]-labeled insulin or [^{125}I]-labeled H2 was assessed by TCA precipitation as described in Materials and Methods (B). Each time point is the mean ± SD for ≥ 5 experiments.

A

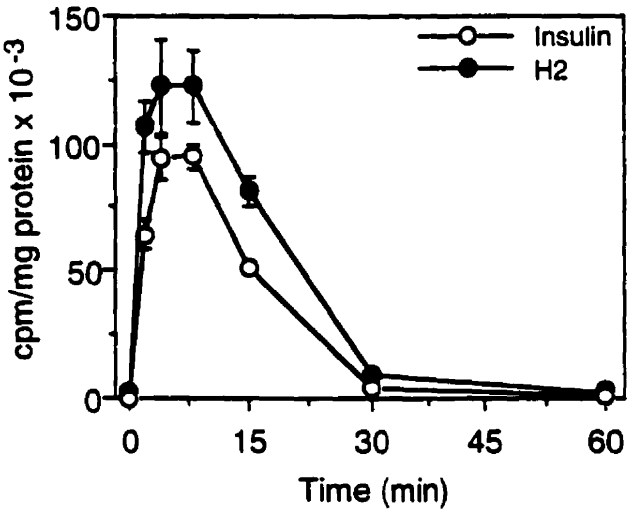
150
100
50
0
cpm/mg protein x 10-3
Insulin
H2
0
15
30
45
60
Time (min)

B

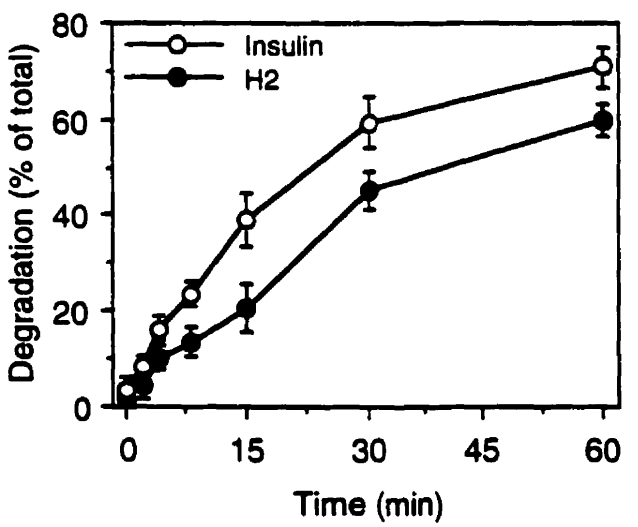
80
60
40
20
0
Degradation (% of total)
Insulin
H2
0
15
30
45
60
Time (min)

Figure 18. Effect of pH on endosomal degradation of radiolabeled insulin or H2.

Endosomal (GE) fractions were isolated from rat livers 4 min after the injection of [^{125}I]-labeled insulin (A) or [^{125}I]-labeled H2 (B). GE fractions were incubated for 0-30 min in pH 4 (—○—), 5 (—●—), 6 (—□—) or 7(—■—) buffer as described in Materials and Methods, after which the amount of degraded ligand was determined by precipitation with TCA.

A Insulin

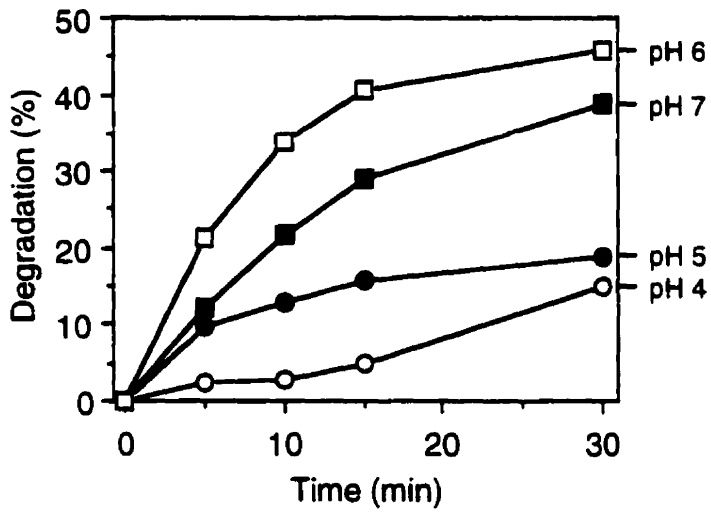

B H2

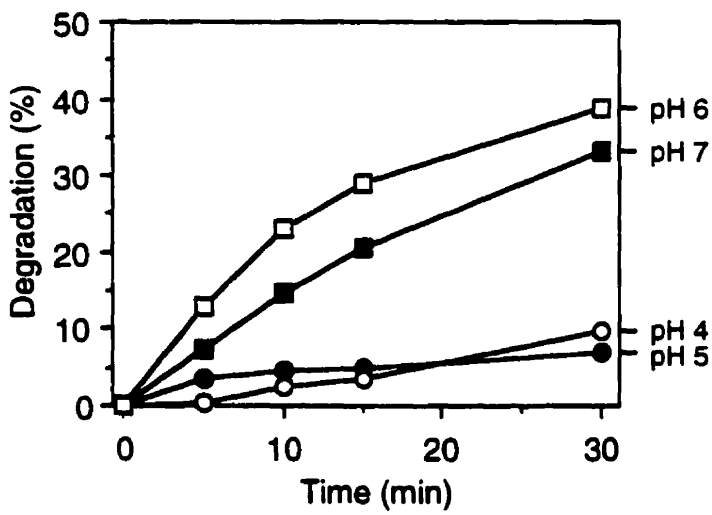

Figure 19. Effect of ATP on endosomal degradation of radiolabeled insulin or H2.

Endosomal (GE) fractions were isolated from rat livers 4 min after the injection of [^{125}I]-labeled insulin (A) or [^{125}I]-labeled H2 (B). The fractions were incubated in buffers of varying pH (pH 3-pH 8.5) for 5 min in the absence (—○—) or presence (—●—) of 1 mM ATP, after which the amount of degraded ligand was determined by TCA precipitation.

A Insulin

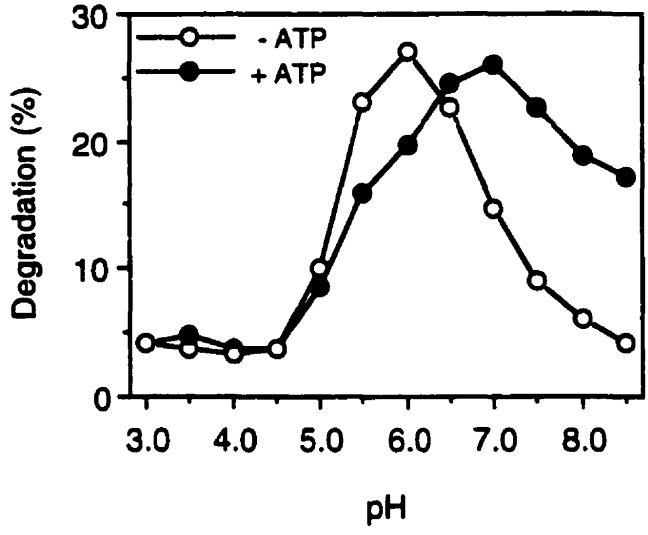

B H2

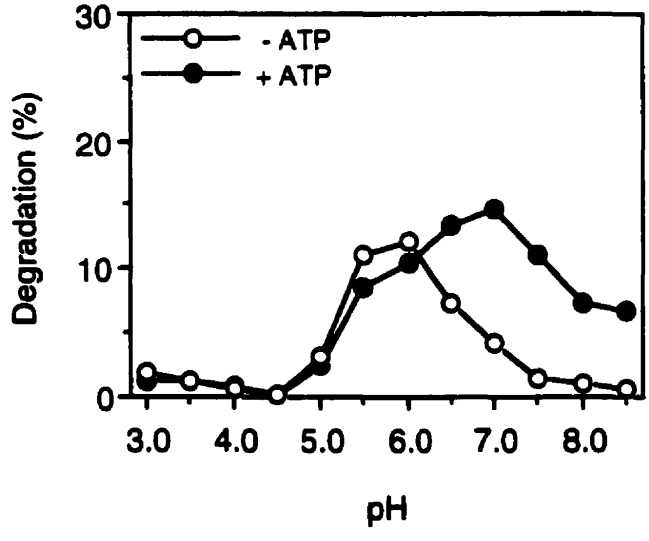

Figure 20. HPLC profiles of insulin or H2 after incubation with soluble endosomal extracts.

Endosomal (GE) fractions were disrupted by hypotonic shock and the soluble GE (SGE) fraction was evaluated for the degradation of insulin and H2. The SGE was incubated with insulin or H2 (10^{-6} M final concentration) for 2 h at pH 5 and 37°C. The proteolytic reaction was then stopped with acetic acid (15% v/v final concentration) and the incubation mixture was analysed by reverse-phase HPLC. Panels A and B show the elution of intact insulin or H2, respectively, both of which had the retention time of ~57 min. The HPLC profiles of insulin and H2 after incubation with the SGE fraction are shown in Panels C and D, respectively. All panels show absorbance profiles at 214 nm.

A Insulin

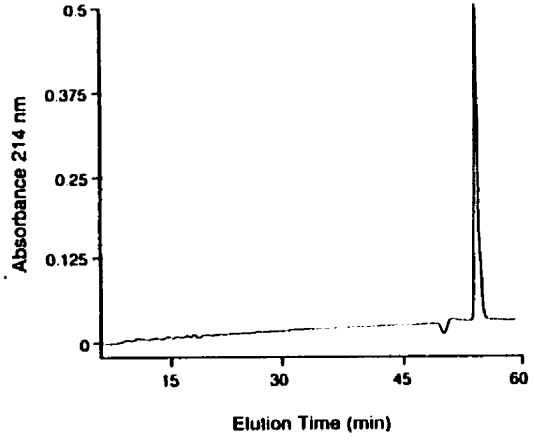

B H2

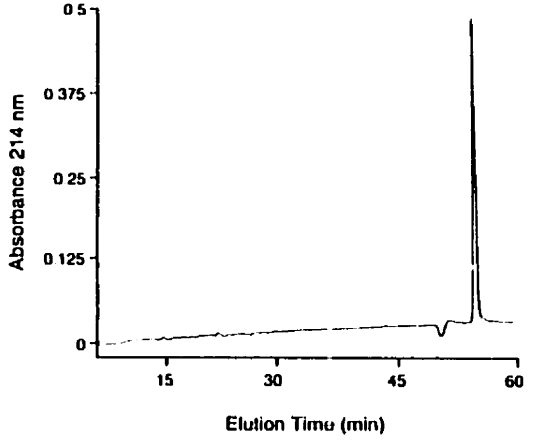

C Insulin + SGE

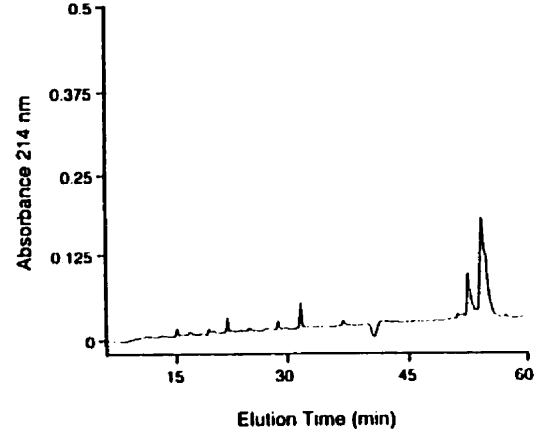

D H2 + SGE

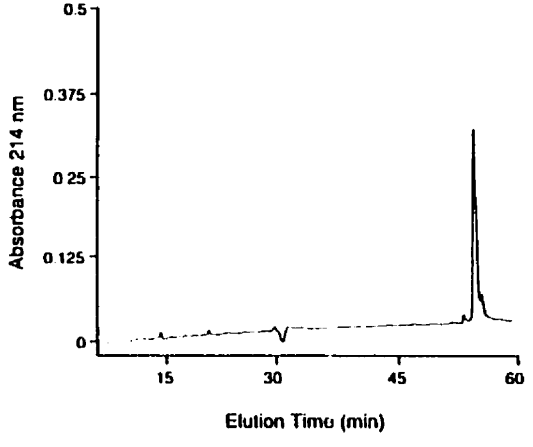

Figure 21. Dissociation of radiolabeled insulin or H2 in liver endosomes.

Rat liver endosomal (GE) fractions were isolated from rat livers at the indicated times after the administration of [^{125}I]-labeled insulin or [^{125}I]-labeled H2. The amount of receptor-bound radiolabeled insulin (□) or H2 (■) was determined by PEG-precipitation in the presence of 0.1% (v/v final) Brij-35. Results (≥ 3 experiments) are expressed relative to the amount of GE-associated (PEG-precipitable in the absence of detergent) radioactivity present at time zero (A). To test pH dependent ligand dissociation, GE fractions were incubated with [^{125}I]-labeled insulin or [^{125}I]-labeled H2 (9 fmol) at the indicated pH for 30-36 h. Free and receptor-bound radiolabeled ligands were separated by the PEG-precipitation assay. Specific binding for insulin (—○—) and H2 (—●—) is expressed as a percentage of total radioactivity added, with corrections made for non-specific binding (B).

A

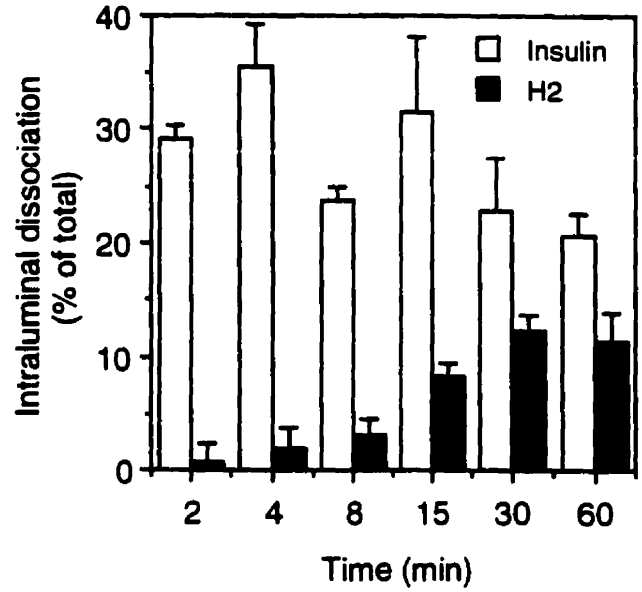
Intraluminal dissociation (% of total)
40
30
20
10
0
Insulin
H2
2
4
8
15
30
60
Time (min)

B

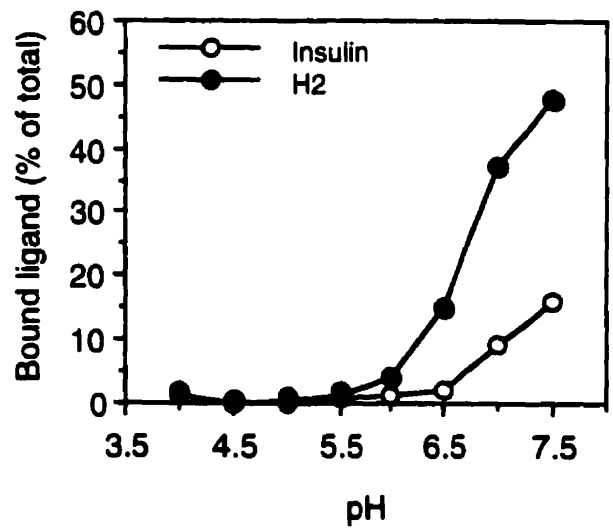
Bound ligand (% of total)
60
50
40
30
20
10
0
Insulin
H2
3.5
4.5
5.5
6.5
7.5
pH

Chapter 3
Insulin receptor traffic and signal transduction in response to insulin or H2 in rat liver

Introduction

Studies on the relationship between RTK endocytosis and signal transduction in rat liver indicated that the EGFR accesses components of the Ras pathway (SHC, GRB2, SOS and Raf-1) and induces nuclear transcription of c-myc, c-fos and c-jun (Chapter 1). We concluded that ligand mediated signaling from the EGFR occurs from both the PM and endosomal apparatus and is amplified by a cytosolic pool of activated molecules (PY-SHC/GRB2/SOS). The IR was observed to be tyrosine phosphorylated at the PM but not the endosomal apparatus and did not access the same mitogenic pathways as the EGFR. This was suggested to be due to the rapid inactivation of IR as it internalizes due to both rapid degradation of ligand and the subsequent dephosphorylation and inactivation of the receptor.

In order to test the hypothesis that IR signaling was quenched by the rapid attenuation initiated by ligand proteolysis we characterized in Chapter 2 an insulin analog, H2, that has altered affinity and a lower k_d for the IR (Hansen *et al.*, 1996). H2 was found to be less efficiently degraded by rat liver endosomal luminal EAI. H2 was also significantly found to be more IR-bound than insulin in endosomes.

In this chapter, the unique properties of the H2 analog were used to test three hypotheses concerning the regulation of IR signal transduction *in vivo*: (1) Alteration of ligand affinity for the IR affects receptor traffic. (2) The reduction of intracellular ligand dissociation from the IR alters the state of receptor tyrosine phosphorylation. (3) Altered IR traffic influences the pattern of signal transduction. This was carried out via subcellular fractionation followed by immunoprecipitation and quantitative immunoblotting as well as Northern analyses. In addition, direct IR kinase activity as well as MAP kinase, glycogen synthase, PKC, JNK and IRS-1 associated PI 3' kinase activities were assessed in rat liver in response to insulin or H2.

Results

Using a well established *in vivo* system (see Chapter 1) we assessed the influence of insulin and H2 on IR trafficking and signaling following ligand-mediated receptor internalization.

Differential effect of insulin and H2 on receptor trafficking

Rat liver PM and GE fractions were isolated following the intraportal injection of a single receptor saturating dose of insulin or H2 (15 μg/ 100 g BW for either ligand). The relative amount of IR in these fractions was assessed by immunoblotting with antibodies raised to the β subunit of the IR (IRβ) and quantitated by phosphoimager (Figure 22). The amount of the IRβ subunit decreased in PM fractions in response to ligand with little difference in the kinetics of net receptor loss from this compartment observed following administration of either insulin or H2 (Figure 22A and B, lanes 1-6). The initial $t_{1/2}$ of IR internalization of ~1 min was identical for both ligands, as was the maximal internalization of 39% of the receptors which was attained within 5 min. The reduced level of IRβ subunit content at the PM was observed for up to 60 min after ligand administration (Figure 22C). Thus, the results indicate that increased receptor occupancy with H2 (Chapter 2) had little influence on the kinetics or extent of recruitment of internalization machinery to the IR, nor did it affect the degree of receptor recycling to the plasma membrane.

Despite similar levels and rates of internalization promoted by either ligand, a marked difference in receptor accumulation was observed in endosomes. In response to insulin administration, maximal IRβ subunit content in GE fractions was attained by 5 min and was maintained for 30 min, after which it decreased (Figure 22A). In contrast, following H2 administration, a continuous IRβ subunit accumulation was observed up to 15 min (Figure 22D). After 60 min of ligand administration, the H2 induced IRβ subunit content in the GE fraction was twice that stimulated by insulin (Figure 22D).

Effect of insulin or H2 on IR tyrosine phosphorylation

Insulin or H2 induced tyrosine phosphorylation of the IRβ subunit was evaluated in PM and GE fractions by immunoblotting with anti-phosphotyrosine antibodies (Figure 23A and B). Within 30 sec of insulin or H2 administration, IRβ subunit tyrosine phosphorylation was observed in PM fractions (Figure 23A and B, lane 2). This signal subsequently declined over 30 min and returned to basal levels after 60 min. Quantitation revealed that the H2 induced IRβ subunit tyrosine phosphorylation was ~25% of that observed after insulin injection (Figure 23C). In endosomes, tyrosine phosphorylated IRβ content peaked 5-15 min post-injection or insulin or H2 (Figure 23A and B, lane 10). The

amount of tyrosine phosphorylated IRβ subunit in the GE fraction was quantitated to be 3 to 5-fold greater in response to H2 than in response to insulin at 15 min post injection (Figure 23D). To further verify the difference of tyrosine phosphorylated IRβ subunit in PM and GE fractions, solubilized fractions were immunoprecipitated with anti-IRβ subunit antibodies and immunoblotted with anti-PY (Figure 24A and B) or anti–IRβ subunit (Figure 24C and D) antibodies and quantitated by phosphoimaging. The ratio of phosphorylated IRβ per IRβ signal was plotted vs. time (Figure 24E and F) and confirms the observation that the phosphorylation of the IRβ subunit is greater in the PM fraction in response to insulin and greater in the GE fraction in response to H2.

To correlate the state of IRβ subunit phosphorylation with the kinase activity of the IR isolated from PM or GE fractions, kinase assays were performed using poly [Glu:Tyr] (4:1) as an exogenous substrate (Figure 25). The IRK activity in PM fractions was observed to be 7-fold greater than basal IRK activity in response to either insulin or H2. In GE fractions, H2 administration resulted in a significantly greater increase in IR kinase activity than insulin (8-fold and 2.5-fold, respectively) (Figure 25B).

These data demonstrate that the extension of ligand occupancy of the IR at the level of the endosome (see Chapter 2) results in alterations in IR traffic, IRβ subunit tyrosine phosphorylation and kinase activity.

Effect of insulin and H2 on the IRS-1 signaling pathway

IRS-1, a major IR kinase substrate, contains a PH and a PTB domain which are believed to be responsible for the interaction of IRS-1 with membrane phosphatidylinositol 4', 5'-bisphosphates and the IR, respectively (see Literature Review). To study the effect of insulin or H2 administration on IRS-1 compartmentalization, PM, GE and cytosolic (Cyt) fractions were assayed for IRS-1 content after ligand administration (Figure 26). The compartment harboring the majority of the IRS-1 signal was the cytosol (Figure 26A and B, lanes 1-6). In response to either insulin or H2 the mobility of IRS-1 was slightly delayed as assessed by SDS-PAGE and may indicate serine phosphorylation. IRS-1 was found in the PM compartment in the absence of ligand and its content and mobility was unaffected by insulin or H2 administration. In the GE fraction, the IRS-1 signal was < 15% than that of the PM fraction and was unaffected in response to ligand (Figure 26A and B, lanes 13-18).

Hansen and colleagues (1996) demonstrated that administration of H2 to CHO-IR cells resulted in an increase of IRS-1 tyrosine phosphorylation over that seen in response to insulin stimulation. To determine if H2 administration in rat liver would result in changes in the level of phosphorylation of IRS-1, IRS-1 was immunoprecipitated from cytosolic

fractions isolated after ligand administration and immunoblotted with anti-phosphotyrosine (Figure 26C) or anti-IRS-1 (Figure 26D) antibodies. EGF, which leads to potent tyrosine phosphorylation of the EGFR in liver parenchyma was used to test for receptor specificity in accessing the IRS-1 pathway. Within 30 sec of ligand administration, tyrosine phosphorylation of IRS-1 was observed in response to all three ligands. The ratio of tyrosine phosphorylated-IRS-1/IRS-1 was quantitated by phosphoimager analysis (Figure 26E). A 7-fold increase in IRS-1 tyrosine phosphorylation was observed within 30 sec of either insulin or H2 administration which declined to a level 3-4 fold above the control by 5 min and remained at this level up to 60 min (Figure 26E). Although EGF administration resulted in a small (2-fold) increase in IRS-1 tyrosine phosphorylation at 30 sec, this effect was transient, and returned to control levels within 5 min.

IRS-1 contains 9 putative PI 3-kinase docking sites (Pawson and Scott, 1997; White, 1998). The association of p85 with these phosphotyrosines of IRS-1 activates the PI 3'-kinase activity (White, 1998). To determine if the PI 3'-kinase recruitment sites were phosphorylated to the same extent in response to both insulin and H2, IRS-1 associated PI 3'-kinase activity was assayed in IRS-1 immunoprecipitates from cytosolic fractions (Figure 26F). The results indicate that there was a 10-fold increase in PI 3'-kinase activity associated with IRS-1 which was maintained up to 60 min after insulin or H2 administration, but was observed transiently (30 sec) after EGF administration.

Effect of insulin and H2 on mitogenic signaling pathways

Insulin stimulation of fibroblasts and CHO-IR cells results in the tyrosine phosphorylation of SHC (Pronk *et al.*, 1993; Sasaoka *et al.*, 1993a). This contrasts with administration of insulin to rat liver (Chapter 1). Stimulation of CHO-IR cells with H2 was shown to result in enhanced IR tyrosine kinase activity as well as enhanced SHC tyrosine phosphorylation, with the effect of H2 being greater than that of insulin. Furthermore, H2 enhanced mitogenicity in the parental CHO cell line as well (Hansen *et al.*, 1996). Since SHC phosphorylation is believed to be effected by the endosomally activated EGFR (Chapter 1) as well as from the endosomally located IGF-1R (Chow *et al.*, 1997), we determined if the endosomally active IR would access and phosphorylate SHC (Figure 27). Neither H2 nor insulin caused a redistribution of SHC to PM and GE fractions, although a rapid and significant recruitment was detected to both membrane compartments in response to EGF stimulation (Figure 27A). Furthermore, cytosolic fractions immunoblotted with anti-phosphotyrosine antibodies revealed tyrosine phosphorylated SHC only after EGF treatment but not after the administration of either H2 or insulin (Figure 27B). Thus,

although endosomal IR kinase activity increases following the administration of H2, the receptor specificity with respect to SHC is maintained in liver *in vivo*.

As a measure of Ras activation in response to ligand administration we assessed Raf-1 mobility shifts in SDS-PAGE, a process proposed to reflect Ras activation and the subsequent hyperphosphorylation and inactivation of Raf-1 (Wartmann *et al.*, 1997). Cytosolic fractions isolated after ligand administration were immunoblotted with antibodies raised to Raf-1 (Figure 28A). Although a mobility shift was observed in response to EGF administration, insulin or H2 did not induce a Raf-1 mobility shift in rat liver cytosol.

A further test was the direct evaluation of MAP kinase activity (Figure 28B). All three ligands tested induced MAP kinase activity. Densitometry revealed that EGF stimulated MAP kinase activity 2-fold over that of insulin and 3-fold over that of H2 at peak time of 5 min post injection. To evaluate the difference in MAP kinase activity in response to insulin and H2, quantitation by phosphoimager analysis was carried out (Figure 28C). This revealed that although the kinetics of MAP kinase activation in response to insulin and H2 were similar, insulin induced MAP kinase activation at 5 min was twice that of H2. By 15 min, MAP kinase activity had returned to basal levels in response to either ligand.

The differences between the prior work of Hansen and colleagues (1996) on the H2 effects on CHO-IR cells and the *in vivo* H2 studies presented here indicates either fundamental differences in the signaling pathways of CHO cells and liver parenchyma or a confound due to the secondary effects of H2 administration *in vivo*. For example, H2 administration may induce a glucagon response secondary to an acute H2-induced hypoglycemic state. This would be predicted to decrease MAP kinase activity (Spector *et al.*, 1997) and alter subsequent downstream signaling. As a test of this hypothesis, we evaluated if glucagon administration could influence ligand induced MAP kinase activation. Since EGF is a potent activator of MAP kinase, the ability of glucagon or H2 to interfere with this induction was tested. Rat liver cytosol was assayed for MAP kinase activity in response to co-injections of EGF (0.1 μg/ 100 g BW or 1 μg / 100 g BW) and receptor saturating doses of H2 (15 μg / 100 g BW) or glucagon (20 μg / 100 g BW). As seen in Figure 28C (inset), glucagon decreased EGF mediated MAP kinase activation by 50% at the 0.1 μg EGF dose and 25% at the 1 μg EGF dose. H2 did not interfere with EGF mediated MAP kinase activity thereby rendering unlikely the hypothesis that H2 signaling was glucagon mediated. This was confirmed by blood glucose levels in response to insulin and H2. In response to either insulin or H2, glucose levels decreased to hypoglycemic levels (3.5 mmol/L) within 15 min of ligand administration.

Early response genes

To further test the consequence of enhanced and prolonged endosomal IR activity in response to H2, early response gene transcription was assessed. As seen in Chapter 1, insulin had little effect on the levels of all three transcripts. Although H2 had little effect on c-fos and c-myc mRNA levels, it caused a 3-fold increase in c-jun mRNA (Figure 29A). The increase in c-jun transcripts in response to H2 was not as great as that seen in response to EGF, but significantly larger than that seen in response to insulin stimulation and may be due to the increased JNK activity observed in cytosolic fractions in response to H2 but not insulin (Figure 29B).

Effect of insulin and H2 on PKC and glycogen synthase

The activation of PKC isoforms has been studied in response to insulin and may be implicated in impaired glycogen synthesis and insulin resistance (Bandyopadhyay *et al.*, 1997). We evaluated the changes in PKC activity in rat liver cytosolic fractions isolated after insulin or H2 administration. PKC activity doubled in response to H2 and had a peak activation 5 min after ligand administration whereas insulin did not stimulate PKC activity in rat liver cytosol (Figure 30A). To assess the specificity of PKC activation, the PKC activity was measured at the peak time of activity (5 min) after ligand administration in the absence or presence of a PKC-α,β and γ inhibitory peptide (corresponding to amino acids 19-36 of PKCα, β and γ). Indeed presence of the inhibitory peptide resulted in attenuated PKC activity in H2 stimulated cytosolic fractions (Figure 30B). Finally, rat liver cytosolic fractions were assessed for their relative content of 6 different PKC isoforms (Figure 30C). PCKα content was increased in response to H2 5 min after ligand administration, while insulin did not cause a redistribution of PKCα. Redistribution of the other isoforms, including PKCδ and ζ, was not observed in response to either insulin or H2 (Figure 30C). These data indicate that the PKCα isoform may account for the increased PKC activity in response to H2 in liver.

Overexpression of PKCα and β has been shown to inhibit insulin-induced increases in glycogen synthase activity in 3T3/L1 adipocytes (Bandyopadhyay *et al.*, 1997). To test the metabolic effects of H2 dependent activation of PKC, we assessed glycogen synthase activity in rat liver. Although an increase in blood glucose levels is the primary stimulus for glycogen synthesis in hepatocytes, insulin has been proposed to play a potentiating role (Villar-Palasi and Guinovart, 1997). Insulin stimulates the deposition of glucose into glycogen at least in part by covalent modification of glycogen synthase. Glycogen synthase "b" (GSb) is the more phosphorylated form and is converted to glycogen synthase "a" (GSa) via dephosphorylation by protein phosphatase 1 (see

Literature Review). Dephosphorylated GS is not dependent on glucose-6-phosphate for function. The activities of GSa and the total GS activity (GSa + GSb) were measured in rat liver cytosol fractions isolated after insulin or H2 administration (Figure 31) and no effect was found on the total glycogen synthase (GSa + GSb) activity. The ratio of GSa/(GSa+GSb) indicated that insulin, but not H2, caused a shift of GSb to GSa peaking at 30 min post injection in rat liver at which time a 70% increase in activity was observed. Thus, the activation of PKC in response to H2 may have resulted in the inhibition of glycogen synthase activity normally observed in liver after IR activation.

Taken together these results define a distinct signaling pathway seen after H2 occupancy of the IR and consequent enhancement of the endosomal IR kinase tyrosine phosphorylation and activation.

Discussion

The coupling of ligand degradation with ligand dissociation ensures complete and rapid dissociation of insulin from its receptor in endosomes (Doherty *et al.*, 1990; Authier, 1994b). H2 dissociates with slower kinetics than insulin from the IR, *in vivo*, despite the acidic environment of the endosome (Chapter 2). Furthermore, dissociated H2 is a poor substrate for degradation by EAI (Chapter 2). As shown here, this enhances endosomal IR phosphorylation and the extension of its activated kinase activity towards exogenous substrates.

Interestingly, increasing ligand affinity for the IR influenced receptor traffic only within endosomes (Figure 22), leading to an enhanced and prolonged content of activated IR in this organelle (Figure 23). The precise molecular explanation for this endosomal specific trafficking event is unknown but has previously been observed for the endosomal EGFR (French *et al.*, 1995). The kinetics and enhanced extent of IR accumulation in the endosome was similar after H2 administration to that seen after EGF induced EGFR accumulation in liver parenchyma (Chapter 1).

No effect was observed on the rate or extent of IR loss from the PM in response to insulin or H2 suggesting that interaction of the IR and the internalization machinery remained unaffected. Hence, enhanced association of H2 with the IR did not alter the efficiency or extent of recruitment into the internalization machinery in liver parenchyma.

Ligand dissociation and IR dephosphorylation

According to the second hypothesis under test, enhanced receptor occupancy may influence the state of receptor activity and tyrosine phosphorylation. Following insulin administration, IR tyrosine phosphorylation was mostly observed at the PM. However, following H2 administration, tyrosine phosphorylation of the IR was now more marked in endosomes. Interestingly although the state of IR phosphorylation was not efficient at the PM in response to H2, its activity was similar to that of insulin stimulated IR (Figure 25). It was in the GE fractions that a marked increase of kinase activity paralleled the increase in tyrosine phosphorylation.

IR signal transduction

The signal transduction pathways accessed by activated IRs have been studied extensively. Aside from the classical IRS-1/2 and SHC pathways emanating from the IR, PKC isoforms have been reported to play a role in insulin signal transduction and glycogen deposition (Bandyopadhyay *et al.*, 1997). The activation of these molecules links insulin stimulation to both metabolic and mitogenic signal transduction pathways. A previous

report which used H2 to study IR signal transduction in CHO-IR cells revealed an enhanced accessing of mitogenic pathways (Hansen *et al.*, 1996). However since the effect was also observed in CHO cells expressing minimal levels of IRs, consideration should be given to binding of H2 to the IGF-1R in these cells. In contrast, adult liver parenchyma does not expresses significant levels of IGF-1Rs (Santos *et al.*, 1994). Hence, the effects of insulin and H2 in liver parenchyma are ascribed to the IR.

The major substrate for the IR tyrosine kinase is IRS-1 (White and Khan, 1994). The peak time of IRS-1 phosphorylation (30 sec) was the same for either insulin or H2 as was the extent of PI 3'-kinase recruitment to IRS-1. EGF stimulated minor IRS-1 tyrosine phosphorylation and a transient PI 3'-kinase activation at 30 sec (Figure 26). Therefore although H2 induced a greater amount of tyrosine phosphorylation and kinase activity of the endosomal IR compared to insulin treatment, IRS-1 was not phosphorylated to a greater extent. This indicates that the amount of activated IR tyrosine kinase at the PM may be sufficient to carry out efficient IRS-1 phosphorylation. Indeed the lower extent of IR tyrosine phosphorylation at the PM after H2 treatment did not affect the IR kinase activity at this locus. These results are consistent with studies in adipocytes and CHO-IR cells where IRS-1 phosphorylation did not require internalization of activated IR (Heller-Harrison *et al.*, 1995).

By assessing the steady state distribution of IRS-1 in liver, the major sites of IRS-1 localization were the cytosol and PM. The accessibility of IRS-1 at the PM in the rat liver may play a major role in IRS-1 phosphorylation by the IR. In contrast to liver endosomes, IRS-1 is localized on internal membranes of adipocytes where it interacts with PI3'-kinase (Kublaoui *et al.*, 1995). Taken together these studies propose that the IR may interact via different mechanisms with IRS-1 at both the level of the PM and the endosome independently and that these differences may be important in the mediation of the different functions of insulin in adipocytes and in liver. Part of this specificity may be a consequence of the anionic phospholipids responsible for membrane recruitment of IRS-1 via its PH domain (Myers *et al.*, 1995).

The adaptor protein SHC has been implicated in mitogenic signaling from the IR in a variety of cultured cells (see Literature Review) and SHC was observed to be tyrosine phosphorylated in control CHO and CHO-IR cells in response to H2 stimulation (Hansen *et al.*, 1996). In rat liver, H2 stimulation prolonged IR activation in the endosome yet SHC phosphorylation remained undetectable by immunoblotting with antiphosphotyrosine antibodies (Figure 27B). SHC has been shown to be associated with a number of intracellular organelles including endosomes (Chapter 1) and the endoplasmic reticulum (Lotti *et al.*, 1996). We assessed the ability of the endosomally tyrosine phosphorylated IR

to recruit SHC in an environment where components of the IR internalization machinery may not be associated with the IR. As with insulin, SHC did not translocate to either PM nor GE fractions in response to H2 (Figure 27A).

EGF and insulin have been shown to activate MAP kinase and act as mitogens in a variety of different cell types (reviewed by Vojtek and Der, 1998). MAP kinase activation has been suggested to regulate Raf-1 activity via a negative feed-back involving serine phosphorylation (Wartmann *et al.*, 1997). Examination of MAP kinase activity in rat liver revealed that the time course of activation by H2 resembled that of insulin but was 50% reduced. Consistent with this observation the Raf-1 mobility shifts were minimal in response to insulin as well as H2 whereas EGF produced a marked mobility shift. Hyperphosphorylation of Raf-1 in response to insulin or H2 was not observed possibly because of the low MAP kinase activity seen in response to these two ligands. In response to EGF, MAP kinase activation was the most efficient and may be responsible for hypershifted Raf-1.

The downstream effects of MAP kinase activation was assessed by the transcription of early response genes. As expected, EGF led to a reproducible activation of transcription of c-jun, c-fos and c-myc while insulin was ineffective. Unexpectedly, H2 increased the level of c-jun mRNA. This may have been partially produced by augmented JNK activity (Figure 29B).

As a physiological consequence of insulin signaling we focused on glycogen synthase activation. Liver is a major store of glycogen and the islets of Langerhans are positioned anatomically to release insulin selectively to liver with a marked effect of insulin and glucose on liver glycogen accumulation (Villar-Palasi and Guinovart, 1997). Here, insulin but not H2, was effective in activating liver glycogen synthase.

Although we cannot rule out completely a confounding effect for the *in vivo* model, receptor saturating doses of insulin and H2 were used thereby allowing for a direct comparison of signaling from the two ligands. An attempt was made to rule out enhanced hypoglycemic effect and rebound glucagon effects. As shown in Figure 28C (inset), H2 did not alter EGF dependent stimulation of MAP kinase whereas glucagon reduced it by 50% at the lowest dose of EGF used (0.1 μg/100 g BW).

Protein kinase C (PKC) has been reported to be involved in the negative regulation of insulin mediated glycogen synthase activity in adipocytes and muscle. Indeed in studies where PKCα and β were overexpressed and activated in 3T3/L1 cells there was an inhibition of insulin dependent glycogen synthase activity (Bandyopadhyay *et al.*, 1997). This would predict that H2 but not insulin could activate PKC activity. We therefore assessed PKC activity in rat liver in response to insulin and H2 in order evaluate the

predicted inverse relationship between ligand mediated activation of glycogen synthase and PKC activity. As predicted, H2, but not insulin, induced an increase in cytosolic PKC activity 5 min after ligand administration. This increase in activity was successfully inhibited with a specific peptide designed to inhibit PKCs α, β, and γ suggesting that one of these three isoforms may be responsive to H2 stimulation in rat liver. Indeed, an H2 dependent increase of the PKCα isoform was found in cytosolic fractions in response to H2. Hence the relocation of activated PKCα to cytosolic fractions may be responsible for the inactivation of glycogen synthase activity in rat liver by H2 (Figure 31).

In conclusion, the alteration of ligand affinity for the IR influences receptor traffic, its tyrosine phosphorylation and kinase activity, and finally downstream signaling pathways. Of note, the MAP kinase, PKC, and JNK pathways were modulated in response to H2. Future studies of the molecular dissection of endosomally activated signaling pathways in *in vivo* models will help elucidate the role endosomal receptor tyrosine kinases play in metabolic and mitogenic signaling.

Figure 22. Insulin receptor internalization in response to insulin or H2 in rat liver.

Rat liver plasma membrane (PM) or endosomal (GE) fractions were isolated at the indicated times after the intraportal injection of receptor saturating doses (15 μg/ 100 g body weight) of insulin (A) or H2 (B). One hundred μg of PM and 50 μg of GE fraction protein were resolved by SDS-PAGE, transferred to nitrocellulose membrane and immunoblotted with anti-insulin receptor β subunit antibodies (A and B). The mobility of the insulin receptor β subunit is indicated (IR β). The IR β subunit content after insulin (—○—) or H2 (—●—) administration in PM (C) and GE (D) fractions was quantitated by phosphoimaging and represented as arbitrary units per gram liver, corrected for yields and recoveries of the respective fractions. Each time point represents the mean of three separate experiments ± SD.

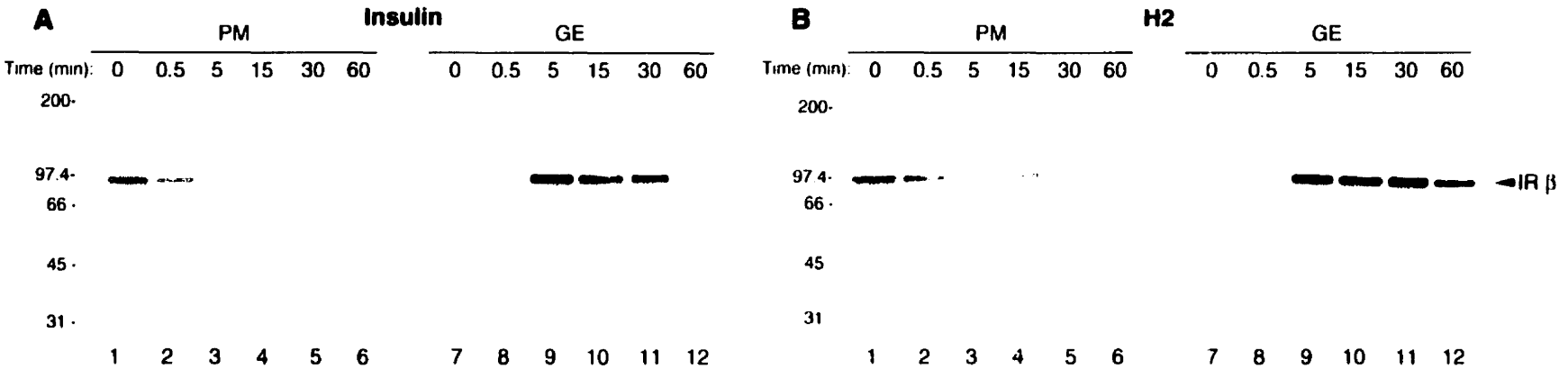
A
Insulin
PM
GE
Time (min): 0 0.5 5 15 30 60 0 0.5 5 15 30 60
200-
97.4-
66 -
45 -
31 -
1 2 3 4 5 6 7 8 9 10 11 12
B
H2
PM
GE
Time (min): 0 0.5 5 15 30 60 0 0.5 5 15 30 60
200-
97.4-
66 -
45
31
IR β
1 2 3 4 5 6 7 8 9 10 11 12

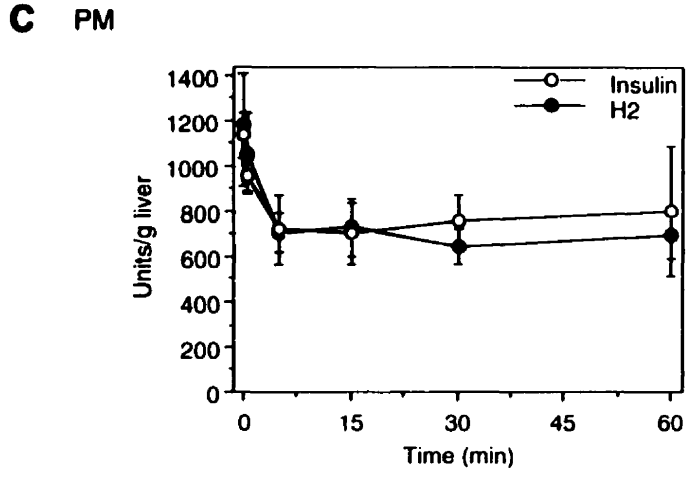
C PM
Insulin
H2
Units/g liver
1400
1200
1000
800
600
400
200
0
0 15 30 45 60
Time (min)

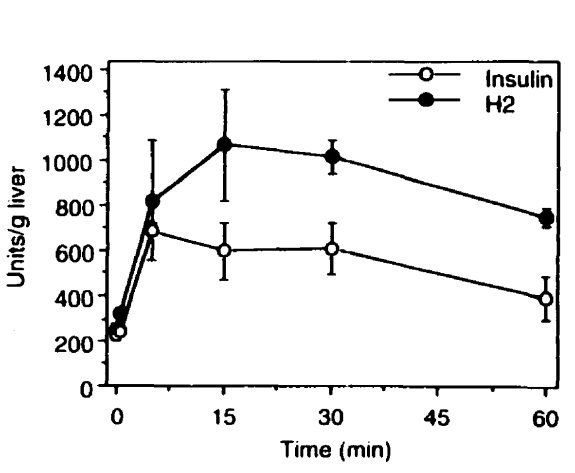
D GE
Insulin
H2
Units/g liver
1400
1200
1000
800
600
400
200
0
0 15 30 45 60
Time (min)

Figure 23. Insulin or H2 mediated insulin receptor phosphorylation in rat liver parenchyma.

Rat liver plasma membrane (PM) or endosomal (GE) fractions were isolated as described in Figure 22 and immunoblotted with anti-phosphotyrosine (αPY) antibodies. The relative amount of tyrosine phosphorylated IR β subunit (94 kDa) in PM (C) and GE (D) fractions after insulin (—○—) and H2 (—●—) administration, was quantitated and expressed as arbitrary units per gram liver. Each datapoint represents the mean of three separate experiments ± SD.

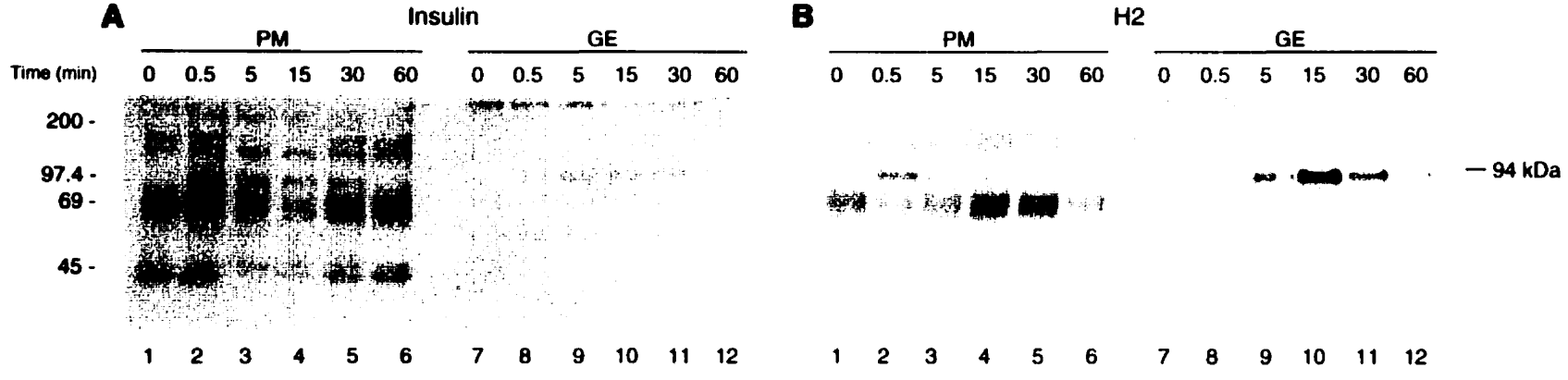
A
Insulin
PM
GE
Time (min)
0 0.5 5 15 30 60 0 0.5 5 15 30 60
200 -
97.4 -
69 -
45 -
1 2 3 4 5 6 7 8 9 10 11 12
B
H2
PM
GE
0 0.5 5 15 30 60 0 0.5 5 15 30 60
— 94 kDa
1 2 3 4 5 6 7 8 9 10 11 12

C PM

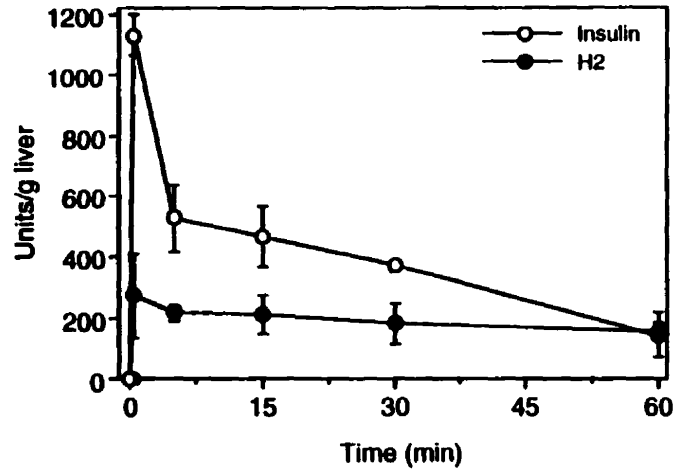
1200
1000
800
600
400
200
0
Units/g liver
Insulin
H2
0
15
30
45
60
Time (min)

D GE

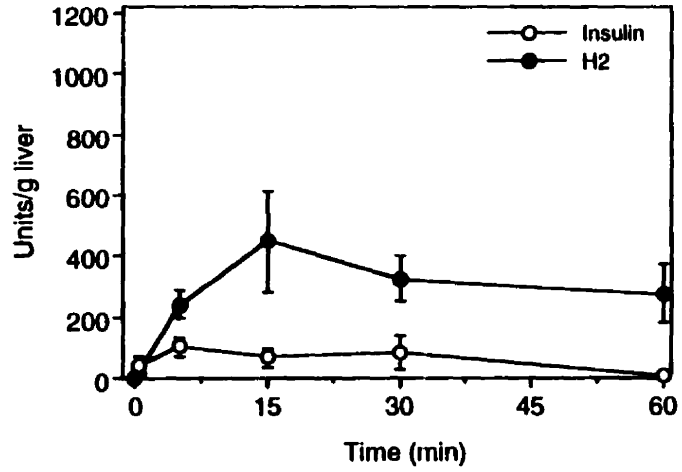
1200
1000
800
600
400
200
0
Units/g liver
Insulin
H2
0
15
30
45
60
Time (min)

Figure 24. Ratio of PY-IR/IR in plasma membranes or endosomes in response to insulin or H2.

Rat liver plasma membrane (PM) or endosomal (GE) fractions were isolated as described in Figure 22 and immunoprecipitated with anti-IR β antibodies. The equivalent of 500 μg of PM fraction and 200 μg of GE fraction protein were immunoprecipitated and immunoblotted with anti-phosphotyrosine (A and B) or anti-IR β antibodies (C and D). The crossreactivity of immunoprecipitating IgG and immunoblotting secondary antibodies is indicated (IgG H). The relative amount of tyrosine phosphorylated IR β subunit (PY-IR β) and IR β in PM and GE fractions after insulin (—○—) and H2 (—●—) administration was quantitated by phosphoimaging and expressed as the ratio of PY-IR/IR (E and F).

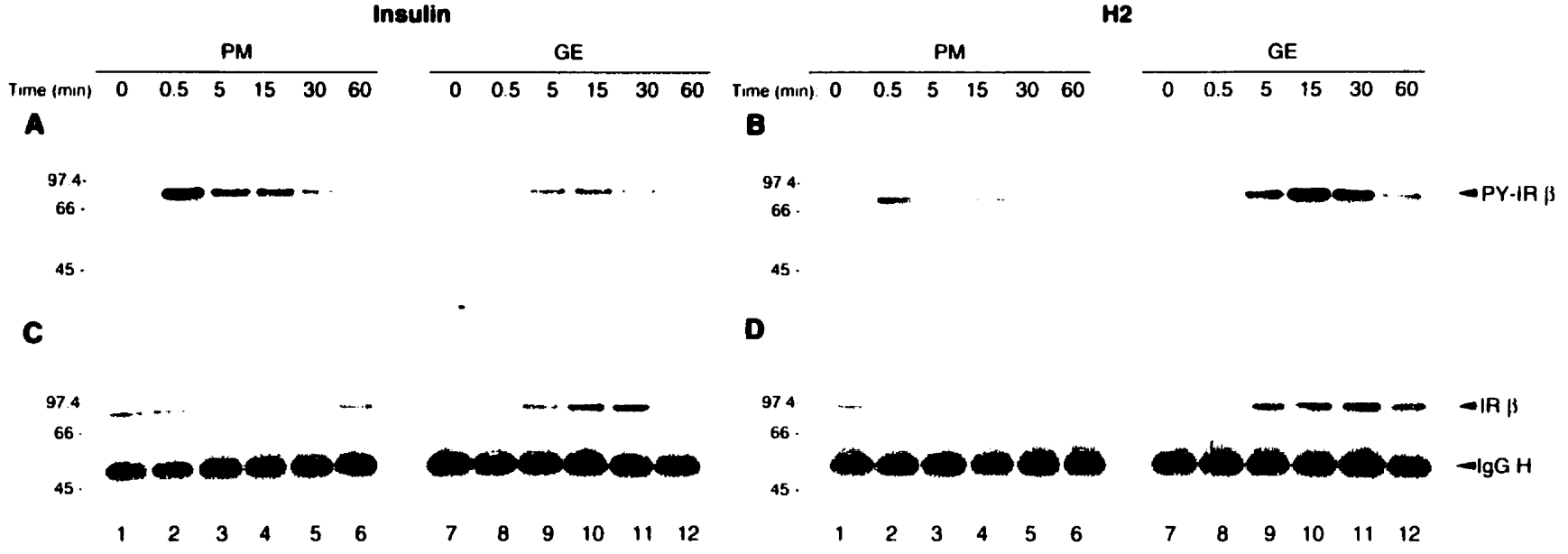
Insulin
H2
PM
GE
Time (min) 0 0.5 5 15 30 60
A
B
C
D
97.4
66
45
PY-IR β
IR β
IgG H
1 2 3 4 5 6 7 8 9 10 11 12

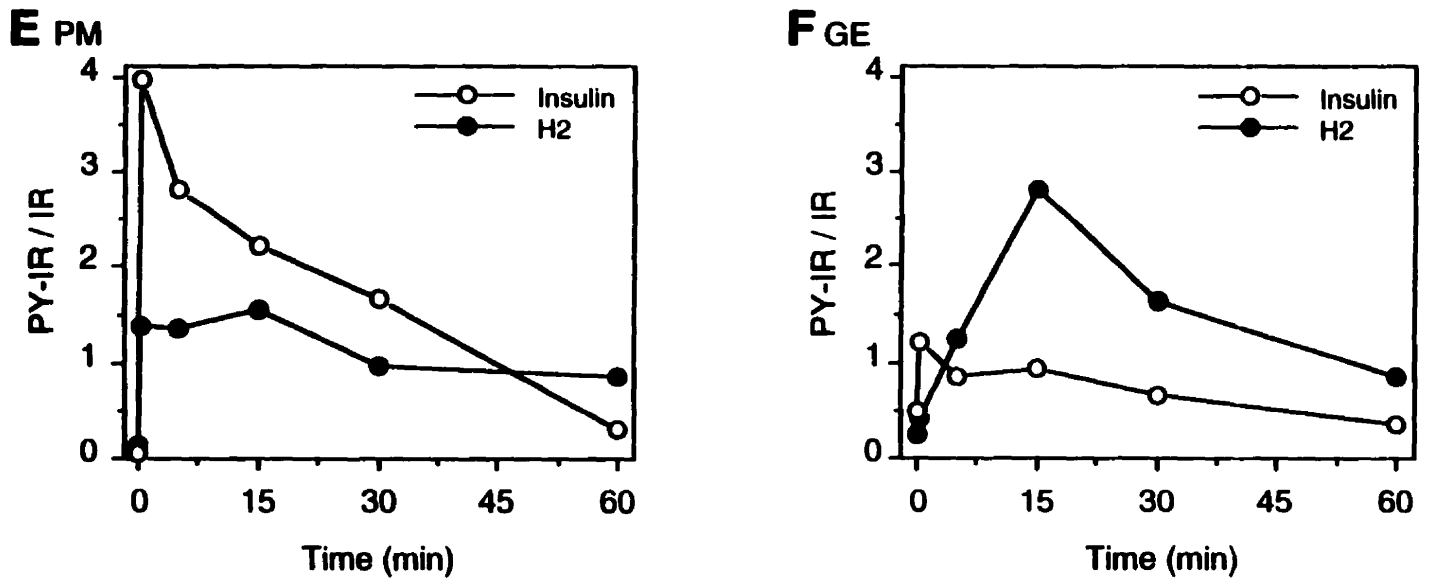
E PM
PY-IR / IR
Insulin
H2
Time (min)
F GE
PY-IR / IR
Insulin
H2
Time (min)

Figure 25. Insulin receptor kinase activity in plasma membranes or endosomes in response to insulin or H2 administration.

Rat liver plasma membrane (PM) or endosomal (GE) fractions were isolated at the indicated times after receptor saturating doses of insulin (—○—) or H2 (—●—) administration. IRs from PM (A) or GE (B) fractions were purified by WGA-Sepharose-chromatography and tyrosine kinase activity was determined by the transfer of [^{32}P] to poly [Glu:Tyr] (4:1) substrate as described in Materials and Methods. Each data point is expressed as IRK activity (pmol/10 min/10 fmol) and represents 2 experiments ± 1/2 difference.

A PM

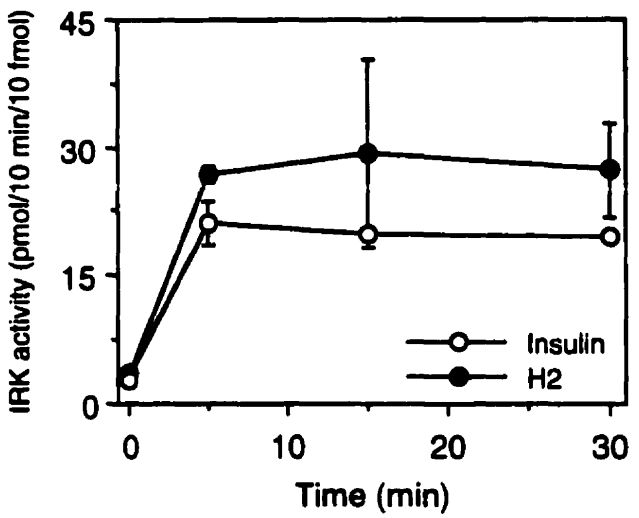
IRK activity (pmol/10 min/10 fmol)
45
30
15
0
0
10
20
30
Time (min)
Insulin
H2

B GE

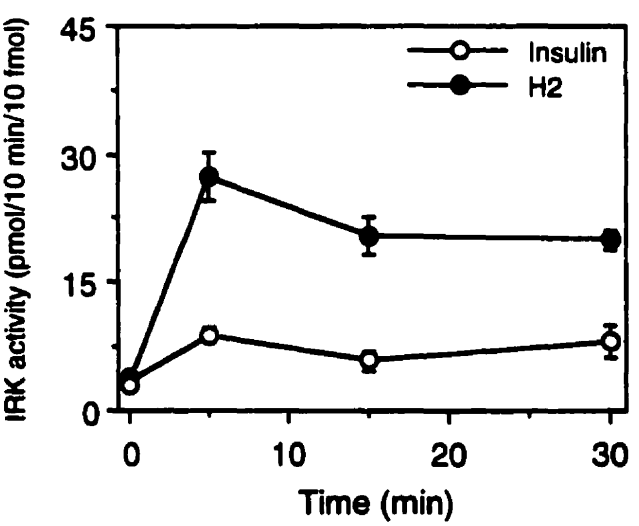
IRK activity (pmol/10 min/10 fmol)
45
30
15
0
0
10
20
30
Time (min)
Insulin
H2

Figure 26. Subcellular localization and phosphorylation of IRS-1 in rat liver parenchyma.

Rat liver cytosolic (Cyt), plasma membrane (PM) or endosomal (GE) fractions were isolated at the indicated times after the injection of insulin or H2 as described in Figure 22. Three hundred micrograms of Cyt, 100 μg of PM and 50 μg of GE fraction protein were resolved by SDS-PAGE and immunoblotted with anti-IRS-1 antibodies (A and B). Rat liver Cyt fractions were isolated at the indicated times after the injection of insulin or H2 (15 μg/100 g body weight) or EGF (10 μg/100 g body weight) and imunoprecipitated with anti-IRS-1 antibodies and immunoblotted with anti-phosphotyrosine (C) or anti-IRS-1 antibodies (D). The band corresponding to tyrosine phosphorylated IRS-1 is indicated as PY-IRS-1. The ratio of tyrosine phosphorylated PY-IRS-1 per unit of IRS-1 was quantitated by phosphoimaging (E). Each data point represents the average of two experiments ± 1/2 difference. IRS-1 immunoprecipitated from rat liver cytosolic fractions was assayed for associated PI 3-kinase activity by the transfer of [^{32}P] to phosphatidylinositol to yield phosphatidylinositol phosphate (indicated as PIP) (F).

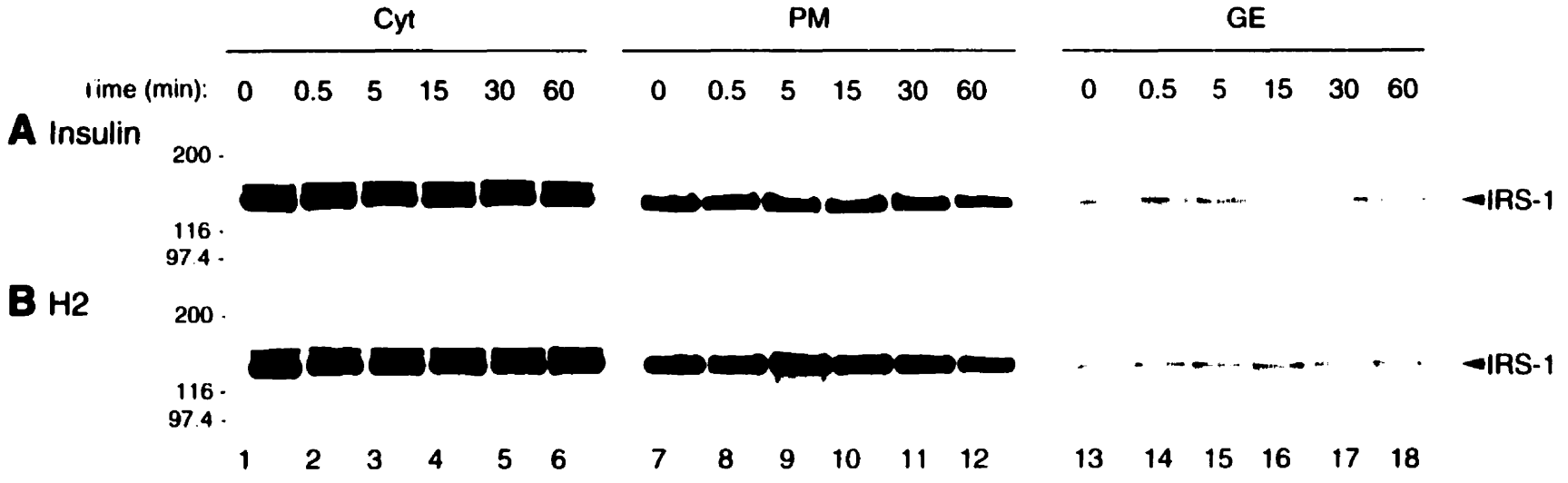
Cyt
PM
GE
Time (min): 0 0.5 5 15 30 60 0 0.5 5 15 30 60 0 0.5 5 15 30 60
A Insulin
200 -
116 -
97.4 -
IRS-1
B H2
200 -
116 -
97.4 -
IRS-1
1 2 3 4 5 6 7 8 9 10 11 12 13 14 15 16 17 18

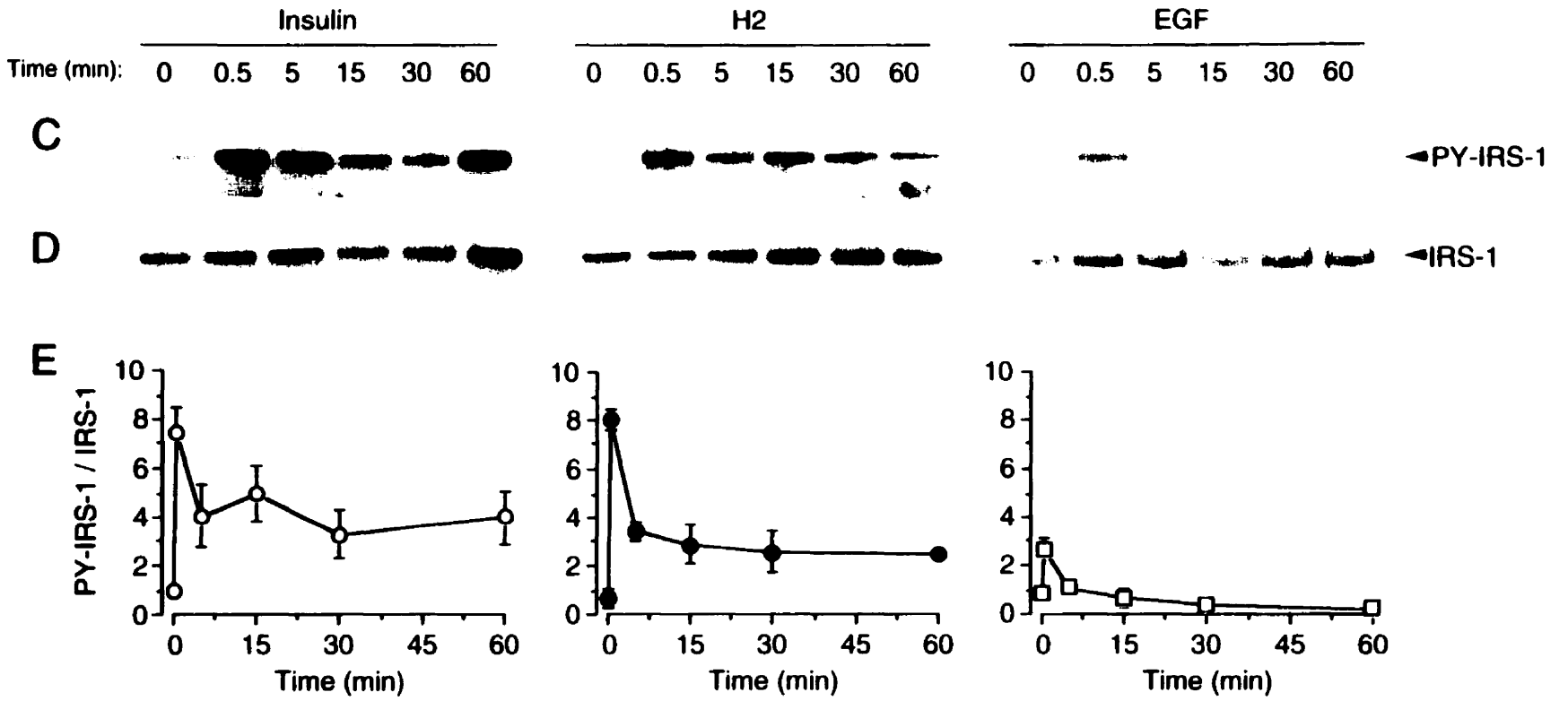
Insulin
H2
EGF
Time (min): 0 0.5 5 15 30 60
C
D
PY-IRS-1
IRS-1
E
PY-IRS-1 / IRS-1
Time (min)

F

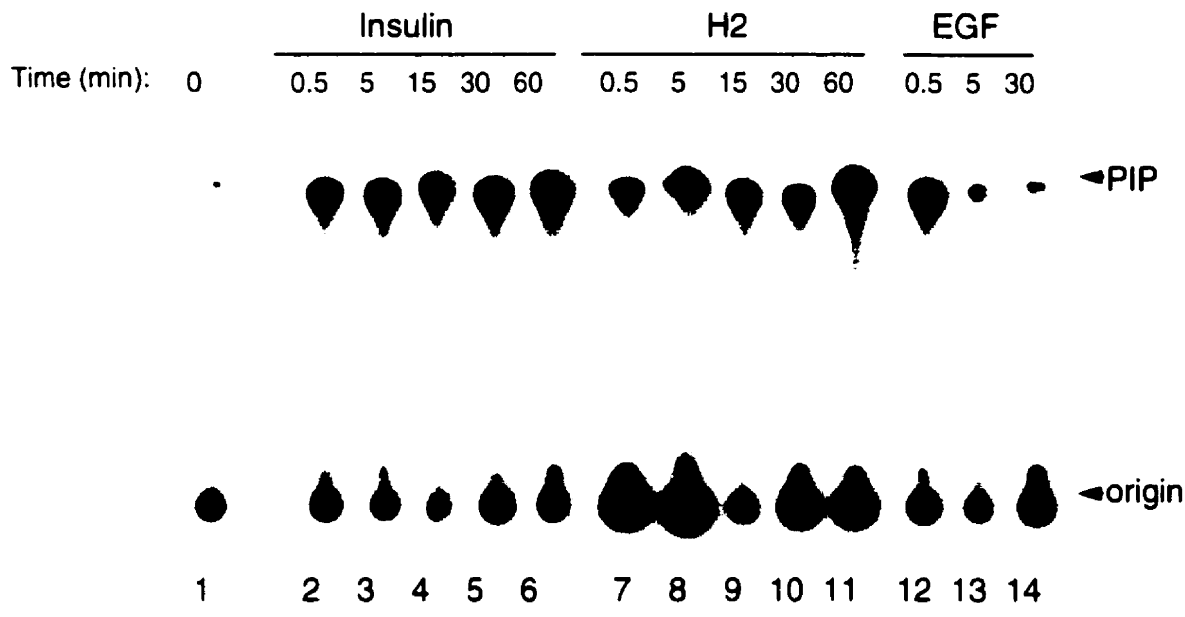
Insulin
H2
EGF
Time (min):
0
0.5 5 15 30 60
0.5 5 15 30 60
0.5 5 30
PIP
origin
1 2 3 4 5 6 7 8 9 10 11 12 13 14

Figure 27. Recruitment of SHC to plasma membranes or endosomes and SHC phosphorylation in cytosol in response to insulin, H2 or EGF administration.

Rat liver cytosolic (Cyt), plasma membrane (PM) or endosomal (GE) fractions were isolated at the indicated times after the injection of insulin, H2 (15 μg/100 g body weight for either ligand) or EGF (10 μg/100 g body weight) as described in Figure 22. One hundred micrograms of Cyt, 100 μg of PM and 50 μg of GE fraction protein were resolved by SDS-PAGE and immunoblotted with anti-SHC antibodies (A). Cyt fractions were immunoblotted with anti-phosphotyrosine antibodies (αPY) and the polypeptide corresponding to tyrosine phosphorylated SHC in indicated as PY-SHC (B).

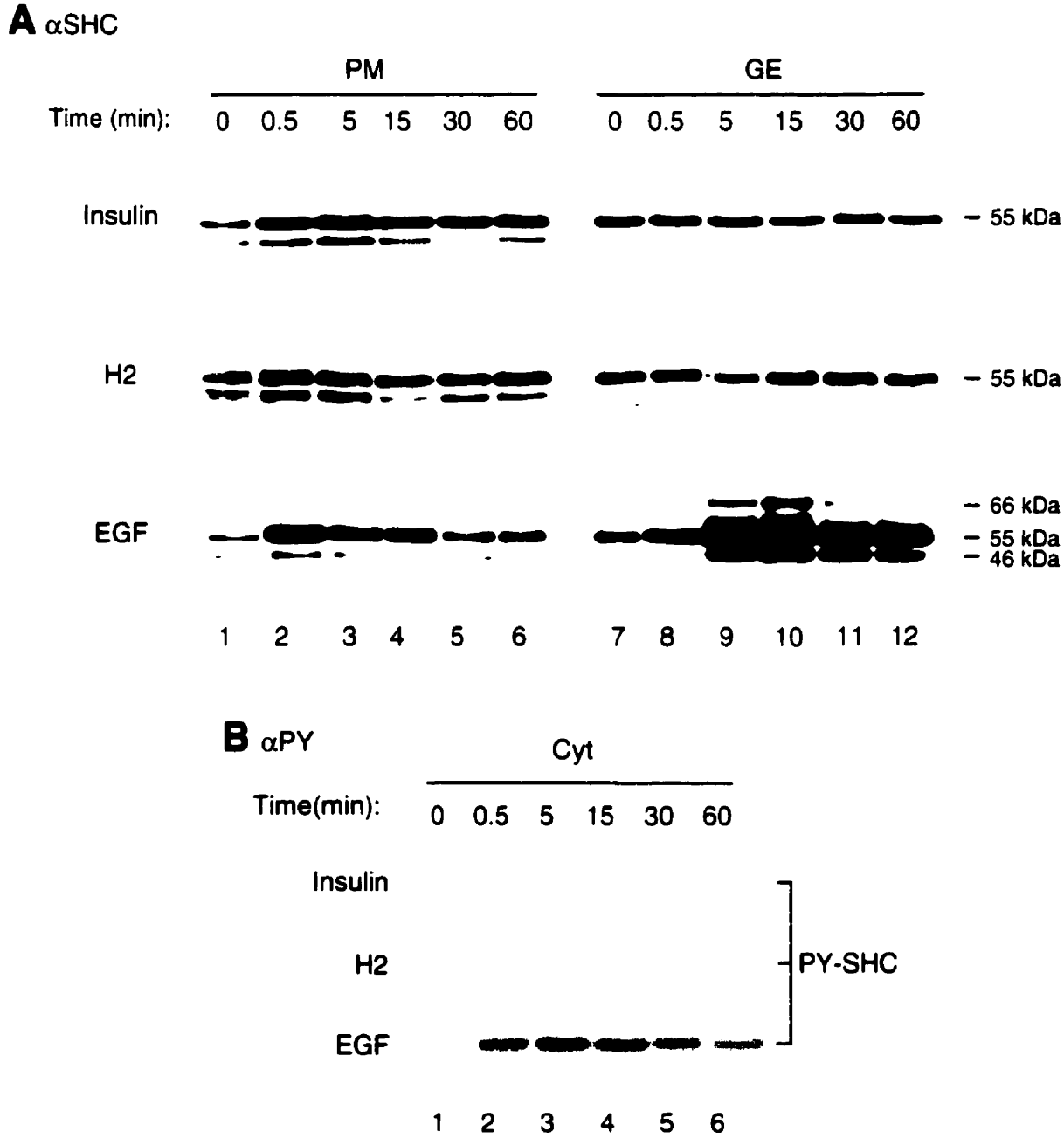
A αSHC
PM
GE
Time (min):
0 0.5 5 15 30 60
0 0.5 5 15 30 60
Insulin
H2
EGF
55 kDa
55 kDa
66 kDa
55 kDa
46 kDa
1 2 3 4 5 6 7 8 9 10 11 12
B αPY
Cyt
Time(min):
0 0.5 5 15 30 60
Insulin
H2
EGF
PY-SHC
1 2 3 4 5 6

Figure 28. Raf-1 mobility in SDS-PAGE and MAP kinase activity in response to insulin, H2 or EGF administration.

Rat liver cytosolic fractions were isolated at the indicated times after the administration of receptor saturating doses of insulin or H2 (15 μg /100 g body weight) or EGF (10 μg /100 g body weight). One hundred micrograms of cytosolic fraction protein were resolved by SDS-PAGE and immunoblotted with anti-Raf-1 antibodies (A). MAP kinase from cytosolic fractions was immunoprecipitated with anti-ERK1 (MAP kinase p44) antibodies and assayed for kinase activity by the transfer of [^{32}P] to myelin basic protein as described in Materials and Methods (B). Quantitation of MAP kinase activity was carried out by densitometry (B) or by phosphoimaging (C). The phosphoimaging data is represented as % of control of three separate experiments ± SD for insulin (—○—) or H2 (—●—). MAP kinase activity was also assessed in cytosolic fractions isolated after the co-injection of EGF (0.1 μg/100 g BW or 1.0 μg/ 100 g BW;□) and H2 (15 μg/ 100 g BW;▨) or glucagon (20 μg/ 100 g BW;■) (C, inset).

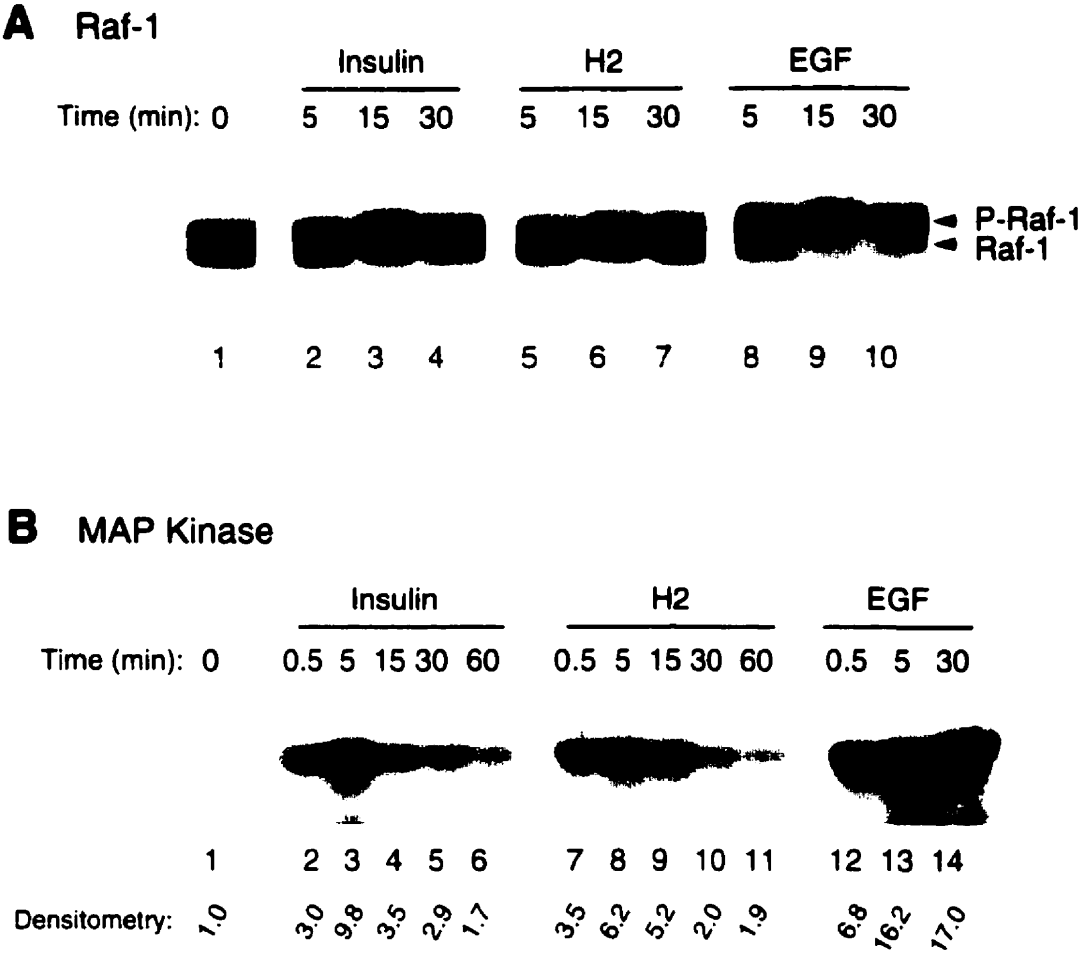
A Raf-1
Insulin
H2
EGF
Time (min): 0
5 15 30
5 15 30
5 15 30
P-Raf-1
Raf-1
1 2 3 4 5 6 7 8 9 10
B MAP Kinase
Insulin
H2
EGF
Time (min): 0
0.5 5 15 30 60
0.5 5 15 30 60
0.5 5 30
1 2 3 4 5 6 7 8 9 10 11 12 13 14
Densitometry:
1.0 3.0 9.8 3.5 2.9 1.7 3.5 6.2 5.2 2.0 1.9 6.8 16.2 17.0
C
MAP kinase activity (% of control)
1200
1000
800
600
400
200
0
0 15 30 45 60
Time (min)
1000
800
600
400
200
0
0.1 1
EGF (μg)

Figure 29. H2-mediated c-jun transcription and JNK activity in rat liver.

Total RNA was isolated from rat livers after the administration of insulin, H2 (15 μg /100 g body weight) or EGF (10 μg /100 g body weight). Twenty micrograms of RNA were electrophoresed, transferred to nylon membrane and subjected to Northern blot analysis with [^{32}P] labeled cDNA probes for c-jun, c-fos or c-myc. Quantitation of the mRNA levels of c-jun, c-fos and c-myc was carried out by phosphoimager analysis (A). Each time point represents the mean of three experiments ± SD. Cytosolic fractions isolated at the indicated times after receptor saturating doses of insulin or H2 (15 μg/100 g body weight) were immunoprecipitated with anti-JNK antibodies and assayed for JNK activity as described in Materials and Methods (B).

A

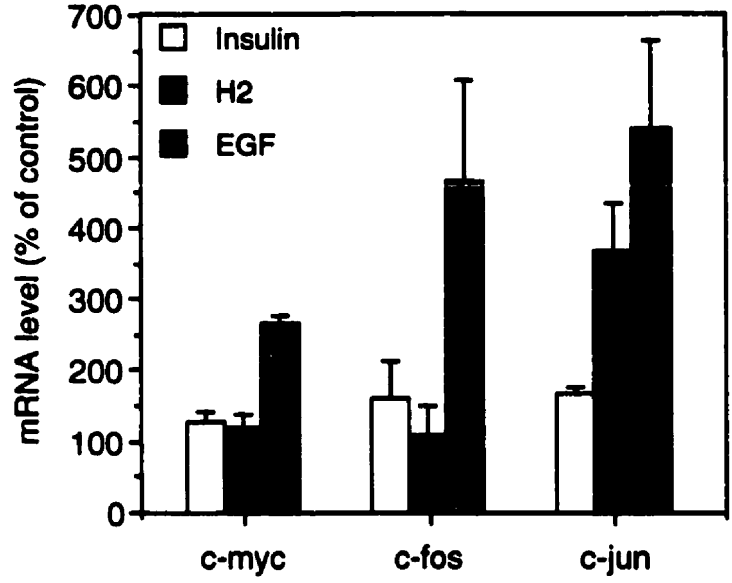
700
600
500
400
300
200
100
0
mRNA level (% of control)
Insulin
H2
EGF
c-myc
c-fos
c-jun

B

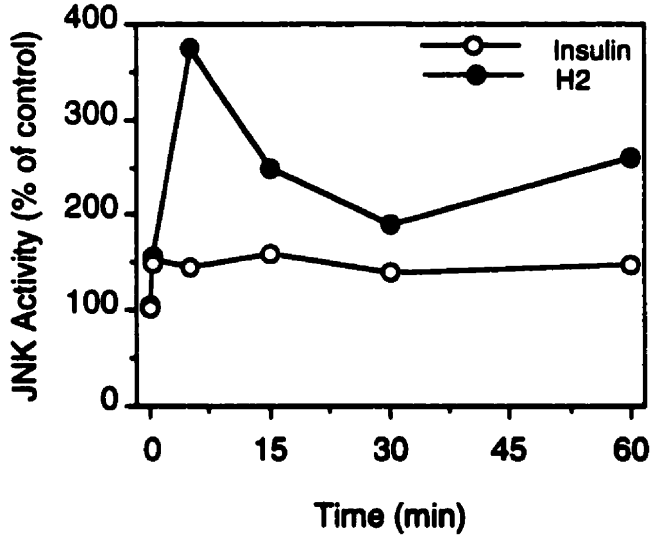
400
300
200
100
0
JNK Activity (% of control)
Insulin
H2
0
15
30
45
60
Time (min)

Figure 30. PKC activity in rat liver cytosol in response to insulin or H2 administration.

Cytosolic fractions were isolated from rat livers at the indicated times after the administration of insulin or H2 (15 μg/100 g body weight). Following partial purification by DEAE-chromatography, the fractions were assayed for insulin (—○—) or H2 (—●—) dependent PKC activity by quantitation of [^{32}P] transfer to myelin basic protein (amino acids 1-14) (A). PKC activity was selectively inhibited with the pseudosubstrate peptide inhibitor as described in Materials and Methods (B). Cytosolic fractions isolated from insulin or H2 treated rats were immunoblotted with 6 PKC isoform-specific (α, β, γ, δ, ε and ζ) anti-PKC antibodies (C).

A

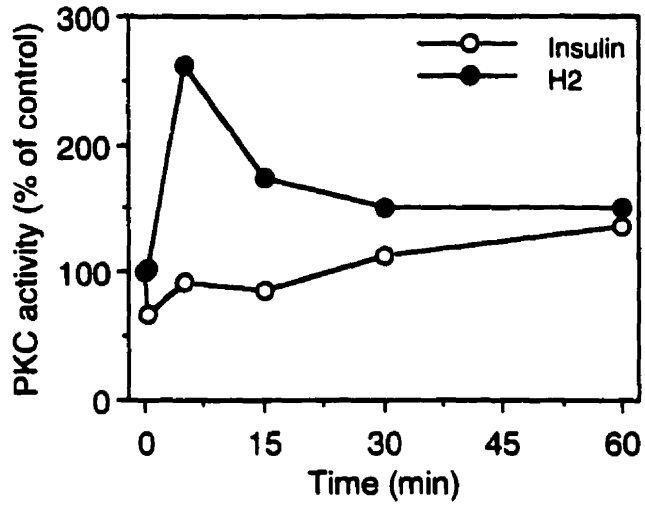
300
200
100
0
PKC activity (% of control)
Insulin
H2
0
15
30
45
60
Time (min)

B

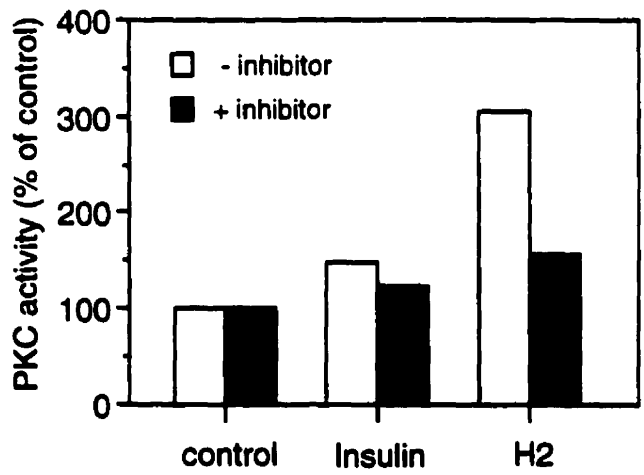
400
300
200
100
0
PKC activity (% of control)
- inhibitor
+ inhibitor
control
Insulin
H2

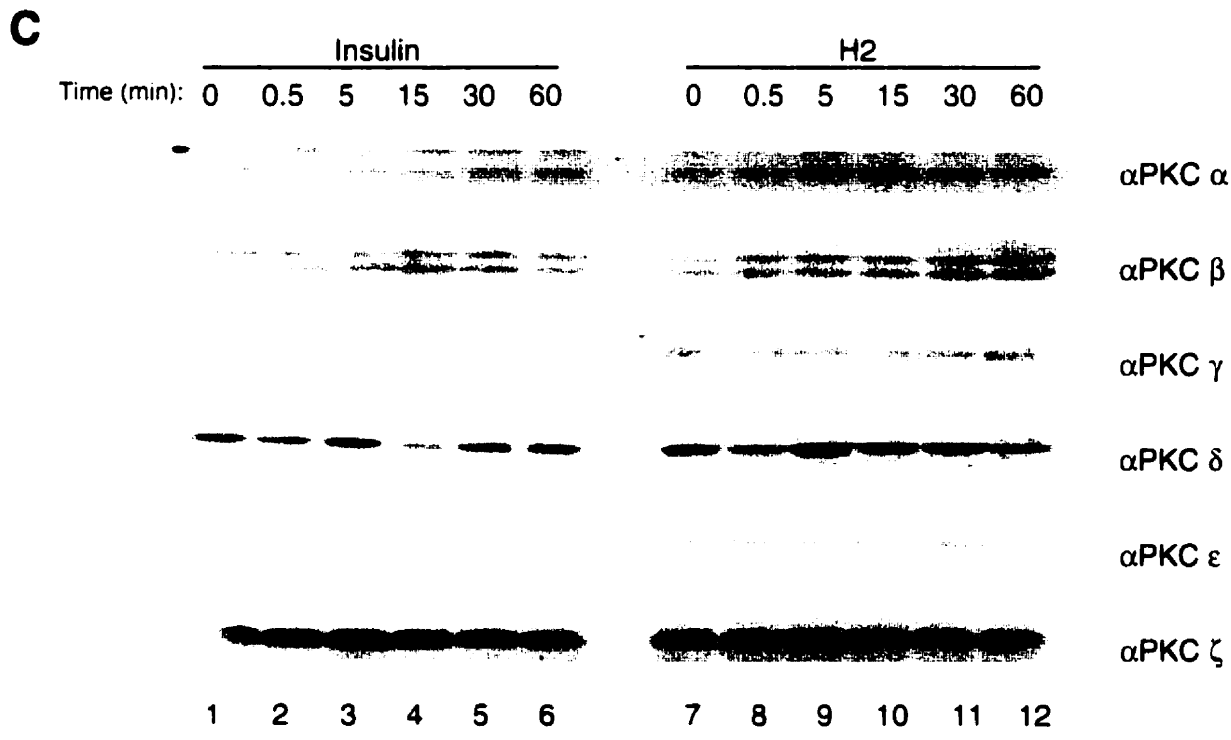
C
Insulin
H2
Time (min): 0 0.5 5 15 30 60
0 0.5 5 15 30 60
αPKC α
αPKC β
αPKC γ
αPKC δ
αPKC ε
αPKC ζ
1 2 3 4 5 6
7 8 9 10 11 12

Figure 31. Glycogen synthase activity in rat liver in response to insulin, H2 or EGF administration.

Liver post-nuclear homogenates from rats treated with insulin (—○—), H2 (—●—) (15 μg/ 100 g body weight) or EGF (10 μg/ 100 g body weight; —□—) were assayed for glycogen synthase (GS) "a" and total GS ("a+b") activity as described in Materials and Methods. Enzyme activity is represented as % control of GSa / GS(a+b) activity. Each time point represents the average of ≥ 3 experiments ± SD.

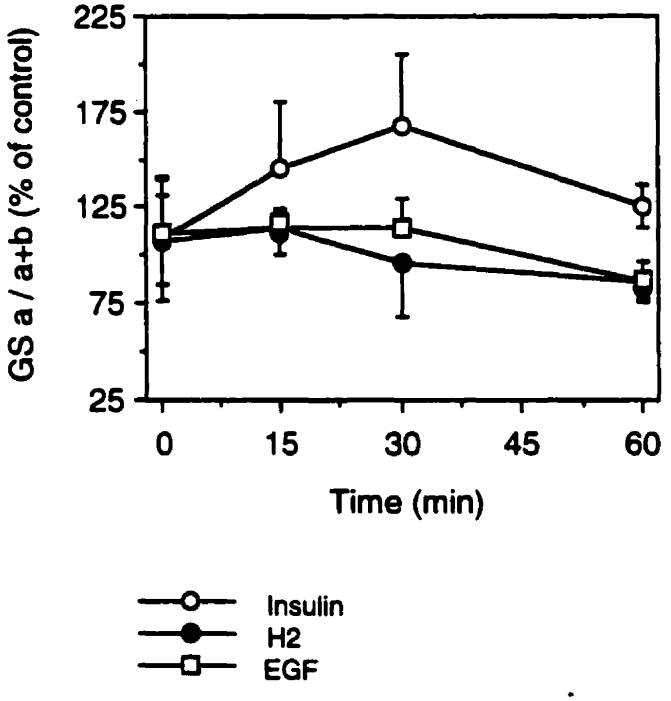
225
175
125
75
25
GS a / a+b (% of control)
0
15
30
45
60
Time (min)
Insulin
H2
EGF

Discussion

Discussion

Receptor tyrosine kinases (RTKs) transmit extracellular signals to the interior of the cell and elicit a number of changes in cellular metabolism, nuclear transcription, protein translation and cytoskeletal structure. Due to common signal transduction pathways from activated RTKs, such as the IR and EGFR, the control of specificity of signal transduction pathways used by RTKs and the regulation of these pathways is postulated to occur at multiple levels in the cell. This is based on the observations that the IR is considered to elicit metabolic responses whereas the EGFR is believed to play a role in mitogenesis. The work presented here has attempted to gain insight into the signal transduction pathways used by the EGF and insulin receptors in a physiological system, rat liver parenchyma. Following the paradigms of studies done on the EGFR, NGFR (trkA), PDGFR, IGF1-R, and IR it was found that receptors signal from specific compartments in the cell (reviewed by Baass *et al.*, 1995). Indeed a link between molecules involved in ligand-mediated receptor endocytosis and cancer have been recently drawn by Floyd and De Camilli (1998). We have therefore studied internalization and the potential role of receptor endocytosis in regulating signaling from RTKs.

Ligand Mediated Receptor Internalization

Signal transduction pathways from the IR and EGFR are initiated at the plasma membrane (see below). However, the binding of ligands induces the rapid internalization of their respective receptors into endosomes (Kay *et al.*, 1986; Khan *et al.*, 1986; Lai *et al.*, 1989a; Burgess *et al.*, 1992; Di Guglielmo *et al.*, 1994).

EGFR internalization from the plasma membrane

The initial $t_{1/2}$ of receptor loss from the plasma membrane was ~1 min for the EGFR and IR in liver parenchyma and indicates that both receptors access the internalization machinery with the same rate. The extent of receptor internalization demonstrates specificity with regards to the molecular machinery involved in endocytosis. A major difference was observed in the bulk of EGFR or IR internalized in response to receptor saturating doses of their respective ligands. The amount of internalized EGFR in response to EGF was 66% whereas the maximum amount of IR internalization was 39% in response to either insulin or H2. The significantly greater extent of EGFR internalization suggests that the regulation of the amount of receptor that is internalized may be a result of the interaction of the receptor with a limited pool of receptor-specific internalization molecules.

Although both the EGFR and IR have NPXY and di-leucine internalization motifs, only IR internalization has been documented to be dependent on these motifs for efficient

internalization (see Literature Review). This indicates that a number of possibilities for the difference in EGFR vs. IR internalization exist. (1) Distinct conformational changes in the receptor tails may allow internalization molecules to access the internalization motifs of the EGFR more efficiently than the IR. (2) The association of SH2/PTB domain containing signaling proteins with the EGFR act as internalization adjuncts. (3) The EGFR may have other internalization motifs absent from the IR carboxy terminus. There is some evidence for the latter two possibilities. The adaptor protein GRB2 associates with both the EGFR and dynamin and has been implicated in EGFR internalization (Wang and Moran, 1996). The EGFR also contains an additional internalization motif found in the carboxy terminus (residues 970-991) that interacts with the adaptor protein AP2.

Association of AP2 with the EGFR has been suggested to be involved in early events of EGFR internalization (reviewed by Schmid, 1997). According to this model, the internalization machinery associates with ligand bound receptors and upon dynamin-aided clathrin coated pit budding from the PM, clathrin and adaptor molecules (including AP2 and Eps15) dissociate from the vesicles and recycle back to the PM. However, the time-course of EGF stimulated association of AP2 with the EGFR shows that association of AP2 with the EGFR is maximum 7-15 min after ligand stimulation (Sorkin *et al.*, 1995). Therefore the majority of AP2 is associated after > 70% of cellular EGFRs have already internalized (Nesterov *et al.*, 1995a). Indeed we have observed an accumulation of AP2 in endosomal fractions in response to EGF and this accumulation is due to the physical association with the EGFR in endosomes (Dahan, S., Di Guglielmo, G.M., Baass, P.C. and J.J.M. Bergeron, manuscript in preparation). Furthermore, mutation of the AP2 binding site in the EGFR tail (residues 970-991) does not impair ligand mediated EGFR internalization (Nesterov *et al.*, 1995b). These observations imply that AP2 is involved in later steps of EGFR sorting and/or signaling as previously proposed by Beck and colleagues (1992).

EGFR traffic in the endosomal apparatus

The endosomal apparatus is positioned both temporally and physically between the plasma membrane and the lysosome. The endosomal lumen becomes progressively more acidic and provides an environment expected to induce the dissociation of internalized ligand/receptor complexes (Authier *et al.*, 1994b). Although EGF is resistant to dissociation from its receptor in endosomes (Lai *et al.*, 1989b), this has not been observed for other EGFR ligands such as TGFα (French *et al.*, 1995). TGFα binds with an identical affinity constant to the EGFR, but dissociates at a higher pH (Ebner and Derynck, 1991). Although both EGF and TGFα induce similar EGFR internalization kinetics, the

targeting of the receptor for degradation in lysosomes was more effective by EGF than TGFα (Ebner and Derynck, 1991; Waterman *et al.*, 1998). We propose that observations on EGFR traffic parallels our results on IR traffic. The IR content in the endosomal apparatus peaked 5 min after insulin stimulation and decreased thereafter to background levels. In contrast, H2 mediated IR accumulation in endosomes was maximal 15 min post-injection and egressed slowly from this compartment (67% of internalized receptors still remained in the GE fraction after 60 min). Therefore by using the EGFR as a paradigm, the effect of H2 on the IR traffic is suggested to be dependent on ligand dissociation.

Signal transduction

In resting hepatocytes, EGF and insulin receptors are expressed on the cell surface. Ligand binding induces receptor dimerization, kinase activation and the transphosphorylation of receptors on defined tyrosine residues (see Literature Review). Progress in understanding the mechanisms of receptor tyrosine kinase signal transduction has been made with the identification of multiple downstream targets of activated receptors.

EGFR signaling at the PM

The tyrosine phosphorylation of the EGFR at specific sites leads to the rapid recruitment and stable association of several downstream signaling molecules. Two of the SHC isoforms (46 and 55 kDa) were recruited to the PM fraction in response to EGF. SHC contains both a PTB and an SH2 domain enabling it to bind two phosphorylated tyrosine residues of the EGFR (Batzer *et al.*, 1995). SHC is also a substrate for the active EGFR tyrosine kinase, however it appears that only a portion of the molecules present are phosphorylated by the EGFR in this compartment. The reason for this is unclear, but may be due to submaximal kinase activity in this compartment. Indeed, the EGFR continues to autophosphorylate as it internalizes with intracellular EGFR having the highest phosphotyrosine content in the cell. This phosphorylation includes phosphorylation at Y^{1173}, a major activation site *in vivo*.

Phosphorylation of SHC provides sites for the binding of the GRB2 SH2 domain and thus may serve as a mechanism to recruit SOS to PM-associated Ras (Pawson and Scott, 1997). GRB2 may also associate with the activated, tyrosine phosphorylated EGFR directly. However, in liver parenchyma, GRB2 was seen associated mainly with endosomal fractions and to a lesser degree with the PM. This may be the consequence of the low levels of SHC phosphorylation at the PM and therefore may provide evidence for the role of SHC in rat liver. It acts as a docking site enabling the association of GRB2 with the EGFR to occur efficiently. Indeed, the endosomal fraction contained both highly

phosphorylated SHC and maximum recruitment of GRB2. This is explained by the observation that the affinity of the GRB2 SH2 domain appears to be greater for tyrosine phosphorylated SHC than phosphotyrosine-modified EGFR (Cussac *et al.*, 1994).

Intracellular EGFR signaling

Internalization of the EGFR has been proposed to represent a desensitization and/or attenuation response since the rapid sequestration of the receptor into endosomes would remove it from its downstream target Ras, the majority of which is constitutively associated with the plasma membrane (Lowy and Willumsen, 1993). In our studies, a second long lived (up to 60 min post injection) complex of phosphorylated SHC/GRB2 and SOS was observed in the cytosol of rat liver following the administration of EGF. The generation of this complex may have been a consequence of the direct phosphorylation and release of SHC by the EGFR and association with GRB2 in the cytosol. Alternatively, this may be a consequence of dissociation of the SHC-GRB2/SOS complex from the EGFR as it internalized. The low levels of GRB2/SOS associated with the EGFR at the PM, in conjunction with the rapid rate of receptor internalization, implies that a physical link between the EGFR-GRB2/SOS complex and Ras may be inefficient. Thus, the generation of a receptor-independent cytosolic pool of phosphorylated SHC-GRB2/SOS complexes may be responsible for the activation of Ras and the subsequent phosphorylation of MAP kinase which is observed during this time.

The cytosolic pool of tyrosine phosphorylated FAK may be a component in EGFR signal transduction. Although it was observed to be phosphorylated up to 60 min after EGF stimulation, the amount of phosphotyrosine-modified FAK was modest in response to EGF in rat liver cytosol. This indicates that FAK may be only one component of the EGF induced phosphorylated molecules that migrate at ~120 kDa in SDS-PAGE. Indeed a number of other molecules may make up the majority of the 120 kDa phosphoprotein signal including p130-cas, a molecule shown to be phosphorylated in response to EGF in Rat1 fibroblasts (Ojaniemi *et al.*, 1997). Nevertheless, the observation of FAK phosphorylation in response to EGF has interesting implications in liver regeneration. In fibronectin stimulated NIH 3T3 cells, FAK was observed to be phosphorylated and associate with GRB2 in an integrin-mediated fashion (Schaepfer *et al.*, 1994). Indeed, liver cells alter their level of expression of both fibronectin and the fibronectin receptor, integrin $\alpha_5\beta_1$, during liver development and regeneration (Stamatoglou *et al.*, 1992).

Although the EGF receptor is eventually targeted to the lysosome for degradation, there may to be a significant period of time in which the receptor in the endosomal compartment may continue to signal. The C-terminal region of the receptor, containing both the active tyrosine kinase domain and the autophosphorylated sites, remains cytosolically oriented and accessible to downstream signal transduction molecules in the cytosol (Wada *et al.*, 1992). The activation of the EGFR was assessed by the hallmark activation site of tyrosine phosphorylation, Y^{1173} (Downward *et al.*, 1984) and the EGFR was observed to be maximally phosphorylated in the endosomal apparatus.

Although initially recruited to the PM, SHC was found to undergo further recruitment, and in particular the 66 kDa isoform of SHC, to the EGFR in the endosomal compartment. Due to recent results indicating that $p66^{SHC}$ may act in the attenuation of the SHC response (Migliaccio *et al.*, 1997) its association with the endosomal EGFR may play a role in signal attenuation. However, the tyrosine phosphorylated 55 kDa isoform of SHC was also observed primarily in this compartment. As well, the EGFR in the endosome appeared to recruit GRB2/SOS to a significantly greater extent than at the PM. The precise role of this complex in the endosome remains to be determined although, the continued presence of the cytosolic pool of phosphorylated SHC-GRB2/SOS in the cytosol may be attributed to the release of this complex from the endosomal receptor, especially at later times (5-60 min) after EGFR internalization. This complex may play a role in activating Ras at the plasma membrane. Such a scenario would serve as an effective amplification mechanism for accessing Ras, over and above that of the physical association at the plasma membrane (Figure 32). This may provide an alternative explanation to the findings whereby truncated EGFRs are transforming (Wells *et al.*, 1990) due to the continued activation of a cytosolic pool of SHC which is itself capable of cell transformation (Pelicci *et al.*, 1992).

The work presented here show that the EGFR , GRB2, SOS and SHC all are part of a common signaling complex in the endosomal apparatus. Such complexes show a precedence of ability of recruitment of guanine nucleotide exchange factors to the endosome and may be a method of signaling of molecules to other G proteins found on the cytoplasmic side of the endosomal membrane. RasGAP associates and internalizes with the EGFR into the endosomal apparatus (Wang *et al.*, 1996) and has been shown to activate the small GTP binding protein Rab5 (Liu and Li, 1998). Rab5 is a local GTPase switch that is localized on early endosomes and controls early endosome fusion. This study demonstrates that the catalytic domain of RasGAP is able to interact physically with Rab5 and stimulate its GTPase activity indicating a possible signal transduction regulation of the Rab5-dependent endosome fusion via RasGAP.

The EGF MAP kinase cascade in the cytosolic fractions indicates that EGF stimulates MAP kinase up to 30 min after EGF stimulation. This causes a hyperphosphorylation of Raf-1 up to 60 min post ligand administration. This implies that Raf-1 is inactivated within 5 min of EGF stimulation and that MAP kinase remains active up to one hour of stimulation. This is consistent with the studies of Lai and colleagues (1989a) in rat liver where a second injection of EGF was ineffectual for both receptor internalization and tyrosine phosphorylation. This suggests that activated MAP kinase may inactivate the EGFR at the PM and prevent further EGF stimulated internalization and signal transduction.

Insulin Receptor signaling at the PM

Challenge of the IR in rat liver led to the activation of its kinase activity and resulted in autophosphorylation at the plasma membrane. However, despite the similar kinase activities of the IR stimulated at the PM in response to insulin or H2, the phosphotyrosine content of the IR was 3-fold higher in response to insulin. The reason is unclear but may indicate that the three phosphorylation sites within the catalytic domain (Y^{1158}, Y^{1162} and Y^{1163}) necessary for activation were phosphorylated in response to both insulin and H2 administration. The carboxy terminal tyrosine residues (Y^{1328} and Y^{1334}) therefore may have been accessed differently in response to insulin or H2 stimulation. Reduced tyrosine phosphorylation did not impinge on IR access to substrate since IRS-1 phosphorylation and its subsequent association with PI 3'-kinase activity were similar in response to insulin or H2. This indicates that the IRS-1 PTB domain-IR interaction site (Y^{972} of the IR) was phosphorylated similarly in response to either insulin of H2.

Unlike the EGFR, IR kinase activation and autophosphorylation of the cytosolic tail results in a tenuous association with the major downstream substrates. This may due to the nature of the tyrosine residues which are available in this receptor after autophosphorylation. These sites do not bind with high affinity to the SH2 and PTB domains of downstream signaling molecules, therefore the interactions are transient. Nevertheless, the major substrate of the IR kinase, insulin receptor substrate-1 (IRS-1), was phosphorylated in response to insulin stimulation (Figure 33). In rat liver a pool of IRS-1 molecules was localized to the PM. A rapid efficient interaction between the receptor and substrate may be essential as a result of the rapid internalization of the receptor. However, no tyrosine phosphorylated IRS-1 could be detected at the PM, which is consistent with the dissociation of phosphorylated IRS-1 into cytosol. Indeed, tyrosine phosphorylated IRS-1 was detected in the cytosol within 30 sec of ligand administration,

and the extent of IRS-1 phosphorylation nor was its association with PI3'-kinase affected by the different ligands used

Despite the numerous potential substrate molecules and interactions described for the EGF and insulin receptors (see Literature Review), only a subset may be physiologically relevant in any given system. The specificity of EGF and insulin receptor signaling in the rat liver appears to be established early after receptor activation. The accessibility of signaling molecules is most likely a consequence of the relative affinities of the various SH2 and/or PTB domains for the tyrosine phosphorylated residues present in each receptor. In addition, there may exist liver specific molecules (PTPases or molecules capable of selectively sequestering downstream substrates away from the activated receptor) which serve to prevent high levels of phosphorylation of other potential targets or their interaction with these receptors.

Intracellular Insulin Receptor signaling

IR internalization is accompanied by the dissociation and degradation of insulin in the endosomal lumen and leads to a decrease in receptor phosphotyrosine content and inactivation (Burgess *et al.*, 1992). Several endosomal mechanisms for the regulation of insulin receptor signaling have been proposed. The endosomal lumen contains insulin degrading activity (EAI) within the endosome (Authier *et al.*, 1994a). The cytosolic face of endosomes contain PTPase activity directed against the IR (Faure *et al.*, 1992). To determine if ligand dissociation and EAI played a role in the regulation of IR signaling from the endosome an insulin analog, H2, was characterized.

The administration of insulin and H2 to rat circulation showed that clearance of either ligand by the liver was faster for insulin than H2. This was attributed to the slower degradation of H2 in the endosomal apparatus. Indeed this slower degradation was correlated with decreased dissociation of H2 from the IR. However, even in the absence of receptors, H2 was a poor substrate for the acidic endosomal insulinase. This tool was then used to show major differences in signaling of the IR that involved the non-traditional pathways of signal transduction.

The results demonstrated that, contrary to the insulin-stimulated IR, receptors stimulated by H2 are not dephosphorylated in the endosome. Therefore the dissociation and degradation of insulin in the lumen of the endosome is required for receptor dephosphorylation. This is potentially due to a conformational change in the receptor that allows specific phosphotyrosine residues access to the endosomal associated PTPase(s). The constant association of H2 with the IR directly tests, *in vivo*, the idea that ligand dissociation is required for receptor inactivation and dephosphorylation.

Studies using the *in vivo* introduction of the PTPase inhibitor, bisperoxo (1,10-phenanthroline) oxovanadate anion (bpV(phen)) showed a selective effect on the phosphotyrosine content of the basal level of IR constitutively present in endosomes (reviewed by Drake and Posner, 1998). Augmentation of the phosphotyrosine content of the endosomal IR led to the enhanced phosphorylation of IRS-1 as well as other downstream effects. By combining our results with those produced using the bpV(phen) compound, a signal transduction model is proposed in rat liver for the IR (Figure 33).

Increased IR kinase activity in the endosomal apparatus in response to H2 administration correlated with lower MAP kinase activity. This was counterintuitive since the augmented endosomal IR signaling was predicted to extend the stimulation of the MAP kinase pathway. This may be explained by the mutual exclusivity of activating MAP kinase pathways and stress induced pathways leading to JNK activation. The JNK pathway leads to the N-terminal phosphorylation and activation of the transcriptional activity of Jun (Minden *et al.*, 1994) which may then autoregulate the AP-1 element in the c-jun promoter. In rat liver, JNK was observed to be inactive and c-jun transcription was absent in response to insulin. In response to H2, the JNK pathway was accessed by H2 and is proposed to have stimulated c-jun transcription, further indicating that an alternative pathway was activated by the endosomal IR (Figure 34).

Although glucose freely enters the liver and does not depend on insulin stimulated glucose transport as is the case of muscle and adipose, it has been suggested to play a potentiating role (Villar-Palasi and Guinovart, 1997). The fact that the liver receives the first bolus of insulin from the pancreas prompted us to test the effect of insulin and H2 on GS activity. As with the observations of c-jun transcription and reduced MAP kinase activity, GS also was reduced in response to H2. In this case, stress pathways may or may not account for these actions. PKC activity has been described to interfere with GS activity and be linked to insulin resistance in Diabetes. Bandyopadhyay *et al.*, (1997) have shown that adipocytes overexpressing PKCα and β impeded insulin stimulated GS activity. Combined with our results, we suggest that the active IR at the endosomal locus may access components that leads to increased PKC activity (Figure 34).

Conclusion

Using subcellular fractionation of rat liver we have attempted to defined signaling transduction pathways from the insulin and EGF receptors in a physiological system. Our results indicate that there are two levels of regulation of signaling from the IR and EGFR in rat liver. The first level of is based on the specificity of molecular interactions of RTKs with their downstream subset of adaptors and/or substrates leading to metabolic vs. mitogenic responses. The second level of regulation is based on molecules in the endosomal apparatus that are involved in modulating RTK traffic and attenuation of signal transduction. The selection of differentiation or metabolic pathways as opposed to pathways involved in cell cycle and growth control for different RTKs may be a consequence of their traffic and subcellular location. The recent advances in the identification of molecules involved in RTK internalization and the realization that they are involved mitogenic responses have added a new facet to the study of receptor mediated endocytosis. The availability of a growing number of reagents for studying RTK signal transduction, membrane traffic, and subcellular compartments indicates that this is will be an area of detailed investigation.

Figure 32. EGFR traffic and signal transduction in rat liver.

The binding of EGF to its cell surface receptor results in the rapid phosphorylation and activation of the EGFR tyrosine kinase and rapid internalization of the EGF-EGFR complexes into endosomes. SHC is found associated with the EGFR at the plasma membrane (PM) or on endosomes and is tyrosine phosphorylated. GRB2 associates with phosphorylated SHC or the EGFR and initiates further downstream effects. EGF induces the phosphorylation of FAK and other 120 kDa proteins as well as SHC in the cytosol. The extended complex of phosphotyrosine-modified SHC/GRB2/SOS in the cytosol, up to 60 min post EGF injection, is postulated to be a result of the dissociation of this complex from the endosomal EGFR. Activation of Ras at the PM elicits a MAP kinase cascade in the cytosol which results in the transcription of c-myc, c-fos and c-jun. The association and/or activities of molecules directly tested are shown in bold. Solid lines represent movement or links that were directly tested and the dashed lines represent postulated movements and/or links.

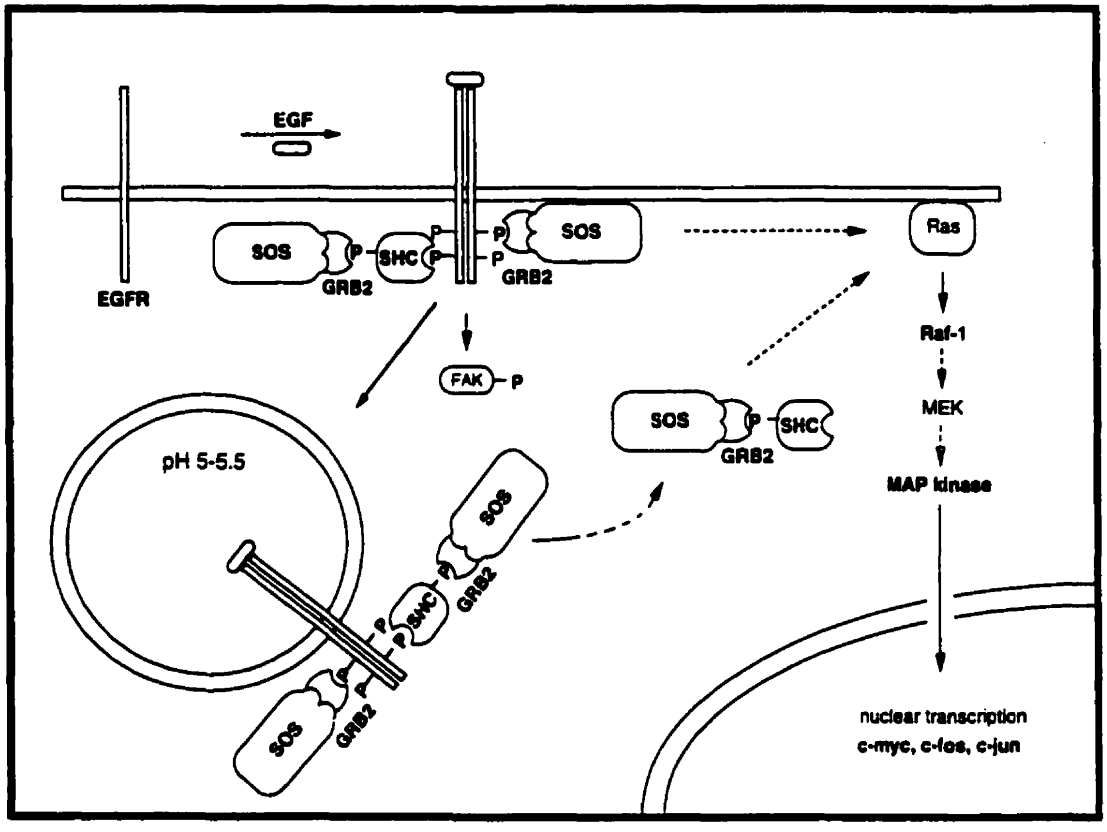
EGF
EGFR
SOS
P
SHC
GRB2
Ras
Raf-1
MEK
MAP kinase
FAK
pH 5-5.5
nuclear transcription
c-myc, c-fos, c-jun

Figure 33. Insulin receptor traffic and signal transduction in rat liver in response to insulin.

Insulin binding to its cell surface receptor results in the rapid phosphorylation and activation of the insulin receptor (IR) tyrosine kinase and internalization of the insulin-IR complexes into endosomes. IRS-1 is postulated to be phosphorylated mainly by PM localized IRs. PI 3'-kinase associates with phosphorylated IRS-1 and initiates further downstream effects. Dephosphorylation of the IR at the endosome attenuates signaling and is coupled to insulin degradation by acidic endosomal insulinase (EAI). Solid lines represent associations or activities directly tested. Dashed lines represent postulated interactions or links.

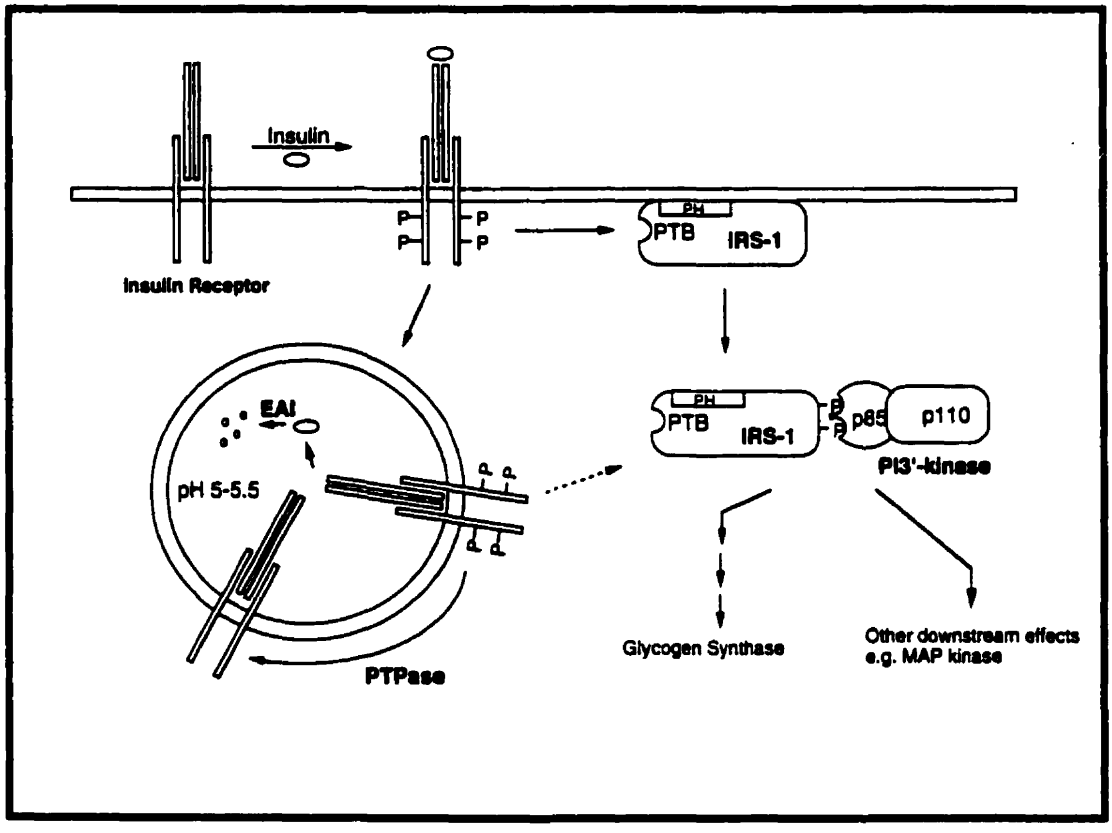
Insulin
Insulin Receptor
P
P
P
P
PH
PTB
IRS-1
EAI
pH 5-5.5
PTPase
PH
PTB
IRS-1
P
P
p85
p110
PI3'-kinase
Glycogen Synthase
Other downstream effects
e.g. MAP kinase

Figure 34. Insulin receptor traffic and signal transduction in rat liver in response to H2.

The insulin analog, H2, binding to the cell surface insulin receptor results in the rapid phosphorylation and activation of the insulin receptor (IR) tyrosine kinase and internalization of the H2-IR complexes into endosomes. IRS-1 may be mainly phosphorylated by PM localized IRs. PI 3'-kinase associates with phosphorylated IRS-1 and initiates further downstream effects. The dephosphorylation of the IR at the endosomal locus is delayed compared to insulin stimulation and is possibly coupled to reduced ligand (H2) dissociation and degradation. Activated IR at the endosomal locus is correlated with increased PKC and JNK activities and lowered glycogen synthase activity. Solid lines represent associations or activities directly tested. Dashed lines represent postulated interactions or links.

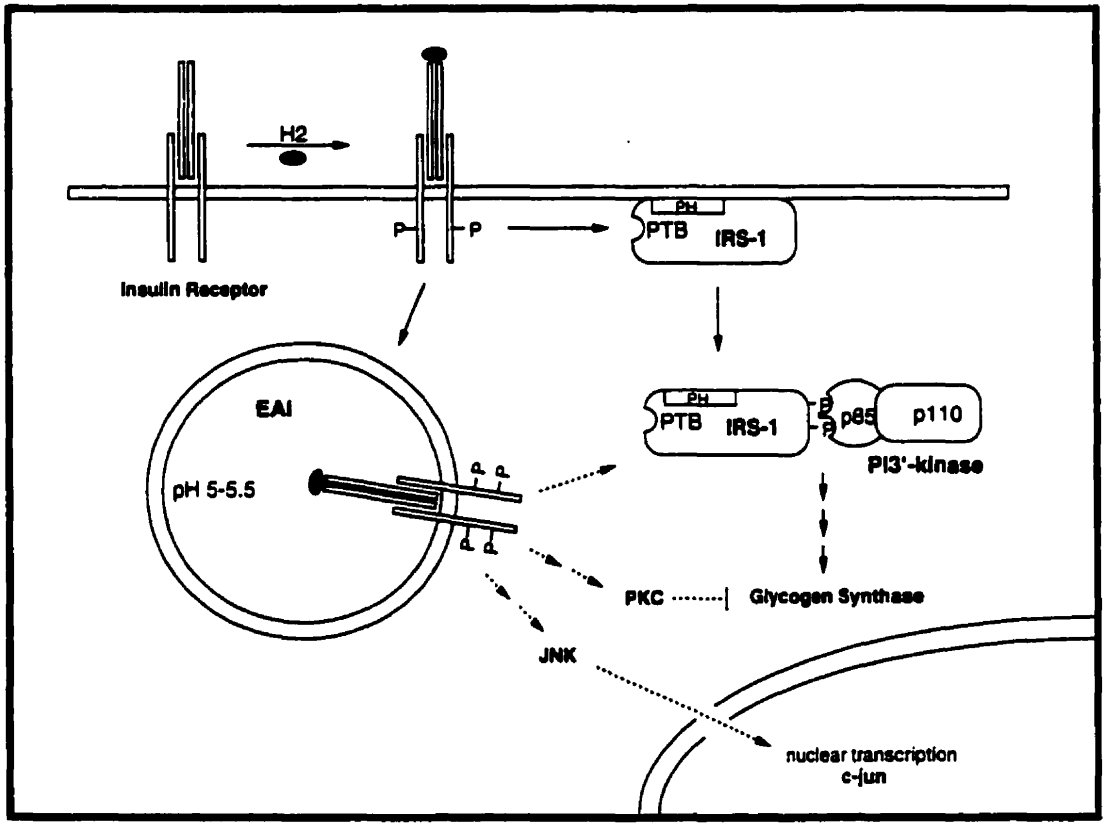
H2
P
P
PH
PTB
IRS-1
Insulin Receptor
EAI
pH 5-5.5
PH
PTB
IRS-1
p85
p110
PI3'-kinase
PKC
Glycogen Synthase
JNK
nuclear transcription
c-jun

Original Contributions

In this work, we have attempted to assess the role of receptor mediated endocytosis and signal transduction *in vivo*. The following original observations are a result of our studies.

1. Using subcellular fractionation and phosphopeptide specific antibodies we demonstrated that the EGFR is phosphorylated on tyrosine-1173 both at the plasma membrane and in endosomes in response to ligand.

2. Our results demonstrate that the signaling complex of SHC, GRB2 and SOS is physically associated with internalized EGFR *in vivo*. In response to EGF injection, SHC was recruited to the PM but was highly tyrosine phosphorylated on endosomal membranes. This was paralleled by the principal recruitment of GRB2 to the endosomal compartment as well as recruitment of SOS at this cellular locus.

3. This is the first work describing a cytosolic pool of phosphorylated SHC in association with GRB2 and SOS in liver parenchyma. This observation is hypothesized to extend Ras stimulation at the plasma membrane.

4. The use of the insulin analog, H2 assessed the effect of ligand dissociation on receptor traffic. We have demonstrated that ligand affinity for the IR does not affect the rate or bulk of IR loss from the plasma membrane. However, an endosomal accumulation of the H2-stimulated IR was observed higher than insulin-stimulated IR and demonstrates that ligand dissociation modifies post-internalization receptor traffic.

5. We have demonstrated that insulin-induced IR phosphorylation at the PM is greater than that observed in response to H2 stimulation. Upon endocytosis, the insulin-stimulated receptor was dephosphorylated, while the H2-stimulated receptor augmented its state of phosphorylation and tyrosine kinase activity.

6. This is the first study investigating the distribution of the insulin receptor substrate, IRS-1, in rat liver subcellular fractions as well as its tyrosine phosphorylation in response to insulin or H2 stimulation. A substantial fraction of cellular IRS-1 was observed localized to the PM but not the endosomal apparatus. Stimulation with insulin or H2 resulted in similar amount of cytosolic IRS-1 tyrosine phosphorylation and association with

PI 3'-kinase activity. Furthermore EGF was seen to transiently phosphorylate IRS-1 and induce its association with PI 3'-kinase.

7. This is the first study comparing the EGF and insulin receptor specificity in accessing the Ras-MAP kinase pathway and nuclear transcription in rat liver. Raf-1 mobility shifts were observed in response to the injection of receptor saturating doses of EGF, but not in response to insulin or H2. MAP kinase activity was also observed in response to ligand in the following order: EGF >> insulin > H2. EGF administration caused an increase in the transcription of the early response genes, c-myc, c-fos and c-jun. Insulin stimulation did not result in the significant increase in transcript levels. H2 stimulation selectively induced an increase in c-jun transcription which correlated with increased JNK activity.

8. Glycogen synthase and PKC activities were assessed in rat liver. The three isoform of PKC that were the most prevalent were α, δ and ζ. Glycogen synthase activity was reduced in response to H2 and we believe this observation to be a result of increased PKC activity and augmented endosomal activation of the IR kinase.

References

References

Abe, Y., Odaka, M., Inagaki, F., Lax, I., Schlessinger, J. and Kohda, D. (1998). Disulfide bond structure of human epidermal growth factor receptor. *J. Biol. Chem.* 273: 11150-11157.

Alessi, D. R., Andjelkovic, M., Caudwell, B., Cron, P., Morrice, N., et al. (1996). Mechanism of activation of protein kinase B by insulin and IGF-1. *EMBO J.* 15, 6541-51.

Anderson, N. G., Li, P., Marsden, L. A., Williams, N., Roberts, T. M. and Sturgill, T. W. (1991). Raf-1 is a potential substrate for mitogen-activated protein kinase in vivo. *Biochem. J.* 277: 573-576.

Araki, E., Lipes, M. A., Patti, M.-E., Brüning, J. C., Haag, B., Johnson, R. S. and Kahn, C. R. (1994). Alternative pathway of insulin signaling in mice with targeted disruption of the IRS-1 gene. *Nature* 372: 186-190.

Authier, F., Di Guglielmo, G. M., Danielsen, G. M. and Bergeron, J. 1998. Uptake and metabolic fate of [his(a8),his(b4),glu(b10),his(b27)]insulin in rat liver in vivo. *Biochem. J.* 332: 421-430.

Authier, F., Mort, J. S., Bell, A. W., Posner, B. I. and Bergeron, J. J. 1995. Proteolysis of glucagon within hepatic endosomes by membrane-associated cathepsins B and D. *J. Biol. Chem* 270:15798-15807.

Authier, F., Posner, B. I. and Bergeron, J. J. M. (1994b). Hepatic endosomes are a major physiological locus of insulin and glucagon degradation in vivo: Cellular Proteolytic Systems. A.J. Ciechanover and A.L. Scwartz, Eds. John Wiley & Sons, Inc., pp. 89-113.

Authier, F., Rachubinski, R. A., Posner, B. I. and Bergeron, J. J. M. (1994a). Endosomal proteolysis of insulin by an acidic thiol metalloprotease unrelated to insulin degrading enzyme. *J. Biol. Chem.* 269: 3010-3016.

Authier, F. and Desbuquois, B. (1991). Degradation of glucagon in isolated liver endosomes. ATP-dependence and partial characterization of degradation products. *Biochem. J.* 280: 211-218.

Avruch, J., Zhang, X.-F. and Kyriakis, J. M. (1994). Raf meets ras: completing the framework of a signal transduction pathway. *Trends Biochem. Sci.* 19: 279-283.

Azpiazu, I., Saltiel, A. R., DePaoli-Roach, A. A. and Lawrence, J. C. (1996). Regulation of both glycogen synthase and PHAS-I by insulin in rat skeletal muscle involves mitogen-activated protein kinase-independent and rapamycin-sensitive pathways. *J. Biol. Chem.* 271: 5033-5039.

Baass P.C., Di Guglielmo G.M., Authier F., Posner B.I. and Bergeron J.J.M. (1995) Compartmentalized signal transduction by receptor tyrosine kinases. *Trends Cell Biol.* 5: 465-470,.

Backer, J. M., Kahn, C. R. and White, M. F. (1989). Tyrosine phosphorylation of the insulin receptor during insulin-stimulated internalization in rat hepatoma cells. *J. Biol. Chem.* 264: 1694-1701.

Backer, J. M., Kahn, C. R. and White, M. F. (1990). The dissociation and degradation of internalized insulin occur in the endosomes of rat hepatoma cells. *J. Biol. Chem.* 265: 14828-14835.

Backer, J. M., Shoelson, S. E., Haring, E. and White, M. F. (1991). Insulin receptors internalize by a rapid, saturable pathway requiring receptor autophosphorylation and an intact juxtamembrane region. *J. Cell Biol.* 115 : 1535-1545.

Backer, J., Myers Jr. M. G., Shoelson, S. E., Chin, D. J., Sun, X.-J., Miralpeix, M., Hu, P., Margolis, B., Skolnik, E. Y., Schlessinger, J. and White, M. F. (1992). Phosphatidylinositol 3'-kinase is activated by association with IRS-1 during insulin stimulation. *EMBO J.* 11: 3469-3479.

Baker, S. J., Keerppola, T. K., Luk, D., Vandenberg, M. T., Marshak, D. R., Curran, T. and Abate, C. (1992). Jun is phosphorylated by several protein kinases at the same sites that are modified in serum-stimulated fibroblasts. *Mol. Cell. Biol.* 12: 4694-4705.

Bandyopadhyay, G., Standaert, M. L., Zhao, L., Yu, B., Avignon, A., et al. (1997). Activation of protein kinase C (alpha, beta, and zeta) by insulin in 3T3/L1 cells. Transfection studies suggest a role for PKC-zeta in glucose transport. *J. Biol. Chem.* 272: 2551-2558.

Bangalore, L., Tanner, A. J., Laudano, A. P. and Stern, D. F. (1992). Antiserum raised against a synthetic phosphotyrosine-containing peptide selectively recognizes $p185^{neu/erbB-2}$ and the epidermal growth factor receptor. *Proc. Natl. Acad. Sci. USA* 89: 11637-11641.

Bar-Sagi, D., Rotin, D., Batzer, A., Mandiyan, V. and Schlessinger, J. (1993). SH3 domains direct cellular localization of signaling molecules. *Cell* . 74: 83-91.

Barford, D. and Neel, B. G. (1998). Revealing mechanisms for SH2 domain mediated regulation of the protein tyrosine phosphatase SHP-2. *Structure*. 6: 249-254.

Baron, V., Alengrin, F. and Van Obberghen, E. (1998). Dynamin associates with Src-Homology Collagen (Shc) and becomes tyrosine phosphorylated in response to insulin. *Endocrinology*. 139: 3034-3047.

Batzer, A. G., Blaikie, P., Nelson, K., Schlessinger, J. and Margolis, B. (1995). The phosphotyrosine interaction domain of SHC binds an LXNPXY motif on the epidermal growth factor receptor. *Mol. Cell. Biol.* 15: 4403-4409.

Beck, K. A., Chang, M., Brodsky, F. M. and Keen, J. H. (1992). Clathrin assembly protein AP-2 induces aggregation of membrane vesicles: A possible role for AP-2 in endosome fusion. *J. Cell Biol.* 119: 787-796.

Begum, N. (1995). Stimulation of protein phosphatase-1 activity by insulin in rat adipocytes. Evaluation of the role of mitogen-activated protein kinase pathway. *J. Biol. Chem.* 270: 709-714.

Benmerah, A., Lamaze, C., Begue, B., Schmid, S. L., Dautry-Varsat, A. and Cerf-Bensussan, N. (1998). AP-2/Eps15 interaction is required for receptor-mediated endocytosis. *J. Cell Biol.* 140: 1055-1062.

Bergeron, J. J. M., Cruz, J., Khan, M. N. and Posner, B. I. (1985). Uptake of insulin and other ligands in receptor rich endocytic components of target cells: the endosomal apparatus. *Annu. Rev. Physiol.* 47: 383-403.

Bergeron, J. J. M., Rachubinski, R., Searle, N., Borts, D., Sikstrom, R. and Posner, B. I. (1980). Polypeptide hormone receptors in vivo: demonstration of insulin binding to adrenal gland and gastrointestinal epithelium by quantitative radioautography. *J. Histochem. Cytochem.* 28: 824-835.

Bergeron, J. J. M., Sikstrom, R., Hand, A. R. and Posner, B. I. (1979). Binding and uptake of ^{125}I-insulin into rat liver hepatocytes and endothelium. *J. Cell. Biol.* 80: 427-432.

Bergeron, J. J., Di Guglielmo, G. M., Baass, P. C., Authier, F. and Posner, B. I. (1995). Endosomes, receptor tyrosine kinase internalization and signal transduction. *Bioscience Reports.* 15: 411-418.

Bernier, M., Liotta, A. S., Kole, H. K., Shock, D. D. and Roth, J. (1994). Dynamic regulation of intact and C-terminal truncated insulin receptor phosphorylation in permeabilized cells. *Biochemistry.* 33: 4343-4351.

Bevan A.P., Drake P.G., Bergeron J.J.M. and Posner B.I. (1996): Intracellular signal transduction: The role of endosomes. *TEM* . 7: 13-21.

Boll, W., Gallusser, A. and Kirchhausen, T. (1995). Role of the regulatory domain of the EGF receptor cytoplasmic tail in selective binding of the clathrin associated complex AP-2. *Curr. Biol.* 5, 1168-1178.

Bollen, M., Vandenheede, J. R., Goris, J. and Stalmans, W. (1988). Characterization of glycogen-synthase phosphatase and phosphorylase phosphatase in subcellular liver fractions. *Biochim. Biophys. Acta.* 969: 66-77.

Boyle, W. J., Smeal, T., Defize, L. H. K., Angel, P., Woodgett, J. R., Karin, M. and Hunter, T. (1991). Activation of protein kinase C decreases phosphorylation of c-jun at site that negatively regulate its DNA-binding activity. *Cell* . 64: 573-584.

Bradford, D. (1976). A rapid and sensitive method for the quantitation of microgram quantities of protein utilizing the principle of protein-dye binding. *Anal. Biochem.* 72: 248-254.

Brady, M. J., Nairn, A. C. and Saltiel, A. R. (1997). The regulation of glycogen synthase by protein phosphatase 1 in 3T3-L1 adipocytes. Evidence for a potential role for DARPP-32 in insulin action. *J. Biol. Chem.* 272: 29698-29703.

Brodsky, F. M., Hill, B. L., Acton, S. L., Nathke, I., Wong, D. H., et al. (1991). Clathrin light chains: arrays of protein motifs that regulate coated-vesicle dynamics. *TIrends. Biochem. Sci.* 16: 208-213.

Buday, L. and Downward, J. (1993). Epidermal growth factor regulates p21ras through the formation of a complex of receptor, GRB2 adapter protein and Sos nucleotide exchange factor. *Cell* 73: 611-620.

Burbelo, P. D. and Hall, A. (1995). 14-3-3 proteins. Hot numbers in signal transduction. *Curr. Biol.* 5: 95-96.

Burgering, B. M., Pronk, G. J., van Weeren, P. C., Chardin, P., and Bos, J. L. (1993). cAMP antagonizes p21ras directed activation of extracellular signal regulated kinase 2 and phosphorylation of mSOS nucleotide exchange factor. *EMBO J.* 12: 4211-4220.

Burgess, J. W., Wada, I., Ling, N., Kahn, M. N., Bergeron, J. J. M., and Posner, B. I. (1992). Decrease in β-subunit phosphotyrosine correlates with internalization and activation of the endosomal insulin receptor kinase. *J. Biol. Chem.* 267: 10077-10086.

Cadena, D. L., Chan, C.-L. and Gill, G. N. (1994). The intracellular tyrosine kinase domain of the epidermal growth factor receptor undergoes a conformational change upon autophosphorylation. *J. Biol. Chem.* 269: 260-265.

Canossa, M., Twiss, J. L., Verity, A. N., Shooter, E. M. (1996). p75(NGFR) and TrkA receptors collaborate to rapidly activate a p75(NGFR)-associated protein kinase. *EMBO J.* 15: 3369-3376.

Carbone, R., Fre, S., Iannolo, G., Belleudi, F., Mancini, P., et al. (1997). eps15 and eps15R are essential components of the endocytic pathway. *Cancer Research.* 57: 5498-5504.

Carpentier, J.-L., and McClain, D. (1995). Insulin receptor kinase activation releases a constraint maintaining the receptor on microvilli. *J. Biol. Chem.* 270: 5001-5006.

Ceresa, B. P., Kao, A. W., Santeler, S. R. and Pessin, J. E. (1998). Inhibition of clathrin-mediated endocytosis selectively attenuates specific insulin receptor signal transduction pathways. *Mol. Cell. Biol.* 18: 3862-3870.

Chakrabarti, R., Joly, M., and Corvera, S. (1993). Redistribution of clathrin coated vesicle adaptor proteins during adipocyte differentiation of 3T3-L1 cells. *J. Cell Biol.* 123: 79-87.

Chang, C.-P., Lazar, C. S., Walsh, B. J., Komuro, M., Collawn, J. F., Kuhn, L. A., Tainer, J. A., Trowbridge, I. S., Farquhar, M. G., Rosenfeld, M. G., Wiley, H. S., and Gill, G. N. (1993). Ligand-induced internalization of the epidermal growth factor receptor is mediated by multiple endocytic codes analogous to the tyrosine motif found in constitutively internalized receptors. *J. Biol. Chem.* 268: 19312-19320.

Charest, A., Wagner, J., Kwan, M. and Tremblay, M. L. (1997). Coupling of the murine protein tyrosine phosphatase PEST to the epidermal growth factor (EGF) receptor through a Src homology 3 (SH3) domain-mediated association with Grb2. *Oncogene.* 14: 1643-1651.

Chavrier, P., Parton, R. G., Hauri, H. P., Simons, K. and Zerial, M. (1990). Localization of low molecular weight GTP binding proteins to exocytic and endocytic compartments. *Cell.* 62: 317-329.

Chen, W. S., Lazar, C. S., Lund, K. A., Welsh, J. B., Chang, C.-P., Walton, G. M., Der, C. J., Wiley, H. S., Gill, G. N. and Rosenfeld, M. G. (1989). Functional independence of the epidermal growth factor receptor from a domain required for ligand-induced internalization and calcium regulation. *Cell.* 59: 33-43.

Chin, D. J., Straubinger, R. M., Acton, S., Näthke, I. and Brodsky, F. M. (1989). 100-kDa polypeptides in peripheral clathrin coated vesicles are required for receptor mediated endocytosis. *Proc. Natl. Acad. Sci. USA* 86, 9289-9293.

Chomczynski, P. and Sacchi, N. (1987). Single-step method of RNA isolation by acid guanidinium thiocyanate phenol chloroform extraction. *Anal. Biochem.* 162: 156-159.

Chow, J. C., Condorelli, G. and Smith, R. J. (1998). Insulin-like growth factor-I receptor internalization regulates signaling via the Shc/mitogen-activated protein kinase pathway, but not the insulin receptor substrate-1 pathway. *J. Biol. Chem.* 273: 4672-4680.

Chow, Y.-H., Pumiglia, K., Jun, T. H., Dent, P. and Sturgill, T. (1995). Functional mapping of the N-terminal regulatory domain in the human Raf-1 protein kinase. *J. Biol. Chem.* 270: 14100-14106.

Chuang, E., Barnard, D., Hettichi, L., Zhang, X.-F., Avruch, J. and Marshall, M. S. (1994). Critical binding and regulatory interactions between Ras and Raf occur through a small, stable N-terminal domain of Raf and specific Ras effector residues. *Mol. Cell. Biol.* 14, 5318-5325.

Cobb, M. H., Boulton, T. G. and Robbins, D. J. (1991). Extracellular signal regulated kinases: ERKs in progress. *Cell Reg.* 2: 965-978.

Coghlan, M. P., Pillay, T. S., Tavare, J. M. and Siddle, K. (1994). Site-specific anti-phosphopeptide antibodies: use in assessing insulin receptor serine/threonine phosphorylation state and identification of serine-1327 as a novel site of phorbol ester-induced phosphorylation. *Biochem. J.* 303: 893-899.

Cohen, P. (1989). The structure and regulation of protein phosphatases. *Ann. Rev. Biochem.* 58: 453-508.

Cohen, S., Carpenter, G. and King, L., Jr. (1980). Epidermal growth factor-receptor-protein kinase interactions. Co-purification of receptor and epidermal growth factor-enhanced phosphorylation activity. *J. Biol. Chem.* 255: 4834-4842.

Collett, M. S. and Erikson, R. L. (1978). Protein kinase activity associated with the avian sarcoma virus src gene product. *Proc. Natl. Acad. Sci. USA.* 75: 2021-2024.

Corvera, S., Chawla, A., Chakrabarti, R., Joly, M., Buxton, J. and Czech, M. P. (1994). A double leucine within the GLUT4 glucose transporter COOH-terminal domain functions as an endocytosis signal. *J. Cell Biol.* 126: 979-989.

Craparo, A., Freund, R. and Gustafson, T. A. (1997). 14-3-3 (epsilon) interacts with the insulin-like growth factor I receptor and insulin receptor substrate I in a phosphoserine-dependent manner. *J. Biol. Chem.* 272: 11663-11669.

Cross, D. A., Alessi, D. R., Cohen, P., Andjelkovich, M. and Hemmings, B. A. (1995). Inhibition of glycogen synthase kinase-3 by insulin mediated by protein kinase B. *Nature.* 378, 785-9.

Cussac, D., Frech, M. and Chardin, P. (1994). Binding of the GRB2 SH2 domain to phosphotyrosine motifs does not change the affinity of its SH3 domain for SOS proline rich motifs. *EMBO J.* 13: 4011-4021.

Damke, H. (1996). Dynamin and receptor-mediated endocytosis. *FEBS Lett.* 389: 48-51.

Daukas, G. and Zigmond, S. H. (1985). Inhibition of receptor-mediated but not fluid-phase endocytosis in polymorphonuclear leukocytes. *J. Cell Biol.* 101: 1673-1679.

De Metys, P., Gu, J.-L., Shymko, R. M., Kaplan, B. E., Bell, G. I. and Whittaker, J. (1990). Identification of a ligand binding region of the human insulin receptor encoded by second exon of the gene. *Mol. Endocrinol.* 4: 409-416.

Decker, S. J. (1993). Transmembrane signaling by epidermal growth factor receptors lacking autophosphorylation sites. *J. Biol. Chem.* 268: 9176-9179.

Dent, P., Lavoinne, A., Nakielny, S., Caudwell, F. B., Watt, P. and Cohen, P. (1990). The molecular mechanism by which insulin stimulates glycogen synthesis in mammalian skeletal muscle. *Nature.* 348: 302-308.

Desbuquois, B., Janicot, M. and Dupuis, A. 1990. Degradation of insulin in isolated liver endosomes is functionally linked to ATP-dependent endosomal acidification. *Eur. J. Biochem.* 193: 501-512

Diehl, A. M. and Rai, R. M. (1996). Regulation of signal transduction during liver regeneration. *FASEB J.* 10: 215-227.

Di Guglielmo, G. M., Baass, P. C., Ou, W. J., Posner, B. I. and Bergeron, J. J. (1994). Compartmentalization of SHC, GRB2 and mSOS, and hyperphosphorylation of Raf-1 by EGF but not insulin in liver parenchyma. *EMBO J.* 13: 4269-4277.

Di Guglielmo, G. M., Drake, P. G., Baass, P. C., Authier, F., Posner B. I. and Bergeron, J. (1998). Insulin receptor internalization and signalling. *Mol. Cell. Biochem.* 182: 59-63.

Doherty II, J.-J., Kay, D. G., Lai, W. H., Posner, B. I. and Bergeron, J. J. M. (1990). Selective degradation of insulin within rat liver endosomes. *J. Cell Biol.* 110: 35-42.

Doiron, B., Cuif, M.-H., Kahn, A. and Diaz-Guerra, M.-J. M. (1994). Respective roles of glucose, fructose, and insulin in the regulation of the liver-specific pyruvate kinase gene promoter. *J. Biol. Chem.* 269: 10213-10216.

Donaldson, R. W. and Cohen, S. (1992). Epidermal growth factor stimulates tyrosine phosphorylation in the neonatal mouse: Association of a M_r 55,000 substrate with the receptor. *Proc. Natl. Acad. Sci. USA* 89: 8477-8481.

Downing, J. R., and Reynolds, A. B. (1991). PDGF, CSF-1, and EGF induce tyrosine phosphorylation of p120, a $pp60^{src}$ transformation-associated substrate. *Oncogene.* 6: 607-613.

Downward, J., Parker, P., and Waterfield, M. D. (1984). Autophosphorylation sites on the epidermal growth factor receptor. *Nature.* 311: 483-485.

Drake, P. G. and Posner, B. I. (1998). Insulin receptor-associated protein tyrosine phosphatase(s) - role in insulin action. *Mol. Cell. Biochem.* 182: 79-89.

Drejer, K., Kruse, V., Larsen, U. D., Hougaard, P., Bjorn, S. and Gammeltoft, S. 1991. Receptor binding and tyrosine kinase activation by insulin analogues with extreme affinities studied in human hepatoma HepG2 cells. *Diabetes.* 40: 1488-1495

Dreyling, M. H., Martinez-Climent, J. A., Zheng, M., Mao, J., Rowley, J. D. and Bohlander, S. K. (1996). The t(10;11)(p13;q14) in the U937 cell line results in the fusion of the AF10 gene and CALM, encoding a new member of the AP-3 clathrin assembly protein family. *Proc. Natl. Acad. Sci. USA.* 93: 4804-4809.

Dudley, D. T., Pang, L., Decker, S. J., Bridges, A. J. and Saltiel, A. R. (1995). A synthetic inhibitor of the mitogen-activated protein kinase cascade. *Proc. Natl. Acad. Sci. USA.* 92: 7686-7689.

Dunn, W. A., and Hubbard, A. L. (1984). Receptor-mediated endocytosis of epidermal growth factor by hepatocytes in the perfused rat liver: Ligand and receptor dynamics. *J. Cell Biol.* 98: 2148-2159.

Ebner, R., and Derynck, R. (1991). Epidermal growth factor and transforming growth factor-α: differential intracellular routing and processing of ligand-receptor complexes. *Cell Reg.* 2: 599-612.

Eckhart, W., Hutchinson, M. A. and Hunter, T. (1979). An activity phosphorylating tyrosine in polyoma T antigen immunoprecipitates. *Cell.* 18: 925-933.

Ek, B., Westermark, B., Wasteson, A. and Heldin, C. H. (1982). Stimulation of tyrosine-specific phosphorylation by platelet-derived growth factor. *Nature.* 295: 419-420.

Faundez, V., Horng, J. T. and Kelly, R. B. (1998). A function for the AP3 coat complex in synaptic vesicle formation from endosomes. *Cell.* 93, 423-432.

Faure, R., Baquiran, G., Bergeron, J. J. M., and Posner, B. I. (1992). The dephosphorylation of insulin and epidermal growth factor receptors. *J. Biol. Chem.* 267: 11215-11221.

Fausto, N., Laird, A. D., and Webber, E. M. (1995). Role of growth factors and cytokines in hepatic regeneration. *FASEB J.* 9: 1527-1536.

Fazioli, F., Minichiello, L., Matoskova, B., Wong, W. T. and Di Fiore, P. P. (1993). eps15, a novel tyrosine kinase substrate, exhibits transforming activity. *Mol. Cell. Biol.* 13: 5814-5828.

Felder, S., Miller, K., Moehren, G., Ullrich, A., Schlessinger, J., and Hopkins, C. R. (1990). Kinase activity controls the sorting of the epidermal growth factor receptor within the multivesicular body. *Cell* 61: 623-634.

Fixman, E. D., Fournier, T. M., Kamikura, D. M., Naujokas, M. A. and Park, M. (1996). Pathways downstream of Shc and Grb2 are required for cell transformation by the tpr-Met oncoprotein. *J. Biol. Chem.* 271: 13116-13122.

Floyd, S. and De Camilli, P. (1998). Endocytosis proteins and cancer: a potential link? *Trends Cell Biol.* 8: 299-301.

Formisano, P., Najjar, S. M., Gross, C. N., Phillips, N., Oriente, F., Kern-Buell, C. L., Accili, D., and Gorden, P. (1995). Receptor-mediated internalization of insulin. *J. Biol. Chem.* 270: 24073-24077.

Formisano, P., Oriente, F., Miele, C., Caruso, M., Auricchio, R., et al. (1998). In NIH-3T3 fibroblasts, insulin receptor interaction with specific protein kinase C isoforms controls receptor intracellular routing. *J. Biol. Chem.* 273: 13197-13202.

Frank, B. H., Peavy, D. E., Hooker, C. S. and Duckworth, W. C. (1983). Receptor binding properties of monoiodotyrosyl insulin isomers purified by high performance liquid chromatography. *Diabetes.* 32: 705-711.

Franke, T. F., Kaplan, D. R., Cantley, L. C. and Toker, A. (1997). Direct regulation of the Akt proto-oncogene product by phosphatidylinositol-3,4-bisphosphate. *Science.* 275: 665-668.

French, A. R. and Lauffenburger, D. A. (1997). Controlling receptor/ligand trafficking: effects of cellular and molecular properties on endosomal sorting. *Annals Biomed. Eng.* 25: 690-707.

French, A. R., Sudlow, G. P., Wiley, H. S., and Lauffenburger, D. A. (1994). Postendocytic trafficking of epidermal growth factor receptor complexes is mediated through saturable and specific endosomal interactions. *J. Biol. Chem.* 269: 15749-15755.

French, A. R., Tadaki, D. K., Niyogi, S. K., and Lauffenburger, D. A. (1995). Intracellular trafficking of epidermal growth factor family ligands is directly influenced by the pH sensitivity of the receptor/ligand interaction. *J. Biol. Chem.* 270: 4334-4340.

Frevert, E. U. and Kahn, B. B. (1996). Protein kinase C isoforms epsilon, eta, delta and zeta in murine adipocytes: expression, subcellular localization and tissue-specific regulation in insulin-resistant states. *Biochem. J.* 316, 865-871.

Frevert, E. U. and Kahn, B. B. (1997). Differential effects of constitutively active phosphatidylinositol 3-kinase on glucose transport, glycogen synthase activity, and DNA synthesis in 3T3-L1 adipocytes. *Mol. Cell. Biol.* 17: 190-198.

Fukui, Y. and H. Hanafusa (1989) Phosphatidylinositol kinase activity associates with viral p60src protein. *Mol. Cell. Biol.* 9: 1651-1658.

Garfield, S., Huber, B. E., Nagy, P., Cordingley, M. G., and Thorgeirsson, S. S. (1988). Neoplastic transformation and lineage switching of rat liver epithelial cells by retrovirus-associated oncogenes. *Mol. Carcinogenesis* 1, 189-195.

Geuze, H. J., Slot, J. W., Strous, G. J., Peppard, J., von Figura, K., et al. (1984). Intracellular receptor sorting during endocytosis: comparative immunoelectron microscopy of multiple receptors in rat liver. *Cell.* 37: 195-204.

Gideon, P., John, J., Frech, M., Lautwein, A., Clark, R., Scheffler, J. E., and Wittinghofer, A. (1992). Mutational and kinetic analyses of the GTPase activating protein (GAP)-p21 interaction: the C-terminal domain of GAP is not sufficient for full activity. *Mol. Cell. Biol.* 12: 2050-2056.

Gille, H., Sharrocks, A. D., and Shaw, P. E. (1992). Phosphorylation of transcription factor p62 TCF by MAP kinase stimulates ternary complex formation at c-fos promoter. *Nature.* 358: 414-417.

Glenney, J. R., Chen, W. S., Lazar, C. S., Walton, G. M., Zokas, L. M., Rosenfeld, M. G., and Gill, G. N. (1988). Ligand-induced endocytosis of the EGF receptor is blocked by mutational inactivation and by microinjection of anti-phosphotyrosine antibodies. *Cell* 52: 675-684.

Goldstein, B. J. (1993). Regulation of insulin receptor signaling by protein-tyrosine dephosphorylation. *Receptor.* 3: 1-15.

Goodnight, J. A., Mischak, H., Kolch, W. and Mushinski, J. F. (1995). Immunocytochemical localization of eight protein kinase C isozymes overexpressed in NIH 3T3 fibroblasts. Isoform-specific association with microfilaments, Golgi, endoplasmic reticulum, and nuclear and cell membranes. *J. Biol. Chem.* 270: 9991-10001.

Greenberg, M. E., and Ziff, E. B. (1984). Stimulation of 3T3 cells induces transcription of c-fos proto-oncogenes. *Nature* 311: 433-438.

Gurney, A. L., Park, E. A., Giralt, M., Liu, J., and Hanson, R. W. (1992). Opposing actions of Fos and Jun on transcription of the phosphoenolpyruvate carboxykinase (GTP) gene. *J. Biol. Chem.* 267: 18133-18139.

Haft, C. R., De La Luz Sierra, M., Hamer, I., Carpentier, J. L. and Taylor, S. I. (1998). Analysis of the juxtamembrane dileucine motif in the insulin receptor. *Endocrinol.* 139: 1618-29.

Hanks, S. K. and Hunter, T. (1995). Protein kinases 6. The eukaryotic protein kinase superfamily: kinase (catalytic) domain structure and classification. *FASEB J.* 9: 576-596.

Hansen, B. F., Danielsen, G. M., Drejer, K., Sorensen, A. R., Wiberg, F. C., et al. (1996). Sustained signalling from the insulin receptor after stimulation with insulin analogues exhibiting increased mitogenic potency. *Biochem. J.* 315, 271-279.

Haring, H. U., Tippmer, S., Kellerer, M., Mosthaf, L., Kroder, G., et al. (1996). Modulation of insulin receptor signaling. Potential mechanisms of a cross talk between bradykinin and the insulin receptor. *Diabetes.* 45: S115-119.

He, W., Rose, D. W., Olefsky, J. M. and Gustafson, T. A. (1998). Grb10 interacts differentially with the insulin receptor, insulin-like growth factor I receptor, and epidermal growth factor receptor via the Grb10 Src homology 2 (SH2) domain and a second novel domain located between the pleckstrin homology and SH2 domains. *J. Biol. Chem.* 273: 6860-6867.

Heller-Harrison, R. A., Morin, M., and Check, M. P. (1995). Insulin regulation of membrane associated insulin receptor substrate 1. *J. Biol. Chem.* 270: 24442-24450.

Henley, J. R., Krueger, E. W., Oswald, B. J. and McNiven, M. A. (1998). Dynamin-mediated internalization of caveolae. *J. Cell Biol.* 141: 85-99.

Herbst, J. J., Opresko, L. K., Walsh, B. J., Lauffenburger, D. A., and Wiley, H. S. (1994). Regulation of post-endocytic trafficking of the epidermal growth factor receptor through endosomal retention. *J. Biol. Chem.* 269: 12865-12873.

Holman, G. D. and Cushman, S. W. (1994). Subcellular localization and trafficking of the GLUT4 glucose transporter isoform in insulin-responsive cells. *Bioessays.* 16: 753-759.

Honegger, A. M., Dull, T. J., Felder, S., Obberghen, E. V., Bellot, F., Szapary, D., Scmidt, A., Ullrich, A., and Schlessinger, J. (1987). Point mutation at the ATP binding site of EGF receptor abolishes protein-tyrosine kinase activity and alters cellular routing. *Cell* 51: 199-209.

Honneger, A., Dull, T. J., Szapary, D., Komoriya, A., Kris, R., Ullrich, A., and Schlessinger, J. (1988). Kinetic parameters of the protein tyrosine kinase activity of EGF-receptor mutants with individually altered autophosphorylation sites. *EMBO J.* 7: 3053-3060.

Hubbard, S. R., Mohammadi, M. and Schlessinger, J. (1998). Autoregulatory mechanisms in protein-tyrosine kinases. *J. Biol. Chem.* 273: 11987-11990.

Hubbard, S. R., Wei, L., Ellis, L. and Hendrickson, W. A. (1994). Crystal structure of the tyrosine kinase domain of the human insulin receptor. *Nature.* 372: 746-754.

Hunter, T. (1996). Tyrosine phosphorylation: past, present and future. *Biochem. Soc. Trans.* 24: 307-327.

Hurel, S. J., Rochford, J. J., Borthwick, A. C., Wells, A. M., Vandenheede, J. R., et al. (1996). Insulin action in cultured human myoblasts: contribution of different signalling pathways to regulation of glycogen synthesis. *Biochem. J.* 320: 871-877.

Hyvönen, M., Macias, M. J., Nilges, M., Oschkinat, H., Saraste, M., and Wilmanns, M. (1995). Structure of the binding site for inositol phosphates in a PH domain. *EMBO J.* 14: 4676-4685.

Iannolo, G., Salcini, A. E., Gaidarov, I., Goodman, O., Jr., Baulida, J., et al. (1997). Mapping of the molecular determinants involved in the interaction between eps15 and AP-2. *Cancer Research.* 57: 240-245.

Issad, T., Tavaré, J., and Denton, R. M. (1991). Analysis of insulin receptor phosphorylation sites in intact rat liver cells by two dimensional phosphopeptide mapping. *Biochem. J.* 275: 15-21.

Ito, T., Sasaki, Y., and Wands, J. R. (1996). Overexpression of human insulin receptor substrate 1 induced cellular transformation with activation of mitogen-activated protein kinases. *Mol. Cell. Biol.* 16: 943-951.

Jaspan, J. B., Polonsky, K. S., Lewis, M., Pensler, J., Pugh, W., Moossa, A. R., and Rubenstein, A. H. (1981). Hepatic metabolism of glucagon in the dog: contribution of the liver to overall metabolic disposal of glucagon. *Am. J. Physiol.* 240: E233-E244.

Joly, M., Kazlauskas, A. and Corvera, S. (1995). Phosphatidylinositol 3-kinase activity is required at a postendocytic step in platelet-derived growth factor receptor trafficking. *J. Biol. Chem.* 270: 13225-13230.

Joly, M., Kazlauskas, A., Fay, F. S. and Corvera, S. (1994). Disruption of PDGF receptor trafficking by mutation of its PI-3 kinase binding sites. *Science.* 263: 684-687.

Kadlec, L. and Pendergast, A. M. (1997). The amphiphysin-like protein 1 (ALP1) interacts functionally with the cABL tyrosine kinase and may play a role in cytoskeletal regulation. *Proc. Natl. Acad. Sci. USA.* 94: 12390-5.

Kahn, C. R., Freychet, P., Roth, J., and Neville, D. M. (1974). Quantitative aspects of the insulin-receptor interaction in liver plasma membrane. *J. Biol. Chem.* 249: 2249-2257.

Kasuga, M., Fujita-Yamaguchi, Y., Blithe, D. L. and Kahn, C. R. (1983). Tyrosine-specific protein kinase activity is associated with the purified insulin receptor. *Proc. Natl. Acad. Sci. USA.* 80: 2137-41.

Kay, D. G., Lai, W. H., Uchihashi, M., Khan, M. N., Posner, B. I., and Bergeron, J. J. M. (1986). Epidermal growth factor receptor kinase translocation and activation in vivo. *J. Biol. Chem.* 261: 8473-8480.

Khan, M. N., Baquiran, G., Brule, C., Burgess, J., Foster, B., Bergeron, J. J. M., and Posner, B. I. (1989). Internalization and activation of the rat liver insulin receptor kinase in vivo. *J. Biol. Chem.* 264: 12931-12940.

Khan, M. N., Savoie, S., Bergeron, J. J. M., and Posner, B. I. (1986). Characterization of rat liver endosomal fractions. *J. Biol. Chem.* 261, 8462-8472.

Klein, H. H., Freidenberg, G. R., Matthaei, S., and Olefsky, J. M. (1987). Insulin receptor kinase following internalization in isolated rat adipocytes. *J. Biol. Chem.* 262: 10557-10564.

Klippel, A., Kavanaugh, W. M., Pot, D. and Williams, L. T. (1997). A specific product of phosphatidylinositol 3-kinase directly activates the protein kinase Akt through its pleckstrin homology domain. *Mol. Cell. Biol.* 17: 338-344.

Knutson, V. P. (1991). Cellular trafficking and processing of the insulin receptor. *FASEB J.* 5: 2130-2138.

Komada, M., Masaki, R., Yamamoto, A. and Kitamura, N. (1997). Hrs, a tyrosine kinase substrate with a conserved double zinc finger domain, is localized to the cytoplasmic surface of early endosomes. *J. Biol. Chem.* 272: 20538-20544.

Kornilova, E., Sorkina, T., Beguinot, L. and Sorkin, A. (1996). Lysosomal targeting of epidermal growth factor receptors via a kinase-dependent pathway is mediated by the receptor carboxyl-terminal residues 1022-1123. *J. Biol. Chem.* 271: 30340-30346.

Kosaka, T. and Ikeda, K. (1983). Reversible blockage of membrane retrieval and endocytosis in the garland cell of the temperature-sensitive mutant of Drosophila melanogaster, shibirets1. *J. Cell Biol.* 97: 499-507.

Kost, D. P. and Michalopoulos, G. K. (1990). Effect of epidermal growth factor on the expression of proto-oncogenes c-myc and c-Ha-ras in short-term primary hepatocyte culture. *J. Cell. Physiol.* 114: 122-127.

Kotani, K., Carozzi, A. J., Sakaue, H., Hara, K., Robinson, L. J., et al. (1995). Requirement for phosphoinositide 3-kinase in insulin-stimulated GLUT4 translocation in 3T3-L1 adipocytes. *Biochem. Biophys. Res. Com.* 209: 343-348.

Kublaoui, B., Lee, J. and Pilch, P. F. (1995). Dynamics of signaling during insulin-stimulated endocytosis of its receptor in adipocytes. *J. Biol. Chem.* 270: 59-65.

Kurten, R. C., Cadena, D. L. and Gill, G. N. (1996). Enhanced degradation of EGF receptors by a sorting nexin, SNX1. *Science.* 272: 1008-1010.

Laemmli, U. K. (1970). Cleavage of structural protein during the assembly of the head bacteriophage T4. *Nature* 277: 680-685.

Lai, W.H., Cameron, P.H., Wada, I., Doherty II, J.-J., Kay, D. G., Posner, B.I., and Bergeron, J.J.M. (1989a). Ligand-mediated internalization, recycling, and downregulation of the epidermal growth factor receptor in vivo. *J. Cell Biol.* 109: 2741-2749.

Lai, W.H., Cameron, P.H., Doherty II, J.-J., Posner, B. I. and Bergeron, J.J.M. (1989b). Ligand-mediated autophosphorylation activity of the epidermal growth factor receptor during internalization. *J. Cell Biol.* 109: 2751-2760.

Lam, K., Carpenter, C. L., Ruderman, N. B., Friel, J. C. and Kelly, K. L. (1994). The phosphatidylinositol 3-kinase serine kinase phosphorylates IRS-1. *J. Biol. Chem.* 269, 20648-20652.

Lamaze, C., Baba, T., Redelmeier, T.E. and Schmid, S.L. (1993). Recruitment of epidermal growth factor and transferrin receptors into coated pits in vitro: differing biochemical requirements. *Mol. Biol. Cell.* 4: 715-727.

Larkin, J. M., Brown, M. S., Goldstein, J. L. and Anderson, R. G. (1983). Depletion of intracellular potassium arrests coated pit formation and receptor-mediated endocytosis in fibroblasts. *Cell.* 33: 273-285.

Lemmon, M. A. and Ferguson, K. M. (1998). Pleckstrin homology domains. *Curr. Top. Microbiol. Immunol.* 228: 39-74.

Li Calzi, S., Choice, C. V. and Najjar, S. M. (1997). Differential effect of pp120 on insulin endocytosis by two variant insulin receptor isoforms. *Am. J. Physiol.* 273: E801-808.

Li, L. and Cohen, S. N. (1996). Tsg101: a novel tumor susceptibility gene isolated by controlled homozygous functional knockout of allelic loci in mammalian cells. *Cell.* 85: 319-329.

Liu, K. and Li, G. (1998). Catalytic domain of the p120 Ras GAP binds to Rab5 and stimulates its GTPase activity. *J. Biol. Chem.* 273: 10087-10090.

Liu, X., and Pawson, T. (1991). The epidermal growth factor receptor phosphorylates GTPase-activating protein (GAP) at tyr-460, adjacent to the GAP SH2 domains. *Mol. Cell. Biol.* 11: 2511-2516.

Lohi, O., Poussu, A., Merilainen, J., Kellokumpu, S., Wasenius, V. M. and Lehto, V. P. (1998). East, an epidermal growth factor receptor- and eps15-associated protein with src homology 3 and tyrosine-based activation motif domains. *J. Biol. Chem.* 273: 21408-21415.

Lotti, L. V., Lanfrancone, L., Migliaccio, E., Zompetta, C., Pelicci, G., et al. (1996). SHC proteins are localized on endoplasmic reticulum membranes and are redistributed after tyrosine kinase receptor activation. *Mol. Cell. Biol.* 16: 1946-1954.

Lowenstein, E. J., Daly, R. J., Batzer, A. G., Li, W., Margolis, B., Lammers, R., Ullrich, A., Skolnik, E. Y., Bar-Sagi, D. and Schlessinger, J. (1992). The SH2 and SH3 domain-containing protein GRB2 links receptor tyrosine kinases to Ras signaling. *Cell.* 70: 431-442.

Lowy, D. R., and Willumsen, B. M. (1993). Function and regulation of ras. *Annu. Rev. Biochem.* 62: 851-891.

Lund, K. A., Lazar, C. S., Chen, W. S., Walsh, B. J., Welsh, J. B., et al. (1990). Phosphorylation of the epidermal growth factor receptor at threonine 654 inhibits ligand-induced internalization and down-regulation. *J. Biol. Chem.* 265: 20517-20523.

Luzio, J. P. and Stanley, K. K. (1983). The isolation of endosome-derived vesicles from rat hepatocytes. *Biochem. J.* 216: 27-36.

Macdonald, S. G., Crews, G. M., Wu, L., Driller, J., Clark, R., Erikson, R. L., and McCormick, F. (1993). Reconstitution of raf-1-MEK-ERK signal transduction pathway in vitro. *Mol. Cell. Biol.* 13: 6615-6620.

Marcu, K. B., Bossone, S. A. and Patel, A. J. (1992). Myc Function and regulation. *Annu. Rev. Biochem.* 61: 809-860.

Margolis, B. L., Lax, I., Kris, R., Dombalagian, M., Honegger, A. M., Howk, R., Givol, D., Ullrich, A. and Schlessinger, J. (1989). All phosphorylation sites of epidermal growth factor (EGF) receptor and HER2/neu are located in their carboxyl-terminal tails. *J. Biol. Chem.* 264: 10667-10671.

Margolis, B., Li, N., Koch, A., Mohammadi, M., Hurwitz, D. R., Zilberstein, A., Ullrich, A., Pawson, T. and Schlessinger, J. (1990). The tyrosine phosphorylated carboxy terminus of the EGF receptor is a binding site for GAP and PLC-γ. *EMBO J.*9: 4375-4380.

Margolis, R. N., Taylor, S. I., Seminara, D., and Hubbard, A. L. (1988). Identification of pp120, an endogenous substrate for the hepatocyte insulin receptor tyrosine kinase, as an integral membrane glycoprotein of the bile canalicular domain. *Proc. Natl. Acad. Sci. U.S.A.* 19: 7256-7259.

Masui, H., Wells, A., Lazar, C. S., Rosenfeld, M. G. and Gill, G. N. (1991). Enhanced tumorigenesis of NR6 cells which express non-down-regulating epidermal growth factor receptors. *Can. Res.* 51: 6170-6175.

Mauro, L. J. and Dixon, J. E. (1994). 'Zip codes' direct intracellular protein tyrosine phosphatases to the correct cellular 'address'. *Trends Biochem. Sci.* 19: 151-155.

Mayer, B. J., and Baltimore, D. (1993). Signaling through SH2 and SH3 domains. *Trends Cell Biol.* 3: 8-13.

Mayer, B. J., and Eck, M. J. (1995). Minding your p's and q's. *Curr. Biol.* 5, 364-367.

McClain, D. A., and Olefsky, J. M. (1988). Evidence for two independent pathways of insulin-receptor internalization in hepatocytes and hepatoma cells. *Diabetes* 37: 806-815.

McLauchlan, H., Newell, J., Morrice, N., Osborne, A., West, M. and Smythe, E. (1998). A novel role for Rab5-GDI in ligand sequestration into clathrin-coated pits. *Curr. Biol.* 8: 34-45.

Mellor, H., Parker, P. J. (1998). The extended protein kinase C superfamily. *Biochem. J.* 332: 281-292.

Messina, J. L. (1989). Regulation of gene expression by insulin. Handbook of Experimental Pharmacology 92: 339-419.

Migliaccio, E., Mele, S., Salcini, A. E., Pelicci, G., Lai, K. M., et al. (1997). Opposite effects of the p52shc/p46shc and p66shc splicing isoforms on the EGF receptor-MAP kinase-fos signalling pathway. *EMBO J.* 16: 706-716.

Miller, T., Jr., Garnache, A. K., Cruz, J., McPherson, R. K. and Wolleben, C. (1986). Regulation of glycogen metabolism in primary cultures of rat hepatocytes. Restoration of acute effects of insulin and glucose in cells from diabetic rats. *J. Biol. Chem.* 261: 785-790.

Miller, T., Jr., Garnache, A. and Vicalvi, J., Jr. (1981). Hormonal regulation of hepatic glycogen synthase phosphatase. *J. Biol. Chem.* 256: 2851-2855.

Minden, A., Lin, A., Smeal, T., Derijard, B., Cobb, M., Davis, R., and Karin, M. (1994). c-jun N-terminal phosphorylation correlates with activation of the JNK subgroup but not the ERK subgroup of the mitogen-activated protein kinases. *Mol. Cell. Biol.* 14: 6683-6688.

Mohn, K. L., Laz, T. M., Melby, A. E., and Taub, R. (1990). Immediate-early gene expression differs between regenerating liver, insulin-stimulated H-35 cells, and mitogen-stimulated Balb/c 3T3 cells. Liver-specific induction patterns of gene 33, phosphoenolpyruvate carboxykinase, and the jun, fos, and egr families. *J. Biol. Chem.* 265: 21914-21921.

Mooney, D., Hansen, L., Vacanti, J., Langer, R., Farmer, S., and Ingber, D. (1992). Switching from differentiation to growth in hepatocytes: control by extracellular matrix. *J. Cell. Physiol.* 151: 497-505.

Mortimore, G. E., King, E., Jr., Mondon, C. E., and Glinsmann, W. H. (1967). Effects of insulin on net carbohydrate alterations in perfused rat liver. *Am. J. Physiol.* 212: 179-83.

Moxham, C. M., Tabrizchi, A., Davis, R. J., and Malbon, C. C. (1996). Jun N-terminal kinase mediates activation of skeletal muscle glycogen synthase by insulin in vivo. *J. Biol. Chem.* 271: 30765-30773.

Myers, M. G., Grammer, T. C., Brooks, J., Glasheen, E. M., Wang, L.-M., Sun, X. J., Blenis, J., Pierce, J. H., and White, M. F. (1995). The pleckstrin homology domain in insulin receptor substrate-1 sensitizes insulin signaling. *J. Biol. Chem.* 270: 11715-11718.

Myers, M. G., Sun, X. J., and White, M. F. (1994). The IRS-1 signaling system. *Trends Biochem. Sci.* 19: 289-293.

Nakamura, T., Yoshimoto, K., Nakayama, Y., Tomita, Y., and Ichihara, A. (1983). Reciprocal modulation of growth and differentiated functions of mature rat hepatocytes in primary culture by cell cell contacts and cell membranes. *Proc. Natl. Acad. Sci. U.S.A.* 80: 7229-7233.

Nesterov, A., Kurten, R. C., and Gill, G. N. (1995a). Association of epidermal growth factor receptors with coated pit adaptins via a tyrosine phosphorylation-regulated mechanism. *J. Biol. Chem.* 270: 6320-6327.

Nesterov, A., Wiley, H. S., and Gill, G. N. (1995b). Ligand-induced endocytosis of epidermal growth factor receptors that are defective in binding adaptor proteins. *Proc. Natl. Acad. Sci. U.S.A.* 92: 9719-8723.

Newton, A. C. (1997). Regulation of protein kinase C. *Curr. Op. Cell Biol.* 9: 161-167.

Northwood, I. C., Gonzalez, F. A., Wartmann, M., Raden, D. L., and Davis, R. J. (1991). Isolation and characterization of two growth factor-stimulated protein kinases that phosphorylate the epidermal growth factor receptor at threonine 669. *J. Biol. Chem.* 266: 23, 15266-15276.

O'Neill, T. J., Craparo, A., and Gustafson, T. A. (1994). Characterization of an interaction between insulin receptor substrate 1 and the insulin receptor by using the two hybrid system. *Mol. Cell. Biol.* 14: 6433-6442.

Odaka, M., Kohda, D., Lax, I., Schlessinger, J., and Inagaki, F. (1997). Ligand-binding enhances the affinity of dimerization of the extracellular domain of the epidermal growth factor receptor. *J. Biochem.* 122: 116-121.

Ojaniemi, M., and Vuori, K. (1997). Epidermal growth factor modulates tyrosine phosphorylation of p130Cas. Involvement of phosphatidylinositol 3'-kinase and actin cytoskeleton. *J. Biol. Chem.* 272: 25993-25998.

Osterop, A. P. R. M., Medema, R. H., Bos, J. L., Zon, G. C. M. v. d., Moller, D. E., Flier, J. S., Moller, W., and Maassen, J. A. (1992). Relation between the insulin receptor number in cells, autophosphorylation and insulin-stimulated ras-GAP formation. *J. Biol. Chem.* 267: 14647-14653.

Palade, G.E. and Bruns R.R. (1968). Structural modifications of plsmalemmal vesicles. *J. Cell. Biol.* 37: 633-649.

Patki, V., Virbasius, J., Lane, W. S., Toh, B. H., Shpetner, H. S., and Corvera, S. (1997). Identification of an early endosomal protein regulated by phosphatidylinositol 3-kinase. *Proc. Natl. Acad. Sci. USA.* 94: 7326-7330.

Pawson, T., and Scott, J. D. (1997). Signaling through scaffold, anchoring, and adaptor proteins. *Science.* 278: 2075-2080.

Peak, M., Rochford, J. J., Borthwick, A. C., Yeaman, S. J., and Agius, L. (1998). Signalling pathways involved in the stimulation of glycogen synthesis by insulin in rat hepatocytes *Diabetologia.* 41: 16-25.

Pearse, B. M. (1976). Clathrin: a unique protein associated with intracellular transfer of membrane by coated vesicles. *Proc. Natl. Acad. Sci. USA.* 73: 1255-1259.

Pearse, B. M. F., and Robinson, M. S. (1990). Clathrin, Adaptins, and Sorting. *Annu. Rev. Cell Biol.* 6: 151-171.

Pease, R. J., Smith, G. D., and Peters, T. J. 1985. Degradation of endocytosed insulin in rat liver is mediated by low-density vesicles. *Biochem. J.* 228: 137-146

Pease, R. J., Smith, G. D., and Peters, T. J. 1987. Characterization of insulin degradation by rat-liver low-density vesicles. *Eur. J. Biochem* 164: 251-257

Pelicci, G., Lanfrancone, L., Grignani, F., McGlade, J., Cavallo, F., Forni, G., Nicoletti, I., Grignani, F., Pawson, T., and Pelicci, P. G. (1992). A novel transforming protein (SHC) with an SH2 domain is implicated in mitogenic signal transduction. *Cell* 70: 93-104.

Peyrard, M., Fransson, I., Xie, Y. G., Han, F. Y., Ruttledge, M. H., et al. (1994). Characterization of a new member of the human beta-adaptin gene family from chromosome 22q12, a candidate meningioma gene. *Hum. Mol. Gen.* 3: 1393-1399.

Pronk, G. J., de Vries-Smits, A. M. M., Buday, L., Downward, J., Maassen, J. A., Medema, R. H., and Bos, J. L. (1994). Involvement of SHC in insulin- and epidermal growth factor induced activation of p21 ras. *Mol. Cell. Biol.* 14: 1575-1581.

Pronk, G. J., McGlade, J., Pelicci, G., Pawson, T., and Bos, J. L. (1993). Insulin-induced phosphorylation of the 46- and 52-kDa SHC proteins. *J. Biol. Chem.* 268: 5748-5753.

Prywes, R., Livneh, E., Ullrich, A., and Schlessinger, J. (1986). Mutations in the cytoplasmic domain of EGF receptor affect EGF binding and receptor internalization. *EMBO J.* 5: 2179-2190.

Quantin, B., and Breathnack, R. (1988). Epidermal growth factor stimulates transcription of c-jun proto-oncogene in rat fibroblasts. *Nature* 344: 538-539.

Rajagopalan, M., Neidigh, J. L., and McClain, D. A. (1991). Amino acid sequences Gly-Pro-Leu-Tyr and Asn-Pro-Glu-Tyr in the submembrane domain of the insulin receptor are required for normal endocytosis. *J. Biol. Chem.* 266: 23068-23073.

Randhawa, R., and Khandelwal, R. L. (1990). Purification and partial characterization of glycogen synthase kinase-3 from rabbit liver. *Mol. Cell. Biochem.* 95: 147-155.

Renfrew, C. A., and Hubbard, A. L. (1991a). Degradation of epidermal growth factor receptor in rat liver. *J. Biol. Chem.* 266: 21265-21273.

Renfrew, C. A., and Hubbard, A. L. (1991b). Sequential processing of epidermal growth factor in early and late endosomes of rat liver. *J. Biol. Chem.* 266: 4348-4356.

Ringerike, T., Stang, E., Johannessen, L. E., Sandnes, D., Levy, F. O., and Madshus, I. H. (1998). High-affinity binding of epidermal growth factor (egf) to egf receptor is disrupted by overexpression of mutant dynamin (k44a). *J. Biol. Chem.* 273: 16639-16642.

Roach, P.J. (1986) : The Enzymes. Boyer, P.D. and E.G. Krebs, Eds. Academic Press Inc. pp. 499-539

Rodriguez-Viciana, P., Warne, P. H., Dhand, R., Vanhaesebroeck, B., Gout, I., Fry, M. J., Waterfield, M. D., and Downward, J. (1994). Phosphatidylinositol-3-OH kinase as a direct target of Ras. *Nature* 370: 527-532.

Rosen, O. M., Herrera, R., Olowe, Y., Petruzzelli, L. M., and Cobb, M. H. (1983). Phosphorylation activates the insulin receptor tyrosine protein kinase. *Proc. Natl. Acad. Sci. USA.* 80: 3237-3240.

Roth, T.F. and Porter K.R. (1964). Yolk protein uptake in the oocyte of mosquito aedes aegypti. L. *J. Cell. Biol.* 20: 313-332.

Rozakis-Adcock, M., McGlade, J., Mbamalu, G., Pelicci, G., Daly, R., Li, W., Batzer, A., Thomas, S., Bruggs, J., Pelicci, P. G., Schlessinger, J., and Pawson, T. (1992). Association of the SHC and Grb2/Sem5 SH2-containing proteins is implicated in activation of the Ras pathway by tyrosine kinases. *Nature* 360: 689-692.

Ruff-Jamison, S., McGlade, J., Pawson, T., Chen, K., and Cohen, S. (1993). Epidermal growth factor stimulates the tyrosine phosphorylation of SHC in the mouse. *J. Biol. Chem.* 268: 7610-7612.

Saad, M. J. A., Araki, E., Miralpeix, M., Rothenberg, P. L., White, M. F., and Kahn, C. R. (1992). Regulation of insulin receptor substrate-1 in liver and muscle of animal models of insulin resistance. *J. Clin. Invest.* 90: 1839-1849.

Sadowski, I., Stone, J. C., and Pawson, T. (1986). A non-catalytic domain conserved among cytoplasmic tyrosine kinases modifies the kinase function and transforming activity of Fujinami sarcoma virus p130$^{gag\text{-}fps}$. *Mol. Cell. Biol.* 6: 4396-4408.

Sakamuro, D., Elliott, K. J., Wechsler-Reya, R., and Prendergast, G. C. (1996). BIN1 is a novel MYC-interacting protein with features of a tumour suppressor. *Nature Genetics.* 14: 69-77.

Salcini, A. E., Confalonieri, S., Doria, M., Santolini, E., Tassi, E., et al. (1997). Binding specificity and in vivo targets of the EH domain, a novel protein-protein interaction module. *Genes & Dev.* 11: 2239-2249.

Sale, G. J. (1992). Serine/threonine kinases and tyrosine phosphatases that act on the insulin receptor. *Biochem. Soc. Trans.* 20: 664-70.

Salteil, A. R. (1994). The paradoxical regulation of protein phosphorylation in insulin action. *FASEB J.* 8: 1034-1040.

Sambrook, J., Fritsh, E. F., and Maniatis, T. (1989). Molecular cloning: A laboratory manual. Second Ed. Cold Spring Harbor Laboratory Press. vol. 1-3.

Sandgren, E. P., Quaife, C. T., Pinkert, C. A., Palmiter, R. D., and Brinster, R. L. (1989). Oncogene-induced liver neoplasia in transgenic mice. *Oncogene* 4: 715-724.

Sandvig, K., Olsnes, S., Petersen, O. W., and Van Deurs, B. (1989). Control of coated-pit function by cytoplasmic pH. *Meth. Cell Biol.* 32: 365-382.

Santos, A., Yusta, B., Fernandez-Moreno, and M. D., Blazquez, E. (1994). Expression of insulin-like growth factor-I (IGF-I) receptor gene in rat brain and liver during development and in regenerating adult rat liver. *Mol. Cell. Endocrinol.* 101: 85-93.

Sasaoka, T., Drazin, B., Leitner, J. W., Langlois, W. J., and Olefsky, J. M. (1994a). Shc is the predominant signaling molecule coupling insulin receptors to activation of guanine nucleotide releasing factor and p21ras-GTP formation. *J. Biol. Chem.* 269: 10734-10738.

Sasaoka, T., Rose, D. W., Jhun, B. H., Saltiel, A. R., Draznin, B., and Olefsky, J. M. (1994b). Evidence for a functional role of Shc proteins in mitogenic signaling induced by insulin, insulin like growth factor-1 and epidermal growth factor. *J. Biol. Chem.* 269: 13689-13694.

Satoh, T., Endo, M., Nakafuku, M., Nakamura, S., and Kaziro, Y. (1990). Platelet-derived growth factor stimulates formation of active p21ras.GTP complex in Swiss mouse 3T3 cells. *Proc. Natl. Acad. Sci. U.S.A.* 87: 5993-5997.

Scheffzek, K., Ahmadian, M. R., Kabsch, W., Wiesmuller, L., Lautwein, A., et al. (1997). The Ras-RasGAP complex: structural basis for GTPase activation and its loss in oncogenic Ras mutants. *Science*. 277: 333-338.

Scherer, P. E., Lisanti, M. P., Sargiacomo, G. B., Mastick, C. C., and Lodish, H. F. (1994). Induction of caveolin during adipogenesis and association of GLUT 4 with caveolin-rich vesicles. *J. Cell Biol.* 127: 1233-1243.

Schlessinger, J. (1986). Allosteric regulation of the epidermal growth factor receptor kinase. *J. Cell Biol.*. 103: 2067-2072.

Schmeichel, K. L., and Beckerle, M. C. (1994). The LIM domain is a modular protein binding interface. *Cell* 79: 211-219.

Schmid, S. L. (1997). Clathrin-coated vesicle formation and protein sorting: an integrated process. *Ann. Rev. Biochem.* 66: 511-548.

Schmid, S. L., and Carter, L. L. (1990). ATP is required for receptor-mediated endocytosis in intact cells. *J. Cell Biol.*. 111: 2307-2318.

Schubert, C., Carel, K., DePaolo, D., Leitner, W., and Draznin, B. (1996). Interactions of protein kinase C with insulin signaling. Influence on GAP and Sos activities. *J. Biol. Chem.* 271: 15311-15314.

Seabright, P. J., and Smith, G. D. 1996. The characterization of endosomal insulin degradation intermediates and their sequence of production. *Biochem. J.*320: 947-956

Seger, R., and Krebs, E. G. (1995). The MAPK signaling cascade. *FASEB J.* 9: 726-735.

Seth, A., Alavrez, E., Gupta, S., and Davis, R. J. (1991). A phosphorylation site located in the NH2-terminal domain of c-Myc increases transactivation of gene expression. *J. Biol. Chem.* 266: 23521-23524.

Settleman, J., Albright, C. F., Foster, L. C., and Weinberg, R. A. (1992a). Association between GTPase activators for Rho and Ras families. *Nature* 359: 153-154.

Settleman, J., Narasimhan, V., Foster, L. C., and Weinberg, R. A. (1992b). Molecular cloning of cDNAs encoding the GAP-associated protein p190: implications for a signalling pathway from ras to the nucleus. *Cell* 69: 539-549.

Sheperd, P. R., Reaves, B. J., and Davidson, H. W. (1996). Phosphoinositide 3-kinase and membrane traffic. *Trends Cell Biol.* 6: 92-97.

Shepherd, P. R., Navé, B. T., and Siddle, K. (1995). Insulin stimulation of glycogen synthesis and glycogen synthase activity is blocked by Wortmannin and rapamycin in 3T3-L1 adipocytes: evidence for the involvement of phosphoinositide 3-kinase and p70 ribosomal protein-S6 kinase. *Biochem. J.* 305: 25-28.

Skolnik, E. Y., Lee, C.-H., Batzer, A., Vicentini, L. M., Zhou, M., Daly, R., Myers, M. J., Backer, J. M., Ullrich, A., White, M. F., and Schlessinger, J. (1993). The SH2/SH3 domain-containing protein GRB2 interacts with tyrosine-phosphorylated IRS-1 and Shc: implications for insulin control of ras signaling. *EMBO J.*12: 1929-1936.

Skouteris, G. G., and Kaser, M. R. (1992). Expression of exogenous c-myc oncogene does not initiate DNA synthesis in primary rat hepatocyte cultures. *J. Cell. Physiol.* 150: 353-359.

Songyang, Z., and Cantley, L. C. (1995). Recognition and specificity in protein tyrosine kinase-mediated signaling. *Trends Biochem. Sci.* 20: 470-475.

Songyang, Z., Shoelson, S. E., Chaudhuri, M., Gish, G., Pawson, T., Haser, W. G., King, F., Roberts, T., Ratnofsky, S., Lechleider, R. J., Neel, B. G., Birge, R. B., Fajardo, J. E., Chou, M. M., Hanafusa, H., Schaffhausen, B., and Cantley, L. C. (1993). SH2 domains recognize specific phosphopeptide sequences. *Cell* 72: 767-778.

Sorkin, A., and Carpenter, G. (1993). Interaction of activated EGF receptors with coated pit adaptins. *Science*. 261: 612-615.

Sorkin, A., Lemmon, M. A., Ullrich, A., and Schlessinger, J. (1994). Stabilization of an active dimeric form of the epidermal growth factor receptor by introduction of an inter-receptor disulfide bond. *J. Biol. Chem.* 269: 9752-9759.

Sorkin, A., McKinsey, T., Shih, W., Kirchhausen, T., and Carpenter, G. (1995). Stoichiometric interaction of the epidermal growth factor receptor with clathrin-associated protein complex AP-2. *J. Biol. Chem.* 270: 619-625.

Sorkin, A., and Waters, C. M. (1993). Endocytosis of growth factor receptors. *Bioessays.* 15: 375-382.

Spector, M. S., Auer, K. L., Jarvis, W. D., Ishac, E. J., Gao, B., et al. (1997). Differential regulation of the mitogen-activated protein and stress-activated protein kinase cascades by adrenergic agonists in quiescent and regenerating adult rat hepatocytes. *Mol. Cell. Biol.* 17: 3556-3565.

Sprang, S. R. (1997). G protein mechanisms: insights from structural analysis. *Ann. Rev. Biochem.* 66: 639-678.

Srivastava, A. K., and Pandey, S. K. (1998). Potential mechanism(s) involved in the regulation of glycogen synthesis by insulin. *Mol. Cell. Biochem.* 182: 135-141.

Stalmans, W., Bollen, M., and Mvumbi, L. (1987). Control of glycogen synthesis in health and disease. *Diab. Metab. Rev.* 3: 127-161.

Stamatoglou, S. C., Enrich, C., Manson, M. M., and Hughes, R. C. (1992). Temporal changes in the expression and distribution of adhesion molecules during liver development and regeneration. *J. Cell Biol.* 116: 1507-1515.

Steer, C. J. (1995). Liver regeneration. *FASEB J.* 9: 1396-1400.

Stenmark, H., Aasland, R., Toh, B. H., and D'Arrigo, A. (1996). Endosomal localization of the autoantigen EEA1 is mediated by a zinc-binding FYVE finger. *J. Biol. Chem.* 271: 24048-24054.

Stephens, L. (1995). Molecules mediating signals. *Biochem. Soc. Trans.* 23: 207-221.

Stokoe, D., Macdonald, S. G., Cadwallader, K., Symons, M., and Hancock, J. F. (1994). Activation of Raf as a result of recruitment to the plasma membrane. *Science* 264: 1463-1467.

Storm, S. M., Cleveland, J. L., and Rapp, U. R. (1990). Expression of the raf family proto-oncogenes in normal mouse tissues. *Oncogene* 5: 345-351.

Sturgill, T. W., Ray, L. B., Erikson, E., and Maller, J. L. (1988). Insulin-stimulated MAP-2 kinase phosphorylates and activates ribosomal protein S6 kinase II. *Nature.* 334: 715-718.

Sun, X. J., Rothenberg, P., Kahn, C. R., Baker, J. M., Araki, E., Wilden, P. A., Cahill, D. A., Goldstein, B. J., and White, M. F. (1991). Structure of the insulin receptor substrate IRS-1 defines a unique signal transduction protein. *Nature* 352: 73-77.

Surmacz, C. A., Wert, J., Jr., Ward, W. F., and Mortimore, G. E. 1988. Uptake and intracellular fate of [14C]sucrose-insulin in perfused rat livers. *Am. J. Physiol* 255: C70-5

Sutherland, C., O'Brien, R. M., and Granner, D. K. (1995). Phosphatidylinositol 3-kinase, but not p70/p85 ribosomal S6 protein kinase, is required for the regulation of phosphoenolpyruvate carboxykinase (PEPCK) gene expression by insulin. *J. Biol. Chem.* 270: 15501-15506.

Sweeney, G., and Klip, A. (1998). Regulation of the Na+/K+-ATPase by insulin - why and how. *Mol. Cell. Biochem.* 182: 121-133.

Takata, Y., Webster, N. J. G., and Olefsky, J. M. (1991). Mutation of the two carboxy terminal tyrosines in an insulin receptor with normal metabolic signaling but enhanced mitogenic signaling properties. *J. Biol. Chem.* 266: 9135-9139.

Tanasijevic, M. J., Myers, M. G., Thoma, R. S., Crimmins, D. L., White, M. F., and Sacks, D. B. (1993). Phosphorylation of the insulin receptor substrate IRS-1 by casein kinase II. *J. Biol. Chem.* 268: 18157-18166.

Tanasijevic, M. J., Myers, M., Jr., Thoma, R. S., Crimmins, D. L., White, M. F., and Sacks, D. B. (1993). Phosphorylation of the insulin receptor substrate IRS-1 by casein kinase II. *J. Biol. Chem.* 268: 18157-18166.

Tanti, J.-F., Grémeaux, T., Obberghen, E. V., and Marcharnd-Brustel, Y. L. (1994). Serine/threonine phosphorylation of insulin receptor substrate 1 modulates insulin receptor signaling. *J. Biol. Chem.* 269: 6051-6057.

Taylor, S. I., Cama, A., Accili, D., Barbetti, F., Quon, M. J., LuzSierra, M. D., Suzuki, Y., Koller, E., Levy-Toledano, R., Wertheimer, E., Moncada, V. Y., Kadowaki, H., and Kadowaki, T. (1992). Mutations in the insulin receptor gene. *Endocrinol.* 13: 566-595.

Taylor, S. I., Najjar, S., Cama, A., and Accili, D. (1991). Structure and function of the insulin receptor. Insulin-like growth factors: Molecular and cellular aspects. D. LeRoth, Ed. CRC Press, Inc. 222-244.

Taylor, S. S., Radzio-Andzelm, E., and Hunter, T. (1995). How do protein kinases discriminate between serine/threonine and tyrosine? Structural insights from the insulin receptor protein-tyrosine kinase. *FASEB J.* 9: 1255-1266.

Thies, R. S., Ullrich, A., and McClain, D. A. (1989). Augmented mitogenesis and impaired metabolic signaling mediated by a truncated insulin receptor. *J. Biol. Chem.* 264: 12820-12825.

Thomas, J. A., Schlender, K. K., and Larner, J. (1968). A rapid filter paper assay for UDPglucose-glycogen glucosyltransferase, including an improved biosynthesis of UDP-14C-glucose. *Anal. Biochem.* 25: 486-499.

Tomic, S., Greiser, U., Lammers, R., Kharitonenkov, A., Imyanitov, E., et al. (1995). Association of SH2 domain protein tyrosine phosphatases with the epidermal growth factor receptor in human tumor cells. Phosphatidic acid activates receptor dephosphorylation by PTP1C. *J. Biol. Chem.* 270: 21277-21284.

Tonks, N. K., Diltz, C. D., and Fischer, E. H. (1988). Purification of the major protein-tyrosine-phosphatases of human placenta. *J. Biol. Chem.* 263: 6722-6730.

Tonks, N. K., and Neel, B. G. (1996). From form to function: signaling by protein tyrosine phosphatases. *Cell.* 87: 365-368.

Tornqvist, H. E., Gunsalus, J. R., Nemenoff, R. A., Frackelton, A. R., Pierce, M. W., and Avruch, J. (1988). Identification of the insulin receptor tyrosine residues undergoing insulin-stimulated phosphorylation in intact rat hepatoma cells. *J. Biol. Chem.* 263: 350-359.

Toth, B., Bollen, M., and Stalmans, W. (1988). Acute regulation of hepatic protein phosphatases by glucagon, insulin, and glucose. *J. Biol. Chem.* 263: 14061-14066.

Touhara, K., Inglese, J., Pitcher, J. A., Shaw, G., and Lefkowitz, R. J. (1994). Binding of G protein βγ-subunits to plextrin homology domains. *J. Biol. Chem.* 269: 10217-10220.

Trahey, M., and McCormick, F. (1987). A cytoplasmic protein stimulates normal N-ras p21 GTPase, but does not affect oncogenic mutants. *Science* 238: 542-545.

Treisman, R. (1995). Journey to the surface of the cell: Fos regulation and the SRE. *EMBO J.* 14: 4905-4913.

Trowbridge, I. S., Collawn, J. F., and Hopkins, C. R. (1993). Signal-dependent membrane protein trafficking in the endocytic pathway. *Ann. Rev. of Cell Biol.* 9: 129-161.

Trüb, T., Choi, W. E., Wolf, G., Ottinger, E., Chen, Y., Weiss, M., and Shoelson, S. E. (1995). Specificity of the PTB domain of SHC for β turn-forming pentapeptide motifs amino-terminal to phosphotyrosine. *J. Biol. Chem.* 270: 18205-18208.

Ushiro, H., and Cohen, S. (1980). Identification of phosphotyrosine as a product of epidermal growth factor-activated protein kinase in A-431 cell membranes. *J. Biol. Chem.* 255: 8363-5.

van der Bliek, A. M., Redelmeier, T. E., Damke, H., Tisdale, E. J., Meyerowitz, E. M., and Schmid, S. L. (1993). Mutations in human dynamin block an intermediate stage in coated vesicle formation. *J. Cell Biol.* 122: 553-563.

van der Geer, P., Hunter, T., and Lindberg, R. A. (1994). Receptor protein-tyrosine kinases and their signal transduction pathways. *Annu. Rev. Cell Biol.* 10: 251-337.

van der Geer, P., and Pawson, T. (1995a). The PTB domain: a new protein module implicated in signal transduction. *Trends Biochem. Sci.* 20: 277-280.

van der Geer, P., Wiley, S., Lai, V. K.-M., Olivier, J. P., Gish, G. D., Stephens, R., Kaplan, D., Shoelson, S., and Pawson, T. (1995b). A conserved amino-terminal SHC domain binds to phosphotyrosine motifs in activated receptors and phosphopeptides. *Curr. Biol.* 5: 404-412.

van der Geer, P., Wiley, S., Gish, G. D., and Pawson, T. (1996). The Shc adaptor protein is highly phosphorylated at conserved, twin tyrosine residues (Y239/240) that mediate protein-protein interactions. *Curr. Biol.* 6, 1435-1444.

Vieira, A. V., Lamaze, C., and Schmid, S. L. (1996). Control of EGF receptor signaling by clathrin-mediated endocytosis. *Science.* 274: 2086-2089.

Villar-Palasi, C., and Guinovart, J. J. (1997). The role of glucose 6-phosphate in the control of glycogen synthase. *FASEB J.* 11: 544-58.

Vojtek, A. B., and Der, C. J. (1998). Increasing complexity of the ras signaling pathway. *J. Biol. Chem.* 273: 19925-19928.

Wada, I., Lai, W. H., Posner, B. I., and Bergeron, J. J. M. (1992). Association of the tyrosine phosphorylated epidermal growth factor receptor with a 55-kD tyrosine phosphorylated protein at the cell surface and in endosomes. *J. Cell Biol.* 116: 321-330.

Wang, B., Balba, Y., and Knutson, V. P. (1996). Insulin-induced in situ phosphorylation of the insulin receptor located in the plasma membrane versus endosomes. *Biochem. Biophys. Res. Com.* 227: 27-34.

Wang, X., Flynn, A., Waskiewicz, A. J., Webb, B. L., Vries, R. G., et al. (1998). The phosphorylation of eukaryotic initiation factor eIF4E in response to phorbol esters, cell stresses, and cytokines is mediated by distinct MAP kinase pathways. *J. Biol. Chem.* 273: 9373-9377.

Wang, Z., and Moran, M. F. (1996). Requirement for the adapter protein GRB2 in EGF receptor endocytosis. *Science.* 272: 1935-1939.

Wang, Z., Tung, P. S., and Moran, M. F. (1996). Association of p120 ras GAP with endocytic components and colocalization with epidermal growth factor (EGF) receptor in response to EGF stimulation. *Cell Growth & Differentiation.* 7: 123-133.

Warren, R. A., Green, F. A., and Enns, C. A. (1997). Saturation of the endocytic pathway for the transferrin receptor does not affect the endocytosis of the epidermal growth factor receptor. *J. Biol. Chem.* 272: 2116-2121.

Wartmann, M., Hofer, P., Turowski, P., Saltiel, A. R., and Hynes, N. E. (1997). Negative modulation of membrane localization of the Raf-1 protein kinase by hyperphosphorylation. *J. Biol. Chem.* 272: 3915-3923.

Waterman, H., Sabanai, I., Geiger, B., and Yarden, Y. (1998). Alternative intracellular routing of ErbB receptors may determine signaling potency. *J. Biol. Chem.* 273: 13819-13827.

Wells, A., Welsh, J. B., Lazar, C. S., Wiley, H. S., Gill, G. N., and Rosenfeld, M. G. (1990). Ligand-induced transformation by a noninternalizing epidermal growth factor receptor. *Science* 247: 962-964.

Wendland, B., McCaffery, J. M., Xiao, Q., and Emr, S. D. (1996). A novel fluorescence-activated cell sorter-based screen for yeast endocytosis mutants identifies a yeast homologue of mammalian eps15. *J. Cell Biol.*. 135: 1485-1500.

White, M. F. (1998). The irs-signalling system - a network of docking proteins that mediate insulin action. Mol. *Cell.* Biochem. 182: 3-11.

White, M. F., and Kahn, C. R. (1994). The insulin signaling system. *J. Biol. Chem.* 269: 1-4.

Willingham, M. C., Pastan, I., Shih, T. Y., and Scolnick, E. M. (1980). Localization of the src gene product of the Harvey strain of MSV to plasma membrane of transformed cells by electron microscopic immunocytochemistry. *Cell* 19: 1005-1014.

Winkler, M. E., O'Connor, L., Winget, M., and Fendly, B. (1989). Epidermal growth factor and transforming growth factor α bind differently to the epidermal growth factor receptor. *Biochemistry* 28: 6373-6378.

Wong, L., and Johnson, G. R. (1996). Epidermal growth factor induces coupling of protein-tyrosine phosphatase 1D to GRB2 via the COOH-terminal SH3 domain of GRB2. *J. Biol. Chem.* 271: 20981-20984.

Wong, W. T., Schumacher, C., Salcini, A. E., Romano, A., Castagnino, P., et al. (1995). A protein-binding domain, EH, identified in the receptor tyrosine kinase substrate Eps15 and conserved in evolution. *Proc. Natl. Acad. Sci. USA.* 92, 9530-9534.

Wu, R., Durick, K., Songyang, Z., Cantley, L. C., Taylor, S. S., and Gill, G. N. (1996). Specificity of LIM domain interactions with receptor tyrosine kinases. *J. Biol. Chem.* 271: 15934-15941.

Wu, R.-Y., and Gill, G. (1994). LIM domain recognition of a tyrosine-containing tight turn. *J. Biol. Chem.* 269: 25085-25090.

Xiao, G. H., Shoarinejad, F., Jin, F., Golemis, E. A., and Yeung, R. S. (1997). The tuberous sclerosis 2 gene product, tuberin, functions as a Rab5 GTPase activating protein (GAP) in modulating endocytosis. *J. Biol. Chem.* 272: 6097-6100.

Yamauchi, K., and Pessin, J. E. (1994). Enhancement or inhibition of insulin signaling by insulin receptor substrate 1 is cell context dependent. *Mol. Cell. Biol.* 14: 4427-4434.

Yamauchi, K., and Pessin, J. E. (1994). Insulin receptor substrate-1 (IRS-1) and Shc compete for a limited pool of Grb2 in mediating insulin downstream signaling. *J. Biol. Chem.* 269: 31107-31114.

Yamauchi, K., Holt, K., and Pessin, J. E. (1993). Phosphatidylinositol 3-kinase functions upstream of Ras and Raf in mediating Insulin stimulation of c-fos transcription. *J. Biol. Chem.* 268: 14597-14600.

Yang, S.-S., and Aelst, L. V., and Bar-Sagi, D. (1995). Differential interactions of human Sos1 and Sos2 with Grb2. *J. Biol. Chem.* 270: 18212-18215.

Yarden, Y., and Ullrich, A. (1988). Growth factor receptor tyrosine kinases. *Annu. Rev. Biochem.* 57: 443-478.

Yasuda, I., Kishimoto, A., Tanaka, S., Tominaga, M., Sakurai, A., and Nishizuka, Y. (1990). A synthetic peptide substrate for selective assay of protein kinase C. *Biochem. Biophys. Res. Com.* 166: 1220-1227.

Yokote, K., Mori, S., Hansen, K., McGlade, J., Pawson, T., Heldin, C.-H., and Claesson-Welsh, L. (1994). Direct interaction between SHC and platelet-derived growth factor β-receptor. *J. Biol. Chem.* 269: 15337-15343.